DEVELOPMENT OF RAPID METHODOLOGIES FOR THE DETERMINATION OF STRONTIUM-90 IN WATER USING TRIPLE-TO-DOUBLE COINCIDENCE RATIO (TDCR) ČERENKOV COUNTING AND LIQUID SCINTILLATION ASSAY TECHNIQUES

DÉVELOPPEMENT DE MÉTHODOLOGIES RAPIDES POUR LA DÉTERMINATION DE STRONTIUM-90 DANS L'EAU À L'AIDE DE TECHNIQUES DE COMPTAGE D'ÉMISSION ČERENKOV PAR RAPPORT DE COÏNCIDENCE TRIPLE-À-DOUBLE (RCTD) ET DE MÉTHODES D'ANALYSE PAR SCINTILLATION LIQUIDE

A Thesis Submitted

to the Division of Graduate Studies of the Royal Military College of Canada

by

Michelle Tayeb

In Partial Fulfilment of the Requirements for the Degree of

Masters in Chemistry and Chemical Engineering in the field of Nuclear Science

January 2015

ACKNOWLEDGEMENTS

First and foremost, I would like to extend my gratitude to the generous assistance, guidance, and support that I received throughout this research endeavour from my supervisors Dr. David Kelly and Dr. Emily Corcoran at the Royal Military College of Canada (RMCC), and Dr. Xiongxin Dai at the Canadian Nuclear Laboratories (CNL), formerly known as Atomic Energy of Canada Limited (AECL). I am grateful for their friendship, insights, and constant encouragement, which were critical to the successful completion of this dissertation. Furthermore, special debt of gratitude is owed to my colleagues at CNL, including Dr. David Lee and Dr. David Rowan, who were instrumental in designing the scope of this dissertation, and to those who assisted with field sample collection and analysis. I am also thankful to my professors and fellow students at RMCC for their support and encouragement during the first four months of my post-graduate studies at RMCC. Moreover, I would like to thank Dr. Hughes Bonin for taking the time to translate the present abstract into French. Additionally, I would like to express my deepest gratitude to my family including my fiancé, father, mother, sister, and brothers for their support and encouragement throughout this research work and writing of this dissertation; their love and prayers will always be remembered.

I would also like to offer my appreciations to the federal Science and Technology program of CNL for their financial support of the research outlined in this dissertation. Additional thanks are due the members of former IsoTrace Accelerator Mass Spectrometry facility, Dr. Xiaolei Zhao and Dr. Liam Kieser, and the Inductively Coupled Plasma-Mass Spectrometry laboratory of the Chalk River Laboratories of CNL for assisting in the mass spectrometry analysis phase of this research. Special thanks are also due to the Canadian Forces Base at Esquimalt, British Columbia, for providing assistance in seawater sample collection for this research.

ABSTRACT

Strontium-90 (^{90}Sr) is an anthropogenic contaminant that is present in the environment from spent nuclear fuel, radioactive waste, and atmospheric fallout from nuclear weapon tests and major nuclear incidents. Strontium-90 is one of the most hazardous and radiotoxic radioisotopes, due to its relative long half-life and high mobility in the environment. Because of its significant health hazards, ^{90}Sr needs to be measured accurately. The radioanalytical capabilities for the determination of ^{90}Sr in the environment are challenged by matrix interferences, which often result in less effective, long, and tedious determination methods. Moreover, a number of shortcomings were found in the current seawater ^{90}Sr methods following the Fukushima Daiichi nuclear power accident in March 2011. Thus, the need for effective, rapid, and simple procedures is on-going.

In the present dissertation, the advancements in modern technologies were used to minimize some of the gaps in current radioanalytical capabilities used for the determination of ^{90}Sr in water. The present work considered techniques at moderate and low levels of detection, and in each case undertook to produce methodologies with increased speed of analysis and greater efficiency. A triple-to-double coincidence ratio (TDCR) Čerenkov counting technique using a Hidex liquid scintillation counter was developed for the indirect determination of ^{90}Sr from ^{90}Y at equilibrium activity concentrations of ^{90}Sr-^{90}Y. The technique was fast and simple with excellent performance test results. For low level ^{90}Sr determination in water, pre-concentration using semi-selective co-precipitation and highly selective extraction chromatography techniques were used. Freshwater ^{90}Sr was determined directly as well as indirectly from ^{90}Sr-^{90}Y equilibrium activity concentrations. The method employed (1) co-precipitation of freshwater ^{90}Sr-^{90}Y using calcium phosphate in alkaline conditions; (2) sequential purification of ^{90}Sr and ^{90}Y on Sr-Resin® and DGA-N® extraction chromatography columns, respectively; and (3) detection of ^{90}Sr by liquid scintillation assay (LSA) at two different time intervals and that of ^{90}Y using both Čerenkov counting and LSA. Seawater ^{90}Sr was determined indirectly from ^{90}Y at equilibrium activity concentrations of ^{90}Sr-^{90}Y. The method used (1) co-precipitation of seawater ^{90}Y using calcium carbonate and hydrous titanium oxide in alkaline conditions; (2) purification of ^{90}Y on DGA-N® resin; and (3) detection of ^{90}Y using both Čerenkov counting and LSA. The methods' performance evaluation demonstrated excellent agreement between measured and expected activities of spiked ^{90}Sr-^{90}Y standard solution. Effective implementation of the freshwater method on natural water samples containing a wide range of ^{90}Sr-^{90}Y concentrations was also achieved.

RÉSUMÉ

Le strontium-90 (^{90}Sr) est un contaminant anthropogénique présent dans l'environnement et provenant de combustible nucléaire usé, de déchets radioactifs, et de retombées atmosphériques des essais d'armements nucléaires et des incidents nucléaires majeurs. Le strontium-90 est l'un des radio-isotopes les plus dangereux et les plus radiotoxiques, à cause de sa demi-vie relativement longue et de sa grande mobilité dans l'environnement. À cause des dangers non négligeables à la santé qu'il représente, le ^{90}Sr se doit d'être mesuré précisément. La radio-analyse visant à la détermination du ^{90}Sr dans l'environnement doit répondre aux défis causés par les interférences des matrices qui rendent souvent les méthodes de détermination moins efficaces, longues et fastidieuses. De plus, un nombre de manquements ont été trouvés pour les méthodes courantes d'analyse du ^{90}Sr dans l'eau de mer à la suite de l'accident de la centrale nucléaire de Fukushima Daiichi en mars 2011. D'où le besoin de procédures efficaces, rapides et simples.

Dans cette thèse-ci, on présente les progrès de technologies modernes qui minimisent certains des manquements des capacités de radio-analyse courante pour la détermination du ^{90}Sr dans l'eau. Le présent travail considère des techniques pour la détection à des niveaux modérés et faibles et, pour chacun des cas, entreprend de développer des méthodologies d'analyse plus rapides et ayant une meilleure efficacité. On a développé une technique de comptage d'émission Čerenkov par rapport de coïncidence triple-à-double (RCTD) en utilisant un compteur par scintillation liquide Hidex pour la détermination indirecte du ^{90}Sr à partir du ^{90}Y en concentrations à l'équilibre d'activité de ^{90}Sr-^{90}Y. La technique ainsi obtenue est rapide et simple avec une excellente performance pour les résultats des tests. Pour la détermination du ^{90}Sr à faible niveau dans l'eau, on a utilisé une pré-concentration par co-précipitation semi-sélective et extraction par chromatographie hautement sélective. La teneur en ^{90}Sr dans l'eau douce a été déterminée directement aussi bien qu'indirectement pour des concentrations de ^{90}Sr-^{90}Y à l'équilibre. La méthode utilisait (1) la co-précipitation de ^{90}Sr-^{90}Y dans l'eau douce par du phosphate de calcium dans des conditions alcalines; (2) une purification séquentielle du ^{90}Sr et du ^{90}Y dans des colonnes d'extraction par chromatographie Sr-Resin® et DGA-N®, respectivement, et; (3) la détection du ^{90}Sr par analyse par scintillation liquide (ASL) pour deux intervalles de temps et, pour le ^{90}Y, la détection à l'aide du comptage Čerenkov et aussi par ASL. La teneur du ^{90}Sr dans l'eau de mer fut déterminée indirectement à partir de celle du ^{90}Y pour des concentrations de ^{90}Sr-^{90}Y à l'équilibre d'activité. Cette méthode comprenait (1) la co-précipitation du ^{90}Y dans l'eau de mer à l'aide de carbonate de calcium et d'oxyde de titane hydraté en conditions alcalines; (2) la purification de ^{90}Y sur résine DGA-N® et; (3) la détection du ^{90}Y par comptage Čerenkov et aussi par ASL. L'évaluation de la performance des méthodes a démontré un excellent accord entre les activités mesurées et attendues de solutions standard de ^{90}Sr-^{90}Y. On a

aussi réussi une mise en œuvre effective de la méthode pour l'eau douce avec des échantillons d'eau naturelle contenant une vaste gamme de valeurs pour les concentrations de ^{90}Sr-^{90}Y.

TABLE OF CONTENTS

LIST OF TABLES

LIST OF FIGURES

LIST OF ACRONYMS

AMS	Accelerator Mass Spectrometry
AL	Action Level
AECL	Atomic Energy of Canada Limited
CCME	Canadian Council of Ministers of the Environment
CNL	Canadian Nuclear Laboratories
CRL	Chalk River Laboratories
CPM	Counts Per Minute
CPS	Counts Per Second
DIC	Dissolved Inorganic Carbon
DOC	Dissolved Organic Carbon
EPA	Environmental Protection Agency (United States)
EXC	Extraction Chromatography
GV	Glass counting vials
ICP-MS	Inductively Coupled Plasma-Mass Spectrometry
IAEA	International Atomic Energy Agency
ICRP	International Commission on Radiological Protection
ISA	Isobar Separator for Anions
KAERI	Korean Atomic Energy Research Institute
LSA	Liquid Scintillation Assay
LSC	Liquid Scintillation Counter
LBL	Lower Bass Lake
MAC	Maximum Acceptable Concentration
MDA	Minimum Detectable Activity
MDC	Minimum Detectable Concentration
MISA	Municipal/ Industrial Strategy for Abatement
MS	Mass Spectrometry
NRX	National Research Experimental (research reactor)
NRU	National Research Universal (research reactor)
OMEE	Ontario Ministry of Environment and Energy
OR	Ottawa River
PPM	Parts Per Million
PL	Perch Lake
PMT	Photomultiplier Tube
PV	Plastic counting vials
ROI	Region of Interest
TDCR	Triple-to-Double Coincidence Ratio
WHO	World Health Organization

LIST OF SYMBOLS AND NOTATIONS

$\mathbf{A_{ia}}$	Added activity
$\mathbf{[A_{ia}]}$	Added activity concentration
$\overline{\upsilon}$	Anti-neutrino
Bq	Becquerel
$\mathbf{Bq \cdot L^{-1}}$	Becquerel per liter
k'	Binding affinity
$\boldsymbol{\varepsilon_{Černk}}$	Cerenkov counting efficiency of sample
$\boldsymbol{\grave{\varepsilon}_{Černk}}$	Cerenkov counting efficiency of sample's duplicate
R	Chemical recovery
$\mathbf{r^2}$	Coefficient of determination
E	Counting efficiency
$\boldsymbol{\varepsilon_{EC}}$	Counting efficiency of electron capture decay of ^{88}Y
$\boldsymbol{\varepsilon_{LSA}}$	Counting efficiency of liquid scintillation assay technique
$\mathbf{CR_b}$	Count rate of background
$\mathbf{CR_s}$	Count rate of sample
$\mathbf{CR_N}$	Count rate of sample subtracted background (net count rate)
T and t	Counting time
k	Coverage factor, equivalent to 1.645 at 95 % confidence interval
λ	Decay constant
D	Decay factor
DY	Decay factor of ^{90}Y
DSr	Decay factor of ^{90}Sr
$\mathbf{\beta^-}$	Electron or beta particle, also called negatron
EC	Electron capture decay
$\mathbf{fg \cdot g^{-1}}$	Femtogram (=10^{-15}g) per gram
Logk	Formation constant of a complex ion
$\boldsymbol{f}$	Fraction of sample measured
γ	Gamma photon
T ½	Half-life
h	Hour
$\mathbf{I_Y}$	In-growth factor of ^{90}Y from ^{90}Sr
$\mathbf{I_1}$	Intensity of light, final
$\mathbf{I_0}$	Intensity of light, initial
A	Mass number
$\mathbf{m \cdot z^{-1}}$	Mass-to-charge ratio
$\mathbf{B_r}$	Mean relative bias
$\mathbf{A_i}$	Measured activity
$\mathbf{[A_i]}$	Measured activity concentration
Logk	Metal-complex formation constant
$\mathbf{\mu g \cdot L^{-1}}$	Micrograms per liter
μs	Microseconds

$\mu S \cdot cm^{-1}$	Microsiemen per centimetre
$\mu g \cdot L^{-1}$	Milligram per liter
min	Minutes
$(M \cdot cm)^{-1}$	Molar absorptivity
$mol \cdot L^{-1}$	Molarity
M	Molarity unit
ns	Nanoseconds
υ	Neutrino
n	Neutron
N	Neutron number
‰	Part per thousand
p	Proton
Z	Proton number, atomic number
R_I	Refractive index
B_{ri}	Relative bias of individual measurement or deviation
sec	Seconds
K_{sp}	Solubility product constant
S_B	Spread in bias or precision
σ	Standard deviation
K	Temperature in Kelvin (*i.e.*, 1K= [°C] + 273.15)
V	Volume of sample measured
x	X-ray

LIST OF CHEMICAL FORMULAS

NH_4OH	Ammonium hydroxide
HCO_3^-	Bicarbonate
Br^-	Bromide
$CaCO_3$	Calcium carbonate
$Ca(NO_3)_2$	Calcium nitrate
$Ca_3(PO_4)_2$	Calcium phosphate
CO_3^{2-}	Carbonate
Cl^-	Chloride
F^-	Fluoride
HCl	Hydrochloric acid
HF	Hydrofluoric acid
PbF_2	Lead fluoride
HNO_3	Nitric acid
NO_2	Nitrogen dioxide
$HClO_4$	Perchloric acid
PO_4^{3-}	Phosphate
H_3PO_4	Phosphoric acid
Na_2CO_3	Sodium carbonate
SrF_2	Strontium fluoride
SrF_3^-	Strontium fluoride anion
DtBuCH18C6	Sr-Resin® [4, 4'(5')-*bis* (tert-butylcyclohexano)-18-crown-6]
SO_4^{2-}	Sulphate
DGA-N®	Y-resin (N,N,N',N'-tetra-n-octyldiglycolamide)
ZrF_2	Zirconium fluoride
ZrF_3^-	Zirconium fluoride anion

Chapter 1: Introduction

Strontium-90 (^{90}Sr) is a product of nuclear fission that is significant in the contexts of environmental contamination and human health. The present preamble identifies the need to develop new methodologies for the analysis of ^{90}Sr by identifying gaps in current capabilities, and outlines the research conducted in this thesis to address these deficiencies. Determination of ^{90}Sr in the environment in the context of routine and emergency events is known to be highly crucial due to the biological risks and hazards associated with the radionuclide. Over several decades a great deal of applied research has centred on the development of analytical methodologies for the determination of ^{90}Sr in the environment. Environmental samples impose tremendous challenges to the effective determination of ^{90}Sr. The major challenges come from interferences from other natural and anthropogenic radiological and chemical constituents found in the environment. In addition, measurements of ^{90}Sr in the environment from the nuclear weapons testing era impose further challenges. In many cases, present day concentrations have reached background levels, which are beyond the detection capabilities of most of available radiometric techniques. However, measurement of these trace concentrations of ^{90}Sr remains a requirement. Thus, more sensitive measurement techniques are needed to meet the sensitivity criteria of the very low levels of ^{90}Sr in the environment.

It is common to find that radiochemical and chemical analyses represent a trade-off between sensitivity, speed, and instrument/labour cost. The present work considers techniques at moderate, low, and very low levels of detection, and in each case endeavours to produce methodologies with increased speed of analysis and greater efficiency. The three developments that formed the initial research structure were based on accelerator mass spectrometry (AMS), extraction chromatography (EXC), and liquid scintillation technology to provide advances at very low, low, and moderate levels of detection, respectively.

In the quest for very low level detection techniques, the determination of radioisotopes by AMS has been developed in recent decades. In AMS, sample atoms are converted into ions which are accelerated in tandem to MeV energies to achieve their separation and analysis on the basis of mass-to-charge ratio, $m \cdot z^{-1}$. AMS is a very sensitive mass spectrometry technique which can measure isotope ratios with high selectivity and precision. Typically, the ratio of the concentrations of the rare and abundant isotopes as low as 10^{-12} to 10^{-16} (*i.e.*, < $fg \cdot g^{-1}$ concentraion of ^{90}Sr) can be measured by AMS. As such, very little sample material is needed (*i.e.*, milligrams). In addition, analyses times are much shorter compared to radiometric techniques. Although AMS is far more sensitive and efficient compared to radiometric measurement techniques, the technique needs further development before it can be feasibly used for routine ^{90}Sr measurements. The

major limitation of ^{90}Sr determination by AMS is that similar mass interferences from atomic constituents, in particular from ^{90}Zr, frequently occur. Development of an AMS method for the determination of ^{90}Sr found at ultra-trace environmental levels was attempted as part of this research dissertation. The technique was designed to reactively remove ^{90}Zr interferences in order to allow for very low ^{90}Sr determination. Unfortunately, two challenges presented themselves: the ubiquitous nature of ^{90}Zr, and the complex and aging nature of the AMS system (IsoTrace, University of Toronto, Toronto, Ontario, Canada). Preliminary results were not encouraging and instrument itself became unavailable. Consequently, ^{90}Sr AMS development work was not pursued within the framework of this research dissertation and is not discussed in detail. It is hoped that the work may proceed once the new AMS facility is set up at the University of Ottawa (Ottawa, Ontario, Canada). A review of the approach employed to measure ^{90}Sr at the IsoTrace AMS facility is discussed in the next chapter.

To achieve low level detection of ^{90}Sr, it is necessary to separate the radionuclide from other radioactive materials and the stable sample matrix. In the past several decades, a wide range of radiochemical techniques have been developed to separate ^{90}Sr from matrix and to produce its accurate determination. Some of the techniques and their limitations are discussed in the next chapter. Although most of the classical techniques have proved to be successful and are used for routine as well as emergency determination of ^{90}Sr, there still exist gaps and limitations in robustness of some of the methodologies. For instance, the ^{90}Sr determination procedures that are used at the Chalk River Laboratories (CRL) site of the Canadian Nuclear Laboratories (CNL) are time consuming, laborious, and expensive. The ^{90}Sr analytical procedures are also challenged by the low ^{90}Sr concentrations that are currently found in CRL effluent waters. Therefore, rapid and more sensitive procedures are needed to effectively measure ^{90}Sr authorized discharges into the environment under routine and normal CRL site operations. Thus, one of the objectives of this research dissertation was to design simple, rapid, sensitive, and effective ^{90}Sr determination methods to be used for CRL site liquid effluent monitoring at low levels of activity. In parallel with this objective was the need to provide similar analyses for more complex matrices. A lack of such methods for determination of ^{90}Sr in seawater was identified following the Fukushima Daiichi nuclear power plant accident in March 2011. Most of the seawater ^{90}Sr procedures are long and tedious and, therefore, inefficient in the situations where radiological discharges into the marine environment need urgent quantification. As a result, a plan for development of a rapid method for the determination of radiostrontium in seawater was initiated by the Analytical Laboratories for the Measurement of Environmental Radioactivity (ALMERA) of International Atomic Energy Agency (IAEA) (ALMERA meeting of 2013, Ottawa, Ontario, Canada). In the context of few seawater radiostrontium determination

methods, this research dissertation aimed to develop a ^{90}Sr seawater method in order to minimize some of the existing gaps.

Situations exist in which any form of preparative chemistry can limit sample throughput and delay in data reporting. In general, direct measurements of ^{90}Sr require its purification from interfering beta (β^-) emitting radionuclides and large quantities of inactive substances that are typically present in the environment. However, ^{90}Sr can be indirectly measured from ^{90}Y when the two radionuclides are in equilibrium activity concentrations (*i.e.*, ^{90}Sr-^{90}Y). Because of its high β^- emission energy, ^{90}Y can be measured using the Čerenkov counting technique. This technique is a rapid screening method, in which sample preparation is not necessary. Thus, the technique is ideal for urgent ^{90}Sr determination, albeit at somewhat higher detection levels. As part of fast and simple method development in this dissertation, efforts were made to develop an advanced and modern Čerenkov counting technique, which is called the triple-to-double coincidence ratio (TDCR) Čerenkov counting, for both freshwater and seawater. Water is an important domain to study based on its capacity to transport radiostrontium and because it is a significant pathway by which radionuclides reach humans. The present work used matrices spiked with known quantities of ^{90}Sr-^{90}Y, including seawater collected from North Pacific Ocean at Esquimalt, British Columbia, Canada. Freshwater samples of river water, lake water, and groundwater were also collected from CRL site of CNL, Chalk River, Ontario, Canada from locations exhibiting documented levels of ^{90}Sr.

The scope of the present research dissertation covered:

- Development of a fast TDCR Čerenkov counting screening technique for the determination of high levels (*i.e.*, ≥ 6 $Bq \cdot L^{-1}$) of ^{90}Sr-^{90}Y in freshwater and seawater;
- Evaluation of the application of the TDCR Čerenkov counting screening technique to CRL surface water and groundwater with high levels (*i.e.*, ≥ 6 $Bq \cdot L^{-1}$) of ^{90}Sr-^{90}Y radioactivity;
- Validation of a radiochemical separation technique followed by liquid scintillating assay method that is found in literature and evaluation of the method's application on CRL surface water and groundwater with different ranges (*i.e.*, ~ 0.2 $Bq \cdot L^{-1}$ to >100 $Bq \cdot L^{-1}$) of radioactivity of ^{90}Sr-^{90}Y; and
- Development of a radiochemical separation technique followed by liquid scintillation counting method for the determination of intermediate-to-high-level (*i.e.*, ~ 0.2 $Bq \cdot L^{-1}$ to > 100 $Bq \cdot L^{-1}$) of ^{90}Sr-^{90}Y in seawater.

Chapter 2: Background Theory

This chapter provides background information on theoretical aspects of the work presented in this dissertation. Within this chapter, the reader is first introduced to general characteristics of Sr and its radioisotopes, in particular, ^{90}Sr. Then, a discussion of sources of ^{90}Sr in the environment, its potential hazards, and, thus, the importance of accurate measurements are presented. Finally, background information about radiometric and mass spectrometric measurement techniques is presented.

2.1. Strontium Radioisotopes

Strontium (Sr) is an alkaline earth metal with 38 protons, an isotopically-dependent number of neutrons in the nucleus, and 38 electrons distributed in five electronic shells K, L, M, N, and O. Strontium has physical and chemical properties similar to other alkaline earth metals, in particular, to Ca. The oxidation state of Sr is +2. Strontium has four naturally occurring stable isotopes [1], which comprise about 0.025 % of the earth's crust [2]. The stable isotopes of Sr (with their natural abundances) are: ^{84}Sr (0.56 %), ^{86}Sr (9.86 %), ^{87}Sr (7.0 %), and ^{88}Sr (82.5 %) [1]. Also, 28 radioisotopes of strontium have been identified to date [1]. Most of the radiostrontium isotopes have short half-lives ($T_{1/2}$) and, therefore, are not perceived as contaminants of concern (*e.g.*,^{104}Sr, $T_{1/2}$=150 ns and ^{74}Sr, $T_{1/2}$=1.2 μs [1]). Two of the sufficiently long-lived radiostrontium isotopes are ^{85}Sr ($T_{1/2}$ = 64.84 days) and ^{89} Sr ($T_{1/2}$=50.53 days) [1]. The longest lived radiostrontium isotope is ^{90}Sr with $T_{1/2}$ of 28.78 years [1]. The long $T_{1/2}$ of ^{90}Sr is particularly important in the context of its high fission yield, 5.73±0.13 %, from thermal fission of ^{235}U [3].

Strontium-90 is an anthropogenic radionuclide introduced into the environment as a result of man-made activities. The production of ^{90}Sr from thermal fission of ^{235}U and its decay process are shown in Eq. (1), [4].

$$^{90}\text{Kr} \xrightarrow{\beta,\gamma\ T_{1/2}=32sec} {}^{90}\text{Rb} \xrightarrow{\beta,\gamma\ T_{1/2}=3min} {}^{90}\text{Sr} \xrightarrow{\beta\ T_{1/2}=29yr} {}^{90}\text{Y} \xrightarrow{\beta\ T_{1/2}=64h} {}^{90}\text{Zr} \quad (1)$$

Strontium-90 is a pure β^- emitter with 100 % emission probability and maximum beta decay energy (E_{max}) of 0.546 MeV [1]. The nucleus of ^{90}Sr possesses excess number of neutrons (N=52) compared to protons (Z=38) and, therefore, it lies outside the locus of stability in a nuclear stability chart [5]. For those radionuclides that are neutron ($^1_0$n) rich and proton ($^1_1$p) deficient, such as ^{90}Sr, the mode of decay is by beta ($^0_{-1}\beta$) emission accompanied with emission of an anti-neutrino ($\overline{\upsilon}$), Eq. (2), [6].

$$^1_0\text{n} \rightarrow\ ^1_1\text{p} + {}^0_{-1}\beta + \overline{\upsilon} \quad (2)$$

Strontium-90 decays to radioactive yttrium-90 (^{90}Y). Yttrium-90 is also a pure β^- emitter, which decays to stable zirconium-90 (^{90}Zr) with E_{max} of 2.280 MeV and short $T_{1/2}$ of 64 hours [1]. The highly energetic β^- particles emitted by ^{90}Y also make ^{90}Sr a hazardous radionuclide; especially because ^{90}Y is often in secular equilibrium with ^{90}Sr. The secular equilibrium between parent and daughter activity concentrations occurs when the $T_{1/2}$ of the parent nuclide is significantly larger than $T_{1/2}$ of the daughter nuclide. In the secular equilibrium condition, the activity concentrations of the parent and daughter nuclides are equal to one another. In the case of aged samples, the equilibrium between ^{90}Sr-^{90}Y is already established, but if the sample is purified, growth of ^{90}Y in ^{90}Sr can occur as time elapses. The growth of ^{90}Y in purified ^{90}Sr as a function of time can be shown as in Figure 1. In the present research, detection measurement of purified samples immediately after purification and also at a time interval (*i.e.* 200-300 h), after purification when the equilibrium was established, was obtained to achieve two independent sets of data and, thus, verification of the measurement results.

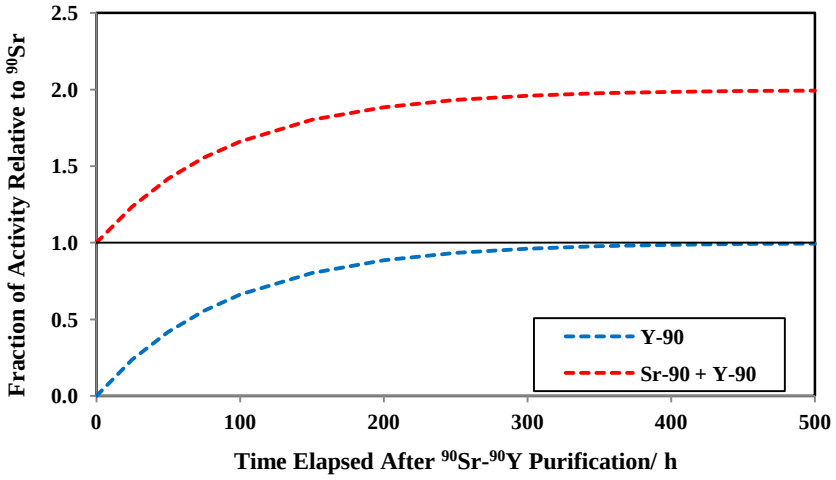

Figure 1. Relationship between purified ^{90}Sr and ^{90}Y decay curves as a function of time

Besides ^{90}Sr, the other two long-lived radiostrontium isotopes are ^{89}Sr and ^{85}Sr. Strontium-89 is also one of the radiotoxic by-products of thermal fission of ^{235}U with a cumulative fission yield of 4.69±0.06 % [3]. The production of ^{89}Sr from thermal fission of ^{235}U and its decay process are shown in Eq. (3), [4].

$$^{89}\mathrm{Kr} \xrightarrow{\beta,\gamma \quad T_{1/2}=3min} {}^{89}\mathrm{Rb} \xrightarrow{\beta,\gamma \quad T_{1/2}=16min} {}^{89}\mathrm{Sr} \xrightarrow{\beta \quad T_{1/2}=51day} {}^{89}\mathrm{Y} \qquad (3)$$

In a similar manner to ^{90}Sr, ^{89}Sr is a pure β^--emitter with more than 99 % emission probability of decay to stable ^{89}Y and E_{max} of 1.495 MeV [1]. The high β^- emission

energy of ^{89}Sr enables its determination by Čerenkov counting technique (Section 2.4.2). Unlike ^{90}Sr, ^{89}Sr from global fallout has decayed away due to it short $T_{1/2}$ of 50.53 days. Hence, in routine analysis of aging environmental samples, ^{89}Sr is not of a concern. In the case of a nuclear fission event, however, because of its high fission yield ^{89}Sr is one of the significant contaminants released into the environment.

Another important radiostrontium isotope is ^{85}Sr. Strontium-85 is also produced from thermal fission of ^{235}U with a cumulative fission yield of 1.31± 0.01 % [3]. Unlike ^{90}Sr and ^{89}Sr, ^{85}Sr decays by electron capture (EC), with 1.065 MeV energy and 100 % emission probability, to stable ^{85}Rb and $T_{1/2}$ of 64.84 days. Strontium-85 lies between two stable isotopes. Its instability and mode of decay reflect complex factors governing nuclear stability. The EC process is seen as proton transformation into a neutron. This mode of decay occurs when the velocity of a particle becomes comparable to the velocities of K-shell electrons. The particle then can grab electrons from the surroundings. As such, a proton of the nucleus combines with an electron ($^{0}_{-1}e$) from an inner shell, most likely K-shell, and converts into a neutron within the nucleus, Eq. (4), [6]. The reaction is accompanied by emission of a neutrino and x-ray (x). Emission of bremsstrahlung radiation, Auger electrons, and γ-rays (γ) can also occur in EC decay mode.

$$^{1}_{1}p + {}^{0}_{-1}e \rightarrow {}^{1}_{0}n + \upsilon + x \qquad (4)$$

After EC decay of ^{85}Sr, a strong γ emission occurs at 0.514 MeV with 96 % emission probability [1], which can be measured by γ spectrometry. Thus, the γ emission enables ^{85}Sr to be used as a radiotracer of Sr in the environment and laboratory settings (*e.g.*, [7, 8]). In this research dissertation, ^{85}Sr was used as a radiotracer for the development of a ^{90}Sr seawater method. Besides ^{85}Sr, the radiotracer ^{88}Y, which is also a 99.8 % EC emitter with 3.623 MeV energy, was used in the seawater method development. Both the EC decay energy and γ mission energy of 0.898 MeV of ^{88}Y were used for radiotracing of ^{90}Y.

2.2. Sources and Hazards of Radiostrontium

Strontium-90 is an anthropogenic radionuclide that is present in the environment on global and local scales. The sources of ^{90}Sr include, authorized discharges from nuclear power plants such as that of CNL, nuclear weapons testing conducted in 1950s and 1960s, and major nuclear incidents such as Fukushima Daiichi nuclear power incident of 2011 and Chernobyl in 1986. Since the nuclear test ban treaty of 1963, a significant decrease in radionuclide signatures have been observed. In general, current ^{90}Sr levels in surface soil typically is found in the range 0.37-37 $mBq{\cdot}g^{-1}$ [9], which can also be expected in the groundwater as ^{90}Sr from surface soil can reach the groundwater by moving down with percolating water. Studies

have reported that industrial radioactive releases of ^{90}Sr generally have little impact on radioactivity levels in surface waters [10].

Besides freshwater, low ^{90}Sr concentrations are also measured in the marine environment. For example, up to 3 $mBq \cdot L^{-1}$ of ^{90}Sr in the surface water of Atlantic Ocean has been reported [11]. In the Pacific Ocean, ^{90}Sr concentrations were 1.2 $mBq \cdot L^{-1}$ before the Fukushima Daiichi nuclear power plant incident of March 2011 [12]. Strontium-90 concentrations in the Pacific Ocean water after the Fukushima Daiichi accident, which were measured in the near-shore water (100-200 km South East from Fukushima) between March and November 2011, ranged from 1.1 $mBq \cdot L^{-1}$ to 85 $mBq \cdot L^{-1}$ [12].

Strontium-90 in the environment is largely dissolved in the water and is, therefore, highly mobile. Thus, ^{90}Sr can easily be dispersed laterally and also transferred among various environmental matrices (*i.e.*, soil, sediment, water, and vegetation). Because of its similar chemistry to Ca, ^{90}Sr follows the biochemical pathways of Ca and can eventually transfer from the environment to humans by ingestion and inhalation. Once ^{90}Sr enters the human body, it can accumulate on the surfaces of the bones, in the same way as Ca. Energetic β^- particles coupled with a moderate isotope $T_{1/2}$ are sufficient to cause detrimental health effects [2]. Because of its capability to cause significant adverse effects to human health, ^{90}Sr has been classified as a high risk radionuclide by the International Atomic Energy Agency, IAEA [13]. Thus, knowledge of the sources and concentrations of ^{90}Sr in the environment, in particular in nuclear operation sites, is crucial. The Canadian guidelines for ^{90}Sr concentrations in drinking water are established in the light of the criteria of the International Commission on Radiological Protection (ICRP). Under normal circumstances, the maximum acceptable concentration (MAC) for ^{90}Sr in drinking water, as defined by Health Canada, is 5 $Bq \cdot L^{-1}$ [14]. The MAC for ^{89}Sr and ^{85}Sr in drinking water are 50 $Bq \cdot L^{-1}$ and 200 $Bq \cdot L^{-1}$, respectively [14]. Also, in the case of a radiological emergency the Action Level (AL) for ^{90}Sr in drinking water and milk is 30 $Bq \cdot L^{-1}$ [15]. The ALs for use in radiological emergency in the screening of food and drinking water have been calculated for those radionuclides expected to be of greater significance to dose if they are ingested. The AL for ^{89}Sr in drinking water and milk is 300 $Bq \cdot L^{-1}$ [15]. There is no AL recommended for ^{85}Sr.

2.3. Radiostrontium Measurement in the Environment

Radiostrontium in the environment is hard to detect because of matrix interferences. Environmental samples (*i.e.*, water, soil, and sediment) are naturally found as mixtures of non-radioactive (*i.e.*, major and trace elements) constituents and sometimes radioactive (*i.e.*, fission and activation products) constituents as well. For example, in the case of natural water, the most abundant non-radioactive dissolved constituents are generally major cations and anions. Major cations of

natural water are Ca^{2+}, Mg^{2+}, Na^{+}, and K^{+} [16]. Major anions of natural water include bicarbonate (HCO_3^{-}), sulfate (SO_4^{-2}), chloride (Cl^{-}), fluoride (F^{-}), and nitrate (NO_3^{-}) [16]. These dissolved constituents mainly come from the relatively abundant elements in the crustal rocks exposed at and near the land surface, which undergo weathering processes including physical and chemical reaction.

The major non-radiological interference to the determination of radiostrontium in the environment comes from Ca. Due to its chemical similarity to Sr, Ca can accompany Sr not only in biochemical pathways, but also in laboratory purification processes. Under circumstances where Ca concentrations are tremendously high, for example in seawater with Ca concentrations of more than 400 $mg{\cdot}L^{-1}$, the separation of Sr from Ca becomes even more challenging. As such, the majority of the methodologies for the determination of ^{90}Sr are tedious, inefficient, and often exceed monitoring capabilities. For instance, following Fukushima Daiichi nuclear power plant accident in 2011, temporal changes of concentrations of several radionuclides (*e.g.*, ^{137}Cs) in surface water adjacent to Fukushima were well documented [12]. The discharge of radiostrontium into the seawater, however, was poorly investigated because of lack of efficient procedures [12]. Monitoring and investigation of radiostrontium can be improved by developing more rapid and efficient radioanalytical techniques.

Besides Ca, other alkaline earth elements, Mg, Ba, and Ra can also interfere with Sr separation techniques. Interference from Mg is much more severe in the case of seawater as Mg concentrations of up to 1,300 $mg{\cdot}L^{-1}$ can be expected in seawater. Separation of Sr from Ba is also important if significantly high concentrations of Ba are expected in the sample. Separation of Ra from Sr is readily achieved because Ra has the least tendency, of all alkaline earth metals, to form complex ions [17].

Strontium-90 in the environment is also hard to detect because of the presence of many β^{-}-emitting radionuclides. In particular, in a radiological emergency resulting from a fission reaction, where excessive concentrations of fission products are released into the environment, accurate determination of ^{90}Sr becomes excessively difficult. Other β^{-} emitting radionuclides can interfere with measurements of ^{90}Sr because in general β^{-} decay emission is not at discrete energy and instead it occurs as a continuous spectrum with a maximum energy. Thus, the spectrum of ^{90}Sr can be hindered by any β^{-} emissions in the energy range of ^{90}Sr (0 - 0.546 MeV). In addition, determination of ^{90}Sr in the environment in a radiological emergency situation imposes further challenges due to the need for urgent measurement of a large number of samples. Therefore, determination techniques that are not only accurate and effective, but that are also rapid and have shorter turnaround time can address the requirements of an emergency situation. For ^{90}Sr measurements in the case of routine as well as emergency, the selection of an efficient measurement

technique is also important. Thus, sample preparation procedure needs to be aligned with the measurement technique to be used. Sample preparation techniques are discussed in the next section.

2.3.1. Sample Preparation Techniques for Determination of Strontium-90 and Yttrium-90

Sample preparation is the key to quality sources produced for measurement. In general, for accurate measurement of an analyte of interest in the environment, preliminary treatment of sample, concentration of the analyte, and its separation from matrix are conducted prior to taking detection measurements. In the analytical procedures for ^{90}Sr, separation of Sr from matrix elements, especially Ca, Mg, and Ba is fairly challenging. The Sr separation includes a wide range of techniques from classical methods using solvent extraction, precipitation, and ion exchange to newer techniques using extraction chromatography (EXC). The majority of the classic separation methods of Sr suffer from various limitations. In many cases (*e.g.*, [13, 18-21]) the separation of Sr from Ca involves multiple and tedious precipitation steps to separate Sr from Ca on the basis of differential solubility of their salts (*i.e.*, nitrates and oxalates). Often Sr separation procedures (*e.g.*, [12, 18, 21, 22]) employ hazardous reagents including fuming nitric acid (*i.e.*, 86 - 95 % HNO_3) and other highly corrosive and concentrated acids (*e.g.*, hydrofluoric acid (HF) and perchloric acid ($HClO_4$)). In the case of seawater, due to high concentrations of Ca, the analysis of a large volume of seawater (*i.e.*, >50 L) uses more than 3 L of fuming HNO_3 for the separation of Sr from Ca [23]. In addition to safety risk, the use of large volumes of fuming HNO_3 for the separation of Sr from Ca makes the method very expensive [24]. Similarly, procedures based on solvent extraction ([11, 20, 25]) require the use of toxic solvents and produce large amounts of liquid waste. Moreover, in the classical methods where procedures are challenged by low chemical recoveries, the method requires evaporation of large volumes (*i.e.*, 50-100 L) of water in order to pre-concentrate small quantities of Sr in the sample [11, 12, 26, 27]. As such, the laboratory processing of the samples must undertake tremendously laborious and time consuming procedures for emergency as well routine operations. The ion-exchange separation procedures of ^{90}Sr [12, 21, 22, 28] also have some shortcomings. In general, ion-exchange procedures require careful pH control as the effective separation from Ca is achieved only within a narrow pH range, which is typically affected by the content of Ca itself in the sample [29].

An efficient approach to overcome the problem of low level samples measurements without the need to process large volumes of water is by pre-concentration using co-precipitation techniques. Co-precipitation is the co-crystallization of metal ion species with similar chemical characteristics [30]. Co-precipitation of metal ions is more effective in salts that are less soluble. The solubility of a salt is quantitatively

measured by solubility-product constant, K_{sp}, Table 1. The K_{sp} is the product of the solubility of the ions in moles per liter in the equilibrium solution between a solid salt and its ions. For example, the solubility equilibrium between calcium carbonate, $CaCO_3$, and calcium phosphate, $Ca_3(PO_4)_2$, salts and their respective ions can be shown in Eq. (5) and Eq. (6), respectively.

$$CaCO_{3(s)} \xleftrightarrow{K_{sp}=[Ca^{2+}]\cdot[CO_3^{2-}]=4.5x10^{-9}@\ 25℃} Ca^{2+}{}_{(aq)} + CO_3{}^{2-}{}_{(aq)} \quad (5)$$

$$Ca_3(PO_4)_{2(s)} \xleftrightarrow{K_{sp}=[Ca^{2+}]^3\cdot[PO_4^{3-}]^2=2.0x10^{-29}@\ 25℃} 3Ca^{2+}{}_{(aq)} + 2PO_4{}^{3-}{}_{(aq)} \quad (6)$$

Table 1. Solubility product constant (K_{sp}) values for Ca and Sr salts at 25°C [31]

Salt	K_{sp}	Unit	Salt	K_{sp}	Unit
$Ca_3(PO_4)_2$	$2.0x10^{-29}$	$mol^{5}\cdot L^{-5}$	$Sr_3(PO_4)_2$	$4.0x10^{-28}$	$mol^{5}\cdot L^{-5}$
$CaCO_3$	$4.5x10^{-9}$	$mol^{2}\cdot L^{-2}$	$SrCO_3$	$9.3x10^{-10}$	$mol^{2}\cdot L^{-2}$
$Ca(OH)_2$	$6.5x10^{-6}$	$mol^{3}\cdot L^{-3}$	$Sr(OH)_2$	$6.4x10^{-3}$	$mol^{3}\cdot L^{-3}$
$CaSO_4$	$2.4x10^{-5}$	$mol^{2}\cdot L^{-2}$	$SrSO_4$	$3.5x10^{-7}$	$mol^{2}\cdot L^{-2}$

In general, for the same number of ions in the salt, the lower the K_{sp} value, the less soluble the salt can be. The very low solubility of $Ca_3(PO_4)_2$ and $CaCO_3$ make them precipitate out of the solution a lot more effectively than some other salts such as calcium hydroxide ($Ca(OH)_2$) and calcium sulphate ($CaSO_4$), Table 1, which are not as frequently used for Sr co-precipitation. Sulfate precipitation is also less frequently used because of the difficulties of dissolving the precipitate [32]. Both phosphate [33- 37], and carbonate [26, 38] co-precipitation of Sr and also Y have been widely used. Yttrium also forms a great variety of insoluble salts under similar conditions as Sr. In the present study, Sr was co-precipitated with Ca as salts of phosphate and carbonate for freshwater and seawater, respectively. Because Sr is chemically analogous to Ca, Sr resembles Ca throughout the co-precipitation process and the Sr-Ca precipitate can be free of most of other matrix interferences. Co-precipitation of Sr with Ca rather than isolation of Sr from Ca in the beginning of sample treatment process is more favourable to Sr. Strontium is found in the environment in trace amounts compared to Ca and, therefore, Sr can be lost if separation of it from Ca is undertaken at the very beginning of the procedure.

In the equilibrium expressions shown in Eq. (5) and Eq. (6), excessive concentrations of Ca need to be present in the aqueous solution in order to shift the equilibrium to the left, towards the solid/precipitate formation. In an experimental study, it was demonstrated that the precipitation of ^{85}Sr is highly dependent on the concentration of Ca in the sample and > 99 % co-precipitation efficiency can be

achieved at Ca concentrations of 16 mM and higher [8]. For freshwater, often additional amounts of Ca are added to ensure sufficient Ca is available for co-precipitation process to take place efficiently. In the case of seawater, because Ca is naturally far more abundant than Sr (*i.e.*, > 50 times more Ca), there is no need for addition of Ca in the co-precipitation step.

Although the uptake of seawater Sr and Y by phosphate is very efficient [18, 34, 35, 37], the phosphate co-precipitation of seawater Sr and Y can also cause major difficulties. The co-precipitation of seawater Sr with $Ca_3(PO_4)_2$ causes a wide variety of ions to co-precipitate along with Sr-Ca. This results in massive precipitate formation, including salts of Mg and Ba. To prevent precipitation of unwanted salts, in this dissertation carbonate co-precipitation is used for seawater and phosphate for freshwater. In the phosphate co-precipitation method, the Ca as in calcium nitrate ($Ca(NO_3)_2$) solution is reacted with phosphoric acid (H_3PO_4) to form $Ca_3(PO_4)_2$ precipitate carrying trace concentrations of Sr that is found as divalent cations in the aqueous solution (*i.e.*, water). In the carbonate co-precipitation method, sodium carbonate (Na_2CO_3) solution is reacted with the dissolved Ca of seawater carrying trace concentrations of Sr. The $Ca_3(PO_4)_2$ and $CaCO_3$ precipitate carrying Sr can subsequently be dissolved in mineral acid (*i.e.*, HCl and HNO_3) solutions and Sr in the aqueous solution can then be separated from Ca. As discussed earlier, in the classical radiochemical methods, separation of Sr from Ca is based on long and tedious procedures. In this research study, purification of Sr and Y from matrix interferences is achieved by a versatile extraction chromatography technique.

2.3.2. Separation of Strontium-90 and Yttrium-90 from Matrix

Accurate and precise determination of ^{90}Sr in the environment requires radiochemical separation of ^{90}Sr from other radioactive and non-radioactive constituents. The purification technique employed in this research study is by a highly selective extraction chromatography (EXC) technique. In EXC, liquid extractants are sorbed on the surface of an inert solid support material [39, 40]. The three main components of an EXC are (i) an inert support (*i.e.*, an organic polymer or porous resin/bead), (ii) a stationary phase (*i.e.*, a liquid extractant such as a crown ether), and (iii) a mobile phase (*i.e.*, an acid solution, usually HNO_3 or HCl) [39]. A diagram of an EXC resin is shown in Figure 2.

The EXC technique has several advantages over conventional separation techniques in which separation of Sr from a matrix requires tedious and time intensive radiochemical procedures. In the EXC technique, the method allows for rapid separation because the extraction process takes place in a thin surface layer whereby a good contact between extractant and the analyte leads to fast exchange kinetics. An additional advantage comes from the use of fewer chemicals, which leads to a reduced amount of waste and consequent improvements in laboratory

practices. The process is also more economical compared to other methods such as solvent extraction and ion exchange. Most importantly, the EXC has high element selectivity. The Sr-selective and Y-selective resins have performed very well for separation of Sr and Y, respectively, from a wide range of matrices such as environmental, biological, and radioactive waste in both routine and emergency operations [4, 22, 27, 34, 36-38, 41-48]. The two types of EXC resins and techniques are introduced in the next sections.

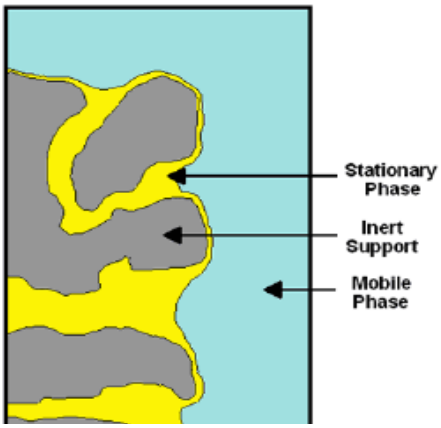

Figure 2. Diagram showing surface of a porous bead used as an extraction chromatography resin [39]

2.3.2.1. Strontium-selective Extraction Chromatography

In the Sr-selective EXC, the extractant is a macrocyclic polyether compound called 4, 4'(5')-*bis* (tert-butylcyclohexano)-18-crown-6 diluted in 1-octanol, which is impregnated on polymer support beads [30, 40]. It is also referred to as DtBuCH18C6 and Sr-Resin®. The octanol of Sr-Resin® enables better extraction ability of the resin by high water uptake, which in turn causes the effective solvation of the Sr nitrate complex [33]. Also, the crown ether is relatively soluble in water, and, therefore, the addition of an inert polymer, which is a hydrophobic substance, reduces the solubility and increases stability of the resin and also the binding power of Sr to the resin [40].

The DtBuCH18C6 forms 40 symmetrically non-degenerate isomers two of which are illustrated in Figure 3 [39]. Due to differences in the conformation of the tert-butylcyclohexano substituents, each of the different stereoisomers of DtBuCH18C6 can exhibit different cation complexation strengths. The molecular modeling calculations have predicted that the 4,4′-DtBuCH18C6 (Figure 3b) forms the most thermodynamically stable complexes with Sr^{2+} [39].

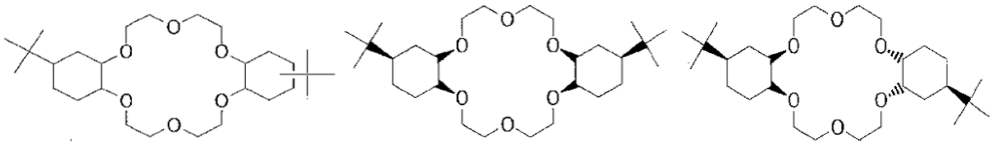

(a) **(b)** **(c)**

Figure 3. Structural representation of the functional group of Sr-Resin®: (a) a generic representation of 4, 4'(5')-*bis*-(tert-butylcyclohexano)-18-crown-6, (b) one of the 4,4'-tert-butyle isomer, and (c) one of the 4,5'-tert-butyle isomers [39]

In general, the 18-crown-6 compounds have the ability to form stable complexes with alkali and alkaline earth cations. Although there is little information available in the literature regarding the mechanisms of interactions specifically between Sr^{2+} and the Sr-Resin®, some general information about crown ethers interaction with cations can deduce the selectivity of the resin for Sr. For example, the ability of the Sr^{2+} to attract DtBuCH18C6 is a Lewis Acid-Base interaction whereby each of the oxygen atoms of the crown ether with two pairs of unshared electrons, Figure 4a, constitute the basis for such an interaction. In addition, it is known that the stability of the complex formed by a particular crown ether and a given metal ion is partly governed by the relative size of the cation and the polymer cavity, which results in both strong and selective metal complex formation [37], Figure 4b and 4c. In the case of $Sr^{2+}$and DtBuCH18C6 complex formation, the polyether ring containing six oxygen atoms provides an effective hole size (~ 0.26 - 0.32 nm [33]) for ionic radius of the Sr^{2+} cation resulting in a thermodynamically stable complex [30, 40]. Moreover, Dietz *et al*. [49] calculated the formation constants for forming cation-crown ether complex formation in water for a number of alkaline earth elements. The conditional formation constant (*i.e.*, indicated as Logk) of the metal-crown ether complex under the experimental conditions tested for Sr^{2+} and 18-crown-6 was calculated to be Logk=3.0±0.2 while that of Ca^{2+} was found to be almost two-orders of magnitude lower at Logk =1.1±0.1 [49].

(a) **(b)** **(c)** **(d)**

Figure 4. Schematic structure of 18-crown-6 (a), its complex formation with a metal cation shown as M^+ in (b) and as a green ball in (c), and a schematic structure of the $Sr(NO_3)_2$-Crown ether complex sorbed onto the Sr-Resin® depicted in (d) where carbon atoms are shown in black, oxygen atoms in red, and nitrogen atoms in gray with crosshatching; *adapted from* [50].

Research and development on the crown ether complex formation with cations has also demonstrated that there are many other factors, such as acidity of the matrix and mobile phase water content that can influence the cation extraction [37]. Horwitz *et al*. investigated the effects of ionic strength of Sr binding onto Sr-Resin® at 0.1-10 M HNO_3 [29, 40]. The extraction equilibrium is shown in Eq. (7) and a schematic structure of the complex shown in Figure 4d.

$$Sr^{2+}_{(aq)} + 2NO_3^-{}_{(aq)} + Crown_{(org.)} \leftrightarrow Sr(NO_3)_2Crown_{(org)} \quad (7)$$

The conjugate ion of the HNO_3 acid, NO_3^-, is a strong base anion exchanger to which Sr, as well as Y, bind stronger than alkaline elements, and some alkaline earth elements such as Mg and Ca [51]. Of the different molarity strengths (*i.e*., 0.1-10 M) of HNO_3 examined by Horwitz *et al*., 8 M HNO_3 was found to be the optimal condition at which the Sr-Resin® is exceptionally selective for Sr over alkali, alkaline earth, and other metal cations, Figure 5.

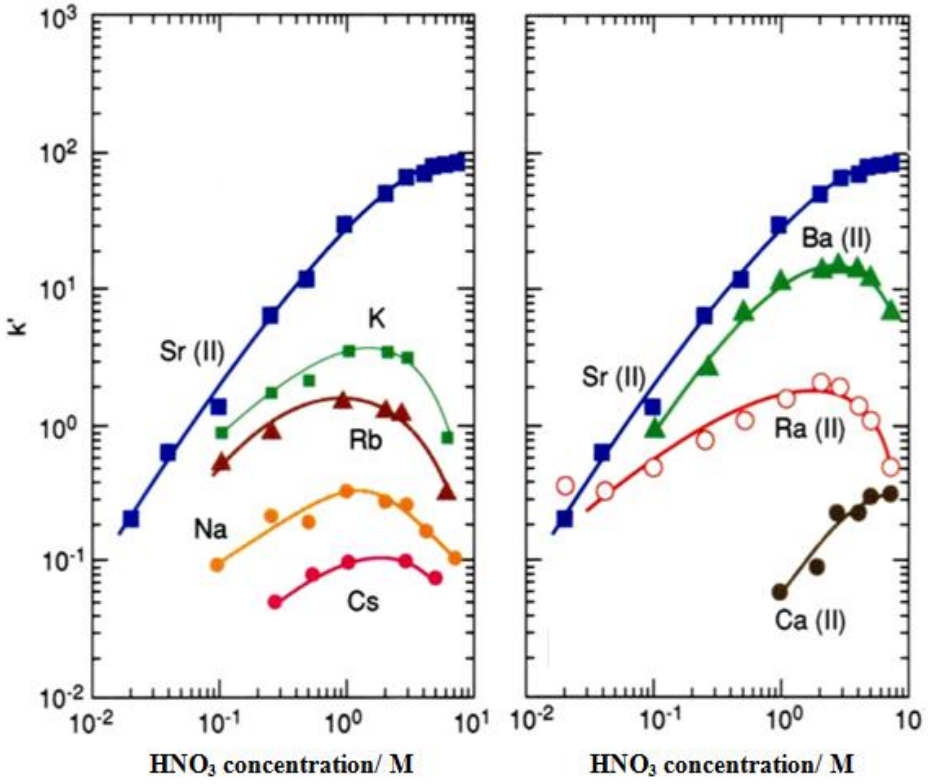

Figure 5. Comparison of binding affinity (*k*') of Sr-Resin® for alkaline and alkaline earth metals; *adapted from* [29, 40]

As shown in Figure 5, in 8 M HNO_3 the binding affinity of Sr for the resin (k'_{Sr}) exceeds that of other alkali and alkaline earth elements by more than two-orders of magnitude, except for Ba. Excellent separation of Sr is achieved from alkali metals and Ca with decontamination factor of more than 100. Thus, separation for radiologically important ^{40}K and Ra isotopes, and chemically important Ca and Mg are achieved. Other acids, such as HCl and H_2SO_4 show comparable pH-dependent binding trends for Sr and interfering ions [52] and are, thus, less effective.

Although the uptake of Sr by Sr-Resin® is much more effective compared to most matrix constituents, under the conditions where the concentrations of those constituents are significantly higher than Sr, they can reduce the uptake efficiency of Sr by competing with Sr for binding sites on the resin. Figure 6 shows the effects of various cations on Sr uptake by Sr-Resin®. As Figure 6 demonstrates, Ca and Na concentrations greater than 0.5 M can significantly reduce the Sr uptake. Similarly, K concentrations greater than 0.01 M can suppress the uptake of Sr by the Sr-Resin®, Figure 6.

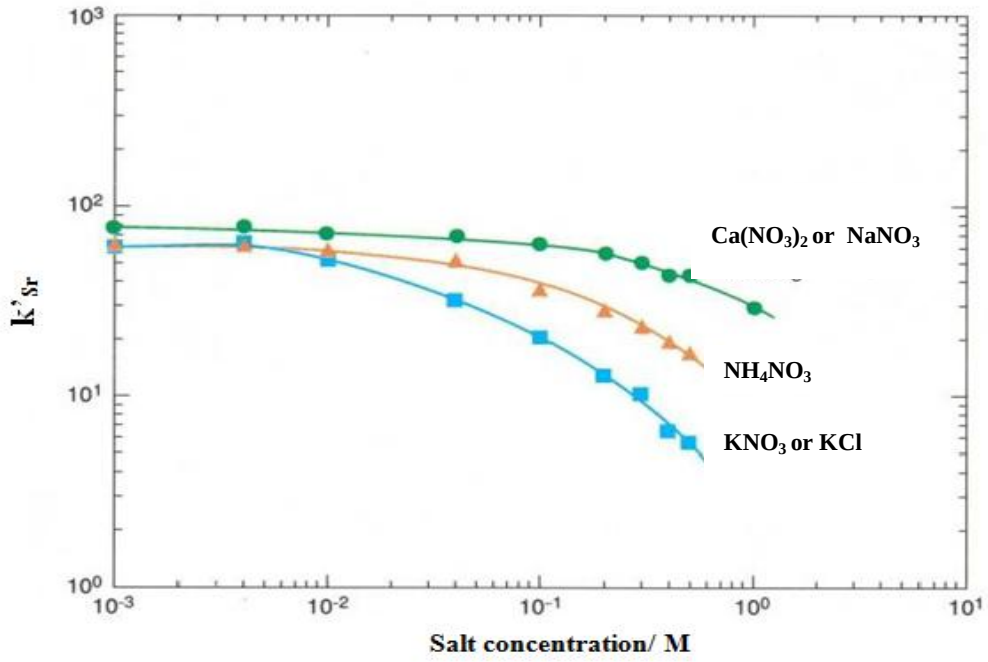

Figure 6. Effect of matrix constituents on Sr retention onto Sr-Resin®; *adapted from* [29]

High concentrations of natural Sr can also reduce the uptake efficiency of Sr by Sr-Resin®, Figure 7.

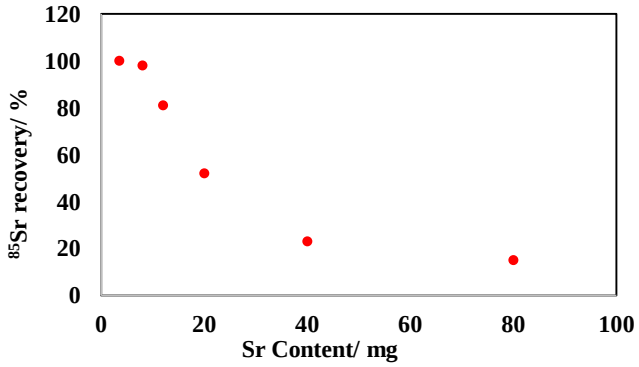

Figure 7. Graphs showing the effect of stable Sr on ^{85}Sr recovery [53]

In general, natural Sr in the environment is by more than six-orders of magnitude more abundant than ^{90}Sr. The maximum capacity of the resin for Sr was experimentally determined to be approximately 21 mg Sr per 2 mL column and working capacity of 10-20 % of maximum capacity is recommended [54].

Additional purification of Sr from the matrix can be achieved during the extraction process. It has been demonstrated that a 2-10 mL wash solution of 3-8 M HNO_3 can effectively remove a variety of unwanted metal ions from the resin resulting in optimal decontamination [29, 41]. The fraction of the elements eluted in the 2-10 mL rinse solution of 3 M HNO_3 is shown in Table 2.

Table 2. Elution behaviour of constituents on a Sr-Resin® column in 2-10 mL of 8 M HNO_3 measured by Inductively Coupled Plasma Atomic Emission Spectroscopy [40]

Element	% element eluted	Element	% element eluted	Element	% element eluted
Na	100	Cu	100	Ag	15
Mg	100	Sr	0	Cd	100
Al	100	Y	100	Ba	0
Ca	100	Zr	91	La	100
Cr	100	Mo	84	Ce	100
Mn	100	Ru	100	Pr	100
Fe	99	Rh	100	Nd	100
Ni	100	Pd	100	Eu	100

Also, it has been demonstrated that Sr is not stripped off the resin with the rinsing solution of 3-8 M HNO_3 because Sr is strongly bound onto the resin at high ionic strengths of the acid and it takes more than 100 mL of the 3 M HNO_3 to pass through the column before measurable breakthrough of Sr occurs [40]. This implies that the resin can be safely and thoroughly rinsed after sample loading and before the bound Sr can be eluted for measurement. The Sr bound onto the resin can be eluted off the column by contacting the organic phase of the resin with

either water or dilute acid (*i.e.*, 0.05 M HNO_3) [40]. Note that in Table 2, Ba does not elute off the column in the 2-10 mL 8 M HNO_3. Column rinsing using additional 8 M HNO_3 is required to elute Ba from the column [37]. Barrium-140 is a fission product and also a β^- emitter, which can interfere with ^{90}Sr-^{90}Y determination if large amounts are present in the sample. However, ^{140}Ba is short-lived, $T_{1/2}$< 13 days, and is not of a concern in aged environmental samples.

As discussed so far, the Sr-Resin® is highly selective for Sr from the mixture of a wide range of matrix interferences. The disadvantage of the Sr-Resin® comes in its affinity towards some elements such as Po, Pb, and some actinides (*i.e.*, Th, U, Np, and Pu), Figure 8. However, Po affinity is low at the pH used for Sr binding, whilst the irreversible interaction of Pb results in its separation during Sr elution. Actinide separation can also be achieved. Uranium and Th are stripped using 8 M HNO_3, whilst the uptake of Pu and Np can be blocked using a complexing agent like oxalic acid (3 M HNO_3/oxalate). In-line actinide selective columns can also be used to selectively remove actinides.

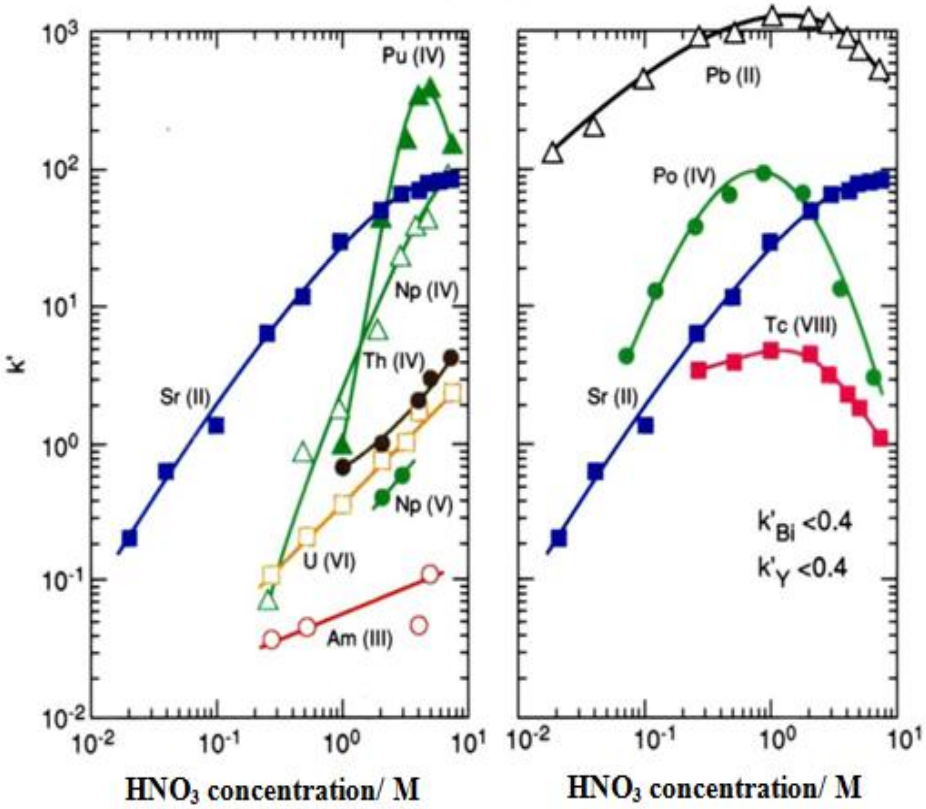

Figure 8. Comparison of binding affinity (*k*') of Sr-Resin® for other elements (transition metals, actinides, and lanthanides); *adapted from* [29, 40]

2.3.2.2. Yttrium-selective Extraction Chromatography

In a similar manner to Sr, Y purification is also achieved using EXC. The resin for extraction of Y is DGA-N® (N,N,N',N'-tetra-n-octyldiglycolamide), Figure 9.

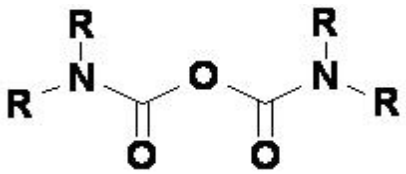

Figure 9. Chemical structure of N,N,N',N'-tetra-n-octyl di-glycol amide [55]

In Figure 9, the four R-groups, which are eight carbon containing chains, comprise the inert support for the resin. The key functional group in the structure is the di-glycol amide. The extraction equilibrium is illustrated by Eq. (8), [56].

$$Y^{3+}_{(aq)} + 3\ DGA + 3NO_3^-{}_{(aq)} \leftrightarrow Y(DGA)_3.(NO_3)_3 \quad (8)$$

Although the DGA-N® resin has been widely used for extraction of Y (*e.g.*, [4, 45, 56], very little information is available in the literature regarding the specific interaction mechanisms between Y and DGA-N® resin. However, the interaction of Y with the resin can be understood from Y chemistry. Yttrium is a transition metal, which exhibits only one oxidation state of +3. The interaction between the Y^{3+} cation and the DGA-N® can be described in terms of Lewis Acid-Base attraction. Although the di-glycol amide is a neutral molecule, both oxygen and nitrogen atoms have unshared pairs of electors which make them electron pair donors and, thus, the ligand acts as the Lewis Base towards Y^{3+}, which is the electron acceptor and, thus, the Lewis Acid. The uptake factor of DGA-N® resin for Y (*k'*) is high in HNO_3 and HCl at 0.01 to 10 M, Figure 10.

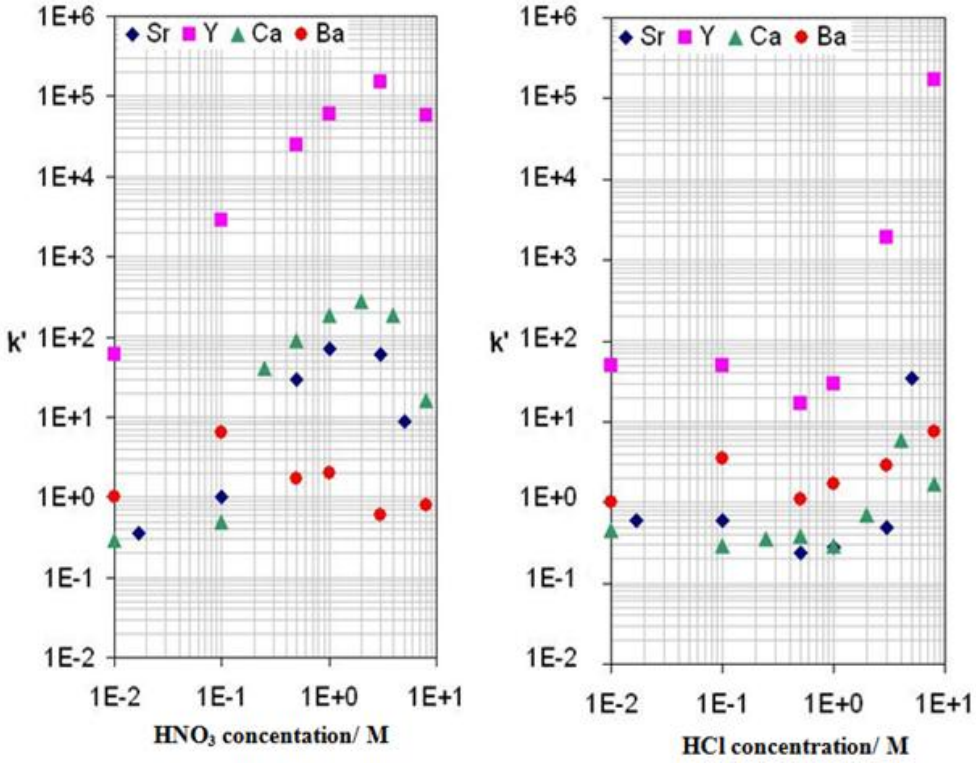

Figure 10. Comparison of binding affinity (*k'*) of DGA-N® resin for different ions; *adapted from* [55]

Besides Y, alkaline earth cations (*i.e.*, Sr, Ca, Ra, and Ba) also show affinity for DGA-N® resin. However, at 8 M acidic solutions of HNO_3 and HCl, Y has a tremendously high *k'* for the DGA-N® resin in comparison to other matrix cations. DGA-N® resin also shows favourable selectivity for Pb, Figure 11, this issue can be eliminated if used in tandem with Sr-Resin®. Once again, actinide binding can be eliminated by the use of actinide specific resins [31, 41].

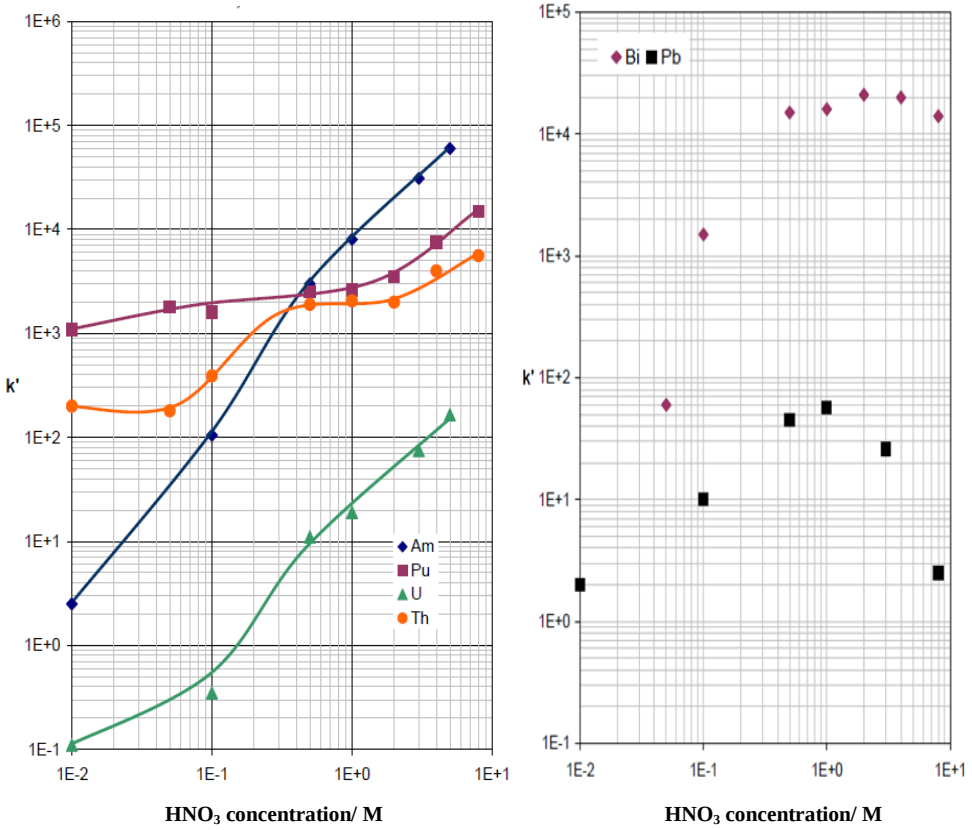

Figure 11. Selectivity of DGA-N® resin for Pb, Bi, and some actinides; *adapted from* [54]

Once separated by EXC, ^{90}Sr and ^{90}Y can be measured for their activities in the sample.

2.4. Strontium-90 and Yttrium-90 Radiometric Detection Techniques

Radiometric techniques, in general, rely on the detection of radiation emitted as a result of radioactive decay of radionuclides. In the case of ^{90}Sr, radioactive decay of ^{90}Sr to ^{90}Y is measured to quantify ^{90}Sr in a sample. The commonly used radiometric detection techniques for ^{90}Sr are by liquid scintillation counting and gas flow proportional (GFP) counting. In the liquid scintillation counting technique using a liquid scintillation counter (LSC), the detection of ^{90}Sr in the sample can be approached by (i) direct determination of ^{90}Sr using an assay technique called the liquid scintillation assay (LSA), and (ii) indirect determination of ^{90}Sr from ^{90}Y using a screening technique called Čerenkov counting. The techniques are further described later in this chapter. In GFP, β^- particles (as well as alpha) ionize the

detector gas (*e.g.*, argon gas) and create ion pairs, which ultimately generate pulses that are registered as counts. The GFP counting technique is commonly used for measurement of gross alpha and gross β^- and occasionally for ^{90}Sr.

Although the background of LSCs is slightly higher than that of GFP counters, liquid scintillation is favoured due to the much better spectral resolution of ^{89}Sr, ^{90}Sr, and ^{90}Y spectra, which enables mathematical determination of the three radionuclides' contributions from a single measurement using different counting windows. The GFP counting technique is also in major disadvantage because of its long and tedious source preparation requirement. In the case of ^{90}Sr measurement, following radiochemical separation, evaporation to dryness, and source preparation are required whereby the purified sample has to be fixed on a stainless steel disc and then measured. The additional processing of samples for GFP counting makes the technique less attractive compared to LSA technique for ^{90}Sr measurement. In addition, the GFP detector system uses a hemispherical volume, hence 2-π geometry. In the 2-π geometry, detection of radiation coming only from the top of the isotropically emitting source is achieved while emissions toward the bottom of the sphere is lost without being detected. Thus, the counting efficiency of GFP counter is 50 % for β^- particle detection. Unlike the GFP, the LSC uses a 4-π geometry detection. Thus, the counting efficiency is 100 % for beta energies using a liquid scintillation counter.

2.4.1. Principle of Liquid Scintillation Counting Technique

The liquid scintillation counting technique is a quantitative radiometric technique for determination of alpha and beta radiations. In the liquid scintillation assay (LSA), an active sample is mixed with a scintillation cocktail and counted on a LSC. The liquid scintillation cocktail is an aromatic solvent containing an organic scintillator (also called fluor) molecule. The π-electron structure of the scintillator molecule, shown in Figure 12, contributes in absorption and emission of light. In the LSA of β^- emitting radionuclides, the kinetic energy of the β^- particle is absorbed by exciting the π-electrons of the molecule into any one of a number of excited states (indicated by S in Figure 12). When the excited molecule relaxes to the ground state (*i.e.,* S_{00} in Figure 12), fluorescence light is emitted in the process. As such, the scintillation cocktail is capable of converting the kinetic energy of charged particles into detectable light. This conversion is linear; the higher the energy of the charged particle the stronger the light output. A schematic of light production by a scintillation cocktail is depicted in Figure 13.

In the process of converting radiation energy into photons of light, the fraction of all incident particle energy that is converted to visible light is called the scintillation efficiency [57]. Many factors contribute to suppress the scintillation efficiency. For example, conditions that suppress the particle energy can also reduce the scintillation efficiency. Because of their shorter ranges compared to γ

rays, the energies of β^- particles (as well as alpha) are largely affected by a number of factors. For instance, various properties of a sample that can contribute to energy suppression could include density, volume, chemical composition, colour, and counting vial material. In the liquid scintillating counting technique, a process that can reduce the efficiency of the conversion of particle energy into light is called quenching. The quenching phenomenon is discussed in further detail later in this section.

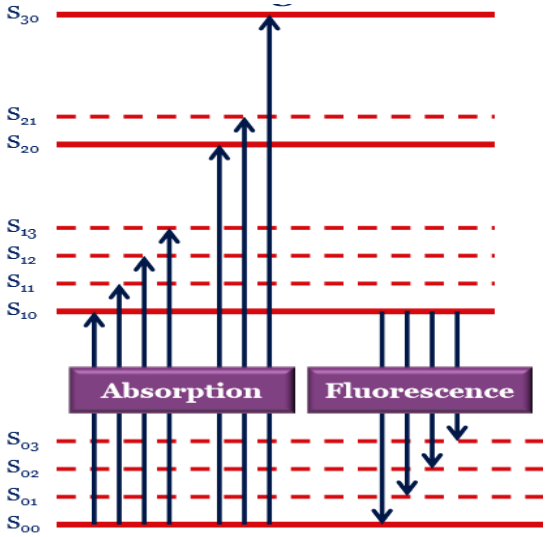

Figure 12. Schematic of energy levels of an organic molecule with π -electron structure; *adapted from* [57].

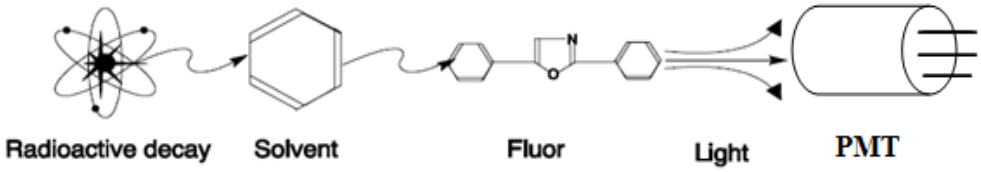

Figure 13. An illustration of the sequence of events in the liquid scintillation process; *adapted from* [58]

Once the light is produced by the scintillation cocktail, it is converted to photoelectrons at the light sensor tubes called photomultiplier tubes (PMTs) of the

LSC detector. A PMT is capable of electron amplification. Once amplified, the electrons are collected at the anode section of PMT and a pulse is produced as an output, which is then recorded by the system [58].

All radiation detectors produce some sort of response for every quantum of radiation that enters it. In the case of LSC, just like any other radiation detector, when charged particles (*i.e.*, alpha and beta) enter the detector, the charged particle deposits all of its energy in the active volume of the detector and pulses are produced. If the detector sees every particle (*i.e.*, beta or alpha) the counting efficiency will be 100 % [57]. However, 100 % efficiency is not achievable for most detector systems and only a fraction of the total efficiency is typically captured. For β^- particles, which have short ranges and interact with energy deposition and excitation, the counting efficiency can be high. The type of efficiency measured in the laboratory using a radioactive source is called the counting efficiency of the source, which is the absolute efficiency (ε_{abs}) expressed by Eq. (9), [57]. The ε_{abs} is the product of intrinsic efficiency of the detector, which is a constant for a given detector, and geometric components (*e.g.*, sample size, density, and other counting conditions).

$$\varepsilon_{abs} = \frac{\text{Number of pulses recorded}}{\text{Number of radiation quanta emitted by source}} \tag{9}$$

One of the main factors that can tremendously suppress counting efficiency of a sample measured on a LSC is quenching. There are two types of quenching: colour and chemical quenching. Colour quenching is the attenuation of photons of light by the colour in the sample. In the case of chemical quenching, the excitation energy of the excited molecule is converted to heat during the transfer of energy from the solvent to the scintillator. Any chemical species in the sample that is electronegative can affect the energy transfer process. Electronegative species can affect the energy transfer process by making the π-electrons of the aromatic solvent less available for efficient energy transfer. Consequently, light output for measurement by the PMT is reduced. As a result of quenching, the overall number of photons produced in the sample is reduced, which in turn reduces the counting efficiency. Counting efficiency is affected by the degree of quenching present in the sample. For example in Figure 14, when the amount of HNO_3 increases in the sample, the sample spectrum amplitude reduces and the spectrum shifts toward the lower energy/channel numbers. The nitrate anion is a strong quenching agent because it has a strong molar absorptivity of 7.24 $(M \cdot cm)^{-1}$ for absorbing radiation light [59]. Thus, the level of quench present in the sample can interfere with the true signal and the degree of such interference is strongly correlated with the level of quench in the sample.

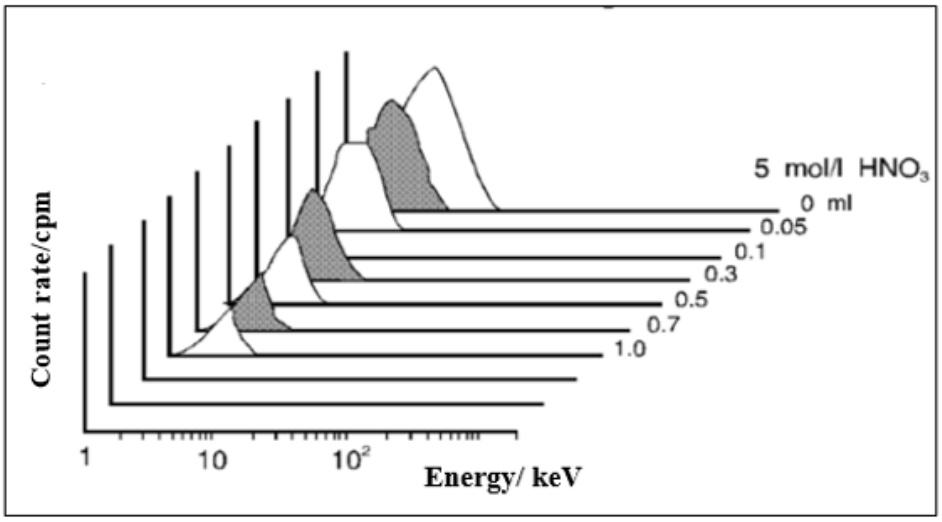

Figure 14. The effect of quenching of 5 M HNO_3 on energy spectrum (of tritium) in liquid scintillation assay technique; *adapted from* [58]

In conventional liquid scintillation counting techniques, the detector is quench calibrated. That means a series of external quench standards are prepared and a quench curve constructed and used to correct the effects of quenching in the sample [60, 61]. Recent advancements have eliminated the need for constructing a quench correction curve. In the modern liquid scintillation technique using a triple-to-double coincidence ratio (TDCR) Hidex LSC, the effects of quenching on the counting efficiency of a sample is automatically corrected. A photo of the Hidex 300SL LSC and its detector assembly are shown in Appendix A. The detector assembly consists of three PMTs, rather than two PMTs that are found in conventional counters. Thus, unlike the conventional double coincidence counting techniques, the TDCR technique uses a triple coincidence counting method. Interferences from quenching and any other factors are reflected in triple coincidence counts and ultimately expressed in the ratio of TDCR. Using the relationship between the sample TDCR and its counting efficiency a correction expression can be developed and applied to automatically correct for the level of quench present in the sample. This approach established the basis for the development of a TDCR Čerenkov counting method for the determination of ^{90}Y in samples as part of this study.

2.4.2. Čerenkov Counting Theory and Application

In addition to the liquid scintillation counting technique, an alternative technique for quantification of ^{90}Sr-^{90}Y is by Čerenkov counting technique. In the Čerenkov counting technique, fast electrons from β^- decay moving in a dielectric and

transparent medium (*e.g.*, water) causes localized electronic polarization of molecules, which rapidly return to the ground state releasing electromagnetic radiation [62]. The electromagnetic radiation released is known as the Čerenkov radiation [62]. Čerenkov radiation is anisotropic whereby photons are emitted as a cone of radiation at a specific angle (~ 40˚) to the direction of travel of β^- particles [62]. The energy threshold of a radionuclide for Čerenkov light production in water is 0.263 MeV [63]. Thus, the technique is highly selective for strong β^--emitters such as ^{90}Y (E_{max} = 2.280 MeV). The secular equilibrium state between ^{90}Sr and ^{90}Y forms the foundation for indirect determination of ^{90}Sr by Čerenkov counting of ^{90}Y. Although, β^- emission energy of ^{90}Sr (E_{max} = 0.546 MeV) is well above the Čerenkov energy threshold in water, Čerenkov light emission of ^{90}Sr is negligible and its contribution to Čerenkov counting efficiency of ^{90}Sr-^{90}Y is acceptably small, only 1-5 % [60, 63- 65]. Čerenkov counting method has several advantages over conventional LSC counting. For example:

i. Alpha emitters and low energy β^- emitters (*e.g.*, ^{3}H with E_{max} = 0.019 MeV and ^{14}C with E_{max} = 0.156 MeV) are discriminated;
ii. Low energy γ emissions of less than 0.430 MeV will not interfere, as they do not produce Compton electrons with energies above 0.263 MeV (threshold energy for Čerenkov counting) [62];
iii. There is no need for sample treatment or mixing of samples with cocktail and, therefore, waste generation is minimized and chemical quenching is eliminated; and
iv. It is a non-destructive technique and, thus, samples can be used for other purposes.

Although the Čerenkov counting technique for measurement of ^{90}Sr-^{90}Y has been widely used for many decades (*e.g.*, [60, 62, 65- 68] the technique can be further developed by the application of emerging technologies such as the TDCR Čerenkov counting technique [69]. The main advantage of the TDCR Čerenkov counting is in its ability to automatically correct for interferences such as colour quenching and variation in sample geometry, which in conventional methods needs external calibration. Therefore, the application of the TDCR allows for the rapid evaluation of interference (*e.g.*, colour quenching and sample geometry) on the activity measurements. One of the objectives of this dissertation was to evaluate the effects of sample geometry and colour quenching on Čerenkov counting of ^{90}Sr-^{90}Y using a TDCR Hidex LSC.

Although the radiometric techniques for the determination of ^{90}Sr have been successfully used, the methods are not sufficiently sensitive to meet the growing demand for more sensitive methods. For example, ^{90}Sr in some cases, such as ^{90}Sr global background studies, is beyond the detection capability of liquid scintillation counting technique. As such, the need for more sensitive measurement techniques

continues. Measurement of trace levels of radiological contaminants in the environment is important in order to assess their hazards. Determination of ^{90}Sr using accelerator mass spectrometry is discussed next.

2.5. Strontium-90 Determination by Accelerator Mass Spectrometry

Mass spectrometry (MS) is a sensitive quantitative technique that can measure isotope ratios with high selectivity and precision. Unlike the radiometric techniques, MS measures radioisotopes directly rather than the by-products of their decay. Therefore, the MS technique is highly suited for the measurement of long-lived isotopes, where many atoms result in few decays. Mass spectrometers analyze sample atoms by producing, separating, and detecting gas-phase ions in vacuum on the basis of mass-to-charge ratio, $m \cdot z^{-1}$. The widely researched MS techniques for ^{90}Sr quantification are the inductively coupled plasma-mass spectrometry (ICP-MS) and the accelerator mass spectrometry (AMS). The ICP-MS is routinely used to quantify major and trace elements at very low concentrations. For the determination of ^{90}Sr, however, the ICP-MS suffers from interferences of atomic and molecular species with masses of 90 (*e.g.*, ^{90}Zr and $^{88}Sr^{1}H_2^{+}$). Even in advanced ICP-MS configurations, where some interference is reactively removed, the detection limits for ^{90}Sr measurement remain somehow higher (*i.e.*, 0.2-3 $pg \cdot g^{-1}$) than expected for MS techniques [46, 70].

AMS is an advanced form of mass spectrometry, which was initially developed in 1977 [71] and used for the quantification of ^{14}C. Later, the technique was further developed to accommodate determinations of ^{36}Cl, ^{129}I, ^{239}Pu [72, 73] and ^{90}Sr [74, 75, 76]. In AMS, sample atoms are converted to negative ion beams by an ion source, for example a Cs^{+} sputter source. The negative ions are then accelerated in tandem to MeV energies to a constant positive high voltage electrode whereby they are changed to positive ions by stripping several electrons in a gas or foil [77]. These ions are then accelerated further through the same potential and then analyzed using electric and magnetic fields which provide information about $m \cdot z^{-1}$ of an ion [77]. A schematic of AMS set-up is illustrated in Appendix A.

Advancements of the AMS system that make it ultra-sensitive include: (i) the use of solid state sample targets, which possess great stability and are less likely to decompose to form interfering fragments during measurements; (ii) use of a Cs^{+} sputter because of its low memory for previous samples [77]; (iii) tandem accelerators that operate in MeV energy range, which efficiently break up interfering molecules (*e.g.*, $^{88}Sr^{1}H_2$) and; (iv) the high resolving power for ^{88}Sr and ^{90}Sr peaks. Despite all the advantages, the major limitation for ^{90}Sr determination by AMS is the isobaric interference from ^{90}Zr [72, 76, 78]. The interference from ^{90}Zr in environmental samples is inevitable as Zr is usually by more than six-orders of magnitude more abundant than ^{90}Sr [70]. The progress made as part of the present project is discussed in Appendix B.

The present chapter has described the basic chemistry of Sr and of the ^{90}Sr daughter, ^{90}Y. Also, the environmental occurrence of ^{90}Sr and established techniques for the separation of ^{90}Sr and ^{90}Y have been discussed, and the analytical techniques described. These discussions represent the underpinning theory and practice used on the experimental work of the present dissertation.

Chapter 3: Field Sample Collection

The method development work in this dissertation used freshwater (*i.e.*, river water, lake water, and groundwater) and seawater. The freshwater and seawater have vastly diverse chemistry. Also, in the case of freshwater, the difference in dynamics of rivers and lakes, which contributes to dilution or concentration of contaminants, makes these surface waters radiologically variable. Thus, the variability in chemistry and radiochemistry of the water samples, which is important for radioanalytical method development, was captured in this study. In this chapter, background about sample locations and a brief procedure for field sample collection are presented. Quality control in field sample collection is also discussed.

3.1. Sampling Locations

Three surface water bodies of the Chalk River Laboratories (CRL) site of the Canadian Nuclear Laboratories (CNL) that have various documented levels of ^{90}Sr constituted the surface water collection sites for this dissertation. They were the Ottawa River, Lower Bass Lake, and Perch Lake with expected ^{90}Sr concentrations of very low, low, and moderate, respectively. Groundwater samples containing various concentrations of ^{90}Sr were also used. For the field collection of surface water samples, a procedure that was in accordance to the environmental quality guidelines of the Canadian Council of Ministers of the Environment (CCME) [79] and Ontario Ministry of the Environment and Energy (OMEE) [80], which is described in Appendix C, was used. The groundwater samples were collected by the CRL groundwater monitoring personnel using CRL internal procedures, the detail of which is not discussed in this dissertation.

3.1.1. Ottawa River

The Ottawa River is the main body of water in CRL site, which has received small and authorized radiological releases as a result of CRL operations (from reactors: National Research Universal and National Research Experimental) for more than 60 years [81]. The releases made to the Ottawa River are measured as part of the environmental routine monitoring and are well below the regulatory limits. The highest ^{90}Sr concentrations observed in the Ottawa River was from global fallout in 1960s. Figure 15 shows temporal decreases in the concentrations of ^{90}Sr in the water of the Ottawa River [82]. Present concentrations of ^{90}Sr in Ottawa River are at ~ 0.1 % of drinking water MAC for ^{90}Sr (*i.e.*, 5 $Bq{\cdot}L^{-1}$) as per the Canadian guidelines for drinking water quality [14]. Such low levels of ^{90}Sr make accurate detection of ^{90}Sr very difficult.

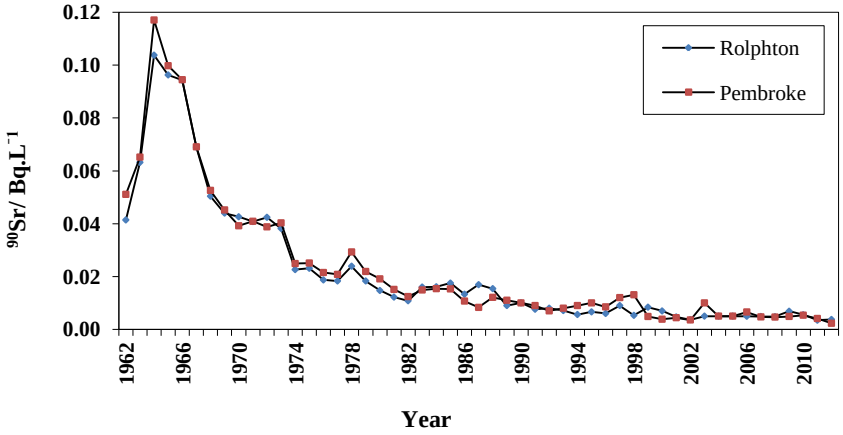

Figure 15. Annual mean concentrations of ^{90}Sr in the water of the Ottawa River upstream (Rolphton) and a downstream (Pembroke) of CRL from 1962-2012 [82]

For the application of methodologies in this dissertation, a total of 11 grab water samples including duplicates were collected from the Ottawa River using the procedure in Appendix C. A map of the sampling locations is shown in Figure 16.

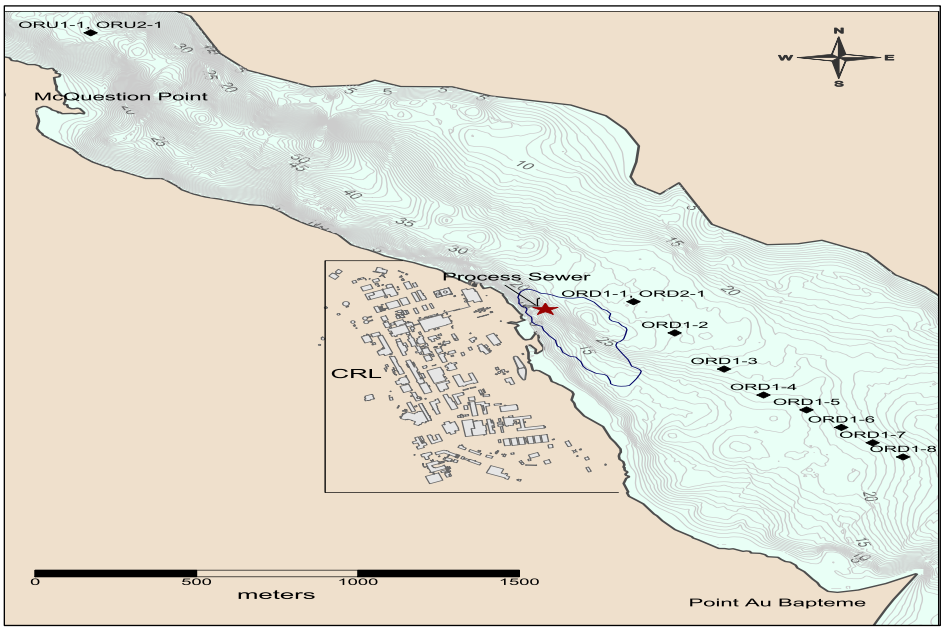

Figure 16. Map of sample locations collected from the Ottawa River

Two samples were collected from approximately 2 km upstream of CRL as a reference location that is expected to be free of CRL potential impacts. The remainder of the nine samples were collected from downstream of CRL discharge zone (indicated by a red star in Figure 16) with sampling location at approximately 100 m distance apart. The sampling points and number of samples are believed to be indicative of a representative set of samples from the Ottawa River at approximately 1.5 km downstream of discharge zone. Also, the number of samples that were collected is considered large enough to produce quality data from statistics point of view. Water samples were collected in new and clean 4-L polyethylene jugs, which were labelled with sample location identification, date, and time of sample collection. Sample identification codes and dates are shown in Table 3.

Table 3. List of freshwater samples collected from the CRL site

Sample code	Collection date	Sample code	Collection date
Ottawa River		Groundwater	
ORU1-1	July 15, 2013	B-WS	Oct. 3, 2013
ORU2-1(Dup)[(1)]	July 15, 2013	C-264	Oct. 24, 2013
ORD1-1	July 15, 2013	610-35	Nov.1, 2013
ORD1-2(Dup)	July 15, 2013	610-36	Nov. 2, 2013
ORD1-2	July 15, 2013	AA-98A	Oct. 22, 2013
ORD1-3	July 15, 2013	C-112	Oct. 9, 2013
ORD1-4	July 15, 2013	AA-69B	Oct. 15, 2013
ORD1-5	July 15, 2013	AA-69C	Oct. 15, 2013
ORD1-6	July 15, 2013	AA-71B	Oct. 15, 2013
ORD1-7	July 15, 2013	AA-68	Oct. 16, 2013
ORD1-8	July 15, 2013	LDA-21	Oct. 11, 2013
		LDA-24	Oct. 9, 2013
Perch Lake		Lower Bass Lake	
PL1-1	July 16, 2013	LBL1-1	July 17, 2013
PL1-2	July 16, 2013	LBL1-2	July 17, 2013
PL1-3	July 16, 2013	LBL1-3	July 17, 2013
PL2-3(Dup)	July 16, 2013	LBL2-3(Dup)	July 17, 2013
PL1-4	July 16, 2013	LBL1-4	July 17, 2013
PL1-5	July 16, 2013	LBL1-5	July 17, 2013
PL1-6	July 16, 2013	LBL2-5(Dup)	July 17, 2013
PL1-7	July 16, 2013	LBL1-6	July 17, 2013
PL1-8	July 16, 2013	LBL1-7	July 17, 2013
PL2-8(Dup)	July 16, 2013	LBL1-8	July 17, 2013

[(1)] (Dup)= Field duplicate sample

3.1.2. Perch Lake

Perch Lake is one of the small lakes on CRL property with an area of ~ 0.45 km^2, maximum depth of 4 m and an average depth of ~ 2 m. Perch Lake water contains significant amounts of humic and fulvic acids, which give the lake water a brownish colour. Perch Lake has received inputs of radionuclides, including ^{90}Sr over the past 50 years from upstream waste management areas as well as through atmospheric deposition [83, 84]. The radionuclides enter Perch Lake via Inlet 1 and Inlet 2 in Figure 17 and give Perch Lake water above background concentrations.

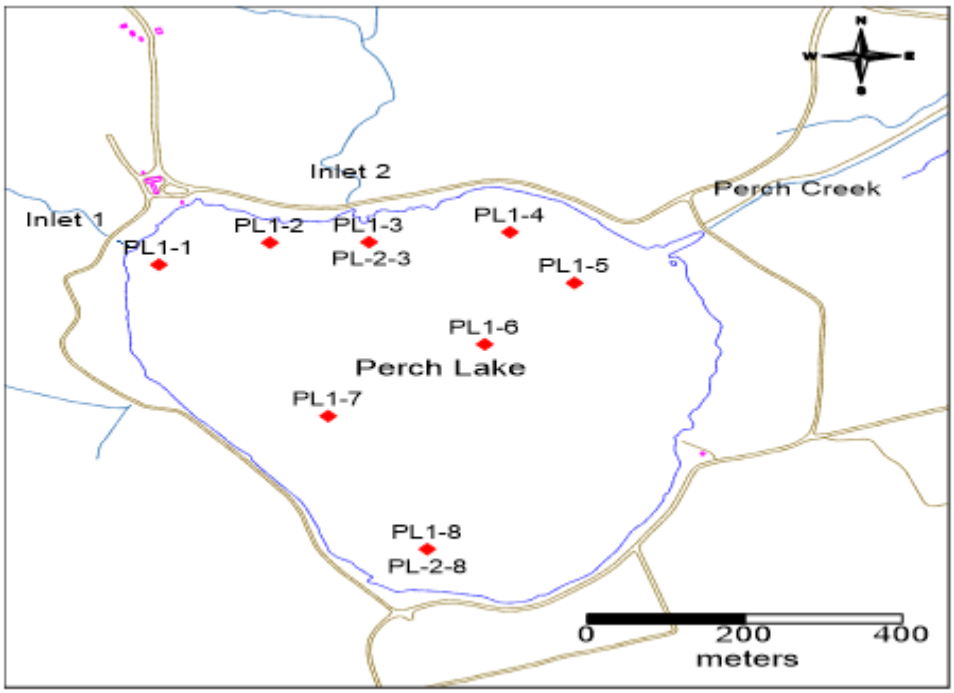

Figure 17. Map of sample locations collected from Perch Lake

The above background concentrations of ^{90}Sr in Perch Lake provide a unique natural laboratory for reseach. Therefore, Perch Lake constitutes an important location for the purpose of ^{90}Sr method development in this research dissertation. A total of 10 grab samples including duplicates were collected using the procedure in Appendix C. Sampling locations are shown in Figure 17. The samples were collected around the parameter and centre of the lake with focus on the northern part where Inlets 1 and Inlet 2 and the outlet are located. The sampling locations and number of samples are believed to be indicative of a representative set of samples collected from Perch Lake. Water samples were collected in new and clean

4-L polyethylene jugs, which were labelled with sample location identification, date, and time of sample collection. Sample identification codes and dates are shown in Table 3.

3.1.3. Lower Bass Lake

Lower Bass Lake is a relatively small and shallow lake on CRL land. Similar to Perch Lake, Lower Bass Lake has received elevated concentrations of ^{90}Sr from underlying contaminated groundwater from historical waste disposal incidents on land that has made its way to underlying aquifers. A passive groundwater treatment facility has successfully reduced ^{90}Sr concentrations of the groundwater flowing into the Lower Bass Lake [85]. Therefore, the lake has low documented concentrations of ^{90}Sr and, thus, is suitable for the application of low level ^{90}Sr methodology developed in this dissertation. A total of 10 grab samples including duplicates were collected using the procedure in Appendix C. The samples were collected around the parameter and centre of the lake, Figure 18. Water samples were collected in new and clean 4-L polyethylene jugs, which were labelled with sample location identification, date, and time of sample collection. Sample identification codes and dates are shown in Table 3.

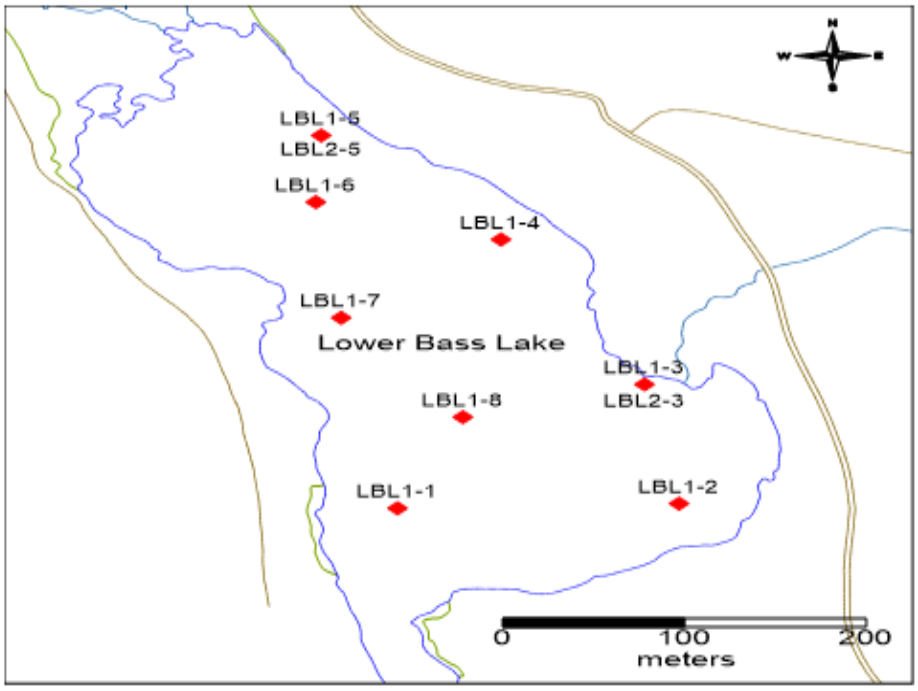

Figure 18. Map of sample locations collected from the Lower Bass Lake

3.1.4. CRL Groundwater

Comprehensive networks of groundwater monitoring wells are located throughout the CRL site. The wells provide water for monitoring of groundwater radiological contaminants originating mainly from waste management and historical incidents on land of CRL site. A selected number of wells from different locations of the CRL site, which have a wide range of ^{90}Sr radioactivity, are used for the application of ^{90}Sr methods. In particular, the high ^{90}Sr concentrations are useful for the application of the TDCR Čerenkov counting screening technique because the surface water and seawater samples used in this research study are not expected to be sufficiently high to meet the detection sensitivity of the method. The collection of CRL groundwater samples was performed by the CRL groundwater monitoring personnel using internal field collection procedures that incorporate the requirements of the Canadian environmental quality guidelines [79, 80]. Twelve groundwater samples of 1 L volume were provided for this research study.

In total, 43 water samples were collected from the CRL site, including surface water, groundwater, and field duplicate samples. Sample identification codes and dates are shown in Table 3.

3.1.5. Seawater

Seawater samples were collected from the North Pacific Ocean at Esquimalt, British Columbia, Canada. The selection of this location for seawater method development was based on the accessibility and ease of obtaining seawater samples. Approximately 20 L of seawater was grabbed in May 2014. The seawater was used for method development in this study.

3.2. Quality Control in Field Sample Collection

A number of quality assurance tools were in place as part of CNL internal QA program to assess the quality of water sampling protocol. Standardized sample collection procedures, chain of custody, and equipment calibration procedures were in accordance to the environmental quality guidelines of the CCME [79], OMEE [80], and Environmental Protection Agency (EPA) [86].

Both blank and duplicate samples were used. The duplicate sample was one of two samples collected at a sampling point at the same time and manner as the sample. The purpose of collecting duplicate samples is to see whether representative samples have been collected from the field and to test the reproducibility of results. As Table 3 indicates, roughly one duplicate sample for every 8-10 samples was collected, which was in accordance with the guidelines requirements of a minimum of 10 % of total sample [79].

The purpose of blank samples was to test for potential contamination of the sample containers, filtering equipment or any other equipment that was used in sample collection, handling, and transportation. The two types of blank samples that were used at the time of sample collection included trip blanks and field blanks, which were prepared in the laboratory from deionized water. Trip blanks were taken to the sampling site and then back to the laboratory without ever being opened. The trip blanks can indicate possible contamination within the bottle. Field blanks, on the other hand, were opened and were subjected to the handling stages such as measurements of pH and electric conductance. Thus, filed blanks were in place to measure possible contamination from the sample collection method, the atmosphere, preservatives, and sample handling methods.

In addition to blank and duplicates, the following practices also ensured the quality of field sample collection:

- A new and clean container was used for each individual sample;
- Prior to filling the container, it was rinsed three times with the sample water in order to remove any plasticizer used in the production of the bottle;
- The sample containers were labelled with a unique sample location identification and date and time of collection at the field site immediately after collection;
- The sample was scanned for any suspended particles, unusual odour or colour;
- The sample bottles were capped at all times and kept cold in a chilled cooler with ice-packs and shipped to the laboratory;
- The samples were collected from various locations of the water body so that a representative set of samples were obtained from the field; and
- The number of samples that were collected was considered large enough to produce quality data from the statistical point of view.

The samples collected were used for the method development and application that are discussed in the next chapter.

Chapter 4: Experimental Design

In this chapter, first non-radiological experimental analyses are discussed. Then, the experimental design for the development of ^{90}Sr-^{90}Y determination methodologies is described.

4.1. Chemical Characterization of Water Samples

Natural samples are likely to contain chemical constituents that interfere with radioanalytical processes such as purification and radiochemical separation of ^{90}Sr from the matrix, therefore, knowledge of the water chemistry was deemed important in this dissertation. Basic characterization (*i.e.*, pH and electric conductance) of water samples was achieved using laboratory standard instrumentation. Characterization of dissolved parameters was performed using specialized techniques and instrumentation, which are introduced in the next section.

4.1.1. Instrumentation/ Techniques

In this section, two fundamental instrumentations are introduced. The first one is the Inductively Coupled Plasma-Mass Spectrometry (ICP-MS), which was used to quantify dissolved metals of the water samples. The second specialized instrument is the Ion Chromatography (IC), which was used to determine the anion concentrations of the water samples.

4.1.1.1. Inductively Coupled Plasma-Mass Spectrometry

The ICP-MS is a technique generally designed for the analysis of dissolved metal constituents in aqueous solutions. The ICP-MS has large analytical capability and superior detection limits, typically in the range of $\mu g \cdot L^{-1}$ to $ng \cdot L^{-1}$ for minor and trace elements, depending on elemental sensitivity and matrix effects. The detection limit is "*the constituent concentration that when processed through the complete method produces a signal with a 99 % probability that it is different from the blank*" [80]. It is the sensitivity of the ICP-MS that makes it a superior method over other methods such as IC for quantification of minute concentrations of dissolved metals in solutions. In addition to superior sensitivity, ICP-MS is capable of rapid multi-element analysis, typically 2-6 minutes per sample.

In general, in the ICP-MS technique, the sample solution is injected in the instrument via a spray chamber that converts the liquid sample into an aerosol. The sample then reaches a high-energy argon plasma source where ionization of atoms takes place [87]. Once the ions are formed, the positively charged ion beams are extracted from the plasma through a differentially pumped vacuum interface and are separated on the basis of their mass-to-charge ratio, $m \cdot z^{-1}$ [87]. Separated ions

are then detected by an electron multiplier or Faraday detector and the ion information processed by a data handling system.

There are many versions of ICP-MS commercially available for various applications. In this dissertation, a Sector Field-ICP-MS with high resolution capability (ELEMENT-XR, Thermo Electron Corp., Bremen, Germany) was used for chemical characterization of water samples as well as for chemical yield determination. Sector Field-ICP-MS uses both magnetic and electrostatic analyzers for mass separation of ions. Magnetic sector is dispersive with respect to mass and energy (*i.e.*, momentum) whereas electrostatic sector is dispersive with respect to energy only [88]. Thus, optimal separation of ions and very low detection limits are achievable by ELEMENT-XR ICP-MS.

4.1.1.2. Ion Chromatography

Ion Chromatography (IC) is a quantitative technique for measurement of anions and cations. The main components of an IC system consist of a sample injector, an ion exchange resin packed column, a conductivity detector, and a data collection system. The resin column of the IC system has ion exchange sites, fixed positive charges for separation and analyses of anions and negative charges for cation analysis. When the dissolved ions in a sample solution make contact with the resin, individual ions attach and detach from the resins at different rates depending on their affinity for the active sites of the resin. Eventually, different ions in the solution elute from the column within a narrow time band specific to that of the ion. The conductivity detector measures the change in conductivity of the eluent species as they pass through the detector. Before running a sample, the ion chromatography system is calibrated using a standard solution. By comparing the data obtained from a sample to that obtained from the known standard, sample ions can be identified and quantified based on their retention times.

Although IC can be used for the determination of both anions and cations, in this dissertation anions were analyzed by IC and cations were analyzed by ICP-MS. A DIONEX ICS1500 (Thermo Scientific Inc., Mississauga, Ontario, Canada) system was used for the determination of anions in this dissertation.

4.1.2. Sample Preparation and Chemical Analysis

After field samples were collected as described in Chapter 3, the samples were taken to the laboratory where they were prepared for various non-radiological and radiological analyses. For those samples where pH and conductivity measurements were not taken in-situ, the measurements were conducted in the laboratory using CRL internal standard procedures that were established in accordance to CCME [79], OMEE [80], and EPA [86] for laboratory measurement of environmental samples as described in Appendix C. In the laboratory, a sub-sample was separated

in a 125-mL polyethylene plastic bottle and measured for pH and specific conductance. The pH and specific conductance measurements were taken on a non-filtered sub-sample. The remainder of the sample was filtered through a 0.45 µm cellulose acetate membrane. This filter porosity is commonly used to separate particulate and dissolved matter. The filtrate was used for chemical and radiological analyses. Sub-samples of filtrate were separated in pre-labelled bottles for each of the chemical analyses of dissolved metals, anions, and dissolved carbon. The remainder of the filtrate was collected in a 2-L high density polyethylene bottles for ^{90}Sr method development. The filtrate was acidified with concentrated HCl solution to 1 % by volume, which adjusted the pH of the filtrate to < 2. The sample bottles were then stored in a fridge with temperature ~ 5˚C until further analysis. The procedures for taking measurements of pH and specific conductance, filtration, and preservation of samples are described in Appendix C.

For Perch Lake water, because of its high suspended particles two to four filter membranes were used per 4 L of the sample filtered. The colour of Perch Lake water was brownish due to the presence of humic and fulvic organic acids contents.

The dissolved metals in water samples were analysed by an ICP-MS ELEMENT-XR in the ICP-MS laboratory of CRL. The method used was in line with the international quality control guidelines as per ISO/IEC 17025, which delineates competency of the laboratory for accuracy and consistency of test results and calibration [89]. The detection limits of the ICP-MS ELEMENT-XR for a number of dissolved parameters is shown in Table 4.

Table 4. Detection limits for the dissolved metals analyzed by Element-XR ICP-MS

Element	MDC /mg·L^{-1}	Element	MDC /mg·L^{-1}
Al	1.00E-03	Mg	1.00E-03
As	5.00E-04	Mn	1.00E-04
B	1.00E-03	Ni	1.00E-04
Ba	5.00E-05	Pb	5.00E-05
Cd	5.00E-05	Rb	2.00E-04
Co	5.00E-05	Sr	5.00E-05
Cr	5.00E-04	Th	2.00E-04
Cs	5.00E-05	U	5.00E-05
Cu	1.00E-04	V	1.00E-04
Fe	1.00E-03	Zn	1.00E-03
La	5.00E-05	Zr	5.00E-05

Dissolved anions were measured in the environmental laboratory of CRL by a DIONEX ICS1500 ion chromatography system as per CRL internal procedure based on EPA method, EPA 300.1 [90]. There is a rigorous quality control process in place in the environmental laboratory of CRL for the analysis of anions by the

DIONEX ICS1500. Instrument calibration and calibration verifications were determined using traceable reference standards. Instrument calibration is performed quarterly and calibration verifications prior to the sample run. The common anions that were determined in water samples were: fluoride (F^-), chloride (Cl^-), bromide (Br^-), sulphate (SO_4^{2-}), and phosphate (PO_4^{3-}). Detection limits of the DIONEX ICS1500 are tabulated in Table 5.

Table 5. Detection limits for anions analyzed by DIONEX ICS1500 Ion Chromatography system

Anion	MDC /mg·L^{-1}
Fl^-	3.00E-02
Cl^-	1.12E-01
Br^-	1.23E-01
PO_4^{3-}	1.79E-01
SO_4^{2-}	1.05E-01

Besides, dissolved metals and anions, dissolved carbon were also determined in the water samples. The dissolved organic carbon (DOC) and dissolved inorganic carbon (DIC) contents were measured as per CRL internal standard method incorporating CCME [79],OMEE [80], and EPA [86]) guidelines for laboratory measurement of environmental samples. The method uses photochemical oxidation by Ultra Violet Persulfate digestion followed by infrared detection using Fusion Carbon Analyzer (Teledyne Tekmar Inc., Mason, Ohaio, U. S. A.) [91]. The instrument is calibrated quarterly using traceable standard solutions for organic and inorganic carbons. The MDC for each of DOC and DIC was 0.05 mg·L^{-1}.

4.2. Methodologies for Determination of Strontium-90

The methodologies developed within this dissertation include a rapid screening technique using Čerenkov counting of ^{90}Y and direct determination of ^{90}Sr using radiochemical purifications followed by liquid scintillation counting techniques. The ^{90}Y and ^{90}Sr measurements were obtained using a low background Hidex liquid scintillation counter (LSC). Γ spectrometry using a high purity germanium (HPGe) detector was also used to measure ^{85}Sr and ^{88}Y, which were the radiotracers for seawater method development. Within this section, first the specialized instrumentation and then the experimental approach to method development of ^{90}Sr are presented.

4.2.1. Specialized Instrumentation

4.2.1.1. Hidex Liquid Scintillation Counter

The radiometric detection of ^{90}Sr and ^{90}Y in this research was obtained by a commercially available triple-to-double coincidence ratio (TDCR) LSC, Hidex 300SL (Hidex Oy, Turku, Finland). The analysis results were reported by MikroWin 2000 software. A Photo of the Hidex 300SL LSC is shown in Appendix A. The detector assembly consists of three photo-multiplier tubes (PMT) with highly reflective measurement chamber design. The arrangement of the three PMTs at 120^{o} angular separation provides optimal measurement geometry and facilitates TDCR counting. The detector chamber is equipped with an automatic adapter from 20-mL to 7-mL vial capacity, which allows for additional counting geometries. The shielding assembly consists of a 7 cm lead shielding in all directions, which enables reduction of background[(2)] effects.

Unlike the conventional double coincidence counting techniques the Hidex LSC uses a TDCR counting method that is made possible by its three PMTs. In the TDCR technique, the triple and double coincidences are measured and the ratio of these coincidences calculated. In general, TDCR is directly proportional to counting efficiency. The relationship between the TDCR and the counting efficiency under different experimental conditions can be used to develop a common expression for correcting the counting efficiency of the radionuclide. This approach was used to develop a TDCR Čerenkov counting technique for the determination of ^{90}Y under various experimental conditions (see Section 4.2.2.1).

For the purpose of ^{90}Sr-^{90}Y detection in this research study, the default energy regions of interest (ROI) were determined using a traceable ^{90}Sr-^{90}Y standard solution counted on the low background Hidex LSC. For the Čerenkov counting of ^{90}Y, the ROI where the ^{90}Y Čerenkov emission was prominent, was found to be channels 50-350 (Figure 19) where the ^{90}Y Čerenkov counting efficiency was found to be ~ 68 %.

For pure β^- emitting radionuclides, for example, ^{90}Sr, ^{90}Y, and ^{32}P, that are counted in liquid scintillation cocktail, the proportionality factor between TDCR and the counting efficiency is 100±15 % [92]. For the liquid scintillation assay (LSA) of ^{90}Sr and ^{90}Y, the ROI where the β^- emission spectra were prominent, was found to be channels 100-800, Figure 19. In this ROI, counting efficiencies of ^{90}Sr and ^{90}Y measured by LSA were ~ 94 %.

[(2)] Background is defined to be ambient signal response recorded by measurement instruments that is independent of radioactivity contributed by the radionuclides being measured in the sample [93].

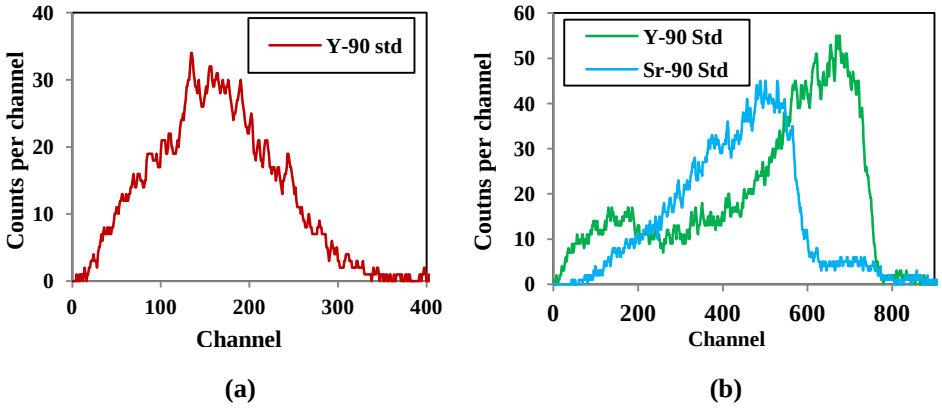

Figure 19. Spectra indicating counting regions of low background Hidex LSC for ^{90}Y Čerenkov emission measured in aqueous solution (a) and ^{90}Y and ^{90}Sr measured in liquid scintillation cocktail solution (b)

4.2.1.2. Gamma Spectroscopy Theory and Application

The γ spectrometer used in this dissertation was a coaxial high purity germanium (HPGe) detector system (Ortec, Oak Ridge, TN, U. S. A.) with 25 % relative efficiency at γ ray energy 1.332 MeV of ^{60}Co. The spectra were analyzed with MAESTRO-32 software. The HPGe detectors are well known for their high resolution capabilities. They are solid state radiation detectors with a high purity Ge being the semiconductor material of detector crystal. The HPGe detectors are built in planar and cylindrical or coaxial configurations. In general, the coaxial configuration is preferred over planar because the coaxial configuration allows for larger detector volumes and, therefore, can incorporate more of the crystal volume into a single finished detector [57]. This is important in the view of the mode of interaction of γ ray with matter, which are the Photoelectric Effect, Compton Scattering, and Paired Production. From the γ spectroscopy perspective, Photoelectric Effect is the preferred mechanism of interaction because in this type of interaction, the total energy of the incident γ photon is absorbed. As for the Compton Scattering and Pair Production, a portion of the energy escapes from the detector volume without being absorbed. As such, the background rate in the spectrum increases. Based on their γ energies, ^{85}Sr with γ energy of 0.514 MeV interacts by Compton Scattering. The ^{88}Y with two γ emissions at 0.898 MeV and 1.836 MeV interacts by both Compton Scattering and Pair Production mechanisms.

The most important factors for accurate γ spectroscopy are the energy and efficiency calibrations for energies of interest. An energy calibration curve can be established using several calibration sources. For efficiency calibration, commercially available point source standards are available. However, the γ

photon's self-absorption within the sample material itself can happen, for instance, when sample has high density, it will absorb too much γ energy compare to low density sample and this will result in lowering the counting efficiency. Therefore, the geometry of the standard used for efficiency calibration needs to match that of the unknown samples to be identified. In this dissertation, peak efficiency calibration for the geometries, in which ^{88}Y and ^{85}Sr were measured by the HPGe γ spectrometer, is described in Appendix D.

4.2.1.3. Ultraviolet-Visible Spectrophotometer

The Ultraviolet-Visible (UV-Vis) spectrophotometry is an analytical technique for quantitative determination of analyte in solutions based on the capability of the analyte to absorb (or emit) electromagnetic radiation in the range of UV-Vis (*i.e.,* ~ 190-700 nm). A UV-Vis spectrophotometer can measure the absorption of the photons of light from a light source by measuring the final intensity of light (I_1) passing through the solution and comparing it to the initial intensity of light (I_0) before it passes through the solution. Thus, absorbance at a particular wavelength of light can be quantitatively measured using Beer- Lambert Law, Eq. (10), [31]. As the concentrations of the analyte increase and the colour of the solution becomes more intense, the amount of light absorbed by the solution increases resulting in lesser light output for measurement by the UV-Vis spectrophotometer.

$$Absorbance = -\ln\left(\frac{I_1}{I_0}\right) \tag{10}$$

The main components of a spectrophotometer are a light source, a chamber for holding the cuvette with liquid sample in it, a monochromator to separate the different wavelengths of light, and a detector. The spectrophotometer used in this research dissertation was a Spectronic 200^{TM} UV-Vis spectrophotometer (Thermo Fisher Scientific, Ottawa, Ontario, Canada) equipped with PiQue^{TM} software. The Spectronic 200^{TM} uses a tungsten-halogen lamp for light source and a charged-coupled device detector.

4.2.2. Experimental Approach

The experimental procedure of the method development for the determination of ^{90}Sr is presented in this section. All references to deionized water indicate pure water obtained from Millipore Direct-Q5^{TM} (Fisher Scientific Inc., Ottawa, Ontario, Canada) water purification system (water resistively of 18.2 MΩ·cm at 25˚C). All reagents used in this study were of analytical grade. All radioisotope standard reference solutions were procured from Eckert and Ziegler Isotope Products (Valencia, CA, U. S. A.). Procurement details of chemical and radiological standards and other laboratory material can be found in Appendix E.

In this section, first the experimental approach to the indirect determination of ^{90}Sr from ^{90}Y using the TDCR Čerenkov counting screening technique for both freshwater and seawater matrices is presented. Then, the methods for radiochemical separation of ^{90}Sr-^{90}Y in freshwater and seawater followed by their liquid scintillation counting are described.

4.2.2.1. TDCR Čerenkov Counting Technique

The procedure for the TDCR Čerenkov counting technique is broken down into three sub-sections to cover the development of the technique and its application on freshwater and seawater. All test measurements were obtained using a low background Hidex LSC.

4.2.2.1.1. Development of TDCR Čerenkov Counting in Freshwater

First, the effect of counting geometry (*i.e.*, sample volume and counting vial type/ size) on the TDCR Čerenkov counting of ^{90}Y was examined. Deionized water, which was acidified using HCl to make up 0.1 M HCl solution, was used as sample matrix. The diluted acidic solution was preferred over deionized water for this test in order to prevent the uptake of the radionuclides by the counting vial. The procedure for making 0.1 M HCl solution from deionized water is described in Appendix F.

Using the 0.1 M HCl solution, the first two sets of samples were prepared in polyethylene plastic scintillation counting vials (PV) of 7-mL and 20-mL capacity. The procedure is described in Appendix G. For each of the vials, varying solution volumes of the 0.1 M HCl were tested. The volumes tested for the 7-mL plastic vials were: 1, 3, 5, and 7 mL. The volumes tested in the 20-mL plastic vials were: 3, 5, 7, 10, 13, 15, 18, and 20 mL. For each volume tested, the samples were prepared in duplicates. Sample information is shown in Table 6. The second two sets of 7-mL and 20-mL vials were prepared in low-potassium borosilicate glass scintillation vials (GV) to compare the effects of vial type on the TDCR Čerenkov counting of ^{90}Y. The sample volumes tested in 7-mL glass vials were 1, 3, 5, and 7 mL solutions of 0.1 M HCl. The volumes tested in the 20-mL glass vials were 10, 15, 18, and 20 mL solutions. The samples were spiked with a known amount (9-10 Bq) of a traceable standard solution of ^{90}Sr-^{90}Y. Duplicate samples were not prepared in glass vials. Blank samples for each of the vials and volume compositions were also prepared using varying volumes of 0.1 M HCl solution.

In order to examine if variation in acid type can influence the TDCR Čerenkov counting of ^{90}Y, an additional set of samples were prepared using 0.1 M HNO_3 solution which was also prepared using deionized water (Appendix F). The geometries using 0.1 M HNO_3 solution consisted of 7-mL vials with volumes of 1,

3, 5, and 7 mL. The samples were prepared in duplicates and corresponding blank samples using 0.1 M HNO_3 were also prepared (Appendix G).

Table 6. Samples prepared for evaluation of effects of variation of sample geometry on the TDCR Čerenkov counting of ^{90}Y. Samples were prepared in plastic vials (PV) and glass vials (GV).

Sample code	Vial size, type	Acid	Vol /mL	A_{ia}[(3)] ^{90}Sr-^{90}Y/ Bq	
				Sample	Duplicate
SrCT3-1	7-mL PV	HCl	1	9.28	9.35
SrCT3-2	7-mL PV	HCl	3	9.33	9.32
SrCT3-3	7-mL PV	HCl	5	9.33	9.23
SrCT3-4	7-mL PV	HCl	7	9.30	9.30
SrCT4-1	20-mL PV	HCl	3	9.33	9.35
SrCT4-2	20-mL PV	HCl	5	9.30	9.35
SrCT4-3	20-mL PV	HCl	7	9.35	9.35
SrCT4-4	20-mL PV	HCl	10	9.36	9.34
SrCT4-5	20-mL PV	HCl	13	9.35	9.33
SrCT4-6	20-mL PV	HCl	15	9.43	9.35
SrCT4-7	20-mL PV	HCl	18	9.32	9.31
SrCT4-8	20-mL PV	HCl	20	9.35	9.33
SrCT5-1	7-mL PV	HNO_3	1	9.33	9.31
SrCT5-2	7-mL PV	HNO_3	3	9.33	9.32
SrCT5-3	7-mL PV	HNO_3	5	9.33	9.30
SrCT5-4	7-mL PV	HNO_3	7	9.29	9.27
SrCT7-1	7-mL GV	HCl	3	9.29	-
SrCT7-2	7-mL GV	HCl	5	9.25	-
SrCT7-3	7-mL GV	HCl	7	9.29	-
SrCT8-1	20-mL GV	HCl	10	9.25	-
SrCT8-2	20-mL GV	HCl	15	9.29	-
SrCT8-3	20-mL GV	HCl	18	9.30	-
SrCT8-4	20-mL GV	HCl	20	9.25	-

To investigate the effect of colour quenching on the TDCR Čerenkov counting technique, a series of quenched samples were prepared in 15 mL deionized water using yellow and brown food-grade dyes for colour quenching. Refer to Appendix G for sample preparation details and Table 7 for sample information. The sample volume of 15 mL was selected for the colour quenching experiment. The brown dye was prepared in the laboratory by mixing red, green, and yellow food-grade

[(3)] A_{ia} = Activity added

dyes in proportions of 1:1:3, respectively. Two sets of plastic vials for each of the yellow and brown dyes and one set of glass vials using yellow dye were prepared by adding increasing drops, equivalent to ~ 0.1 mL increments, of the food-grade dyes. A small amount of the sample from each vial was tested for maximum light absorption, which was quantified on the UV-Vis spectrophotometer. The instrument was calibrated for zero absorption and 100 % transmission using deionized water sample in a quartz cuvette. Subsequently, samples containing various amounts of yellow and brown dye solutions were scanned over the visible light continuous spectrum and a spectrum of absorbance obtained. An initial measurement of the sample vials was obtained on the Hidex LSC. Subsequently, the vials were spiked with a known amount (8-10 Bq) of ^{90}Sr-^{90}Y standard solution and recounted. The blank samples consisted of unquenched deionized water spiked with ^{90}Sr-^{90}Y (8-10 Bq) and were used for background subtraction.

Table 7. Sample prepared for evaluation of colour quenching on the TDCR Čerenkov counting of ^{90}Y

Sample Cod	Sample Description	Dye /mL	A_{ia} ^{90}Sr-^{90}Y /Bq
SrCT11-Blk	20 PV, Blank	0	8.79
SrCT11-1	20 PV, Yellow	0.1	8.89
SrCT11-2	20 PV, Yellow	0.2	8.81
SrCT11-3	20 PV, Yellow	0.3	8.83
SrCT11-4	20 PV, Yellow	0.4	8.88
SrCT11-5	20 PV, Yellow	0.5	8.86
SrCT11-6	20 PV, Yellow	0.6	8.87
SrCT11-7	20 PV, Yellow	0.7	8.86
SrCT11-8	20 PV, Yellow	0.8	8.85
SrCT11-Blk	20 PV, Blank	0	8.79
SrCT12-1	20 PV, Brown	0.1	8.85
SrCT12-2	20 PV, Brown	0.2	8.85
SrCT12-3	20 PV, Brown	0.3	8.84
SrCT12-4	20 PV, Brown	0.4	8.86
SrCT12-5	20 PV, Brown	0.5	8.84
SrCT12-6	20 PV, Brown	0.6	8.85
SrCT12-7	20 PV, Brown	0.7	8.87
SrCT12-8	20 PV, Brown	0.8	8.87
SrCT13-1	20 GV, Blank	0	8.77
SrCT13-2	20 GV, Brown	0.1	8.75
SrCT13-3	20 GV, Brown	0.2	8.78
SrCT13-4	20 GV, Brown	0.3	8.73
SrCT13-5	20 GV, Brown	0.4	8.81
SrCT13-6	20 GV, Brown	0.5	8.80

Another experimental condition evaluated as part of the method development, was to delineate the effects of different radionuclides on TDCR Čerenkov counting of ^{90}Y. Appendix G describes sample preparation details and Table 8 shows sample information for the test of effect of other radionuclides on ^{90}Y TDCR Čerenkov counting.

Table 8. Samples prepared for evaluation of effects of other radionuclides on the TDCR Čerenkov counting of ^{90}Y

Radionuclide	A_{ia} ^{90}Sr-^{90}Y/Bq	
	20-mL PV	20-mL GV
^{90}Sr-^{90}Y	9.25	13.2
^{90}Sr-^{90}Y Dup	8.89	13.2
^{89}Sr	9.85	10.2
^{89}Sr Dup	9.88	10.2
^{32}P	13.2	15.0
^{32}P Dup	13.2	13.2
^{210}Pb-^{210}Bi	9.75	9.67
^{210}Pb-^{210}Bi Dup	9.86	9.75
^{137}Cs	9.87	9.85
^{137}Cs Dup	9.85	9.87
^{60}Co	11.6	11.1
^{60}Co Dup	12.1	10.7
^{40}K	24.3	8.26
^{40}K Dup	23.7	16.7

Single radionuclide-containing samples were prepared using 15 mL of 0.1 M HCl in 20-mL plastic and glass scintillation counting vials. Besides ^{90}Y, pure β^- emitting radionuclides tested were ^{32}P, ^{89}Sr,^{210}Bi (in equilibrium with ^{210}Pb) as well as mixed β^--γ emitting radionuclides including: ^{60}Co,^{137}Cs, and ^{40}K. The ^{40}K solution was prepared in the laboratory from KCl salt in deionized water and its radioactivity calculated from its natural abundance (0.0117 % [1, 94]) and specific activity (31.72 Bq·g^{-1} [94]). A known amount of the standard reference solutions of the radionuclides were dispensed gravimetrically to the vials. Duplicate samples were prepared for each radionuclide. A blank sample using 15 mL of 0.1 M HCl solution was also prepared. Samples were counted on the Hidex LSC.

4.2.2.1.2. Development of TDCR Čerenkov Counting in Seawater

The development of the TDCR Čerenkov counting of a seawater matrix involved the evaluation of colour quenching effects and the effects of other radionuclides in the matrix on the ^{90}Y TDCR Čerenkov counting. Procedures were comparable with those for freshwater using a 10-11 Bq spike of ^{90}Sr and ^{90}Y in secular equilibrium, Table 9 and 10.

Table 9. Detail of seawater colour quenching test

Sample code[4]	Dye /mL	A_{ia} ^{90}Sr-^{90}Y /Bq	Sample code	Dye /mL	A_{ia} ^{90}Sr-^{90}Y /Bq
SWY-Qnch0	0	11.1	SWY-Qnch3	0.5	10.9
SWY-Qnch1	0.1	11.0	SWY-Qnch4	0.7	11.0
SWY-Qnch2	0.2	11.0	SWY-Qnch5	1.0	11.0

Table 10. Radionuclides tested in 15 mL seawater

Radionuclide	A_{ia} ^{90}Sr-^{90}Y /Bq	Radionuclide	A_{ia} ^{90}Sr-^{90}Y /Bq
^{90}Y	10.9	^{137}Cs	11.8
^{32}P	11.0	^{60}Co	10.3
^{210}Bi	11.6	^{40}K	15.7

4.2.2.1.3. Application of TDCR Čerenkov Counting on Freshwater

After the TDCR Čerenkov counting technique was developed, the application of the method was examined using natural freshwater samples that were obtained from the CRL site. The water samples had a wide range of ^{90}Sr-^{90}Y radioactivity and colour (*e.g.*, green-brownish) in them. A ~ 20 mL from each of the CRL surface water and groundwater samples was pipetted into a 20-mL PV. A blank sample was also prepared using 20 mL deionized for background subtraction.

All samples that were prepared in Section 4.2.2.1 were measured for ^{90}Y Čerenkov emission on a low background Hidex LSC. Counting time was at least 0.5 h so that the 1 sigma (σ) counting error was < 2 %.

4.2.2.2. Radiochemical Separation and Liquid Scintillation Counting

This section describes the experimental approach undertaken to separate ^{90}Sr and ^{90}Y from the matrix. For the freshwater samples, a literature based pre-concentration technique using calcium phosphate, $Ca_3(PO_4)_2$, co-precipitation was used to precipitate ^{90}Sr and ^{90}Y. For the seawater samples, a two-step co-precipitation technique using calcium carbonate, $CaCO_3$, and hydrous titanium oxide (denoted as HTiO) was developed in this dissertation. After they were pre-

[4] In the sample identification codes, for example, SWY-Qnch0, SWY indicates seawater sample spiked with ^{90}Sr-^{90}Y standard. Qnch0 through Qnch 5 mean "colour quenched" seawater with Qnch0 representing non-quenched sample and Qnch5 denoting highest degree of colour quenching.

concentrated, the ^{90}Sr and ^{90}Y were purified using element-selective extraction chromatography (EXC) technique and measured on the low background Hidex LSC. The pre-concentration, purification, and measurement procedures are described in the next sections.

4.2.2.2.1. Pre-concentration of Strontium in Freshwater

One of the most common methods of concentrating trace quantities of an analyte is by co-precipitating it along with a major analyte that is found in the same solution. In this research study, Sr was co-precipitated with Ca. Because Sr is analogous to Ca, therefore, Sr resembles Ca in the co-precipitation step. To ensure that Ca is in excess, often Ca is added to the solution in the co-precipitation step. For the co-precipitation of freshwater, ~ 80 mg of Ca in the form of 1 M $Ca(NO_3)_2$ solution was added to each 1 L water sample.

For the co-precipitation of Sr with Ca in freshwater samples, approximately 1 L samples were processed in 1-L glass beakers. To each sample 1 mg of standard solutions of stable Sr (*i.e.*, ^{88}Sr at 1.0 $mg{\cdot}mL^{-1}$) and stable Y (*i.e.*, ^{89}Y, 1.0 $mg{\cdot}mL^{-1}$) were added for chemical yield determinations. Chemical yield is an estimate of the analyte during analytical processing and is defined as the ratio of the amount of radiotracer or carrier determined in a sample analysis to the amount of radiotracer or carrier originally added to a sample [86]. The chemical yield is used as a correction factor to determine the amount of radionuclide (analyte) originally present in the sample. The Sr and Y stable tracers used in this procedure were determined by ICP-MS. The detail procedure of $Ca_3(PO_4)_2$ co-precipitation is described in Appendix H.

After adding the tracers and mixing well, 1 mL of water from the beaker was removed and used for ICP-MS determination of Sr in the beginning of the procedure. Subsequently, 1 mL of concentrated phosphoric acid (H_3PO_4) was added to each sample. Then, the pH of the solution was raised to 10 using concentrated ammonium hydroxide (NH_4OH) solution, which was added drop-wise while stirring and pH monitored using a pH paper. The $Ca_3(PO_4)_2$ precipitate started forming around pH of 8. The solution was then centrifuged (at 4000 rpm for 5 min), supernatant discarded, and precipitate retained. The final precipitate weighed on average approximately 10 g with a pre-concentration factor of 100 fold. The precipitate was washed (in deionized water) to get rid of unwanted soluble salts, centrifuged, and the precipitate retained. The precipitate was solubilized in 10 mL concentrated HNO_3 and used for column chromatography separation. The flow chart of the procedure is shown in Figure 20.

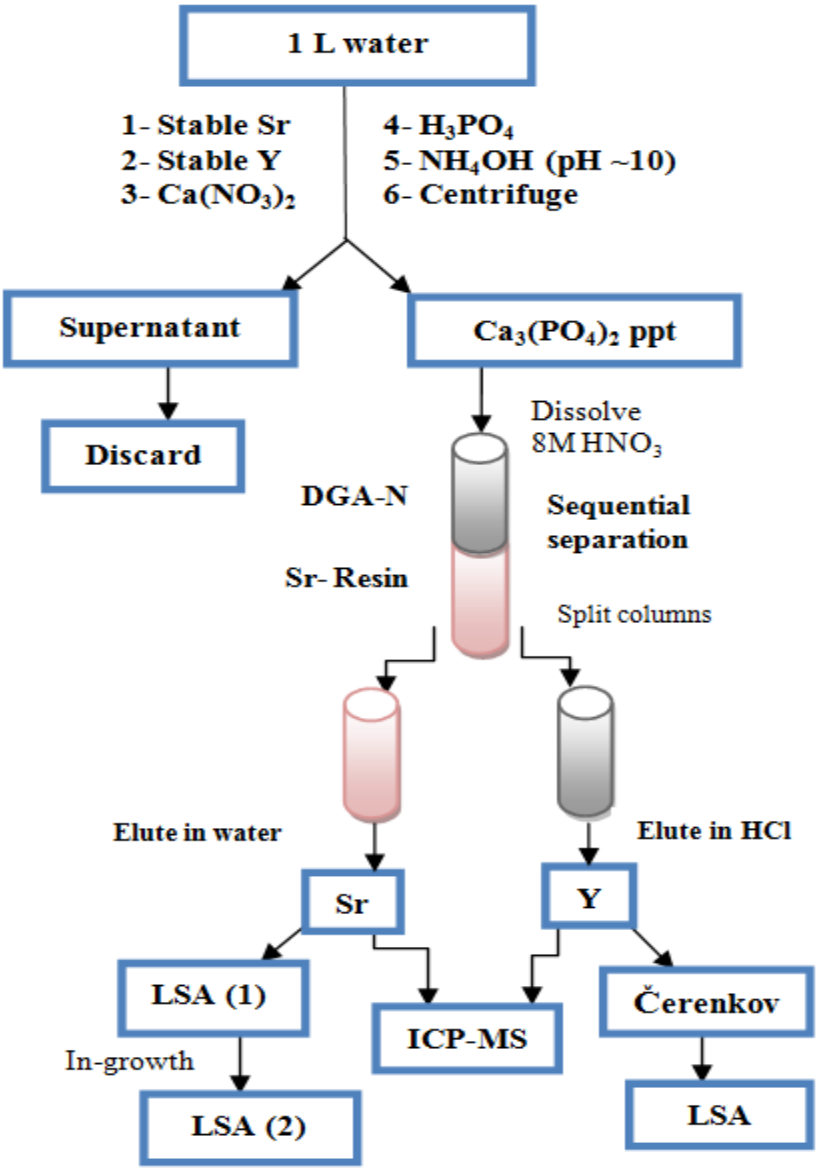

Figure 20. Flow chart of freshwater sample preparation

Twenty five samples of freshwater, which were obtained from the CRL site (see Table 3) were pre-concentrated using the procedure described above. They were: eight samples from Perch Lake, nine samples from Lower Bass Lake, three

samples from Ottawa River, and five groundwater samples. Sample information is presented in Table 11.

Table 11. Natural samples prepared for freshwater column separation method

Sample code	Sr added /mg	Y added /mg	MS_{sample} [5] /g
PL1-1	1.03	1.06	1.00
PL1-3	1.00	1.00	1.00
PL1-3Dup	1.00	1.00	1.00
PL1-5	1.00	1.01	0.990
PL1-6	1.00	1.00	1.00
PL1-7	1.01	1.01	1.00
PL1-8	1.01	1.01	1.01
PL2-8(Dup)	1.01	1.01	0.987
LBL1-1	1.00	1.00	0.996
LBL1-1Dup	1.01	1.01	0.974
LBL1-3	1.01	1.01	1.00
LBL2-3(Dup)	1.01	1.01	0.983
LBL1-4	1.03	1.06	1.00
LBL1-5	1.00	1.00	1.00
LBL1-7	1.01	1.01	0.940
LBL1-7Dup	1.00	1.00	0.989
LBL1-8	1.00	1.00	0.989
B-WS	1.00	1.00	0.989
AA-69B	0.652	0.748	1.21
AA-69C	1.07	1.02	1.00
AA-69C-Dup	0.636	0.732	1.23
AA-71B-Dup	0.665	0.772	1.24

In addition to natural samples, 10 spiked and four procedural blank samples were prepared from 1 L deionized water for method validation using the $Ca_3(PO4)_2$ technique. In Figure 20 for the spiked samples, a known amount of a traceable ^{90}Sr-^{90}Y standard solution and also stable tracers of Sr and Y were added in the initial step of the procedure. Spiked samples consisted of six samples (Spike 1 through Spike 6 in Table 12) for validating the reproducibility of the method, which were spiked at ~ 5 $Bq{\cdot}L^{-1}$ of the ^{90}Sr-^{90}Y standard solution. For the method linearity demonstration, four spiked samples in the range of 0.5-100 $Bq{\cdot}L^{-1}$ were prepared, Table 12.

[5] MS_{sample} = aliquot removed for ICP-MS analysis

Table 12. Spiked and blank samples prepared for validation of freshwater method

Sample code	Sr added /mg	Y added /mg	$[A_{ia}]$ ^{90}Sr-^{90}Y /Bq·L^{-1}	MS_{sample} /g
Spike 1	1.00	1.00	4.36	0.989
Spike 2	1.00	1.00	4.91	0.998
Spike 3	0.70	0.713	5.41	1.24
Spike 4	1.07	1.09	6.49	1.00
Spike 5	1.06	1.07	6.43	0.999
Spike 6	1.06	1.07	6.21	0.852
Spike 7	1.06	1.07	0.753	0.992
Spike 8	1.06	1.07	1.15	1.00
Spike 9	1.01	1.01	24.2	0.996
Spike 10	1.02	1.02	99.5	0.607
Blank 1	1.00	1.00	None	0.989
Blank 2	1.00	1.00	None	0.924
Blank 3	1.00	1.00	None	0.999
Blank 4	0.710	1.10	None	1.00

4.2.2.2.2. Pre-concentration of Yttrium in Seawater

Low level ^{90}Sr-^{90}Y from seawater needs to be pre-concentrated prior to measurement. In this dissertation, seawater ^{90}Sr-^{90}Y was pre-concentrated using a two-step co-precipitation technique. The technique used calcium carbonate, $CaCO_3$, and hydrous titanium oxide, HTiO.

Seawater samples of 1 L were processed in 1-L glass beakers. The samples were spiked with a known amount of ^{90}Sr-^{90}Y standard reference solution at different levels in the range of 0.5-100 Bq·L^{-1}. Each sample was spiked with 1 mg of stable Y carrier (*i.e.*, ^{89}Y) for gravimetric yield option. Additionally, known amounts (10-12 Bq) of each of ^{88}Y and ^{85}Sr were also added for quick radiotracing options by γ spectroscopy in all samples except for 0.5 Bq·L^{-1} samples, which were radiotraced by ^{85}Sr only because ^{88}Y signal would have interfered with low-level ^{90}Y. Stable Sr tracing was also employed in order to monitor separation of Y-Sr at various stages of the method development. For Sr tracing, the intrinsic stable Sr content of seawater in samples was ~ 6 mg·L^{-1}. After addition of the tracers and adequate stirring, 1 mL of water from the beaker was removed and used for ICP-MS determination of stable isotopes in the beginning of the procedure. Subsequently, the samples, which were previously acidified, were adjusted to a pH in the range of 5-6 using concentrated NH_4OH solution. Then, ~ 25 mL of 2.6 M Na_2CO_3 solution was added to each sample, with continuous stirring, and pH adjusted to a pH in the range of 9.5-10 using concentrated NH_4OH solution. The sample was centrifuged in a 500-mL polycarbonate centrifuge tubes at 4000 rpm for 5 min and the supernatant separated. The precipitate was dissolved in 10 mL concentrated HNO_3

solution, transferred into a 20-mL plastic scintillation vial, and counted on a HPGe γ spectrometer for 0.5 h. Subsequently, and aliquot was removed for the stable isotopes analysis by ICP-MS. Then, the sample solution was transferred to a 500-mL beaker and diluted with deionized water to 250 mL. Subsequently, approximately 230 mg of Ti^{3+} as in 20 % titanium trichloride, $TiCl_3$, solution was added to the sample and pH adjusted to 8.0-8.5 using concentrated NH_4OH solution. The HTiO precipitate was formed and separated by centrifuging at 4000 rpm for 5 min. The time was recorded for ^{90}Y decay correction. Subsequently, the precipitate was dissolved in 15 mL concentrated HNO_3 solution, transferred into a 20-mL plastic scintillation vial, and counted on a HPGe γ spectrometer for 0.5 h. Then, from the dissolved precipitate solution, an aliquot was withdrawn for chemical yield determination of stable Y and Sr. The samples were then ready for column separation. The final precipitate weighed on average approximately 9 g giving a pre-concentration factor of more than 110. For co-precipitation procedure details, refer to Appendix H.

A total of 11 seawater spiked and four seawater procedural blanks were prepared. Of the 11 spiked samples, six samples were for validating the reproducibility of the method, which were spiked at ~ 5 $Bq{\cdot}L^{-1}$ of ^{90}Sr-^{90}Y standard solution. The remainder five spiked samples in the range of 0.5-100 $Bq{\cdot}L^{-1}$ of ^{90}Sr-^{90}Y were used for the method linearity performance test. Sample information is shown in Table 13 and the procedure flow chart is shown in Figure 21.

Table 13. Spiked and blank seawater samples prepared for validation of seawater ^{90}Y separation method

Sample code	Y added /g	$[A_{ia}]^{90}Sr$-^{90}Y /$Bq{\cdot}L^{-1}$	^{88}Y tracer /$Bq{\cdot}L^{-1}$	^{85}Sr tracer /$Bq{\cdot}L^{-1}$	Ti^{3+} /mg
SWY-1	1.07	5.02	12.6	11.4	211
SWY-2	1.06	4.95	12.8	11.7	229
SWY-3	1.07	5.00	12.8	11.7	228
SWY-4	1.07	5.98	12.6	10.9	232
SWY-5	1.02	4.72	10.9	10.4	231
SWY-6	1.02	4.72	11.0	10.4	231
SWY-7	1.06	0.58	None	10.5	231
SWY-8	1.02	0.59	None	10.5	231
SWY-9	0.99	20.0	12.7	12.3	231
SWY-10	1.06	33.7	12.7	12.3	233
SWY-11	1.02	93.6	12.4	10.7	233
SWBlank1	1.02	None	None	None	230
SWBlank2	1.02	None	None	None	231
SWBlank3	1.02	None	None	None	229
SWBlank4	1.02	None	None	None	231

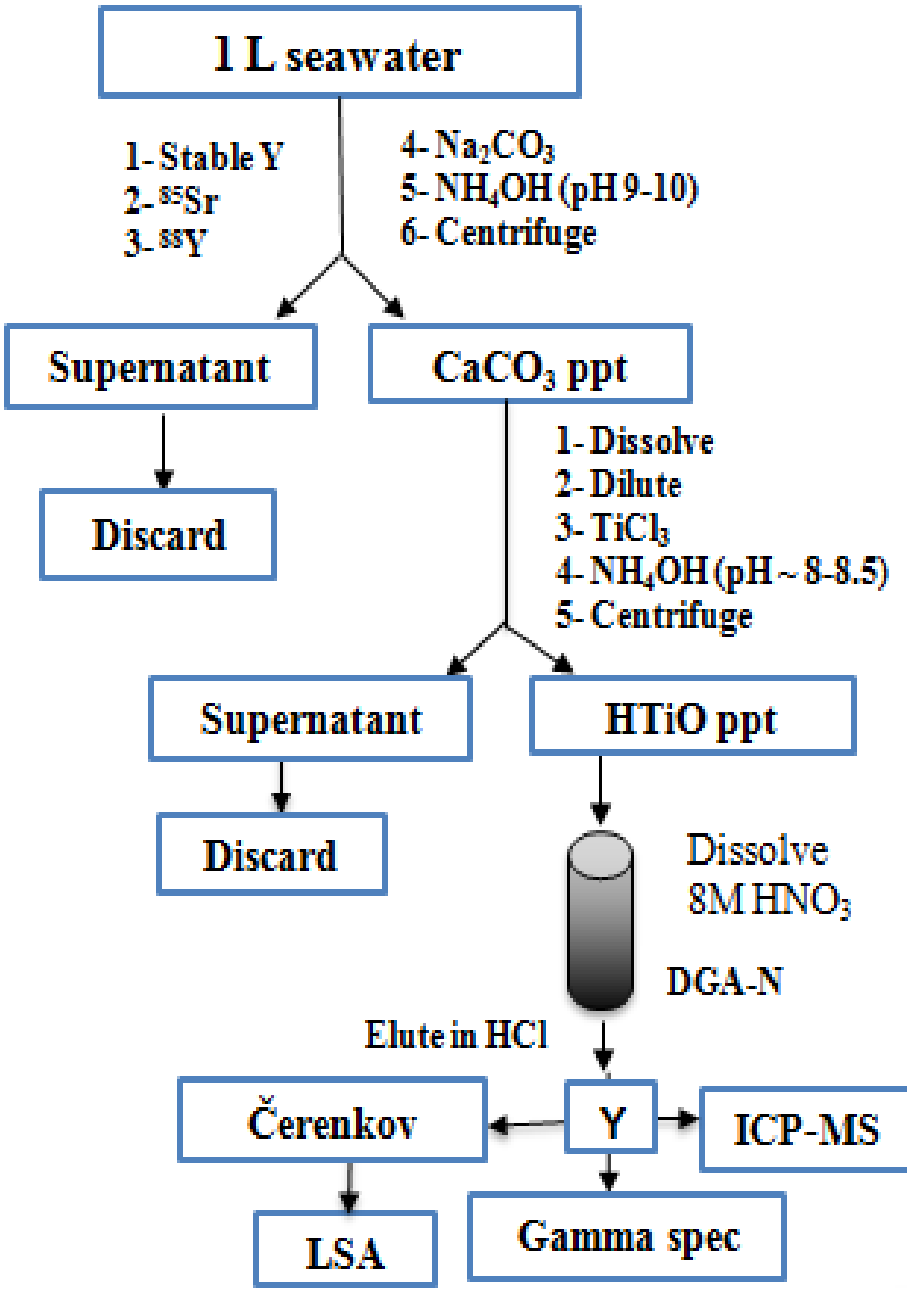

Figure 21. Flow chart of seawater sample preparation

4.2.2.2.3. Chromatographic Extraction of Strontium-90 and Yttrium-90

Element-selective extraction chromatography (EXC) was used to separate ^{90}Sr and ^{90}Y from freshwater and ^{90}Y from seawater. Both Sr-Resin® and DGA-N® resin columns were used for extraction of ^{90}Sr and ^{90}Y, respectively, from freshwater and only DGA-N® resin for extraction of ^{90}Y from seawater. The Sr-Resin® and DGA-N® extraction resins (pre-packed in 2-mL cartridges) were assembled in tandem with DGA-N® columns on the top of Sr-Resin® columns as shown in the schematic in Figure 22. A vacuum box with related accessories was used to assemble the chromatographic columns. After they were assembled, the columns were pre-conditioned using 10 mL deionized water first followed by 10 mL of 8 M HNO_3. The columns were then ready for sample loading and extraction (Step 1 in Figure 22). A photo of the vacuum box apparatus is shown in Appendix A. For apparatus set-up, column conditioning, and separation procedure refer to Appendix I.

For column separation of samples, the sample solutions, which were dissolved precipitate solutions of 8 M HNO_3 ($Ca_3(PO_4)_2$ carrying Sr for freshwater and HTiO carrying Y for seawater) were loaded onto the pre-conditioned columns of Sr-Resin® and DGA-N® (both columns used for freshwater and only DGA-N® for seawater method). The vacuum flow rate was maintained at ≤ 1 ml·min^{-1} for the sample solutions. Then, the column was rinsed with 10 mL of 8 M HNO_3 solution to get rid of unwanted matrix constituents (Step 2 in Figure 22).

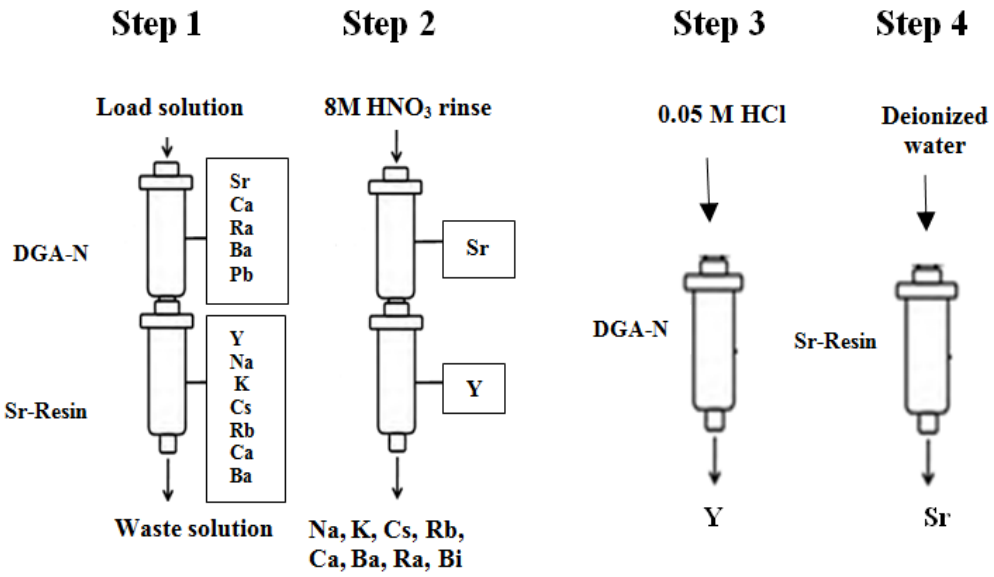

Figure 22. Schematic of column separation procedure using Sr-Resin® and DGA-N®

The end time of column rinsing was recorded for decay correction of ^{90}Sr and ^{90}Y (this time is the start of ^{90}Y in-growth in ^{90}Sr activity). Subsequently, the resins were each assembled separately on a vacuum box with new and clean accessories (*i.e*., inner and out tips and loading solution reservoir). The Sr from Sr-Resin® was eluted using 8 mL deionized water (steps 3 in Figure 22) and Y from DGA-N® using 10-15 mL of 0.05 M HCl (steps 4 in Figure 22). The eluate solutions were collected in pre-weighed 20-mL polyethylene plastic scintillation vials and weighed. An aliquot (~ 0.5 mL) from each vial was withdrawn for chemical yield determination of stable Sr and Y. The aliquots were diluted to 20 mL using 0.1 M HNO_3 solution and sent to the ICP-MS laboratory of CRL for analysis.

4.2.2.2.4. Measurement of Strontium-90 and Yttrium-90

Once eluted from the columns, the samples were counted on the low background Hidex LSC. The eluate solutions of the DGA-N®, which were eluted in 20-mL polyethylene plastic scintillation vials, were first counted for Čerenkov emission of ^{90}Y. The sample vials were simply placed on the LSC and counted for 1 h (some samples were counted for 0.5 h due to unavailability of the instrument for longer counting times). After Čerenkov counting was completed, the same samples were analyzed by liquid scintillation assay (LSA) technique. In the LSA, 8 mL of the purified solution was mixed with 12 mL Ultima Gold AB (UGAB) liquid scintillation cocktail solution. Similarly, the eluate solutions of the Sr-Resin® column, which were also eluted in 20-mL polyethylene plastic scintillation vials, were mixed with 12 mL Ultima Gold AB (UGAB) liquid scintillation cocktail solution. All LSA samples were measured for ^{90}Sr and ^{90}Y on the Hidex LSC for 1 h. The choice and volume of the cocktail solution UGAB for stripping solution samples, deionized water and 0.05 M HCl, with low ionic strength were consistent with recommendations in the literature [59].

4.3. Quality Control

Quality control measures were in place to ensure the quality of the measurement results obtained in this dissertation. Laboratory quality control samples (*i.e.*, spiked and procedural blank) were prepared using deionized water and processed following through the entire procedure except for the addition of radioactivity into the blank sample. The purpose of method blank was to ensure that there is no elevated radioactivity produced during the procedure, which could contribute to the radioactivity of the unknown samples. Spiked samples were prepared using deionized water that was spiked with a known amount of ^{90}Sr-^{90}Y traceable standard solution, and processed following through the entire procedure. In addition to procedural blank, reagent blank sample was also prepared. The reagent blank was a blank sample matching the matrix in which the analyte was measured for its radioactivity. For example, for the LSA of sample, the reagent blank was prepared by mixing of deionized water and the scintillation cocktail in proportions

matching that of the samples (*i.e.*, 8 mL water and 12 mL cocktail solution). The purpose of the reagent blank was to subtract the background registered counts by the LSC from the raw sample counts in order to obtain net counts of sample.

Besides spiked and blank samples, duplicate samples were also analyzed. For the TDCR Čerenkov counting technique, samples were prepared in duplicates. Duplicate samples of unknown freshwater were also analyzed for each of the TDCR Čerenkov counting and radiochemical separation techniques.

In summary, the present chapter has described sample preparation procedures for the determination of ^{90}Sr and ^{90}Y in freshwater and seawater matrices and also the chemical characterization of the water samples. Analytical techniques that were used to measure both chemical and radiological parameters were also described in this chapter. The measurement results obtained from the chemical and radiological analyses of the water samples described in the chapter formed the foundation of the present dissertation and are discussed in the next chapter.

Chapter 5: Results and Discussions

5.1. General Discussion

In this chapter, both non-radiological and radiological results are reported. The non-radiological characterization of the water was important in the context of radioanalytical method development in this dissertation. In the present chapter, the non-radiological results are presented first. Then, the results of method development for ^{90}Sr-^{90}Y in freshwater and seawater are discussed.

5.2. Non-radiological Test Results and Discussion

All water samples were tested for physical parameters such as pH, temperature, electric conductance. The results are shown in Appendix J (Table J-1 shows surface water and Table J-2 shows groundwater results). The water pH is an important parameter indicating conditions where cationic species such as Sr can enter the dissolved phase. The pH of the water samples measured was in the range of 6.37-7.82, which spans neutrality in a moderately narrow range. Such pH ranges for CRL surface waters are expected due to poorly buffered capacity of the Canadian Shield, particularly because these areas receive higher than average inputs of acidic precipitation on a regular basis [95].

Electric conductance reflects the total dissolved concentrations of ions in the water samples. The electric conductance of the lake water and groundwater samples was found to be higher than that of the Ottawa River water and correlated to higher concentrations of dissolved solids.

The main dissolved constituents of water that contribute to the major dissolved component of water are Ca^{2+}, Mg^{2+}, Na^{+} and K^{+}, which are likely from weathering and leaching of igneous rocks. For the purpose of the development work in the present dissertation, the dissolved metals concentrations needed to be characterized prior to radiochemical experiments in order to assess the level of interferences from the water matrix. The water samples were analyzed for a number of dissolved elements using Inductively Coupled Plasma- Mass Spectroscopy (ICP-MS). The most important dissolved metals for the purpose of the present research work were those that potentially interfere with Sr and Y radiochemical separation as discussed in Section 2.3.2.1 and Section 2.3.2.2. Mean concentrations of the potentially interfering dissolved metals analyzed in the freshwater and seawater samples along with their MDC (minimum detectable concentration) are shown in Table 14. The concentrations of individual samples are shown in Appendix J.

Table 14. Mean concentrations (±1σ) of non-radiological constituents of freshwater and seawater samples

Analyte	MDC /mg·L^{-1}	Ottawa River /mg·L^{-1}	Perch Lake /mg·L^{-1}	L. Bass Lake /mg·L^{-1}	Groundwater /mg·L^{-1}	Seawater /mg·L^{-1}
Na	2.00E-02	2.14E+00±0.03E+00	1.17E+01±0.23E+01	7.60E+00±0.05E+00	7.78E+01±6.20E+01	9.10E+03±0.14E+03
K	5.00E-02	5.92E-01±0.23E-01	7.97E-01±1.60E-01	9.67E-01±0.14E-01	2.91E+00±2.60E+00	3.10E+02±0.30E+02
Rb	2.00E-04	1.18E-03±0.05E-03	1.29E-03±0.27E-03	1.59E-03±0.03E-03	2.00E-03±1.30E-03	9.30E-02±0.35-02
Cs	5.00E-06	8.91E-06±1.00E-06	8.78E-06±0.67E-06	< MDC	8.25E-06±3.10E-06	3.90E-03±0.42E-03
Mg	4.00E-02	1.78E+00±0.02E+00	2.22E+00±0.44E+00	1.93E+00±0.01E+00	4.61E+00±4.00E+00	1.14E+03±0.01E+03
Ca	3.00E-02	6.75E+00±0.08E+00	6.25E+00±1.30E+00	5.59E+00±0.03E+00	1.73E+01±1.90E+01	2.90E+02±0.30E+02
Sr	6.00E-05	2.60E-02±0.02E-02	4.21E-02±0.85E-02	4.79E-02±0.03E-02	1.14E-01±0.89E-01	6.25E+00±0.01E+00
Y	1.00E-05	< MDC	< MDC	< MDC	< MDC	< MDC
Ba	5.00E-05	1.10E-02±0.02E-02	1.56E-02±0.29E-02	1.41E-02±0.01E-02	7.93E-02±6.20E-02	6.85E-03±1.10E-03
Fe	9.00E-03	1.57E-01±0.03E-01	1.32E+00±0.25E+00	7.02E-01±0.08E-01	3.97E+00±5.30E+00	1.05E-02±0.21E-02
Pb	5.00E-05	1.08E-04±0.02E-04	2.76E-04±0.05E-04	5.80E-05±0.30E-05	1.07E-03±2.20E-03	2.45E-03±0.14-03
U	5.00E-05	6.32E-05±0.10E-05	< MDC	< MDC	4.46E-03±5.60E-03	2.30E-03±0.14-03
Th	2.00E-04	< MDC	< MDC	< MDC	4.80E-04±2.41E-04	< MDC
F	3.00E-02	< MDC	3.38E-02±0.20E-02	< MDC	NT[6]	NO[7]
Cl	1.12E-01	1.50E+00±0.11E+00	2.65E+00±0.25E+00	1.56E+01±0.04E+01	NT	2.33+04±0.19E+04
Br	1.23E-01	< MDC	< MDC	< MDC	NT	5.11E+01±1.00E+01
PO_4	1.79E-01	1.19E-01±0.10E-01	< MDC	< MDC	NT	2.22E+00±0.17E+00
SO_4	1.05E-01	5.06E+00±0.28E+00	3.95E+00±0.23E+00	2.65E+00±0.08E+00	NT	2.85+03±0.54E+03
DOC	5.00E-01	6.49E+00±0.42E+00	13.3E+00±3.9E+00	4.64E+00±0.23E+00	NT	1.51E-01±0.04E-01
DIC	5.00E-01	3.68E+00±0.20E+00	2.68E+00±1.10E+00	3.89E+00±0.85E+00	NT	2.15E+01±0.01E+01

[6] NT=Not tested. Anions were not tested in groundwater samples.
[7] NO=Not observed. Concentration peaks of F were hindered by abundant concentrations of Cl.

As expected, Sr was found in trace concentrations in all freshwater samples and Y was mainly below the MDC of $1.0x10^{-5}$ $mg{\cdot}L^{-1}$. The mean concentrations of Na^+ and K^+ in CRL surface waters were similar to those reported for other Canadian freshwaters such as Niagara River, Rainy River, and St. Lawrence River [16]. The mean concentration of Ca^{2+} and Mg^{2+} found in the CRL surface waters, however, were much lower than those of Niagara River, Rainy River, and St. Lawrence River [16], reflecting the different geology of its catchment area. The peak in Na^+ concentrations of CRL groundwater samples is a result of road salt, which is commonly observed in CRL surface water and groundwater. In general, the concentrations found in the freshwater samples in this dissertation were three to four orders of magnitude lower than those that can adversely affect radiochemical separation of Sr and Y on their respective resins. For example, the highest mean concentration of freshwater Na^+, K^+, and Ca^{2+} found in CRL groundwater were ~ 78 $mg{\cdot}L^{-1}$, 3 $mg{\cdot}L^{-1}$, and 17 $mg{\cdot}L^{-1}$, respectively. As shown in Figure 6, only at or above concentrations of 0.5 M of Na^+ and Ca^{2+} and 0.01 M of K^+ can the binding affinity of Sr for Sr-Resin® be suppressed.

In the seawater, the major cations were found at concentrations that were much higher than freshwater, as expected. The concentration of Na^+, K^+, Mg^{2+} and Ca^{2+} found in seawater were ~ 9100 $mg{\cdot}L^{-1}$, 310 $mg{\cdot}L^{-1}$, 1140 $mg{\cdot}L^{-1}$, and 290 $mg{\cdot}L^{-1}$, respectively. Such high concentrations would have significantly interfered with separation of Sr and Y on their respective extraction resins. Thus, separation of Sr and Y from excessive concentrations of these cations was important and achieved in the co-precipitation step (refer to Chapter 4, Section 4.2.2.2.2).

Knowledge of concentrations of actinides in freshwater and seawater was also crucial in the light of the binding tendency of some of the actinides to the chromatography extraction resins as described in Section 2.3.2. As illustrated by Table 14, the Th and U concentrations of both freshwater and seawater were very close to or below the detection limit. Although the U in groundwater and seawater was found above detectable concentrations, the U was not expected to cause any major difficulties in the determination of ^{90}Sr and ^{90}Y because (i) the concentrations are very low (in $\mu g{\cdot}L^{-1}$ - $mg{\cdot}L^{-1}$ ranges) and (ii) even at similar concentration to ^{90}Sr and ^{90}Y, the U under the acidic conditions used in this experiment (*i.e.*, 8 M HNO_3) has 50 to 1000 times lower binding affinity for Sr-Resin® (Figure 8) and DGA-N® (Figure 11), respectively. Thus, they cannot successfully compete with Sr and Y for binding. Therefore, Th and U were presumed to cause no major difficulties in radiochemical separation of ^{90}Sr and ^{90}Y in the present research.

Anions and dissolved carbons were analyzed in surface water and seawater. Anions and carbon were not analyzed in groundwater samples because the samples that were provided, by the CRL groundwater monitoring personnel, for this dissertation

were acidified at the time of collection from the field as per the groundwater monitoring protocol (the collection of groundwater samples for the purpose of this dissertation was not in the scope of this research work). The anions analysis cannot be performed on acidified samples. The anions and dissolved carbon concentrations of individual surface water samples are shown in Table J-5 and Table J-6, respectively, Appendix J. Mean concentrations of anions and dissolved carbons for each of the Ottawa River, Perch Lake, and Lower Bass Lake and also of the seawater are presented in Table 14. Of the main anions, Cl^- is dominant in many CRL surface water and groundwater where the source of high Cl^- concentrations is linked to road salt. The anion concentrations measured in the CRL surface water were similar to those reported for other Canadian freshwaters such as Niagara River, Rainy River, and St. Lawrence River [16]. In general, in those samples detected, the anions concentrations were below the maximum allowable concentrations of drinking water, where applicable, or below aesthetic objective (AO) levels as per the drinking water guidelines of Health Canada [14]. The dissolved organic carbon (DOC) concentrations were found to be higher in the surface water samples than the dissolved inorganic carbon (DIC) concentrations. A variety of on land and aquatic vegetation surrounding the watersheds of CRL site contribute to the high DOC concentrations. Conversely, in the seawater, the DIC concentrations were 100 times higher than DOC, as expected.

In general, the results of all chemical parameters were as expected for natural and seawater. The chemical characterization of water samples provided the fundamental knowledge that was essential in understanding the level of matrix interference towards the radiochemical separation procedures of freshwater and seawater ^{90}Sr-^{90}Y.

5.3. Radioanalytical Method Development Results and Discussion

5.3.1. TDCR Čerenkov Counting Technique

5.3.1.1. Development of TDCR Čerenkov Counting Technique

The objective of the TDCR Čerenkov counting technique was to offer simple and fast determination moderate to high levels of ^{90}Sr-^{90}Y (at secular equilibrium activity concentrations) under various experimental conditions. In general, experimental factors that attenuate Čerenkov light and also the counting efficiency are: (i) solution volume; (ii) counting vial material; (iii) presence of colour; and (iv) presence of other high energy β^- and mixed β^--γ emitters. To correct for the effects of such factors, often calibration of the instrument is required.

In the TDCR Čerenkov counting technique, the triple coincidences are strongly suppressed by experimental conditions that attenuate the Čerenkov light which eventually reduce both the TDCR and the counting efficiency. If the relationship

between the TDCR and counting efficiency is known, the TDCR can be used to correct for the effects of any experimental variations on the counting efficiency. In the present dissertation, the relationship between the TDCR and counting efficiency of ^{90}Y was found using colour quenching, as the only variable, and then the same expression was used to evaluate the performance of the method under any other given experimental conditions. Colour quenching factor was used as the variable of choice because it causes the most unfavourable condition in the Čerenkov counting technique due to significant absorption of Čerenkov light by the sample colorant. Sample vials of 15 mL deionized water were spiked with various amounts of yellow and brown food-grade dyes and known (*i.e.*, 8-10 Bq) added activities, A_{ia}, of ^{90}Sr-^{90}Y standard and Čerenkov counted using a low background Hidex LSC. The ^{90}Y count rates were obtained, Table 15, and used in Eq. (11) to obtain the counting efficiency of ^{90}Y:

$$Counting\ Eff\ = \frac{CR_S - CR_b}{A_{ia}} \tag{11}$$

where CR_s and CR_b are sample and background count rates (cps), respectively.

Table 15. TDCR and counting efficiencies of spiked and colour quenched samples (± combined statistical and non-statistical uncertainties at 1σ) measured on Hidex LSC.

Sample code	Dye type	Dye /mL	A_{ia} ^{90}Y /Bq	Net TDCR	CR_N[8] /cps	Counting Eff /%
SrCT11-Blk	Blank	0	8.79±0.11	0.72±0.02	5.98±0.10	68.0±1.4
SrCT11-1	Yellow	0.1	8.85±0.11	0.66±0.02	5.88±0.10	66.4±1.4
SrCT11-2	Yellow	0.2	8.81±0.11	0.61±0.02	5.52±0.10	62.7±1.3
SrCT11-3	Yellow	0.3	8.83±0.11	0.59±0.02	5.41±0.09	61.2±1.3
SrCT11-4	Yellow	0.4	8.88±0.11	0.55±0.02	5.16±0.09	58.1±1.3
SrCT11-5	Yellow	0.5	8.86±0.11	0.53±0.02	5.04±0.09	56.9±1.2
SrCT11-6	Yellow	0.6	8.87±0.11	0.49±0.02	4.82±0.09	54.4±1.2
SrCT11-7	Yellow	0.7	8.86±0.11	0.47±0.02	4.35±0.09	49.1±1.1
SrCT11-8	Yellow	0.8	8.85±0.11	0.45±0.02	4.60±0.09	52.0±1.2
SrCT12-1	Brown	0.1	8.85±0.11	0.63±0.02	5.65±0.10	63.9±1.4
SrCT12-2	Brown	0.2	8.85±0.11	0.52±0.02	4.69±0.09	53.0±1.3
SrCT12-3	Brown	0.3	8.84±0.11	0.46±0.02	4.38±0.08	49.6±1.2
SrCT12-4	Brown	0.4	8.86±0.11	0.40±0.02	4.26±0.08	48.1±1.1
SrCT12-5	Brown	0.5	8.84±0.11	0.37±0.02	3.70±0.08	41.9±1.1
SrCT12-6	Brown	0.6	8.85±0.11	0.30±0.02	3.20±0.07	36.1±1.0
SrCT12-7	Brown	0.7	8.87±0.11	0.28±0.02	2.87±0.07	32.3±0.9
SrCT12-8	Brown	0.8	8.87±0.11	0.24±0.02	2.75±0.07	31.0±0.9

[8] CR_N = Net count rate

The counting efficiencies for a wide range of coloured samples were plotted as a function of triple to double coincidences, Figure 23. The empirical relationship between TDCR and Čerenkov counting efficiency of ^{90}Y, $\boldsymbol{\varepsilon_{Cernk}}$, was determined as expressed by Eq. (12) with a strong coefficient of determination, $r^2 = 0.980$.

$$\varepsilon_{Cernk} = 0.9 \cdot (TDCR)^{0.75} \quad (12)$$

Once the correlation between the TDCR and Čerenkov counting efficiency of ^{90}Y was determined, the expression was used to correct the effects of counting condition variables, such as sample geometry and also colour quenching itself, on the counting efficiency of ^{90}Y.

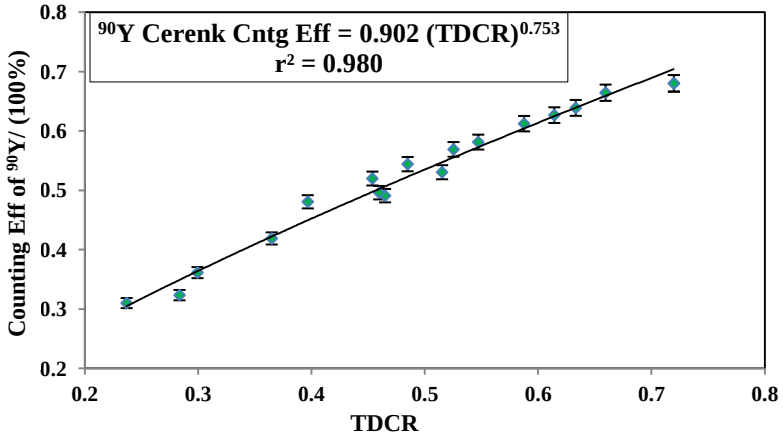

Figure 23. Čerenkov counting efficiency of ^{90}Y in colour quenched samples as a function of TDCR. Error bars indicate combined statistical and systematic uncertainties in counting efficiency at 1σ.

The effects of geometry on counting efficiency of ^{90}Y were evaluated using (i) various volumes of aqueous solutions of 0.1 M HCl and 0.1 M HNO_3; (ii) vial type made from polyethylene plastic and glass; and (iii) vial sizes of 7-mL and 20-mL. Sample geometry is an important parameter because Čerenkov radiation is anisotropic whereby photons are emitted as a cone of radiation at a specific angle to the direction of travel of β^- particles [62]. Variations, such as sample volume and counting vial size and type, in the pathway of travelling Čerenkov photons can eventually influence their detection efficiency by the photomultiplier tubes (PMTs) of the detector. As described in Chapter 4, the vials were spiked with a known amount (*i.e.*, ~ 8-10 Bq) of ^{90}Sr-^{90}Y standard solution and the Čerenkov emission of ^{90}Y was measured on a TDCR Hidex LSC. A summary of geometry test results are presented in Table 16 and detailed analytical results are shown in Table K-1, Appendix K. The sample geometries examined were 7-mL and 20-mL plastic vials (PV) at various 0.1 M HCl and 0.1 M HNO_3 solution volumes and 7-mL and 20-

mL glass vials (GV) at various 0.1 M HCl solution volumes. The mean counting efficiency (±1σ) of various 0.1 M HCl volumes measured in the 7-mL and 20-mL PVs were 72±1 % and 70±1 %, respectively, Table 16 and Figure 24.

Table 16. TDCR Čerenkov counting results of ^{90}Y measured in plastic vials (PV) and glass vials (GV)

Sample code	Sample geometry	A_{ia} ^{90}Sr-^{90}Y /Bq	TDCR	$\varepsilon_{Čerenk}$ /%	A_i[9] ^{90}Y /Bq	B_{ri}[10] /%
SrCT3-1	7 PV, 1mL HCl	9.28	0.74	71.9	8.94	-3.7
SrCT3-2	7 PV, 3mL HCl	9.33	0.76	73.1	8.78	-5.9
SrCT3-3	7 PV, 5mL HCl	9.33	0.74	72.2	8.80	-5.6
SrCT3-4	7 PV, 7mL HCl	9.30	0.73	71.3	8.83	-5.1
SrCT3-1Dup	7 PV, 1mL HCl	9.35	0.74	72.0	8.87	-5.1
SrCT3-2Dup	7 PV, 3mL HCl	9.32	0.75	72.8	8.77	-5.9
SrCT3-3Dup	7 PV, 5mL HCl	9.30	0.74	72.1	8.78	-5.6
SrCT3-4Dup	7 PV, 7mL HCl	9.30	0.73	71.4	8.93	-4.1
Mean±1σ				*72±1*		
B_r[11]						*-5.1*
S_B[12]						*0.8*
SrCT4-1	20 PV, 3mL HCl	9.33	0.70	69.0	9.26	-0.8
SrCT4-2	20 PV, 5mL HCl	9.30	0.72	70.5	9.00	-3.3
SrCT4-3	20 PV, 7mL HCl	9.35	0.72	70.1	9.20	-1.6
SrCT4-4	20 PV, 10mL HCl	9.36	0.73	71.0	9.11	-2.6
SrCT4-5	20 PV, 13mL HCl	9.35	0.72	70.6	9.00	-3.8
SrCT4-6	20 PV, 15mL HCl	9.43	0.72	70.6	9.21	-2.4
SrCT4-7	20 PV, 18mL HCl	9.32	0.72	70.5	9.03	-3.1
SrCT4-8	20 PV, 20mL HCl	9.35	0.72	70.4	8.97	-4.0
SrCT4-1Dup	20 PV, 3mL HCl	9.35	0.69	68.3	9.37	0.2
SrCT4-2Dup	20 PV, 5mL HCl	9.35	0.72	70.0	9.14	-2.3
SrCT4-3Dup	20 PV, 7mL HCl	9.35	0.73	71.2	9.00	-3.8
SrCT4-4Dup	20 PV, 10mL HCl	9.38	0.73	70.8	9.22	-1.7
SrCT4-5Dup	20 PV, 13mL HCl	9.33	0.73	70.7	8.98	-3.8
SrCT4-6Dup	20 PV, 15mL HCl	9.35	0.73	70.8	9.03	-3.4
SrCT4-7Dup	20 PV, 18mL HCl	9.31	0.72	70.0	8.96	-3.8
SrCT4-8Dup	20 PV, 20mL HCl	9.33	0.71	69.3	9.03	-3.2
Mean±1σ				*70±1*		
B_r						*-2.7*
S_B						*1.2*

[9] A_i = measured activity
[10] B_{ri} = Relative bias of individual measurement
[11] B_r = Relative bias of replicate sets of samples
[12] S_B = Spread in bias (precision)

Table 16 continues

Sample code	Sample geometry	A_{ia} ^{90}Sr-^{90}Y /Bq	TDCR	$\varepsilon_{Čerenk}$ /%	A_i ^{90}Y /Bq	B_{ri} /%
SrCT5-1	7 PV, 1mL HNO_3	9.33	0.72	70.1	8.95	-4.0
SrCT5-2	7 PV, 3mL HNO_3	9.33	0.73	70.9	8.91	-4.4
SrCT5-3	7 PV, 5mL HNO_3	9.33	0.73	71.4	8.97	-3.9
SrCT5-4	7 PV, 7mL HNO_3	9.29	0.72	70.2	8.83	-5.0
SrCT5-1Dup	7 PV, 1mL HNO_3	9.31	0.73	70.8	9.02	-3.1
SrCT5-2Dup	7 PV, 3mL HNO_3	9.32	0.73	71.0	8.93	-4.2
SrCT5-3Dup	7 PV, 5mL HNO_3	9.30	0.74	71.6	8.98	-3.4
SrCT5-4Dup	7 PV, 7mL HNO_3	9.27	0.71	69.8	8.98	-3.1
Mean±1σ				*71±1*		
B_r						*-3.9*
S_B						*0.7*
SrCT7-1	7 GV, 3mL HCl	9.29	0.64	64.4	9.32	0.3
SrCT7-2	7 GV, 5mL HCl	9.25	0.61	62.2	9.60	3.7
SrCT7-3	7 GV, 7mL HCl	9.28	0.58	59.8	9.48	2.1
SrCT8-1	20 GV, 10mL HCl	9.25	0.64	64.5	9.42	1.7
SrCT8-2	20 GV, 15mL HCl	9.28	0.62	62.9	9.41	1.3
SrCT8-3	20 GV, 18mL HCl	9.30	0.60	61.5	9.28	-0.3
SrCT8-4	20 GV, 20mL HCl	9.25	0.58	59.5	9.50	2.7
Mean±1σ				*62±2*		
B_r						*1.7*
S_B						*1.4*

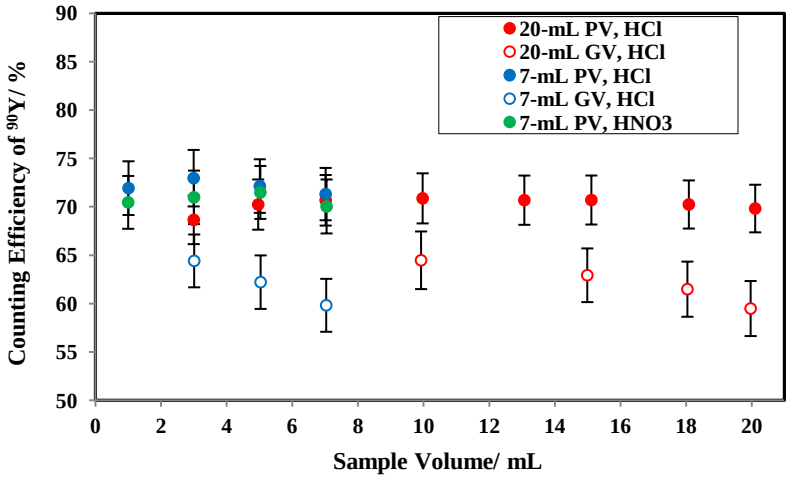

Figure 24. Counting efficiency of ^{90}Y counted in plastic (PV) and glass vials (GV) as a function of sample volume; *adapted from* [96]. Error bars indicate combined statistical and systematic uncertainties in counting efficiencies at 1σ.

Mean counting efficiency of various 0.1 M HNO_3 volumes measured in the 7-mL PVs was 71±1 %. Counting efficiencies measured in GVs were lower than those of PVs and were in the range of 59-64 % with mean of 62±2 %. Inspection of the data in Table 16 and Figure 24 indicates that the counting efficiencies obtained in PVs did not change with variation in sample solution types and volumes. To statistically test this hypothesis, a two-tailed paired t-distribution test was conducted at 5 % significance level. There were six different observations that were statistically analyzed, Table 17. They were:

(1) 0.1 M HCl volumes of 3, 5, and 7 mL counted in 7-mL PV;
(2) 0.1 M HNO_3 volumes of 3, 5, and 7 mL counted in 7-mL PV;
(3) 0.1 M HCl volumes of 3, 5, and 7 mL counted in 7-mL GV;
(4) 0.1 M HCl volumes of 3, 5, and 7 mL counted in 20-mL PV;
(5) 0.1 M HCl volumes of 10, 15, 18, and 20 mL counted in 20-mL PV; and
(6) 0.1 M HCl volumes of 10, 15, 18, and 20 mL counted in 20-mL GV.

Also, where duplicate samples existed, they were also analyzed. Note: similar sample volumes constitute a pair and, therefore, all data points could not have been paired and evaluated using this statistical tool.

Table 17. Counting efficiencies of geometry tests that were statistically evaluated

		Observations						
		(1)	**(2)**	**(3)**	**(4)**		**(5)**	**(6)**
Vial size		7-mL	7-mL	7-mL	20-mL		20-mL	20-mL
Vial type		PV	PV	GV	PV		PV	GV
Aqueous solution		HCl	HNO_3	HCl	HCl		HCl	HCl
Vol /mL		**$\varepsilon_{Čerenk}$ /%**				**Vol /mL**	**$\varepsilon_{Čerenk}$ /%**	
Sample	3	73.1	70.9	64.4	69.0	10	71.0	64.5
	5	72.2	71.4	62.2	70.5	15	70.6	62.9
	7	71.3	70.2	59.8	70.1	18	70.5	61.5
						20	70.4	59.5
Duplicate	3	72.8	71.0	-	68.3	10	70.8	-
	5	72.1	71.6	-	70.0	15	70.8	-
	7	71.4	69.8	-	71.2	18	70.0	-
						20	69.3	-

Parallel observations based on sample volume as shown in Table 17 were used in pairs and their p-values obtained using MS Excel, Table 18. As Table18 demonstrates, at 5 % significance level, the probability-value was higher for paired observations corresponding to variations in sample volume and vial size. As such, variation in counting efficiencies were not statistically different between (i) sample

volumes; (ii) vial sizes of 7-mL and 20-mL; and (ii) types of aqueous solutions tested (*i.e.*, HCl vs HNO_3). This implies that in the TDCR Čerenkov counting technique, the variation in sample geometry, which in conventional techniques causes changes in counting efficiency, was automatically corrected. Thus, counting efficiencies were not significantly changed when sample geometry changed.

Table 18. Two-tailed paired t-distribution statistical test results

Paired observation	p-value sample	p-value duplicate	ε_{Cerenk} of pairs different:
(1) & (2)	0.08	0.09	No
(1) & (3)	0.01	0.01	Yes
(1) & (4)	0.12	0.22	No
(5) & (6)	0.003	0.002	Yes

However, variation between plastic and glass vials was observed. The variation in counting efficiencies was statistically different when vial types changed between plastic and glass vials, paired observations (1) and (3), and (5) and (6) in Table 17. The difference in counting efficiencies between plastic and glass vials can be attributed to two main factors. First, the Čerenkov light reflection in the plastic vial may have contributed to higher counting efficiency in plastic vials because unlike glass, the light that cannot pass through polyethylene plastic is reflected away from the vial [97]. When reflected away, the Čerenkov light, which originally possesses an anisotropic behaviour, may be seen as if it is an isotropic source emitting in all directions and, therefore, can be detectable more effectively. Secondly, the variation in counting efficiencies between plastic and glass vials may be due to variation in index of refraction, R_I, of the counting media. For plastic medium with R_I =1.52, the β^- particle's threshold energy ($E_{threshold}$) for the production of Čerenkov radiation as a function of R_I is 0.167 MeV as per Eq. (13) [98]. For borosilicate glass medium with R_I =1.48, the β^- particle's $E_{threshold}$ for the production of Čerenkov radiation is 0.183 MeV [98]. This implies that the lower $E_{threshold}$ for detection of Čerenkov photons in plastic counting vials, compared to that of the glass vials, may have resulted in higher Čerenkov counting efficiency in plastic vials as the β^- particles travel in the lower threshold energy medium [98]).

$$E_{threshold}(MeV) = 0.511 \cdot \left[\left(1 - \frac{1}{(R_I)^2}\right)^{-1/2} - 1\right] \quad (13)$$

Once the ε_{Cerenk} was found as per Eq. (12), the measured activity (A_i) determined by the TDCR Čerenkov counting, which is detonated as $A_{Y\ TDCR,}$ was obtained as expressed by Eq. (14):

$$A_i = A_{Y\ TDCR}\ (Bq) = \frac{CR_s - CR_b}{\varepsilon_{Cerenk}} \quad (14)$$

where CR_s and CR_b are sample and background count rates (of the blank sample) in counts per second (cps), respectively, in the ^{90}Y default region of interest (ROI), which were channels 50-350 on low background Hidex LSC. Measured activities are tabulated in Table 16. The bias and precision in measured activities of spiked samples were assessed to delineate the performance of the method. Relative bias for individual sample measurements (B_{ri}) was obtained as per Eq. (15):

$$B_{ri}(\%) = \left(\frac{A_i - A_{ai}}{A_{ia}}\right) \cdot 100 \quad (15)$$

where A_i and A_{ai} represent measured activity and added or expected activity of individual samples, respectively. The relative precision (S_B) was also calculated as expressed by Eq. (16) to show the dispersion in bias measurements:

$$S_B(\%) = \left(\sqrt{\frac{\sum_i^{N_r}(B_{ri} - B_r)^2}{N_r - 1}}\right) \cdot 100 \quad (16)$$

where N_r represents the number of replicate measurements and B_r is the mean of B_{ri} of replicate samples. The B_{ri} and B_r of all sample geometry tests were within 6 % and S_B within 1 % of the expected values, Table 16. This deviation of ±6 % is also illustrated in Figure 25 where the ratios of measured-to-expected activities of all geometries tested are shown as a function of sample volume.

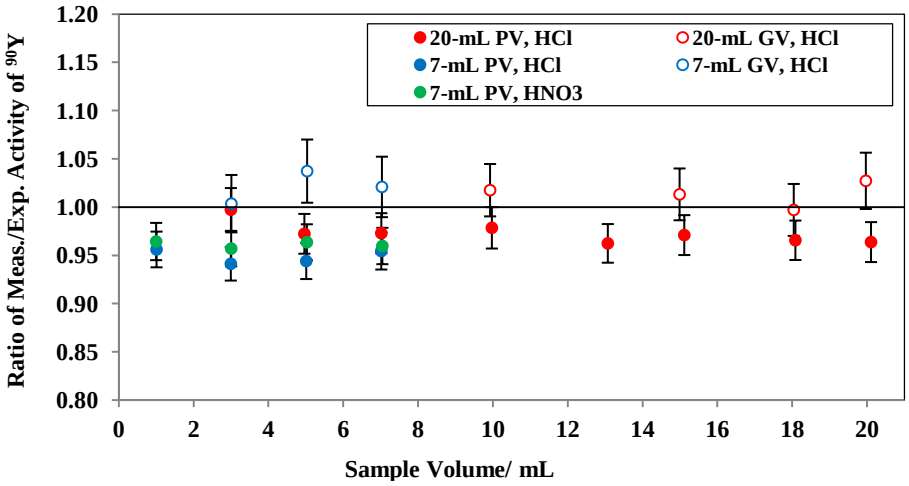

Figure 25. The ratio of measured-to-expected activities of ^{90}Y in equilibrium with ^{90}Sr measured in plastic (PV) and glass vials (GV) using various volumes of 0.1 M HCl and 0.1 M HNO_3; *adapted from* [96]. Error bars indicate combined statistical and systematic uncertainties at 1σ.

Besides counting geometry, sample colour quenching variation was also corrected using the empirical expression developed in the present dissertation, Eq. (12). Conventionally, colour quenching effect in LSA technique is corrected using a quench curve, however, colour qunching effect in Čerenkov counting technique cannot be corrected by any means. In the TDCR technique, however, the effect of quenching on Čerenkov efficiency was corrected based on the measured TDCR values. Deionized water samples having a wide range of quantities of added yellow and brown colours and known quantities of ^{90}Sr-^{90}Y were counted on the Hidex LSC for Čerenkov emission of ^{90}Y in the presence of colour quenching. A summary of the results is tabulated in Table 19 and details shown in Table K-2, Appendix K.

Table 19 demonstrates that as the amount of dye in the sample increased, the counting efficiency gradually decreased. The decrease in counting efficiency for samples that were colour quenched using various amounts of the colorants and counted in PVs was by ~ 20 % for yellow and ~ 40 % for brown quenched samples. Similarly, the decrease in counting efficiency was significant when brown quenched samples were counted in GV. The decrease in counting efficiency is attributable to the amount of light that the colorant in the sample can absorb and the consequent reduction in the light output for detection by the PMTs of the LSC. An absorption measurement of quenched samples was obtained using a UV-Vis spectrophotometer, Figure 26. The absorption spectra were 350 - 500 nm for yellow and 350 - 600 nm for brown colorants. These spectra coincide with the spectral response range of the PMTs (Electron Tubes 9102KA PMTs, sensitivity range ~ 290 - 630 nm, peak at ~ 370 nm) in the Hidex 300SL LSC. Therefore, absorption by the colorant resulted in reduced counting efficiency, which implies that changes in counting efficiency can be related directly to quench. The change in counting efficiency due to colour quenching was effectively corrected using the TDCR Čerenkov counting technique. As Table 19 shows the relative bias for individual spiked samples were within 5 % and 8 % for each of yellow and brown dyes, respectively. The deviation in measured activities can also be expressed as the ratio of measured-to-expected activities as a function of counting efficiency of quenched samples as illustrated in Figure 27. The greater deviations for brown dye may be attributed to its greater absorption.

Table 19. Colour quenching test results using 15 mL coloured deionized water measured in 20-mL vials

Sample code	Vial type	Dye type	Dye amount /mL	A_{ia} ^{90}Sr-^{90}Y /Bq	ε_{Cerenk} /%	A_i ^{90}Y /Bq	B_{ri} /%
Blank1	PV	None	0	8.80	70.3	8.51	-3.3
SrCT11-1	PV	Yellow	0.1	8.85	65.9	8.92	0.9
SrCT11-2	PV	Yellow	0.2	8.81	62.4	8.84	0.3
SrCT11-3	PV	Yellow	0.3	8.83	60.4	8.95	1.4
SrCT11-4	PV	Yellow	0.4	8.88	57.3	9.02	1.5
SrCT11-5	PV	Yellow	0.5	8.86	55.5	9.07	2.4
SrCT11-6	PV	Yellow	0.6	8.87	52.3	9.22	4.0
SrCT11-7	PV	Yellow	0.7	8.86	50.7	8.58	-3.1
SrCT11-8	PV	Yellow	0.8	8.85	49.8	9.24	4.5
Mean±1σ					*58±7*		
Br							*1.0*
S_B							*3.9*
Blank2	PV	None	0	8.80	70.3	8.51	-3.3
SrCT12-1	PV	Brown	0.1	8.85	63.9	8.85	0.0
SrCT12-2	PV	Brown	0.2	8.85	54.7	8.58	-3.1
SrCT12-3	PV	Brown	0.3	8.84	50.2	8.73	-1.3
SrCT12-4	PV	Brown	0.4	8.86	45.0	9.46	6.8
SrCT12-5	PV	Brown	0.5	8.84	42.3	8.76	-0.9
SrCT12-6	PV	Brown	0.6	8.85	36.4	8.78	-0.8
SrCT12-7	PV	Brown	0.7	8.87	35.0	8.20	-7.5
SrCT12-8	PV	Brown	0.8	8.88	30.6	9.00	1.4
Mean±1σ					*48±13*		
Br							-0.9
S_B							3.9
Blank3	GV	None	0	8.77	61.9	8.95	2.1
SrCT13-2	GV	Brown	0.1	8.75	57.9	9.06	3.5
SrCT13-3	GV	Brown	0.2	8.76	54.0	9.14	4.0
SrCT13-4	GV	Brown	0.3	8.73	52.3	9.15	4.7
SrCT13-5	GV	Brown	0.4	8.81	50.8	9.06	2.8
SrCT13-6	GV	Brown	0.5	8.80	46.5	9.24	4.9
Mean±1σ					*54±5*		
Br							*3.7*
S_B							*1.1*

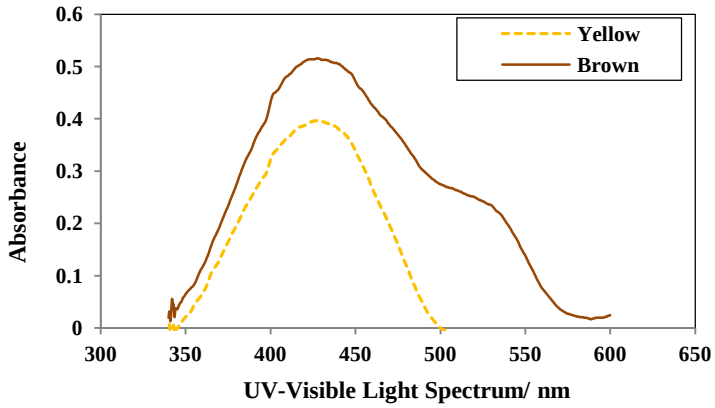

Figure 26. Absorbance spectra of yellow and brown dyes [96]

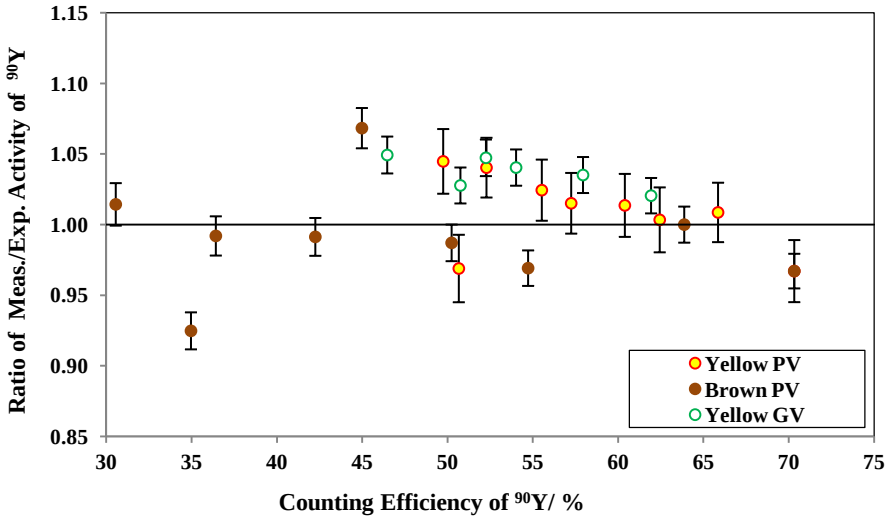

Figure 27. The ratio of measured-to-expected activities of ^{90}Y in equilibrium with ^{90}Sr containing yellow and brown dyes counted in plastic (PV) and glass vials (GV) as a function of counting efficiency [96]. Error bars indicate combined statistical and systematic uncertainties at 1σ.

The TDCR Čerenkov counting technique was also evaluated in the presence of other radionuclides that potentially cause interference for ^{90}Sr-^{90}Y in environmental samples. These radionuclides are shown in Table 20 and have emission energies above the energy threshold for radionuclide Čerenkov emission. Known amounts of each radionuclide was spiked in 15 mL of 0.1 M HCl solution in both PV and GV and measured on the Hidex LSC. Samples were prepared in duplicates and the mean counting efficiencies of sample and its duplicate obtained. Details of the

analysis of this test are presented in Table K-3 and Table K-4 in Appendix K. Using emission probabilities shown in Table 20, the total average energy (E_{avg}) was calculated for each radionuclide and used to demonstrate the change in Čerenkov counting efficiency as a function of radionuclide E_{avg}, Figure 28. In Table 20 and Figure 28, the counting efficiency of the radionuclides other than the ^{90}Y was determined as expressed by Eq. (11) and that of ^{90}Y was determined using Eq. (12). The E_{avg} rather than E_{max} was used as E_{avg} is a representative of a large proportion of β^- emission. According to Figure 28, for the pure beta emitters (^{90}Y, ^{32}P, ^{89}Sr, and ^{210}Bi), the relationship between E_{avg} and Čerenkov counting efficiency was a natural logarithm function, with strong coefficient of determination ($r^2 \geq 0.98$) and a threshold E_{avg} of ~ 0.3 MeV. Mixed β^--γ emitters (^{40}K, ^{137}Cs, and ^{60}Co) have contributions from both β^- and γ emissions. These β^--γ emitters ^{60}Co and ^{137}Cs, each with respective E_{avg} of ~ 0.1 and ~ 0.2 MeV of β^-, showed roughly 10 % Čerenkov counting efficiency. Similar Čerenkov counting efficiencies for ^{60}Co, ^{137}Cs, and ^{40}K were also reported in previous studies using conventional Čerenkov counting technique [62, 65].

Table 20. Properties of radionuclides used for TDCR Čerenkov counting and their counting efficiencies measured in plastic vials (PV) and glass vials (GV)

Radionuclide tested	E_{avg} /MeV	$I^{(13)}$	Total E_{avg} /MeV	Counting Eff in PV /%	Counting Eff in GV /%
^{90}Y (equilib. with ^{90}Sr)	0.934	1.000	1.119	70.5	63.8
	0.186	0.001			
^{89}Sr	0.585	1.000	0.774	48.9	41.8
	0.189	0.000			
^{32}P	0.695	1.000	0.695	55.1	48.3
^{210}Bi (equilib. with ^{210}Pb)	0.389	1.000	0.389	18.6	14.2
^{137}Cs	0.416	0.056	0.174	8.53	6.29
	0.174	0.944			
^{60}Co	0.096	0.999	0.095	8.02	7.22
	0.626	0.001			
	0.275	0.000			
^{40}K	0.561	0.893	0.561	44.0	37.9

$^{(13)}I$= Emission probability

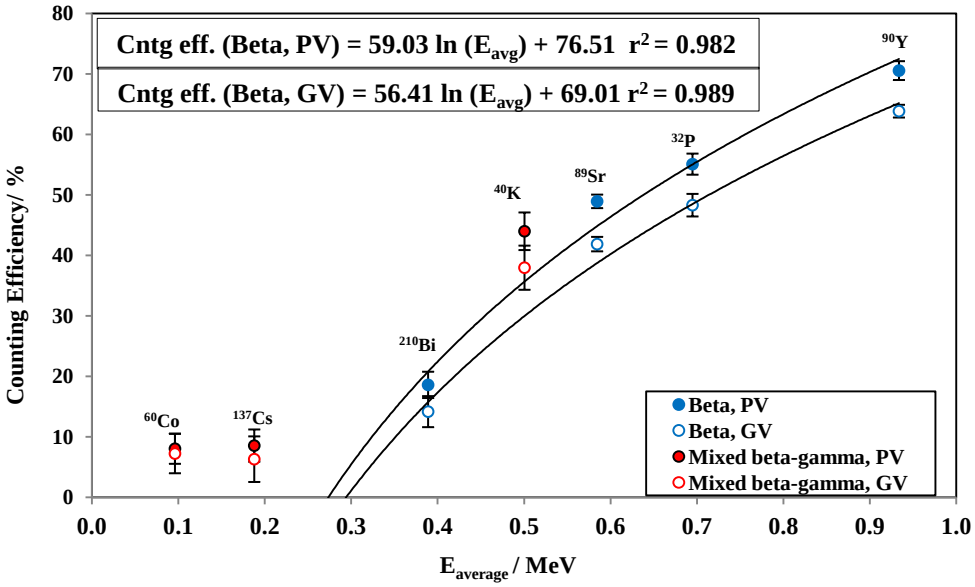

Figure 28.Čerenkov counting efficiency of different radionuclides as a function of their E_{avg} [96] measured in plastic (PV) and glass counting vials (GV). Error bars indicate combined statistical and systematic uncertainties at 1σ.

The results demonstrated that the ^{90}Y Čerenkov counting efficiency is improved by the TDCR Čerenkov counting technique. Overall, the TDCR Čerenkov efficiencies for ^{90}Y were ~ 70 % or higher, which is greater than those found in the literature under similar counting conditions, for example: 68 % [67]; 65 % [68]; 60 % [66]; 50 % [65]; 49 % [63]; 47 % [60]; and 34 % [20]. Only special conditions such as use of a wavelength shifter and dry state sample counting studies in the literature have reported enhanced Čerenkov counting efficiencies at or higher than 70 % [62, 98].

Gamma energies greater than 0.43 MeV, generally, can produce electrons with energies above the threshold energy for producing Čerenkov light (*i.e.*, 0.263 MeV in water). In the case of ^{60}Co, the exhibited Čerenkov counting efficiency is believed to be from the two strong γ ray emissions at 1.173 MeV and 1.332 MeV each with probabilities of ~ 100 %. Similarly, the ^{137}Cs γ emission of 0.6617 MeV at 85 % emission probability is believed to be strong enough to contribute to Čerenkov efficiency. Thus, the 10 % Čerenkov counting efficiency for each of ^{60}Co and ^{137}Cs is attributed to their γ emissions rather than their β^- emission. Potassium-40 efficiency is similarly augmented by its γ emission of 1.461 MeV at ~11 % emission probability. Most significantly, ^{90}Sr with E_{avg} of ~ 0.195 MeV exhibits insignificant Čerenkov counting efficiency. Thus, ^{90}Sr contribution to Čerenkov counting in the ^{90}Sr-^{90}Y equilibrium is negligible.

The decay spectra of those potentially interfering radionuclides (in Table 20) were obtained to assess their contribution to ^{90}Y Čerenkov counting, Figure 29. Their decay spectra overlapped with the ^{90}Y Čerenkov spectrum. This implies that the radionuclides that were tested can contribute to counts in the counting window of ^{90}Y Čerenkov counting (channels 50-350 on Hidex LSC) if they are present in significant quantities in the sample. Thus, a separation of ^{90}Sr-^{90}Y from other radionuclides remains desirable and is discussed in this chapter.

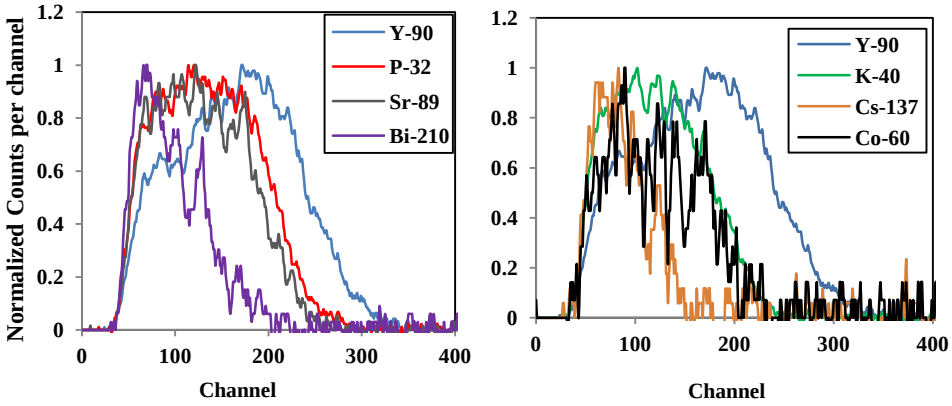

Figure 29. Comparison of spectra of pure beta emitting radionuclides to that of ^{90}Y (a) and mixed beta-gamma emitting radionuclides to that of ^{90}Y; *adapted from* [96]. The spectra were obtained by a low background Hidex LSC.

The TDCR Čerenkov counting method detection limit as in minimum detectable concentration (MDC) of ^{90}Y was determined for each sample geometry using Currie method expressed by Eq. (17) [99]:

$$\mathrm{MDC\ (Bq \cdot L^{-1})} = \frac{k^2 + 2 \cdot k \cdot \sqrt{2 \cdot B}}{T \cdot R \cdot \mathrm{E} \cdot f \cdot V} \qquad (17)$$

where k is the coverage factor [(14)] = 1.645 for a 95 % confidence interval; B is the background counts; T is the counting time (s), which was 1800 sec; R is the chemical recovery and R=1 because there was no chemical preparation involved in this method; E is the Čerenkov counting efficiency of ^{90}Y as per Eq. (12); f is the fraction of sample measured and f=1 because the entire sample was measured; and V is sample volume (L) analyzed, which ranged from 0.001 L to 0.02 L for the development of the method. For example, for SrCT4-8 with 20 mL volume, its

[(14)] The coverage factor is a value by which the combined standard uncertainty is multiplied to give the expected uncertainty [93].

corresponding blank sample SrCT4-Blk8 with 893 counts (Table K-1, Appendix K) in the ROI of ^{90}Y, counting efficiency of $\varepsilon_{Čerenkov}$ = 70.4 % in Table 16, and a counting time of 1800 sec, the MDC was obtained as shown below:

$$\text{MDC}\ (\text{Bq}\cdot\text{L}^{-1}) = \frac{(1.645)^2 + 2\,(1.645)\,\sqrt{2\,(893)}}{1800\cdot\ 1\cdot 0.704\cdot 1\cdot 0.02} = 5.59\ \text{Bq}\cdot\text{L}^{-1}$$

Thus, the MDC for 20 mL sample volume counted in plastic vial on the low background Hidex LSC for 0.5 h was found to be ~ 6 Bq·L^{-1}. The MDCs of similar volumes measured in glass vials were ~ 8 Bq·L^{-1}, which was higher than those measured in plastic vials due to lower counting efficiency of GV. Therefore, for measurement of unknown natural samples using this method, sample volumes between 18-20 mL were measured in PV (discussed in the next section).

Overall, the TDCR Čerenkov method was fast and efficient and had a moderate detection limit. Also, it was successfully employed for the determination of ^{90}Sr-^{90}Y in the freshwater and seawater samples, which are discussed next.

5.3.1.2. Freshwater and Seawater Strontium-90 and Yttrium-90 Determination Using TDCR Čerenkov Counting Technique

Approximately 20 mL of freshwater samples that were collected from various locations of the CRL site (described in Chapter 3) were measured for ^{90}Y (in equilibrium with ^{90}Sr) by a low background Hidex LSC. Most of the CRL freshwater samples were found to have ^{90}Y activity concentrations, [A_i], that were below the detection limit of the TDCR Čerenkov counting method (*i.e.*, 6 Bq·L^{-1}). Those groundwater samples that showed ^{90}Sr-^{90}Y concentrations > MDC are tabulated in Table 21 with their measured activities determined by the TDCR Čerenkov counting method. The details of sample measurements are presented in Table K-5, Appendix K.

Table 21. Freshwater ^{90}Y activity concentrations (± combined statistical and systematic uncertainties at 1σ) measured by TDCR Čerenkov counting technique on Low background Hidex LSC with a 1 h counting time

Sample code	Vol /mL	[A_i] ^{90}Y /Bq·L^{-1}	MDC /Bq·L^{-1}
AA69B	19	469±11	4.7
AA69C	19	86±5	6.1
AA69C Dup	19	78±4	5.1
AA71B	18	358±9	4.9
AA68A	18	2202±42	4.7
AA68A Dup	20	2291±44	4.2
LDA21	20	13116±239	4.2
LDA24	20	1231±22	4.2

The freshwater results shown in Table 21 demonstrated that the TDCR Čerenkov counting technique can be successfully used for natural water samples. In order to validate if the TDCR Čerenkov counting method can determine ^{90}Sr-^{90}Y in seawater, the method was challenged by colour quenching of the seawater sample. In addition, the effect of other radionuclides on seawater was examined for ^{90}Y, Table 22. Quenched seawater was prepared by adding a yellow dye into seawater samples and spiking the samples with a known amount of ^{90}Sr-^{90}Y standard as described in Chapter 4. As observed earlier in the case of quenched samples of 0.1 M HCl solution, the counting efficiency dropped as seawater quenching level increased, Figure 30. Although the counting efficiencies dramatically dropped as the level of sample quenching increased, the deviation in the measured activities, B_{ri}, was within ±6 % of expected activities, Table 22.

Table 22. Spiked and colour quenched seawater ^{90}Y activity concentrations measured by TDCR Čerenkov counting technique on Hidex LSC and a counting time of 0.5 h

Sample code	A_{ia} ^{90}Sr-^{90}Y /Bq	ε_{Cerenk} /%	A_i ^{90}Y /Bq	B_{ri} /%
SWY-Qnch 0	11.1	70.4	10.6	-5.5
SWY-Qnch 1	11.0	69.3	10.6	-4.6
SWY-Qnch 2	11.0	66.0	10.6	-4.0
SWY-Qnch 3	10.9	57.1	11.2	1.5
SWY-Qnch 4	11.0	54.6	10.9	-1.4
SWY-Qnch 5	11.0	52.1	10.9	-1.4
Mean±1σ		*62±8*		
B_r				*-2.6*
S_B				*2.6*

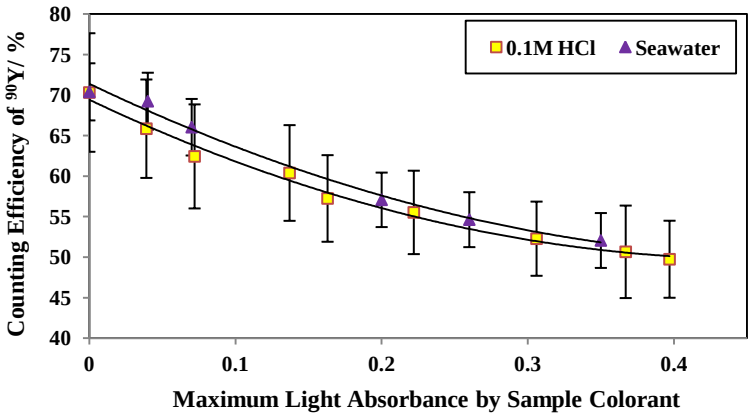

Figure 30. Comparison of counting efficiencies of seawater and freshwater as a function of maximum light absorption by yellow sample colorant measured by UV-Vis spectrophotometer. Error bars indicate combined statistical and systematic uncertainties in counting efficiencies at 1σ.

The TDCR correction for Čerenkov counting efficiency, expressed as the ratio of measured-to-expected activities is illustrated in Figure 31. Similar to 0.1 M HCl solution, the correction for seawater quenched seawater was also effective; measured activities were within ~ 5 % of expected values.

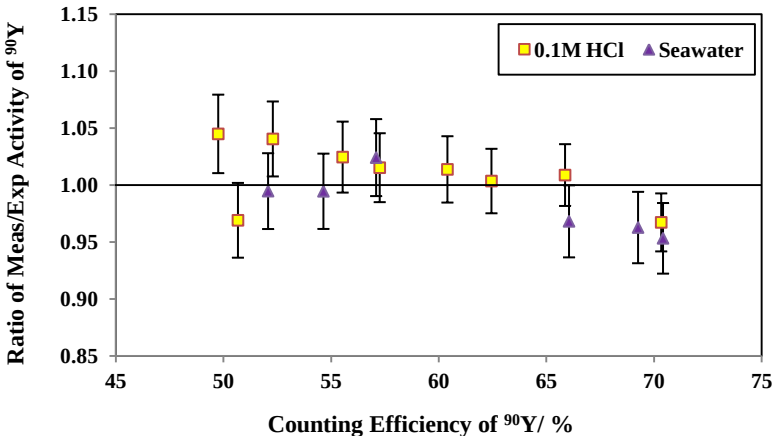

Figure 31. Ratios of measured-to-expected activities of ^{90}Y measured in coloured seawater. Error bars indicate combined statistical and systematic uncertainties in counting efficiencies at 1σ.

In addition, in parallel to freshwater method development, the effect of other radionuclides on seawater ^{90}Y was evaluated. The radionuclides measured were: ^{32}P, ^{40}K, ^{210}Pb-^{210}Bi, ^{137}Cs, and ^{60}Co. The Čerenkov counting efficiency as a function of the radionuclide E_{avg} is illustrated by Figure 32.

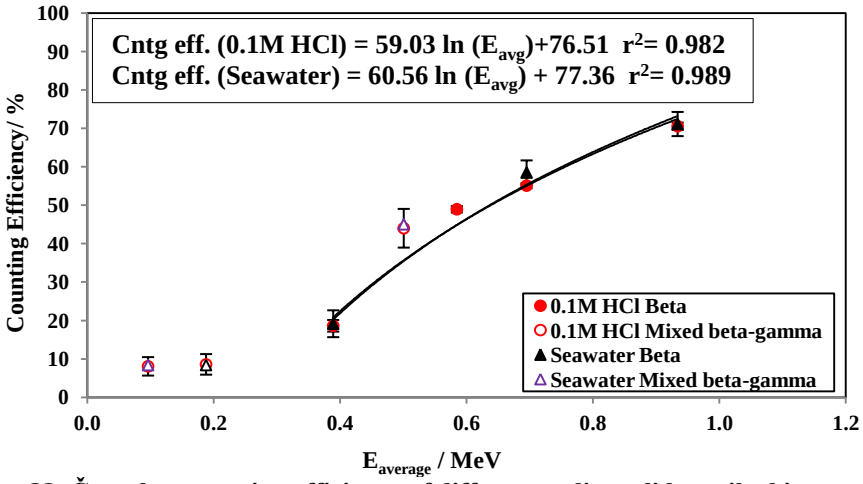

Figure 32. Čerenkov counting efficiency of different radionuclides spiked in seawater and 0.1 M HCl shown as a function of their E_{avg}. Error bars indicate combined statistical and systematic uncertainties in counting efficiencies at 1σ.

In Figure 32, the trend observed for seawater is in parallel to the trend obtained using 0.1 M HCl in the development of the method, Section 5.3.1.1. Thus, the radionuclides interference is the same for both freshwater and seawater. This interference can be low in situations where concentrations of ^{90}Sr-^{90}Y is several times higher than other high energy pure β^- or mixed β^--γ emitting radionuclides which can emit Čerenkov light, for example, in a radiological emergency event. In such events, in which often a large batch of samples are required testing, the TDCR method can be used as a screening test to segregate the high and low level samples. Those samples that screen lower than the detection limit of this method can then be rigorously analyzed for their ^{90}Sr-^{90}Y content using separation methods. Separation techniques for freshwater and sweater are discussed in the next section.

5.3.2. Determination of Freshwater and Seawater Strontium-90 and Yttrium-90 Using Radiochemical Separation Techniques

In the previous section of this chapter, it was found that due to the moderate detection limits of the TDCR Čerenkov counting technique (~ 6 Bq·L^{-1} for 20 mL and 0.5 h counting time on Hidex LSC), the technique falls short in detection of low and very low activity concentrations of ^{90}Sr-^{90}Y in water. Thus, for accurate determination of low and very low concentrations of ^{90}Sr-^{90}Y pre-concentration and isolation of ^{90}Sr-^{90}Y from matrix are required. In this section, the results for radiochemical separation of ^{90}Sr-^{90}Y are discussed. Freshwater ^{90}Sr-^{90}Y was pre-concentrated using calcium phosphate, $Ca_2(PO_4)_3$, and seawater ^{90}Sr-^{90}Y was pre-concentrated using calcium carbonate, $CaCO_3$ and hydrous titanium oxide (HTiO) co-precipitation techniques. After pre-concentration, the ^{90}Sr and ^{90}Y were extracted from the matrix on Sr-Resin® and DGA-N® resin, respectively. Table 23 and Table 24 show summary of samples that were prepared and analyzed as described in Chapter 4 and their results are discussed in this section.

Table 23. Number and type of samples analyzed using radiochemical separation techniques

	Number of samples analyzed	
	Freshwater	**Seawater**
Natural samples & duplicates analyzed without spiking	25	none
Spiked samples analyzed for method validation	10	11
^{90}Sr-^{90}Y spiked at drinking water MAC (5 Bq·L^{-1})	6	6
^{90}Sr-^{90}Y spiked at drinking water AL (30 Bq·L^{-1})	1	1
^{90}Sr-^{90}Y spiked at ~ 0.5-1 Bq·L^{-1} (several times < MAC)	2	2
^{90}Sr-^{90}Y spiked at ~ 100 Bq·L^{-1} (several times > AL)	1	1
^{90}Sr-^{90}Y spiked at other level: ~ 20 Bq·L^{-1}	0	1
Procedural blank	4	4
Total # of samples analyzed	**39**	**15**

Table 24. Experimental approach for the determination of ^{90}Sr-^{90}Y

Type of sample analyzed	Freshwater	Seawater
Natural samples & duplicates (not spiked)	25	none
Spiked samples	10	11
Procedural blank	4	4
Stable isotope for chemical yield tracing	Stable Sr and Y	Stable Sr & Y
Radioisotope for chemical yield tracing	none	^{88}Y and ^{85}Sr
Co-precipitation technique used	$Ca_3(PO_4)_2$	$CaCO_3$ and HTiO
Column separation resins	Sr-Resin® and DGA-N®	DGA-N®
Measurement techniques used	^{90}Y Čerenkov, ^{90}Y LSA, and ^{90}Sr LSA	^{90}Y Čerenkov and ^{90}Y LSA
Tracer measurement technique	ICP-MS	ICP-MS and γ-spec.

5.3.2.1. Freshwater Strontium-90 and Yttrium-90 Determination Using Radiochemical Separation Techniques

The main challenge with ^{90}Sr-^{90}Y separation comes from matrix interferences from the major dissolved cations of water, such as Na^+, K^+, Mg^{2+}, and Ca^{2+}. In the case of freshwater samples used in this dissertation, the concentrations of the major cations were from 10 to 100 times higher than natural Sr concentrations, Table 14. As per the discussions of dissolved interfering ions and their binding capabilities onto the extraction resins in Section 2.3.2, the major cations found in the water samples in this research study were below the levels that can adversely affect the separation of Sr and Y on their respective resins. The combined dissolved cations concentrations, on the other hand, may potentially interfere with accurate determination of low and very low level ^{90}Sr activity concentrations in water, if not treated. Therefore, separation of low and very low level ^{90}Sr-^{90}Y from the matrix was deemed important prior to their detection measurement. Separation of ^{90}Sr-^{90}Y in freshwater samples was performed using radiochemical methods available in literature. The ^{90}Sr-^{90}Y in water was separated from the matrix using calcium phosphate, $Ca_2(PO_4)_3$, co-precipitation followed by extraction of ^{90}Sr and ^{90}Y on Sr-Resin® and DGA-N® resin columns, respectively. The purified samples were measured on a low background Hidex LSC in four different ways in order to gain confidence in measurement results. The methods were: (i) TDCR Čerenkov counting of ^{90}Y immediately after its elution from DGA-N® resin; (ii) liquid scintillation assay (LSA) of ^{90}Y immediately after its Čerenkov counting; (iii) initial LSA measurement of ^{90}Sr immediately after its elution from Sr-Resin®; and (iv) a second measurement of the LSA sample in (iii) after the in-growth of ^{90}Y in ^{90}Sr (7-12 days after column separation of ^{90}Sr). Measurement details are presented

in Appendix L. The shape of spectral emission by each of the four different measurement techniques is illustrated by Figures 33.

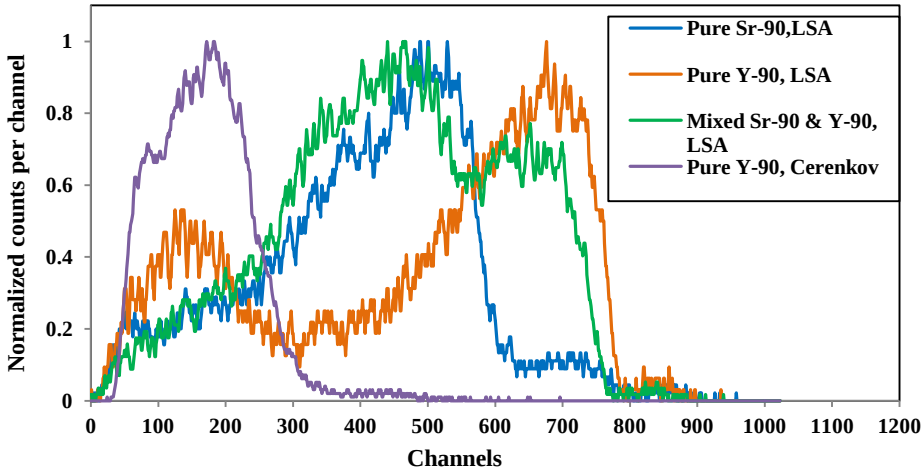

Figure 33. An example of shapes of spectra of purified ^{90}Sr-^{90}Y standard measured by four different techniques on a low background Hidex LSC

For each of the analysis techniques, the registered decay rate (also referred to as count rate) in the default counting regions of interest, ROI, (*e.g.*, ROI 50-350 for purified ^{90}Y Čerenkov counting in Figure 33) were processed for calculating the measured activities, A_i. The activity concentration of purified ^{90}Y ($A_{Y\ Cerenk}$) by Čerenkov counting technique was determined as expressed by Eq. (18). The activity concentration of purified ^{90}Y by LSA technique ($A_{Y\ LSA}$) was determined as per Eq. (19). The activity concentration of ^{90}Sr by LSA technique ($A_{Sr\ LSA}$) was determined using Eq. (20), [41].

$$[A_i] = A_{Y\ Cerenk}\ (Bq \cdot L^{-1}) = \frac{\frac{CR_s}{(\varepsilon_{Cerenk})_s} - \frac{CR_b}{(\varepsilon_{Cerenk})_b}}{R \cdot f \cdot V \cdot DY_{Cerenk}} \quad (18)$$

$$[A_i] = A_{Y\ LSA}\ (Bq \cdot L^{-1}) = \frac{\frac{CR_s}{(\varepsilon_{LSA})_s} - \frac{CR_b}{(\varepsilon_{LSA})_b}}{R \cdot f \cdot V \cdot DY_{LSA}} \quad (19)$$

$$[A_i] = A_{Sr\ LSA}\ (Bq \cdot L^{-1}) = \frac{\frac{CR_s}{(\varepsilon_{LSA})_s} - \frac{CR_b}{(\varepsilon_{LSA})_b}}{R \cdot f \cdot V \cdot (DSr_{LSA} + I_Y)} \quad (20)$$

In Eq. (18), Eq. (19), and Eq. (20): CR_s and CR_b are sample and blank count rates (cps), respectively, in the default ROI of ^{90}Y Čerenkov counting (*i.e.*, channels 50-350) in Eq. (18), and ^{90}Y and ^{90}Sr LSA (*i.e.*, channels 100-800) in Eq. (19) and Eq. (20); $(\varepsilon_{Cerenk})_s$ and $(\varepsilon_{Cerenk})_b$ are sample and blank Čerenkov counting

efficiencies, respectively; *R* is the chemical recovery*; f* is the fraction of sample measured; and *V* is the volume (L) of water analyzed. In Eq. (18), ε_{Cerenk} is the TDCR Čerenkov counting efficiency obtained as per Eq. (12); and DY_{Cerenk} is ^{90}Y Čerenkov decay factor as per $DY_{Cerenk}=e^{-(T_1-T_0)\cdot\lambda_Y}$, where T_0 is the time (sec) of the end of extraction of ^{90}Y on the DGA-N® and ^{90}Sr on the Sr-Resin® (simultaneous extraction), T_1 is the start of Čerenkov counting of ^{90}Y on the Hidex LSC (see Appendix I), and λ_Y is ^{90}Y decay constant (sec^{-1}). In Eq. (19) and Eq. (20), ε_{LSA} is the LSA counting efficiency and is proportional to the ratio of triple-to-double coincidence counts, TDCR, with the proportionality factor between TDCR and ε_{LSA} of 1. In Eq. (19), DY_{LSA} is the decay factor of ^{90}Y, $DY_{LSA}=e^{-(T_2-T_0)\cdot\lambda_Y}$, where T_2 represents the time (sec) of start of LSA of ^{90}Y on the Hidex LSC. In Eq. (20), DSr_{LSA} is the decay factor of ^{90}Sr LSA, $DSr_{LSA}=e^{-(T_3-T_0)\cdot\lambda_{Sr}}$, where T_3 represents the time (sec) of start of LSA of ^{90}Sr on the Hidex LSC, and λ_{Sr} is ^{90}Sr decay constant (sec^{-1}); and I_Y is the in-growth factor of ^{90}Y from ^{90}Sr and is obtained as per Eq. (21), [41]:

$$I_Y = \frac{\lambda_Y}{\lambda_Y - \lambda_{Sr}} \times \left(e^{-\lambda_{Sr}\cdot(T_3-T_0)} - e^{-\lambda_Y\cdot(T_3-T_0)}\right) \quad (21)$$

Depending on the method of analysis, the value for *f* was slightly different. In the Čerenkov counting, $f=1$ because in this method the entire eluted sample was measured. In the LSA method, because a small aliquot was removed for the recovery analysis, therefore, $f \leq 0.95$.

The chemical recovery, *R*, was determined from the ratio of the initial amounts of the analyte in the sample (*i.e.*, Sr_i or Y_i) to that of the final amounts (*i.e.*, Sr_f or Y_f) that were determined by ICP-MS as per Eq. (22). The chemical recoveries of Sr and Y are tabulated in Table 25.

$$R\,(\%) = \left(\frac{Y_i}{Y_f}\right)\cdot 100 \quad (22)$$

The chemical recovery of both Sr and stable Y were consistently high. Mean chemical recovery (±1 σ) of the stable Sr and Y in the purified sample (unknown samples, spiked samples, and procedural blank samples combined) were 81±13 % and 83±10 %, respectively. Higher chemical recoveries (*i.e.*, > 83) would have been attainable had precipitation occurred at pH >10. However, higher pH conditions can also produce massive precipitates and time demanding dissolution steps, which can consequently delay sample turnaround time. The chemical recoveries were used to correct for the loss of the analyte during the radiochemical separation procedure.

Table 25. Chemical recoveries of stable Sr and Y tracers in freshwater samples

Sample code	Sr_R [15] /%	Y_R [16] /%	Sample code	Sr_R /%	Y_R /%
PL1-1	95.3±4.1	80.7±4.0	B-WS	81.2±6.0	81.4±4.0
PL1-3	93.6±4.7	68.2±3.5	AA69B	80.0±3.9	78.4±4.1
PL1-3Dup	80.6±3.8	84.3±4.0	AA69C	81.2±5.0	100±5.2
PL1-5	57.2±2.9	83.4±4.0	AA69CDup	81.2±4.8	82.3±4.1
PL1-6	81.2±6.0	82.4±3.9	AA71B	82.3±1.6	71.6±3.7
PL1-7	62.5±3.2	86.4±4.5	Spike 1	89.3±4.5	63.1±3.1
PL1-8	50.5±2.5	82.0±4.3	Spike 2	90.1±4.9	100±5.2
PL2-8	100±5.9	84.4±4.3	Spike 3	77.5±4.1	81.7±4.2
LBL1-1	81.2±6.0	88.9±5.0	Spike 4	95.6±4.2	81.9±3.9
LBL1-1Dup	50.0±3.0	80.0±4.0	Spike 5	87.2±4.2	80.6±4.0
LBL1-3	100±3.7	85.9±4.4	Spike 6	79.3±4.0	80.0±3.8
LBL2-3(Dup)	94.9±4.0	84.7±4.1	Spike 7	87.5±4.0	86.5±3.8
LBL1-4	94.4±3.9	77.6±3.7	Spike 8	100±5.6	80.5±3.7
LBL1-5	76.5±3.8	100±5.0	Spike 9	88.7±4.2	84.7±4.5
LBL1-7	98.9±4.9	76.7±3.4	Spike 10	66.8±3.1	84.4±4.2
LBL1-7Dup	78.5±4.0	86.1±4.3	MethodBlank 1	81.3±5.6	76.6±3.7
LBL1-8	81.3±5.3	60.2±3.0	MethodBlank 2	63.8±3.1	96.1±4.6
ORD1-1	81.2±6.0	81.4±4.0	MethodBlank 3	81.2±5.0	100±5.2
ORD1-2	81.2±6.0	100±5.0	MethodBlank 4	78.6±4.0	75.7±3.8
ORD1-3	59.0±2.2	63.0±3.0			
Mean±1σ		**Sr_R: 81±13%**	**Y_R: 83±10%**		

The method performance was evaluated using spiked deionized water in the range of 0.75 $Bq{\cdot}L^{-1}$ to ~ 99 $Bq{\cdot}L^{-1}$, Table 26. The bias and precision in measured activities of spiked samples were determined to delineate accuracy and repeatability of the method, respectively, and are shown in Table 26. Relative bias for individual sample measurements (B_{ri}) was obtained as per Eq. (15). Replicates of six spiked samples at approximately 5 $Bq{\cdot}L^{-1}$, were used to show the bias in the six replicate measurements, which is shown as B_r in Table 26. The relative precision (S_B) was also calculated as per Eq. (16) to show the dispersion in B_r of the six replicates. The B_{ri} of all four measurement methods was in the range of -16 to 9 %, which is within ±20 % acceptance criteria for effluent monitoring of CRL site [100].

[15] Sr_R = Chemical recovery of stable Sr
[16] Y_R = Chemical recovery of stable Y

Table 26. ^{90}Y and ^{90}Sr determined in spiked freshwater samples after radiochemical separation. Four methods of measurement were used.

Measurement method		**^{90}Y Čerenkov**		**^{90}Y LSA**		**^{90}Sr LSA (1)**		**^{90}Sr LSA (2)**	
Method code		(i)		(ii)		(iii)		(iv)	
Sample code	$[A_{ia}]^{90}Sr$-^{90}Y /Bq·L^{-1}	$[A_i]^{90}Y$ /Bq·L^{-1}	B_{ri} /%	$[A_i]^{90}Y$ /Bq·L^{-1}	B_{ri} /%	$[A_i]^{90}Sr$ /Bq·L^{-1}	B_{ri} /%	$[A_i]^{90}Sr$ /Bq·L^{-1}	B_{ri} /%
Spike 1	4.36	4.51	3.6	4.00	-7.0	3.86	-11	3.92	-9.9
Spike 2	4.91	4.84	-1.4	4.72	-3.1	4.73	-3.5	4.41	-10
Spike 3	5.41	5.51	1.8	5.32	-0.6	5.91	9.2	5.67	4.7
Spike 4	6.49	5.46	-16	5.64	-13	5.63	-13	5.65	-13
Spike 5	6.43	5.67	-12	5.79	-9.7	5.52	-14	5.52	-14
Spike 6	6.21	5.35	-14	5.49	-11	5.21	-16	5.28	-15
Spike 7	0.75	0.65	5.7	0.59	-4.5	0.71	-6.3	0.77	1.8
Spike 8	1.15	1.10	-4.2	1.03	-9.5	0.99	-14	0.99	-14
Spike 9	24.2	23.1	-4.6	23.8	-1.6	24.4	0.8	24.3	0.3
Spike 10	99.5	95.0	-4.4	98.7	-0.25	94.0	-5.5	93.2	-6.3
B_r			-6.2		-7.3		-8.2		-9.6
S_B			8.5		4.7		9.6		7.3

Note: Shaded area represents reproducibility test samples and their statistics.

In addition to precision and bias, method linearity was also demonstrated over a range from 0.75 Bq·L^{-1} to ~ 100 Bq·L^{-1}. This range was selected to cover a linear dynamic range several times lower and higher than the drinking water maximum acceptable concentration (MAC) of 5 Bq·L^{-1} [14] and action level (AL) of 30 Bq·L^{-1} [15] as the Canadian drinking water guidelines. The range also covered MAC of 10 Bq·L^{-1} as per the World Health Organization (WHO) guidelines for drinking water [101]. The linearity of the four measurement methods was analyzed and shown in Figure 34a for ^{90}Y and in Figure 34b for ^{90}Sr measurements. Figure 34 is plotted using logarithm scale in order to better illustrate the wide range of data points.

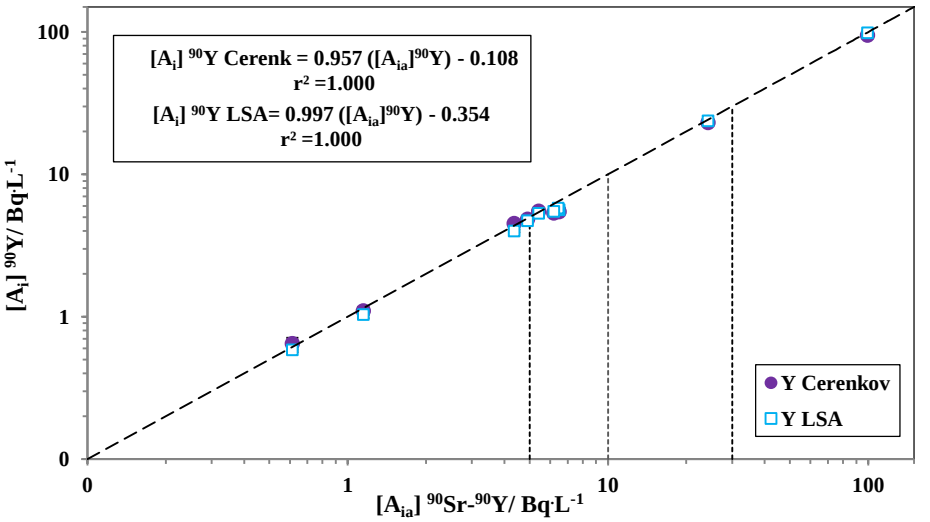

(a)

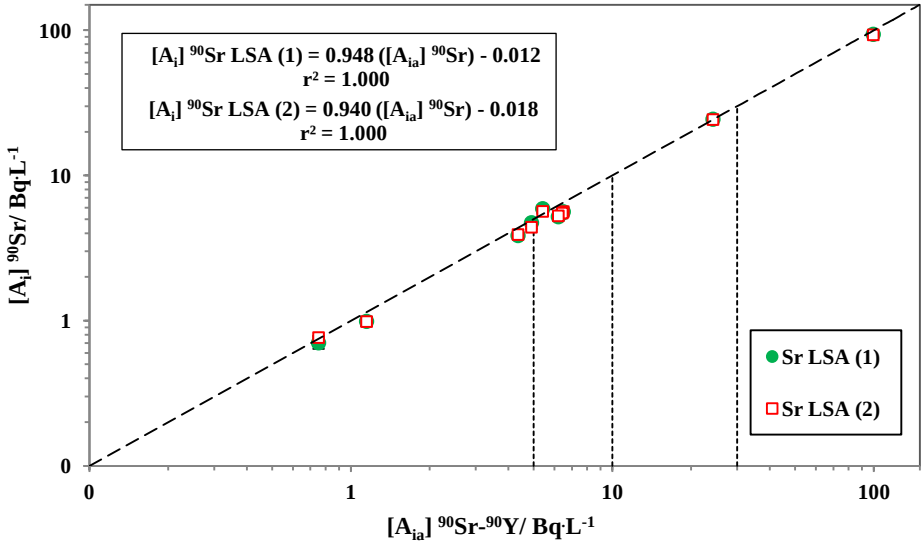

(b)

Figure 34. An illustration of freshwater spiked samples' measured activity concentrations, $[A_i]$, as a function of expected activity concentrations, $[A_{ia}]$. The $[A_i]$ of ^{90}Y by Čerenkov counting and LSA are shown in (a) and $[A_i]$ of ^{90}Sr by LSA are shown in (b). Diagonal hatched lines represents 1:1 ratio between $[A_i]$ and $[A_{ia}]$. Vertical hatched lines from left to right show regulatory limits for ^{90}Sr in drinking water at 5 $Bq{\cdot}L^{-1}$ (Health Canada), 10 $Bq{\cdot}L^{-1}$ (WHO), and 30 $Bq{\cdot}L^{-1}$ (Health Canada action level). The error bars (too small to show on log scale plot) represent combined statistical and systematic uncertainties at 1σ.

A linear regression model y = a +b*x was achieved with the "best line" with r^2 value of 1.000 for all methods of ^{90}Y measurement (Figure 34). In order to determine the spread on the constant "a" and slope "b" of the best line, the expressions for the standard deviation of the slope σ_b and the standard deviation of the intercept σ_a at 95 % confidence interval were obtained using standard methods of regression analysis [102]. The uncertainties in slope and intercept for each of the methods are shown in Table 27. The small uncertainties in the slope and constant values of the line of best fit indicate that excellent linearity between expected and measured activities was established.

Table 27. Regression analysis of line of best fit for measured activities of ^{90}Y

Measurement Method	Best line regression	r^2	b±σ	a±σ
^{90}Y Čerenkov	$[A_i] = 0.957 ([A_{ia}]) - 0.108$	1.000	0.957±0.010	- 0.108±0.330
^{90}Y LSA	$[A_i] = 0.997 ([A_{ia}]) - 0.354$	1.000	0.997±0.007	- 0.354±0.232
^{90}Sr LSA(1)	$[A_i] = 0.948 ([A_{ia}]) - 0.012$	1.000	0.948±0.018	- 0.012±0.590
^{90}Sr LSA(2)	$[A_i] = 0.940 ([A_{ia}]) - 0.018$	1.000	0.940±0.017	- 0.018±0.563

For the spiked deionized water samples measured by the four different methods mentioned above, a two-tailed paired-t-test was conducted to evaluate the difference in the ^{90}Y measured activities. The null hypothesis was stated that at 5 % significance level the differences in paired measurement methods are not significant. The statistical results showed that probability (p) values were greater than 0.05 at each paired measurement, Table 28. Therefore, the null hypothesis was not rejected and it was stated that the paired measurements were not statistically different from each other.

Table 28. Statistical test of two-tailed paired t-test for freshwater spiked samples at 5 % significance level

Paired measurement method	p-value	$[A_i]$ significantly different:
(^{90}Y Čerenkov) & (^{90}Y LSA); (i) & (ii)	0.34	No
(^{90}Y Čerenkov) & (^{90}Sr LSA (1)); (i) & (iii)	0.93	No
(^{90}Y Čerenkov) & (^{90}Y LSA (2)); (i) & (iv)	0.56	No
(^{90}Y LSA) & (^{90}Sr LSA(1)); (ii) & (iii)	0.43	No
(^{90}Y LSA) & (^{90}Sr LSA (2)); (ii) & (iv)	0.37	No
(^{90}Sr LSA (1)) & (^{90}Sr LSA (2)); (iii) & (iv)	0.17	No

In parallel with spiked samples, the unknown freshwater samples that were collected from the CRL site were measured using the four measurement methods discussed earlier and the results are tabulated in Table 29.

Table 29. ^{90}Sr and ^{90}Y measured activities (± combined statistical and systematic uncertainties at 1σ) determined in natural fresh water samples using four different methods of measurement on a low background Hidex LSC. Counting time was 1 h with exception of a few measured by Čerenkov counting for 0.5 h (shaded).

Measurement method	**^{90}Y Čerenkov**		**^{90}Y LSA**		**^{90}Sr LSA (1)**		**^{90}Sr LSA (2)**	
Measurement method code	(i)		(ii)		(iii)		(iv)	
Sample code[17]	$[A_i]^{90}$Y /Bq·L^{-1}	MDC /Bq·L^{-1}	$[A_i]^{90}$Y /Bq·L^{-1}	MDC /Bq·L^{-1}	$[A_i]^{90}$Sr /Bq·L^{-1}	MDC /Bq·L^{-1}	$[A_i]^{90}$Sr /Bq·L^{-1}	MDC /Bq·L^{-1}
PL1-1	6.51±0.11	0.103	6.44±0.07	0.080	5.92±0.08	0.081	6.07±0.09	0.079
PL1-3	6.45±0.11	0.080	6.48±0.06	0.063	4.72±0.07	0.063	5.50±0.09	0.062
PL1-3Dup	6.10±0.08	0.075	6.53±0.07	0.078	6.48±0.08	0.080	6.34±0.10	0.078
PL1-5	6.31±0.08	0.075	6.52±0.07	0.078	6.58±0.08	0.080	6.37±0.10	0.077
PL1-6	6.71±0.11	0.088	6.00±0.06	0.061	6.18±0.07	0.062	6.37±0.09	0.062
PL1-7	6.12±0.08	0.075	6.31±0.07	0.079	6.63±0.08	0.081	6.17±0.10	0.078
PL1-8	6.26±0.08	0.077	6.49±0.07	0.080	6.23±0.08	0.080	6.10±0.10	0.077
PL2-8(Dup)	6.12±0.08	0.075	6.32±0.07	0.079	6.05±0.08	0.081	5.78±0.09	0.079
LBL1-1	0.21±0.07	0.140[18]	0.28±0.03	0.057	0.35±0.03	0.057	0.34±0.03	0.055
LBL1-1 Dup	0.37±0.04	0.094	0.37±0.04	0.090	0.41±0.05	0.091	0.38±0.05	0.087
LBL1-3	0.34±0.04	0.087	0.43±0.04	0.089	0.39±0.05	0.091	0.39±0.05	0.087
LBL2-3(Dup)	0.48±0.04	0.088	0.46±0.04	0.088	0.37±0.04	0.088	0.35±0.05	0.085
LBL1-4	0.32±0.06	0.120	0.41±0.04	0.089	0.33±0.04	0.091	0.36±0.05	0.087

[17] Sample codes having "(Dup)", with brackets, represent field duplicate samples and "Dup", without brackets, indicate laboratory duplicate analysis of the same sample.

[18] MDC value is slightly higher because the sample was counted on a different Hidex LSC, which had a slightly higher background than the low-background Hidex LSC, which was used for measurement of all other samples. This MDC value was not included in the mean calculation.

Table 29 Continues

Measurement method	**^{90}Y Čerenkov**		**^{90}Y LSA**		**^{90}Sr LSA (1)**		**^{90}Sr LSA (2)**	
Measurement method code	(I)		(II)		(III)		(IV)	
Sample code	$[A_i]^{90}Y$ /Bq·L^{-1}	MDC /Bq·L^{-1}	$[A_i]^{90}Y$/ /Bq·L^{-1}	MDC /Bq·L^{-1}	$[A_i]^{90}Sr$ /Bq·L^{-1}	MDC /Bq·L^{-1}	$[A_i]^{90}Sr$ /Bq·L^{-1}	MDC /Bq·L^{-1}
LBL1-5	0.28±0.07	0.140[18]	0.30±0.03	0.057	0.30±0.03	0.057	0.39±0.03	0.058
LBL1-7	0.56±0.03	0.100	0.34±0.03	0.070	0.27±0.04	0.068	0.34±0.04	0.0657
LBL1-7 Dup	0.45±0.04	0.090	0.44±0.04	0.089	0.47±0.05	0.091	0.41±0.05	0.087
LBL1-8	0.44±0.05	0.101	0.36±0.03	0.070	0.24±0.04	0.070	0.30±0.04	0.066
ORD1-1	< MDC	0.160	<MDC	0.053	<MDC	0.023	<MDC	0.066
ORD1-2	0.15±0.04	0.130	<MDC	0.075	<MDC	0.077	<MDC	0.073
ORD1-3	< MDC	0.140	<MDC	0.050	<MDC	0.028	<MDC	0.066
B-WS	<MDC	0.140	0.13±0.03	0.072	<MDC	0.075	<MDC	0.070
AA69B	488±20	0.070	471±15	0.050	518±22	0.080	507±32	0.080
AA69C	92.0±5.1	0.080	86.6±4.6	0.060	82.0±6.0	0.090	85.2±7.0	0.090
AA69C Dup	84.1±4.8	0.080	80.7±4.4	0.060	97.8±5.3	0.080	99.9±7.9	0.080
AA71B	343±14	0.070	333±11	0.050	364±17	0.080	360±24	0.080
Method Blank 1	0.17±0.05	0.130	<MDC	0.070	<MDC	0.080	<MDC	0.080
Method Blank 2	<MDC	0.120	<MDC	0.070	<MDC	0.070	<MDC	0.070
Method Blank 3	0.21±0.03	0.100	<MDC	0.070	<MDC	0.110	<MDC	0.130
Method Blank 4	<MDC	0.140	<MDC	0.097	<MDC	0.100	<MDC	0.100
MDC: Mean±1σ	***0.081±0.023 (1 h)*** ***0.130±0.009 (0.5 h)***		***0.072±0.014***		***0.076±0.018***		***0.078±0.015***	

Note: The results for PL1-3 LSA (1) and LBL1-7 measured by ^{90}Y Čerenkov counting was artificially lower and higher, respectively compared to other methods of measuremnt. The Instrument electronics may have contributed to these variations.

The MDCs for the 1 L freshwater samples and procedural blanks were determined as per Eq. (17), Table 29. The mean MDC for ^{90}Y measured by Čerenkov counting was 0.13 Bq·L^{-1} for 0.5 h counting time and 0.08 Bq·L^{-1} for 1 h counting time on the Hidex LSC. The MDC for ^{90}Y measured by LSA was 0.07 Bq·L^{-1} for a counting time of 1 h. The MDC for ^{90}Sr measured by LSA was 0.08 Bq·L^{-1}, for both the first and second measurements, for a counting time of 1 h. The MDC for Čerenkov counting method with counting time of 0.5 h was slightly higher due to shorter counting time, as expected. However, this MDC at 0.13 Bq·L^{-1} was still only at ~ 3 % of the MAC of 5 Bq·L^{-1}. This implies that if longer counting times are not achievable, the Čerenkov counting method with a counting time of 0.5 h can reliably be used for the detection of very low concentrations of ^{90}Sr-^{90}Y.

The activity concentrations of the water samples measured using the four measurement methods were very similar. The Ottawa River water samples were either below or very close to the detection limit. The very low concentrations that were found in the three samples indicated that the measurement techniques developed in this dissertation cannot precisely determine such low concentrations of ^{90}Sr-^{90}Y in the Ottawa River water. Therefore, the analysis of the remainder of the Ottawa River water samples was not attempted. In the Perch Lake and Lower Bass Lake water samples, the ^{90}Sr and ^{90}Y activity concentrations that were found were sufficiently above the MDCs, and therefore, can be reliably reported. In addition, the determination of the activity concentrations using the four different methods provided confidence in the results. To demonstrate that the activities determined from the four measurement methods were not significantly different, a two-tailed paired-t-distribution test was conducted at 5 % significance level. The statistical results showed that p-values were greater than 0.05 at each paired measurement, Table 30. Therefore, the paired measurements were not found to be statistically different at 95 % confidence interval.

Table 30. Statistical test results of the two-tailed paired t-distribution for natural freshwater samples at 5 % significance level

Paired measurement method	Perch Lake p-value	L. Bass Lake p-value	[A_i] significantly different:
(^{90}Y Čerenkov) & (^{90}Y LSA); (I) & (II)	0.95	0.95	No
(^{90}Y Čerenkov) & (^{90}Sr LSA (1)); (I) & (III)	0.41	0.59	No
(^{90}Y Čerenkov) & (^{90}Y LSA (2)); (I) & (IV)	0.12	0.87	No
(^{90}Y LSA) & (^{90}Sr LSA(1)); (II) & (III)	0.26	0.22	No
(^{90}Y LSA) & (^{90}Sr LSA (2)); (II) & (IV)	0.06	0.67	No
(^{90}Sr LSA (1)) & (^{90}Sr LSA (2)); (III) & (IV)	0.93	0.28	No

A comparison of the activity results obtained by the TDCR Čerenkov counting method and column separation method would have provide additional verification in the results of the unknown freshwater samples that were collected from the CRL

site. However, a vast majority of the natural water samples were below the detection limit of the TDCR Čerenkov counting method, 6 $Bq{\cdot}L^{-1}$. Thus, they could not be used for this comparison. Only a small number of samples, which were above the detection limit of the TDCR Čerenkov counting technique and were also measured using radiochemical separation, were available to be compared. Table 31 and Figure 35 show a comparison of all methods.

Table 31. Comparison of ^{90}Sr-^{90}Y activity concentrations (± uncertainties at 1σ) of natural freshwater samples obtained from five different measurement methods

Method	None-purified $TDCR_{Čerenk}$	Purified (radiochemical separation)			
		$TDCR_{Čerenk}$	LSA	LSA (1)	LSA (2)
Sample code	$[A_i]^{90}Y$-^{90}Sr /$Bq{\cdot}L^{-1}$	$[A_i]^{90}Y$ /$Bq{\cdot}L^{-1}$	$[A_i]^{90}Y$ /$Bq{\cdot}L^{-1}$	$[A_i]^{90}Sr$ /$Bq{\cdot}L^{-1}$	$[A_i]^{90}Sr$ /$Bq{\cdot}L^{-1}$
AA-69-B	469±13	488±20	471±15	518±22	507±32
AA-69-C	86±7	92±5	87±5	98±6	100±8
AA-69-C Dup	78±7	84±5	81±4	82±5	85±7
AA-71-B	358±11	343±14	333±11	364±17	360±24

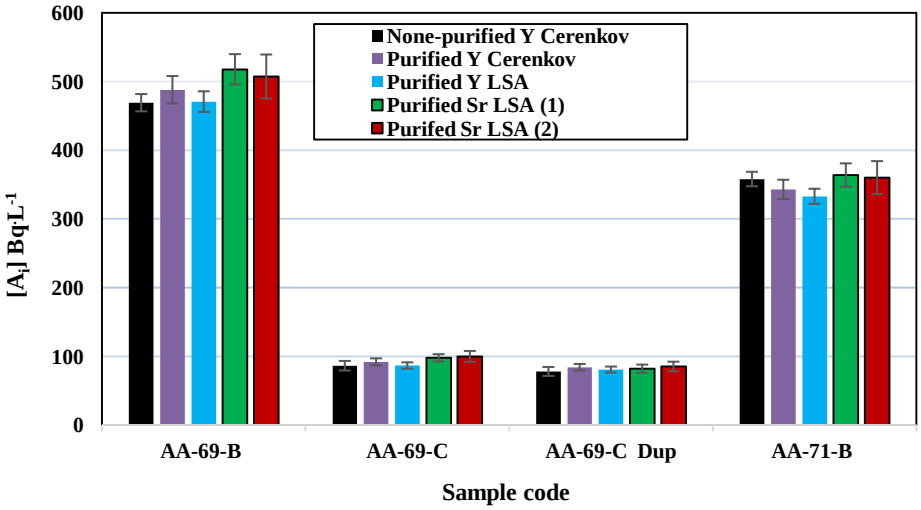

Figure 35. Comparison of ^{90}Sr-^{90}Y measured activity concentrations in unknown freshwater samples using five different measurement methods. Error bars indicate combined statistical and systematic uncertainties at 1σ.

The statistical test of two-tailed paired t-distribution test was performed to evaluate whether or not the activity concentrations of those samples that were analyzed using all five measurement methods were significantly different. The null hypothesis was stated that the differences in activity concentration found from each paired measurement method were not significant from each other at 5 % significance level. The statistical results demonstrated that the p-values were

greater than 0.05 for all pairs, Table 32. Therefore, it was concluded that the five measurement methods were not statistically different from each other.

Table 32. Statistical test of two-tailed paired t-test at 5 % significance level for natural freshwater samples measured using 5 different methods

Paired Measurement Method	p-value	$[A_i]$ different from $[A_{ia}]$:
None-purified ^{90}Y Čerenkov & purified ^{90}Y Čerenkov	0.62	No
None-purified ^{90}Y Čerenkov & purified ^{90}Y LSA	0.50	No
None-purified ^{90}Y Čerenkov & purified ^{90}Sr LSA (1)	0.20	No
None-purified ^{90}Y Čerenkov & purified ^{90}Sr LSA (2)	0.15	No
^{90}Y Čerenkov & ^{90}Y LSA	0.06	No
^{90}Y Čerenkov & ^{90}Sr LSA (1)	0.16	No
^{90}Y Čerenkov & ^{90}Y LSA (2)	0.07	No
^{90}Y LSA & ^{90}Sr LSA (1)	0.11	No
^{90}Y LSA & ^{90}Sr LSA (2)	0.06	No
^{90}Sr LSA (1) and ^{90}Sr LSA (2)	0.53	No

The results and discussion provided in the present section demonstrated that both ^{90}Sr and ^{90}Y methods offer comparable, accurate, and efficient methods for the determination of low, moderate, and high ^{90}Sr and ^{90}Y radioactivity concentrations in freshwater. Thus, either of the ^{90}Sr and ^{90}Y methods can be implemented for routine monitoring of ^{90}Sr in surface water and groundwater of CRL site of CNL with concentrations above the detection limits described. For some locations, for example, the Ottawa River water, the current methods are unavoidably incapable of detecting the very low concentrations (*i.e.*, ≤ 0.08 Bq·L^{-1}) of ^{90}Sr-^{90}Y. However, the procedures can be expanded to accommodate larger sample volumes and increased counting times, which theoretically should offer improved detection capabilities. As such, further experimentation is required to demonstrate if such adaptations of the current method can practically offer any improvements. Further examinations, however, are not in the scope of the present dissertation.

5.3.2.2. Seawater Yttrium-90 Determination Using Radiochemical Separation Techniques

The determination of ^{90}Sr in seawater is far more challenging than freshwater due to the increased concentrations of dissolved constituents, which interfere with radiochemical separation or Sr and Y. The chemical characterization of seawater that was used in this dissertation found the concentrations of the major cation Na^+, Mg^{2+}, K^+, and Ca^{2+} to be at 9100 mg·L^{-1}, 1140 mg·L^{-1}, 310 mg·L^{-1}, and 290 mg·L^{-1}, respectively, Table 14. The dissolved Na^+ and K^+ are not expected to co-precipitate with Sr and Y and, therefore, are less interfering to Sr analysis. The main

interfering species are Mg^{2+} and Ca^{2+}, which due to their chemical similarities to Sr, co-precipitate with Sr. In the present dissertation, in which seawater ^{90}Sr was determined from ^{90}Y at equilibrium concentrations, a two-step co-precipitation using ($CaCO_3$) and hydrous titanium oxide (HTiO) removed residual salt contents including excess amounts of Ca^{2+} and Mg^{2+}.

$CaCO_3$ co-precipitation has advantages over calcium phosphate ($Ca_3(PO_4)_2$), which is also commonly used for precipitation of Sr-Y in environmental samples (*e.g.*, in [33, 103]), because the uptake of excessive amounts of Ca and also Mg by CO_3^{2-} is unfavourable. The uptake of unwanted cations can also be minimized by carefully controlling the pH of the precipitating solutions at both $CaCO_3$ and HTiO precipitation stages. For these reasons, a $CaCO_3$ precipitation method was explored in the present work. In a preliminary experiment the pH dependency of ^{90}Y uptake was examined. In this experiment, samples of 40 mL seawater spiked with known amounts of ^{90}Sr-^{90}Y standard solution were processed at different pH conditions and ^{90}Y in the precipitates measured. In the $CaCO_3$ co-precipitation step, although the uptake of ^{90}Y by the precipitate was above 90 % at all pH conditions evaluated, the precipitate weight increased in a linear fashion as pH increased from 8.5 to 12.5, Figure 36a. Because it was very important to minimize the mass of the final precipitate, the pH for this step of the precipitation was adjusted to no more than pH 10 at which the ^{90}Y uptake was above 95 %. Similarly, the optimal pH of the HTiO co-precipitation for the minimum mass of HTiO co-precipitate and maximum ^{90}Y recovery was investigated. For this test, all other conditions, including pH of the first co-precipitation, was kept constant. The optimal pH at which the uptake of the ^{90}Y was ~ 90 % was achievable with pH of 8-9.5, Figure 36b. The careful control of pH at the precipitation steps and the use of HTiO enabled selective uptake of Y from the seawater and its separation from Ca and Mg, majority of which remained in the supernatant in the second stage of the co-precipitation. As a result, the wet weight of the final precipitate formed from 1 L seawater was on average less than 10 g, which was small enough to re-dissolve in a sufficiently small volume of HNO_3 solution for purification on a single DGA-N® resin column. Thus, the addition of Ti^{3+} not only removed residual salt content, but it also effectively pre-concentrated Y. The Ti^{3+}, which has a purple colour in $TiCl_3$ solution, is a strong reducing agent. Upon addition to the acidic matrix, the Ti^{3+} immediately oxidized to Ti^{4+}, which was indicated by its immediate loss of colour and formation of white precipitate. Formation of a white precipitate eliminates the potential for colour quenching interferences if Čerenkov counting is to be performed at this stage. Also, the Ti^{4+} does not cause interference during radiochemical separation on the DGA-N® resin because it does not tend to bind onto the DGA-N® resin [104].

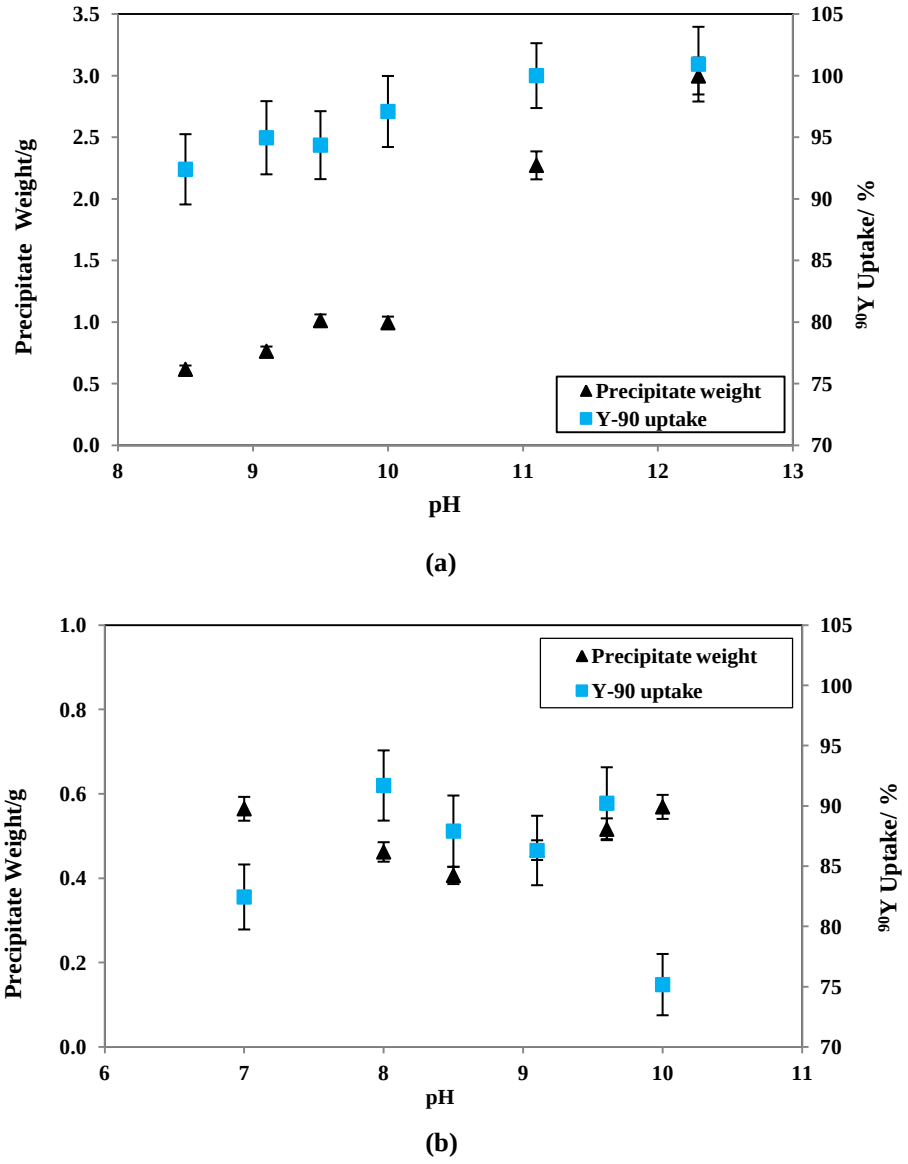

Figure 36. $CaCO_3$ precipitate weight and ^{90}Y uptake as a function of pH (a) and HTiO precipitate weight and ^{90}Y uptake as a function of pH (b); *adapted from* [105]

In the present method unlike Y, the Sr uptake by $CaCO_3$ was found to be low. Maximum uptake of Sr by $CaCO_3$ co-precipitation was found to be ~ 60 %. Such low yield presented itself as the main challenge in the direct determination of seawater ^{90}Sr. Therefore, indirect determination of ^{90}Sr from ^{90}Y was pursued instead.

After their separation and purification on the DGA-N® resins, the purified samples were measured on a low background Hidex LSC by TDCR Čerenkov counting of ^{90}Y immediately after its elution from DGA-N® resin and also by subsequent liquid scintillation assay (LSA) of ^{90}Y. The two independent measurement offered reliability in results. In addition, further verification was also achieved by both stable and radiotracing of Sr and Y. The chemical recovery was traced in five different ways at various stages of the procedure: (i) tracing stable Y in the $CaCO_3$ and HTiO co-precipitates and purified samples; (ii) tracing stable Sr in the $CaCO_3$ and HTiO co-precipitates and purified samples; (iii) tracing ^{88}Y using its γ emission in the $CaCO_3$ and HTiO co-precipitates and purified samples; (iv) tracing ^{88}Y using its electron capture (EC) emission by LSA in the purified samples; and (v) tracing ^{85}Sr using its γ emission in the $CaCO_3$ and HTiO co-precipitates and purified samples.

The stable Y and Sr chemical recoveries were determined from the ratio of the initial amount of the analyte (*i.e.,* Sr or Y) to that of the final amounts as per Eq. (22). The Sr and Y contents of seawater samples were analyzed by ICP-MS. The details of stable Y and stable Sr chemical recoveries are shown in Tables L-5 and Table L-6, respectively, in Appendix L. A summary of chemical recovery results for all methods of analyses are shown in Table 33. The chemical recovery of stable Y was consistently high in all stages of the procedure. Mean chemical recovery of stable Y in the $CaCO_3$, HTiO, and purified spiked and blank seawater samples (n=15) were 93±3 %, 94±7 %, and 88±7 %, respectively. Natural Sr content of seawater, which was found to be 7.0±0.5 $mg \cdot L^{-1}$ on average (n=15) (See Table L-6, Appendix L), was also traced throughout the procedure in spiked and blank seawater samples. On average, 48±7 % stable Sr precipitated by $CaCO_3$ and only 22±4 % remained in the HTiO co-precipitate. As expected, no Sr was detected in purified samples.

Table 33. Chemical recoveries measured in seawater samples at various stages of the procedure

		$CaCO_3$ precipitate				HTiO precipitate			
Method of tracing chemical recovery (R)		**Stable Y ICP-MS**	**^{88}Y γ-spec**	**Stable Sr ICP-MS**	**^{85}Sr γ-spec**	**Stable Y ICP-MS**	**^{88}Y γ-spec**	**Stable Sr ICP-MS**	**^{85}Sr γ-spec**
Sample code	**$[A_{ia}]^{90}$Sr-^{90}Y /Bq·L^{-1}**	**Y_R /%**	**$^{88}Y_R$ [19] /%**	**Sr_R /%**	**$^{85}Sr_R$ [20] /%**	**Y_R /%**	**$^{88}Y_R$ /%**	**Sr_R /%**	**$^{85}Sr_R$ /%**
SWY-1[21]	5.02	94.4±7.0	NM[22]	58.4±3.5	NM	92.8±6.7	NM	22.6±1.1	NM
SWY-2	4.95	97.5±7.4	NM	62.3±5.5	NM	88.2±6.5	NM	22.4±1.9	NM
SWY-3	5.00	87.6±6.4	NM	57.0±5.1	NM	89.7±6.8	NM	21.3±1.8	NM
SWY-4	5.98	93.5±6.1	87.1±8.2	47.7±3.8	34.0±4.7	89.6±6.2	68.9±7.0	18.3±1.5	5.8±2.8
SWY-5	4.72	94.5±6.2	88.5±12.0	40.7±3.1	58.5±6.9	91.6±6.0	104±14	16.9±1.3	13.6±3.3
SWY-6	4.72	93.3±7.4	96.7±12.5	44.9±3.3	66.4±7.1	88.4±6.7	95.5±12	18.1±1.3	11.1±3.6
SWY-7	0.58	93.7±7.2	NS[23]	44.8±3.5	30.2±3.5	88.2±7.0	NS	20.0±1.6	16.1±2.3
SWY-8	0.59	93.5±7.0	NS	45.5±3.2	65.0±7.1	83.3±6.4	NS	17.3±1.3	18.9±3.7
SWY-9	20.0	95.7±7.8	80.3±8.4	47.3±4.0	38.6±4.3	93.8±7.2	72.2±8.8	18.1±1.4	11.2±2.8
SWY-10	33.7	94.5±7.1	81.6±8.5	46.3±3.6	39.7±4.6	92.6±6.9	88.2±7.7	17.7±1.4	8.5±2.8
SWY-11	93.6	95.0±7.4	97.7±8.9	53.5±4.2	50.7±5.7	91.3±7.4	85.8±8.2	19.4±1.5	8.6±2.8
SWBlank-	-	84.7±6.8	NS	40.4±2.6	NS	109±9.1	NS	25.2±1.7	NS
SWBlank-	-	93.4±7.3	NS	39.0±2.7	NS	108±7.9	NS	25.1±1.6	NS
SWBlank-	-	95.0±6.9	NS	44.6±3.0	NS	100±8.7	NS	29.7±1.9	NS
SWBlank-	-	93.9±7.3	NS	45.3±2.9	NS	100±11	NS	30.9±2.0	NS
Mean±1σ (all data)		*93±3(n=15)*		*48±7*		*94 ±7(n=15)*		*22±4(n=15)*	
Mean±1σ (shaded data)		*94±1(n=6)*	*89±7 (n=6)*	*46±4(n=8)*	*48±14(n=8)*	*91±3(n=6)*	*86±13(n=6)*	*18±1(n=8)*	*12±4(n=8)*

[19] $^{88}Y_R$= Chemical recovery of ^{88}Y
[20] $^{85}Sr_R$= Chemical recovery of ^{85}Sr
[21] SWY=Seawater spiked samples
[22] NM=Not measured; sample was spiked, but not tested due to unavailability of gamma spectrometer
[23] NS=Not spiked; sample was not spiked with the radiotracer

Table 33 Continues

		Purified sample		
Method of tracing chemical recovery (R)		**Stable Y ICP-MS**	**^{88}Y γ-spec**	**^{88}Y EC LSA**
Sample code	**A_{ia} ^{90}Sr-^{90}Y/ Bq·L^{-1}**	**Y_R/ %**	**$^{88}Y_R$/ %**	**$^{88}Y_R$/ %**
SWY-1	5.02	88.0±6.3	77.7±6.9	78.2±6.9
SWY-2	4.95	82.9±6.0	93.7±7.3	82.3±7.2
SWY-3	5.00	81.8±6.4	82.7±6.5	81.3±7.2
SWY-4	5.98	104±7.0	90.1±6.4	96.3±8.4
SWY-5	4.72	87.5±5.6	87.6±7.4	85.2±7.5
SWY-6	4.72	86.1±6.5	89.0±7.3	84.2±7.4
SWY-7	0.58	93.7±7.5	NS	NS
SWY-8	0.59	86.6±6.9	NS	NS
SWY-9	20.0	88.8±7.0	88.7±6.8	87.4±7.6
SWY-10	33.7	88.3±6.5	88.0±6.8	89.0±7.7
SWY-11	93.6	96.1±7.6	88.7±6.7	92.0±8.0
SWBlank-1	-	79.6±6.7	NS	NS
SWBlank-2	-	85.9±6.6	NS	NS
SWBlank-3	-	88.3±6.5	NS	NS
SWBlank-4	-	88.6±7.0	NS	NS
Mean±1σ (all data points)		*88±7% (n=15)*	*87±5 (n=9)*	*85±6 (n=9)*
Mean±1σ (shaded data points)		*92±7 (n=6)*	*89±1 (n=6)*	*89±5 (n=6)*

Note: In Table above, shaded areas represent those samples for which all methods of chemical recovery at all stages of the procedure were attainable and, therefore, their mean recoveries calculated for accurate comparison of the chemical recovery across different methods.

The radiotracers ^{88}Y and ^{85}Sr in the samples were traced by measuring their γ emission on the HPGe gamma spectrometer, which was calibrated for ^{88}Y and ^{85}Sr before measurements were obtained (see Appendix D). Yttrium-88 has two γ emissions at 0.898 MeV and 1.836 MeV with emission probabilities of 93.7 % and 99.2 %, respectively [1], of which the 0.898 MeV γ ray was found to have a higher peak efficiency (1.26 %) than the 1.836 MeV γ ray (0.70 %) for the desired measurement geometry. Therefore, the 0.898 MeV peak was preferably used for the activity determination of ^{88}Y in Eq. (23):

$$[A_i] = A_\gamma\ (Bq \cdot L^{-1}) = \frac{CR_N}{\varepsilon_\gamma \cdot I \cdot f \cdot V \cdot D} \tag{23}$$

where CR_N is the net sample count rate (cps); ε_γ is the γ ray peak efficiency; I is the γ ray emission probability; D is the decay factor; and f and V are as before (see Eq. (18)). The peak efficiency for ^{85}Sr γ ray of 0.514 MeV was 2.38 %, which was used in Eq. (23) for ^{85}Sr activity determination. Results of ^{88}Y and ^{85}Sr gamma spectroscopy are presented in Tables L-7 and Table L-8, respectively, in Appendix L and a summary of chemical recovery end results are shown in Table 33.

Besides its γ emission, the EC emission of ^{88}Y at 3.623 MeV was also traced by LSA on the Hidex LSC for additional verification. In a separate experiment, the counting efficiency, ε_{EC} , of a standard ^{88}Y source solution spiked in the UGAB scintillation cocktail was found to be 40±3 %, which was used in Eq. (24) to determine ^{88}Y in the purified samples mixed with UGAB scintillation cocktail:

$$[A_i] = A_{EC}\ (Bq \cdot L^{-1}) = \frac{CR_S - CR_b}{\varepsilon_{EC} \cdot f \cdot V \,.\, D} \tag{24}$$

Once the measured activities of ^{88}Y and ^{85}Sr were determined, the ratios of measured-to-expected activities were used to indicate the chemical recoveries of the radiotracers at various stages of the procedure. The radiotracing option also enabled rapid chemical yield determination in samples. The detailed results of ^{88}Y measured by EC in shown in Tables L-9 (Appendix L) and a summary of chemical recovery end results are shown in Table 33.

The γ rays of ^{88}Y and ^{85}Sr in the spiked seawater samples were traced using gamma spectroscopy in the co-precipitates $CaCO_3$ and HTiO (except for three samples due to unavailability of the instrument) and also in the purified sample. Radiotracing using ^{88}Y was used for samples (n=9) with ^{90}Y added activity of ~ 5 $Bq{\cdot}L^{-1}$ and higher as ^{88}Y was found to interfere with low level ^{90}Y. Mean (±1σ) chemical recovery of ^{88}Y measured by gamma spectroscopy in the six spiked samples in the co-precipitates $CaCO_3$ and HTiO, and purified samples were 89±7 %, 86±13 %, and 89±1 %, respectively. In the purified samples, mean chemical recovery of ^{88}Y based on its EC decay measured by LSA was 85±6 %. A comparison of recovery

results in Table 33 shows that the mean chemical yield of ^{88}Y (both γ and EC tracing) and stable Y are very similar and within their respective uncertainty ranges.

Radiotracing using ^{85}Sr was used in all 11 spiked seawater samples, but measurement of three samples were not obtained due to unavailability of the instrument. In the eight samples tested, the mean ^{85}Sr recovery in the $CaCO_3$ and HTiO precipitates were 48±14 % and 12±4 %, respectively. In the same eight samples, the mean stable Sr was very similar to mean ^{85}Sr: 46±4 % in $CaCO_3$ and 18±1 % in HTiO precipitate, Table 33.

For a ratio of ^{88}Y activity concentrations to ^{90}Y activity concentrations of 0.4 and higher a clean signal for ^{88}Y EC was achieved. However, if this ratio is small, ^{90}Y peak tailing in the default counting region of ^{88}Y on the LSC (ROI 100-300) becomes significant, which overestimates ^{88}Y measured activities. Such an effect was observed when the ratio of ^{88}Y activity concentration to ^{90}Y activity concentration was small. Therefore, for the samples with ^{90}Y spiked activity concentrations greater than 5 $Bq \cdot L^{-1}$ having ^{88}Y activity concentration to ^{90}Y activity concentration ratios of smaller than 0.4, the contribution of ^{90}Y into ^{88}Y was subtracted and accurate ^{88}Y radiochemical yield was achieved. If ^{88}Y is employed as a radiotracer using this method, one has to carefully choose the quantity of ^{88}Y to be used.

The determination of activity concentrations of ^{90}Y in seawater used the same equations as those of freshwater (Eq. (18) and Eq. (19)). In the decay factor calculations for seawater Čerenkov counting method, $DY_{Cerenk}=e^{-(T_1-T_0)\cdot\lambda_Y}$, the T_0 and T_1 were replaced by t_0 (time of end of HTiO co-precipitation) and t_1 (time of start of ^{90}Y Čerenkov counting on the Hidex LSC), respectively, to indicate seawater ^{90}Y decay correction time records. Similarly, in the decay factor calculations for seawater LSA method, $DY_{LSA}=e^{-(T_2-T_0)\cdot\lambda_Y}$, T_0 and T_2 were replaced by t_0 and t_2 (time of start of ^{90}Y LSA on the Hidex LSC), respectively. Other parameters were the same for both freshwater and seawater. The detailed results of seawater activity concentrations measured by Čerenkov counting and LSA techniques are shown in Table L-10 and L-11, respectively (Appendix L). A summary of final results are tabulated in Table 34.

Table 34. ^{90}Y measured in spiked seawater by Čerenkov and LSA using different tracing methods

Chem recovery analysis method		**Stable Y**				**^{88}Y γ-spec**				**^{88}Y EC**	
Measurement method		Čerenkov		LSA		Čerenkov		LSA		LSA	
Method code		(a)		(b)		(c)		(d)		(e)	
Sample code	$[A_{ia}]^{90}Y$-^{90}Sr /Bq·L^{-1}	$[A_i]^{90}Y$ /Bq·L^{-1}	B_{ri} /%	$[A_i]^{90}Y$ /Bq·L^{-1}	B_{ri} /%	$[A_i]^{90}Y$ /Bq·L^{-1}	B_{ri} /%	$[A_i]^{90}Y$ /Bq·L^{-1}	B_{ri} /%	$[A_i]^{90}Y$ /Bq·L^{-1}	B_{ri} /%
SWY-1	5.02	4.56	-9.2	4.70	-6.5	5.15	2.4	5.32	5.9	5.29	5.3
SWY-2	4.95	4.70	-5.1	4.84	-2.3	4.14	16	4.28	-13	4.88	-1.5
SWY-3	5.00	4.99	-0.2	4.92	-1.7	4.92	-1.6	4.86	-2.7	4.95	-1.1
SWY-4	5.98	5.25	-12	5.81	-2.8	5.83	-2.5	6.45	7.9	6.04	1.0
SWY-5	4.72	5.04	6.9	4.36	-7.6	5.04	6.8	5.34	13	4.48	-5.0
SWY-6	4.72	5.03	6.5	4.67	-1.0	4.87	3.1	5.02	6.2	4.78	1.2
SWY-7	0.581	0.54	-7.8	0.59	0.9	NS	NS	NS	NS	NS	NS
SWY-8	0.587	0.61	4.1	0.56	-5.5	NS	NS	NS	NS	NS	NS
SWY-9	20.0	19.2	-4.3	20.4	1.6	19.2	-4.2	20.4	1.7	20.7	3.2
SWY-10	33.7	31.8	-5.8	33.6	-0.4	31.9	-5.3	33.7	0.0	33.3	-1.2
SWY-11	93.6	103	9.7	93.6	0.0	111	19	101	8.3	97.8	4.4
B_r			*-2.2*		*-3.6*		*-1.4*		*2.8*		*-2.7*
S_B			*8.0*		*2.7*		*8.1*		*9.5*		*3.4*

Note: Shaded area represents reproducibility test samples and their statistics.

For ^{90}Y decay correction in the present seawater method, the delay between the HTiO co-precipitation and counting the purified sample on the LSC (*i.e.*, t_1-t_0 and t_2-t_0) was only 2-3 h. Minimizing the delay time is highly important for two main reasons: (i) ^{90}Y has a short half-life of 64 h, which decays very quickly and in the low level samples the uncertainty in measurement results increases; and (ii) the delay is particularly significant because approximately half of the sample ^{90}Sr remains in the $CaCO_3$ precipitate and only ~ 20 % of ^{90}Sr remains for analysis after HTiO co-precipitation. Given such factors, the decay and in-growth correction for ^{90}Y can become quite challenging if there is a significant delay between co-precipitation and counting. Also, decay correction between first and second stages of the co-precipitation was deemed insignificant as half of ^{90}Sr was still in the sample and the delay in time was < 1 h. In addition, in the present work, counting times of 1 h mean that ^{90}Y decay during counting can be neglected, but longer counting times would require decay correction.

In order to gain confidence in measurement results, as illustrated by Table 34, the activity concentrations of ^{90}Y in the purified samples were obtained in five different ways: (a) Čerenkov counting using stable Y recovery correction; (b) LSA using stable Y recovery correction; (c) Čerenkov counting using ^{88}Y recovery correction based on γ spectroscopy of ^{88}Y; (d) LSA using ^{88}Y recovery correction based on γ spectroscopy of ^{88}Y; and (e) LSA using ^{88}Y recovery correction based on the ^{88}Y EC emission measured by LSA on Hidex LSC.

Because the ^{88}Y is not separable from ^{90}Y, it shows 10 -15 % of its LSA emission in the ^{90}Y default ROI (channels 300-800). Thus, mathematical correction for the radiotracer ^{88}Y was required (Appendix M). To avoid the mathematical correction step, the use of ^{88}Y can be eliminated since tracing by stable Y is sufficient for routine and also emergency situations using the present method.

The ^{90}Y measured in the spiked seawater samples, which were obtained using five different methods, were statistically analyzed to determine if the measurement results were significantly different. A two-tailed paired t-distribution test at 5 % significance level was performed with the hypothesis stating that the paired methods are not significantly different from each other. The statistical analysis illustrated by Table 35 demonstrated that p-values were greater than 0.05 at each paired measurement, which indicated that the null hypothesis cannot be rejected. Thus, the measured activities were not statistically different at 95 % confidence interval. This implies any methods of chemical recovery tracing and radioactivity measurement can give comparable results.

Table 35. Statistical test of two-tailed paired t-distribution test for seawater spiked samples measured in five different ways

Paired methods description	p-value	$[A_i]$ different from $[A_{ia}]$:
(Čerenkov; stable Y) & (LSA; stable Y); a & b	0.53	No
(Čerenkov; stable Y) & (Čerenkov; ^{88}Y by γ); a & c	0.32	No
(Čerenkov; stable Y) & (LSA; ^{88}Y by γ); a & d	0.26	No
(Čerenkov; stable Y) & (LSA; ^{88}Y by EC); a & e	0.87	No
(LSA; stable Y) & (Čerenkov; ^{88}Y by γ); b & c	0.42	No
(LSA; stable Y) & (LSA &; ^{88}Y by γ); b & d	0.23	No
(LSA; stable Y) & (LSA; ^{88}Y by EC); b & e	0.23	No
(Čerenkov; ^{88}Y by γ) & (LSA; ^{88}Y by γ); c & d	0.62	No
(Čerenkov; ^{88}Y by γ) & (LSA; ^{88}Y by EC); c & e	0.49	No
(LSA; ^{88}Y by γ) & (LSA; ^{88}Y by EC); d & e	0.26	No

The method performance was evaluated using 1 L spiked seawater samples that were spiked with a known quantity of ^{90}Sr-^{90}Y standard, at activity equilibrium concentrations, in the range of 0.58 $Bq{\cdot}L^{-1}$ to ~ 94 $Bq{\cdot}L^{-1}$, Table 34. The bias and precision in measured activities of the spiked samples were determined to delineate accuracy and repeatability of the method, Table 34. Relative bias for individual sample measurements (B_{ri}) was obtained as per Eq. (15). Replicates of six spiked samples at approximately 5 $Bq{\cdot}L^{-1}$, were used to show the bias in the six replicate measurement, which is shown as B_r in Table 34. The relative precision (S_B) was also calculated as per Eq. (16) to show the dispersion in B_r of the six replicates. The B_{ri} of all five measurement methods shown in Table 34 was within ± 13 %. This indicated good agreement between the expected and measured ^{90}Y activity concentrations.

In addition, method linearity was demonstrated over a range from 0.58 $Bq{\cdot}L^{-1}$ to ~ 94 $Bq{\cdot}L^{-1}$. This range was selected in parallel to freshwater spiked samples, which correspond to several times lower and higher than the drinking water MAC of 5 $Bq{\cdot}L^{-1}$ [14] and AL of 30 $Bq{\cdot}L^{-1}$ [15]. The linearity of measurement methods was analyzed for ^{90}Y measured by Čerenkov counting and LSA whereby the chemical recovery correction was based on stable Y, Figure 37. Excellent linearity with $r^2 \geq 0.997$ for both methods of measurement was established. The standard deviation of the slope (σ_b) and intercept (σ_a) at 95 % confidence interval were obtained, Table 36. The small uncertainties in the slope "b" and constant "a" of the line of best fit indicate that excellent linearity between expected and measured activities was established in Figure 37.

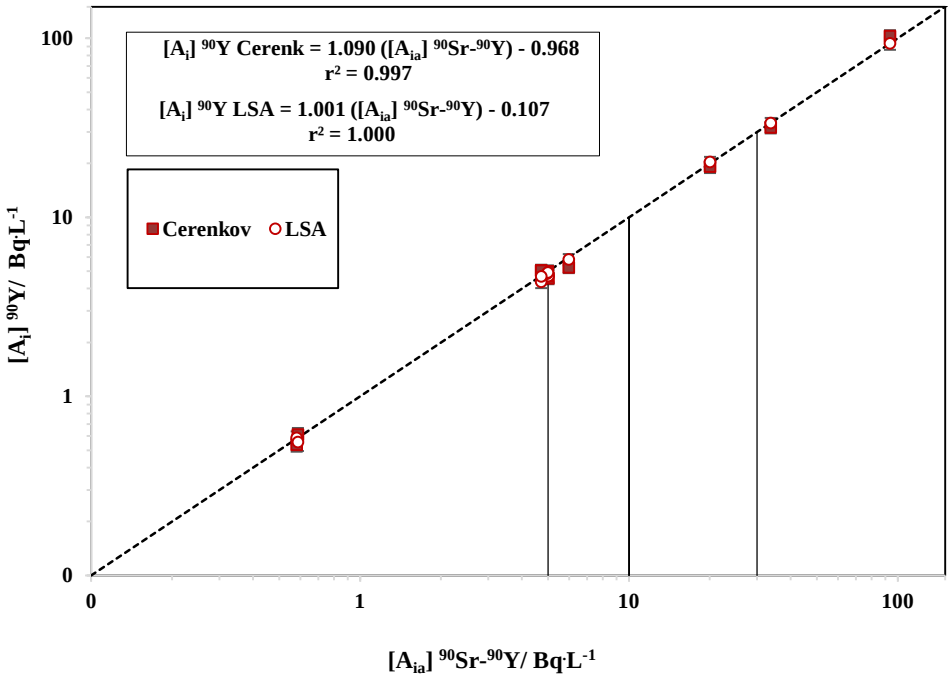

Figure 37. An illustration of measured activity concentrations, $[A_i]$, as a function of expected activity concentrations, $[A_{ia}]$. Diagonal hatched line represents 1:1 ratio between $[A_i]$ and $[A_{ia}]$. Vertical lines from left to right represent the MACs at 5 $Bq{\cdot}L^{-1}$ and 10 $Bq{\cdot}L^{-1}$ for ^{90}Sr in drinking water as per Health Canada and WHO guidelines, respectively, and AL at 30 $Bq{\cdot}L^{-1}$ as per Health Canada guidelines. The error bars, which are too small to show on log scale, indicate combined statistical and systematic uncertainties at 1σ; *adapted from* [105].

Table 36. Regression analysis of line of best fit for measured activities of ^{90}Y

Measurement Method	Best line regression	r^2	b±σ	a±σ
^{90}Y Čerenkov	$[A_i] = 1.090\ ([A_{ia}]) - 0.968$	0.997	1.090±0.044	-0.968±1.347
^{90}Y LSA	$[A_i] = 1.001\ ([A_{ia}]) - 0.107$	1.000	1.001±0.005	-0.107±0.150

The MDCs for the 1 L water samples and procedural blanks were determined as per Eq. (17). The mean MDCs for ^{90}Y in 1 L seawater measured by Čerenkov counting and LSA using stable Y chemical recovery correction were 0.11 $Bq{\cdot}L^{-1}$ and 0.18 $Bq{\cdot}L^{-1}$, respectively, for 1 h counting time on the low background Hidex LSC, Table 37.

Table 37. MDC values for ^{90}Y measured in 1 L blank seawater samples by Čerenkov counting and LSA techniques using a low background Hidex LSC and a counting time of 1 h

	MDC/ Bq·L^{-1}	
Sample code	**Čerenkov**	**LSA**
SWBlank-1	0.118	0.190
SWBlank-2	0.109	0.191
SWBlank-3	0.104	0.182
SWBlank-4	0.108	0.167
Mean±1σ	0.11±0.01	0.18±0.01

Often, radiostrontium is found at the mBq·L^{-1} levels or lower in seawater. If the objective is to detect the very low concentrations of ^{90}Sr-^{90}Y in seawater, then processing of liters of seawater is unavoidably required. Using the method developed in the present dissertation, better detection capabilities may be achieved by expanding the methods to cover larger sample volumes and longer counting times. Theoretically, for a 4 L seawater sample, the detection limit can be estimated to be less than 0.05 Bq·L^{-1} while the final precipitate can be small enough to dissolve in 40-50 mL HNO_3 solution and still be separated on a single DGA-N® resin. This hypothesis, however, needs practical demonstration. Conversely, the procedure can be used for smaller volumes of seawater whereby higher detection limits fit the purpose. For example, for 100 mL seawater sample the detection limit can be approximated to be 1 Bq·L^{-1}, which is a factor of five below the MAC for ^{90}Sr in drinking water and 30 times lower than the AL for emergency situations as per the Canadian guidelines. Furthermore, the detection limit of 1 Bq·L^{-1} is a factor of 10 below the WHO (World Health Organization) recommended concentration of ^{90}Sr in drinking water, which is 10 Bq·L^{-1} based on 0.1 mSv·y^{-1} of committed effective does [101]. Rapidly processing seawater volumes of 100 mL with detection limit of 1 Bq·L^{-1} could prove to be very effective in the emergency application of this method whereby sample collection and analysis times can be significantly reduced.

Overall, the results presented in this section demonstrated that the seawater method performed well in the radiochemical separation and indirect measurement of low, moderate, and high concentrations of ^{90}Sr from ^{90}Y in seawater. Although the method has limitations with respect to ^{90}Sr direct determination, it can be effectively used in radiological emergency circumstances such as storage bay leakage into the seawater and also for emergency events given that ^{90}Sr and ^{90}Y equilibrium has been established. In general, the major challenges of accurate and rapid determination of ^{90}Sr during emergency situations comes from interferences from activities of shorter-lived Sr and Y nuclides. That is mainly because the shorter lived nuclides from a fission event can be present in 1-2 orders of magnitude higher than that of ^{90}Sr [32]. However, a vast majority of Sr and Y

isotopes have very short $T_{1/2}$ and will decay after a couple of days following a release scenario [32]. Longer-lived isotopes, however, can present themselves as major interferences to ^{90}Sr-^{90}Y determination. For example, ^{89}Sr can be present in the sample and can show high β^- emissions, which can interfere with ^{90}Y detection. Using the present method, the ^{89}Sr is not an issue because all Sr isotopes are similarly discarded by the DGA-N® column extraction chromatography. If ^{85}Sr is present in the sample, then the use of ^{85}Sr as a radiotracer will interfere with the intrinsic ^{85}Sr. As such, ^{85}Sr radiotracing should be avoided and only stable Sr used for tracing the chemical recovery.

If ^{89}Sr that is released into the environment from a fission event needs to be quantified using this method, then the $CaCO_3$ precipitate can be Čerenkov counted and ^{89}Sr quantified. Chemical recovery of Sr in $CaCO_3$ was found to be 48±7 % on average (Table 33). Although the chemical recovery of ~ 50 % is not desirable for ^{90}Sr determination, however, for ^{89}Sr the chemical recovery can still result in effective determination. That is because (i) the ratio of ^{89}Sr/^{90}Sr is high in a fresh fission release event; and (ii) the regulatory limits for ^{89}Sr, which are not as stringent as those for ^{90}Sr, can be conveniently met. For example, in the case of a radiological emergency the Action Level for ^{89}Sr and ^{90}Sr in drinking water are 300 $Bq{\cdot}L^{-1}$ and 30 $Bq{\cdot}L^{-1}$, respectively [15]. Under normal circumstances, the MAC of ^{89}Sr and ^{90}Sr in drinking water, as defined by Health Canada, are 50 $Bq{\cdot}L^{-1}$ and 5 $Bq{\cdot}L^{-1}$, respectively [14]. The advantage of ^{89}Sr Čerenkov counting in $CaCO_3$ precipitate is that the precipitate is small enough (~ 15g) to be re-dissolved in a total volume of ~ 20 mL acid and counted in a scintillation counting vial. The ^{90}Y Čerenkov contribution can be mathematically corrected once the final and purified sample (after HTiO precipitation and column separation steps) is measured by both ^{90}Y Čerenkov and LSA techniques.

With respect to the other Y isotopes, the ^{88}Y is not expected to be in the sample because in the case of both fission event and rod-bay storage leakage, there is no ^{88}Y expected to be released into the environment. However, ^{91}Y may be present because ^{91}Y is a fission product with a 5.849 % yield from thermal neutron fission of ^{235}U [3] and $T_{1/2}$ of 58.51 days [1]. The production and decay process of ^{91}Y is illustrated by Eq. (25), [32]:

$$^{91}\mathrm{Kr} \xrightarrow{\beta,\gamma\ T_{1/2}=9sec} {}^{91}\mathrm{Rb} \xrightarrow{\beta,\gamma\ T_{1/2}=58sec} {}^{91}\mathrm{Sr} \xrightarrow{\beta,\gamma\ T_{1/2}=10h} {}^{91}\mathrm{Y} \xrightarrow{\beta\ T_{1/2}=59d} {}^{91}\mathrm{Zr} \qquad (25)$$

The ^{91}Y can be present in a fission event and until a couple of years after the incident, but not in a rod bay leakage event because rod bays are in general aged storages where short-lived radionuclides such as ^{91}Y are not present in significant quantities. In the Čerenkov counting method, ^{91}Y with high energy of 1.545 MeV, which is above the threshold energy for Čerenkov light emission, will interfere with ^{90}Y. Therefore, the interference from ^{91}Y is unavoidable. In such cases, the

direct determination of ^{90}Sr is preferred. Alternatively, mathematical corrections can be applied to subtract the ^{91}Y contribution, if the current method of indirect determination of ^{90}Y is used. In the case of a fission event, because of short $T_{1/2}$ of ^{90}Y, its build up is much faster (from ^{90}Sr at high concentrations) than the decay of ^{91}Y with $T_{1/2}$ of 58.51 days. Therefore, upon secular equilibrium establishment between ^{90}Sr and ^{90}Y, the present method can be used and ^{91}Y contribution subtracted. Historically, a fission type of emergency situation is a highly rare event compared to radioactivity leakage incidents at nuclear power plants, in which case the present seawater method can be successfully used.

The results and discussions presented in this chapter demonstrated that the methods for the determination of ^{90}Sr-^{90}Y in freshwater and seawater that were developed as part of this dissertation were effective, rapid, and simple. Multiple measurement methods offered confidence in analytical results. The methods' accuracy and precision were also validated.

Chapter 6: Summary and Conclusions

The objective of the research outlined in this dissertation was to address some of the gaps in current radioanalytical capabilities for the determination of ^{90}Sr-^{90}Y in the environment. Methodologies developed in the present dissertation considered techniques at moderate, low, and very low levels on detection with increased speed of analysis and greater efficiency. The three developments that formed the initial scope of this dissertation were based on accelerator mass spectrometry (AMS), extraction chromatography (EXC), and liquid scintillation technology.

The preliminary results of ^{90}Sr determination by AMS technique demonstrated proof of principle. However, further method development was needed in order to meet the detection sensitivity requirements of the very low environmental concentrations. Further optimization of the technique, unfortunately, was not achieved within the time frame of this dissertation because the resources became unavailable.

Recent advancement in radiochemical separation and liquid scintillation counting techniques were used to design methodologies for the determination of ^{90}Sr-^{90}Y at low to moderate detection capabilities. A triple-to-double coincidence ratio (TDCR) Čerenkov counting method for indirect determination of freshwater and seawater ^{90}Sr form ^{90}Y at equilibrium activity concentrations was developed. The technique was rapid and simple without the need for any chemical treatment. The method's performance was challenged in the presence of colour quenching and variations in sample size and counting vial geometry. The results demonstrated that in the TDCR Čerenkov counting technique, the variation in sample geometry, which in conventional techniques causes changes in counting efficiency, was automatically corrected and, therefore, the counting efficiencies were not significantly changed when sample geometry changed. Similarly, the colour quenching results showed that the TDCR Čerenkov counting technique is capable of correcting the effects of colour quenching without the need for external quench calibration curve. The measured activities deviation from expected were within 8 % maximally. The method's detection limit was found to be ~ 6 $Bq{\cdot}L^{-1}$ for 20 mL sample volume and 0.5 h counting time on a low background Hidex liquid scintillation counter (LSC). Also, the method's implementation on naturally coloured freshwater samples with moderate to high ^{90}Sr-^{90}Y radioactivity was successfully achieved.

To achieve low level detection of ^{90}Sr in water, its separation from other radioactive materials and the stable sample matrix is necessary. The radiochemical separation used in the present research employed pre-concentration by co-precipitation followed by highly selective extraction EXC purification techniques. Freshwater ^{90}Sr was determined directly as well as indirectly from ^{90}Sr-^{90}Y. The

method employed (1) co-precipitation of freshwater ^{90}Sr-^{90}Y using calcium phosphate in alkaline conditions; (2) sequential purification of ^{90}Sr and ^{90}Y on Sr-Resin® and DGA-N® EXC columns, respectively; and (3) detection of ^{90}Sr by liquid scintillation assay (LSA) at two different time intervals and that of ^{90}Y using both Čerenkov counting and LSA. Seawater ^{90}Sr was determined indirectly from ^{90}Y at equilibrium activity concentrations of ^{90}Sr-^{90}Y. The method used (1) co-precipitation of seawater ^{90}Y using calcium carbonate and hydrous titanium oxide in alkaline conditions; (2) purification of ^{90}Y on DGA-N® resin; and (3) detection of ^{90}Y using both Čerenkov counting and LSA. The Čerenkov counting and LSA techniques provided independent sets of data and, thus, reliability of the methods. The chemical recovery was traced using stable Sr and Y isotopes in freshwater method and stable isotope tracing as well as radiotracing using ^{88}Y and ^{85}Sr in seawater method. The multiple methods of chemical recovery correction of the measured activities provided multiple and independent sets of data, which were comparable and, hence, validated the reliability of measurement results. The methods' performance evaluation demonstrated excellent agreement between measured and expected activities of spiked ^{90}Sr-^{90}Y standard solution in the range of 0.75 $Bq{\cdot}L^{-1}$ to 100 $Bq{\cdot}L^{-1}$, which covers maximum allowable concentration (MAC) of ^{90}Sr in drinking water under normal circumstances (*i.e.,* 5 $Bq{\cdot}L^{-1}$) as well as the Action Level (AL) limits in the case of a radiological emergency (*i.e.,* 30 $Bq{\cdot}L^{-1}$). The freshwater methods detection limit for all methods of measurement (^{90}Y Čerenkov counting and LSA and ^{90}Sr LSA) were $\leq$ 0.08 $Bq{\cdot}L^{-1}$ for 1 L water and 1 h counting on the Hidex LSC. The seawater method detection limit for ^{90}Y measured by Čerenkov counting and LSA techniques were 0.11 $Bq{\cdot}L^{-1}$ and 0.18 $Bq{\cdot}L^{-1}$, respectively, for 1 L seawater and a counting time of 1 h.

Effective implementation of the freshwater method on natural water samples from the Chalk River Laboratories (CRL) of the Canadian Nuclear Laboratories (CNL) at a wide range of ^{90}Sr-^{90}Y concentrations was also achieved. This implies that the freshwater method developed as part of this dissertation will be implemented in the environmental monitoring program of CRL for the determination of ^{90}Sr-^{90}Y in radiological effluents. The seawater method aims to minimize some of the existing gaps in the determination techniques. The results of the seawater ^{90}Sr-^{90}Y method have been accepted for publication in a peer-reviewed journal.

Chapter 7: Recommendation

Based on the results obtained in the present dissertation, the following recommendations can be made for future use and improvement of the methods developed in this dissertation:

1. For the determination of ^{90}Sr-^{90}Y with documented levels above 6 Bq·L^{-1} (*i.e.*, the method detection limit), it is recommended that the samples should be first screened using the TDCR Čerenkov counting method. In doing so, those samples that are well above the detection limit of this method are rapidly and reliably measured without the need for radiochemical separation of ^{90}Sr-^{90}Y from the matrix. Those samples that are found to be below the method's detection limit can then be processed for radiochemical separation of ^{90}Sr-^{90}Y using the methods described in the present dissertation. This assures fast and inexpensive method of analysis and also segregates high and low level samples in an unknown sample batch.

2. The development of freshwater ^{90}Sr determination in the present work used simultaneous measurements of direct ^{90}Sr and indirect determination of ^{90}Sr (from ^{90}Y at equilibrium concentrations). For routine application of the freshwater method, however, it is not necessary to obtain simultaneous measurements because both methods can provide equally reliable results. Thus, to reduce cost of analysis and laboratory processing of samples, either ^{90}Sr or ^{90}Y methods can be used. Because measurement of ^{90}Y relies on the established equilibrium between ^{90}Y and ^{90}Sr and requires immediate counting as the radionuclides is very short-lived where long delays can cause huge uncertainties in low level measurements, therefore, direct ^{90}Sr method may be more convenient.

3. For seawater method developed in this dissertation, multiple methods of chemical recovery were assessed and the results compared very well. Because radiotracing using ^{88}Y requires mathematical subtraction of ^{88}Y contributions in ^{90}Y counting window, therefore, it is recommended that stable Y should be used for chemical recovery tracing using this method.

4. The methods developed as part of this dissertation fell short in the detection of the very low concentrations of ^{90}Sr-^{90}Y in water. In general, detection of the ultra-low concentrations in both freshwater and seawater is beyond the capabilities of the radiometric techniques. To address this limitation, the Accelerator Mass Spectrometry (AMS) determination of ^{90}Sr, which was initially in the scope of this research dissertation, will be revisited once the new AMS facility is commissioned at the University of Ottawa.

REFERENCES

[1] Korea Atomic Energy Research Institute, Table of Nuclides. Available from: http://atom.kaeri.re.kr/ [Accessed: 10 February 2013]

[2] Argonne National Laboratory, Environmental Science Division. Human Health Fact Sheet on Strontium, 2006.

[3] Nicholas A. L., Aldama D. L., Verpelli M., Handbook of Nuclear Data for Safeguards. International Atomic Energy Agency. IAEA-INDC (NDS)-0534, 2008

[4] Groska J., Molnar Z., Bokori E., Vajda N., Simultaneous Determination of ^{89}Sr and ^{90}Sr: Comparison of Methods and Calculation Techniques. *Journal of Radioanalytical and Nuclear Chemistry (2012) 291:707-715*

[5] Lockheed M., Nuclides and Isotopes. Chart of the Nuclides. KAPL Inc. 16th Edition, 2002

[6] Bonin W. H., Health Physics and Radiation Protection. RMC-CCE-HWB-90-1 Rev. 1, 1990

[7] Priebe E., Lee D. R., Reactive Sandpacks for *In-situ* Treatment of Construction Dewatering Effluent. *AECL Nuclear Review (2013) 2 :85-87.* Available from: www.cnl.ca

[8] Burge R. S., The Precipitation of Radioactive Strontium from Urine. *Applied Radiation and Isotopes (1962) 13:565-571*

[9] International Atomic Energy Agency, Assessment of Radiological Consequences and Evaluation of Protective Measures- The International Chernobyl Project. IAEA-TECDOC-03254, 1992

[10] Durham R. W., Joshi S. R., Radionuclide Concentration in Two Sewage Treatment Plants on Western Lake Ontario, Canada. *Journal of Radioanalytical Nuclear Chemistry (1979) 54:367-370*

[11] Borcherding J., Nies H., An Improved Method for the Determination of ^{90}Sr in Large Samples of Seawater. *Journal of Radioanalytical and Nuclear Chemistry (1986)* 98:127-131

[12] Casacuberta N., Masque P., Garcia-Orellana J., Garcia-Tnorio R., Buesseler K. O., ^{90}Sr and ^{89}Sr in Seawater of Japan as a Consequence of the Fukushima Daiichi Nuclear Accident. *Biogeosciences (2013) 10:*3649-3659

[13] International Atomic Energy Agency, Categorization of Radioactive Sources. Vienna, Austria. IAEA-TECDOC-1344, 2003

[14] Health Canada, Guidelines for Canadian Drinking Water Quality-Guideline Technical Document, Radiological Parameters. ISBN: 978-1-100-16767-1, May 2009

[15] Health Canada, Canadian Guidelines for the Restriction of Radiological Contaminated Food and Water Following a Nuclear Emergency- Guidelines and Rationale. ISBN 0-662-30278-8, 2000

[16] John D. H., Hydrogeochemistry of rivers and lakes, The Geology of North America, Vol. 0-1, Surface Water Hydrology, The Geological Society of America, 1990

[17] National Analytical Management Program, U. S. Department of Energy. Radiochemistry Webinars, Radium Chemistry. Available from: www.wipp.energy.gov/namp [Accessed: 27 August 2013]

[18] Marie L., ^{90}Sr in Environmental Matrices. Procedure Manual, Sr-03-RC. 1: HASL-300, 1997

[19] Bojanoski R., Knapinska-Skiba D., Determination of Low-Level ^{90}Sr in Environmental Materials: A Novel Approach to the Classical Method. *Journal of Radioanalytical and Nuclear Chemistry (1990) 138:207-218*

[20] Martin J. E., Measurement of ^{90}Sr in Reactor Wastes by Čerenkov Counting of ^{90}Y. *Applied Radiation and Isotopes (1987) 38(11):953-957*

[21] Boni A. L., Determination of Total Radiostrontium in Biological Samples Containing Large Quantities of Calcium. *Analytical Chemistry (1963) 35:586-593*

[22] Chu T. C., Wang J. J., Lin Y. M., Radiostrontium Analytical Method Using Crown-ether Compound and Čerenkov Counting and its Application in Environmental Monitoring. *Applied Radiation and Isotopes (1998) 49:1671-1675*

[23] Chen Q., Hou X., Yu Y., Dahlgaard H., Nielson S. P., Separation of Sr from Ca, Ba and Ra by Means of $Ca(OH)_2$ and $Ba(Ra)Cl_2$ or $Ba(Ra)SO_4$ for the Determination of Radiostrontium. *Analytical Chemistry (2002) 466:109-116*

[24] Popov L., Hou X., Nielson S. P., Yu Y., Djingova R., Kulef I., Determination of Radiostrontium in Environmental Samples Using Sodium Hydroxide for Separation of Strontium from Calcium. *Journal of Radioanalytical and Nuclear Chemistry (2006)* 269:161-173

[25] Vanura P., Jedinakova-Krizova V., Yoshioka A., Extraction Separation of Strontium and Yttrium Radionuclides by Hydrogen Heptachlorodicarbollycobaltate in the Presence of Bebzo-15-crown 5. *Journal of Radioanalytical and Nuclear Chemistry (2002) 251:511-514*

[26] Rocco G., Broecker W. S., The Vertical Distribution of ^{137}Cs and ^{90}Sr in the Oceans. *Journal of Geophysical Research (1963) 68:4501- 4512*

[27] Grahek Z., Rozmaric M., Determination of Radioactive Strontium in Seawater. *Analytical Chemistry (2005) 534:271-279*

[28] Owens D. L., Practical Principles of Ion Exchange Water Treatment. Tall Oaks Publishing Inc., 1985

[29] Horwitz P. E., Chiarizia R., Dietz M. L., A Novel Strontium-selective Extraction Chromatographic Resin. *Solvent Extraction and Ion Exchange (1992)* 10:313-336

[30] National Analytical Management Program, U. S. Department of Energy. Radiochemistry Webinars, Actinide Chemistry Series, Source Preparation for Alpha Spectroscopy. Available from: www.wipp.energy.gov/namp [Accessed: 20 May 2014]

[31] Brown T. L., LeMay H. E., Bursten B. E., Burdge J. R., Chemistry-The Central Science. 9th Edition, Pearson Education Inc. (2003)

[32] Vajda N., Kim C.-K. Determination of Radiostrontium Isotopes: A Review of Analytical Methodologies. *Applied Radiation and Isotopes (2010)* 68:*2306-2326*

[33] Maxwell S. L., Culligan B. K., Utsey R. C., Rapid Determination of Radiostrontium in Seawater Samples. *Journal of Radioanalytical and Nuclear Chemistry (2014) 298:867-875*

[34] Maxwell S. L., Culligan B. K., Shaw P. J., Rapid Determination of Radiostrontium in Large Soil Samples. *Journal of Radioanalytical and Nuclear Chemistry (2013) 295:965-971*

[35] Shiraishi K., Ko S., Arae H., Ayama K., Rapid Analysis Technique for Sr, Th, and U in Urine samples. *Journal of Radioanalytical and Nuclear Chemistry (2007)* 273:307-310

[36] Alvarez A., Navarro N., Method for Actinides and ^{90}Sr Determination in Urine Samples. *Applied Radiation and Isotopes (1996) 47:869-873*

[37] Dietz M. L., Horwitz E. P., An Improved Method for Determining ^{89}Sr and ^{90}Sr in Urine. *Health Physics (1991)* 61:871-877

[38] International Atomic Energy Agency, Rapid Simultaneous Determination of ^{89}Sr and ^{90}Sr in Milk: A Procedure Using Čerenkov and Scintillating Counting. IAEA/AQ/27, 2013

[39] Eichrom Technologies Inc., Purification of 4,4'(5')-di-t-butylcyclohexano-18-crown-6. U.S. 70913338 B2, 15 August 2006. Available from: www.eichrome.com [Accessed: July 2013]

[40] Horwitz E. P., Chiarizia R., Dietz M. L., The Application of Novel Extraction Chromatographic Materials to the Characterization of Radioactive Waste Solutions. *Journal of Radioanalytical and Nuclear Chemistry (1992)* 161:575-583

[41] Dai X., Cui Y., Kramer-Tremblay S., A Rapid Method for Determining Strontium-90 in Urine Samples. *Journal of Radioanalytical and Nuclear Chemistry (2013) 296:363-368*

[42] Sadi B. B., Li C., Jodayree S., Lai E. P., Kochermin V., Kramer G. H., A Rapid Bioassay Method for the Determination of ^{90}Sr in Human Urine Sample. *Radiation Protection Dosimetry (2010) 140:41-48*

[43] Li C., Sadi B. B., Moodie G., Daka J. N., Lai E. P., Kramer G. H., Field Development Technique for ^{90}Sr Emergency Bioassay. *Radiation Protection Dosimetry (2009) 136:82-86*

[44] Temba E., Amaral A. M., Monteiro R. P., Separation and Determination of ^{90}Sr in Low- and Intermediate Level Radioactive Wastes Using Extraction Chromatography and LSC. *Journal of Radioanalytical and Nuclear Chemistry (2011) 290:631-635*

[45] Vyas C. K., Joshiro P. M., Manchanda V. K., Separation of ^{90}Y from ^{90}Sr Using Sequential Multiple Column Extraction Chromatography. *Journal of Radioanalytical and Nuclear Chemistry (2014) 300:445-450*

[46] Taylor V. F., Evans R. D., Cornett R. J., Determination of ^{90}Sr in Contaminated Environmental Samples by Tuneable Bandpass Dynamic Reaction Cell ICP-MS. *Analytical and Bioanalytical Chemistry (2007) 387:343-350*

[47] Maxwell S. L., Culligan B. K., New Column Separation Method for Emergency Urine Samples. *Journal of Radioanalytical and Nuclear Chemistry (2009) 279:105-111*

[48] Tovedal A., Nygren U., Lagerkvist P., Vesterlund A., Rameback H., Methodology for Determination of ^{89}Sr and ^{90}Sr in Radiological Emergency: II. Method Development and Evaluation. *Journal of Radioanalytical and Nuclear Chemistry (2009)* 282:461-466

[49] Dietz M. L., Chiarizia R., Horwitz E. P., Bartsch R. A., Talanov V., Effect of Crown Ethers on the Ion-exchange Behaviour of Alkaline Earth Metals. Toward Improved Ion Exchange Methods for the Separation and Pre-concentration of Radium. *Analytical Chemistry (1997) 69:3028-3037*

[50] TrisKem International Inc., Product Sheet. Available from: *www.triskem-international.com* [Accessed: Oct 2014]

[51] Grahek Z., Karanovic G., Nodilo M., Rapid Determination of $^{89, 90}$Sr in Wide Range of Activity Concentrations by Combination of Yttrium, Strontium Separation and Čerenkov Counting. *Journal of Radioanalytical and Nuclear Chemistry (2012) 292:555-569*

[52] Grahek Z., Rozmaric M., Possibility of Rapid Determination of Low-level ^{90}Sr Activity by Combination of Extraction Chromatography Sepration and Čerenkov Counting. *Analytica Chimica Acta (1999):237-247*

[53] Eichrom Technologies Inc., www.eichrome.com [Accessed: 25 February 2013]

[54] Eichrom Technologies Inc., Eichrom Technologies' Product Catalogue for 2013. Available from: www.eichrom.com [Accessed: 30 May 2014]

[55] Eichrom Inc. DGA-N® Resin: Update on Properties and Applications. Bratislava, 10 Nov 2006. Available from: www.eichrome.com. [Accessed: 25 July 2014]

[56] Horwitz E. P., McAlister D. R., Bond A. H., Barrans R. E., Novel Extraction Chromatographic Resins Based on Tetraalkyldiglycolamides: Characterization and Potential Applications. *Solvent Extraction and Ion Exchange (2005) 23:319-344*

[57] Knoll G. F., Radiation Detection and Measurement, 4th Edition, Wiley & Sons Inc. (2010)

[58] L'Annunziata M. F., Handbook of Radioactivity Analysis, 3rd Edition, Academic Press (2012)

[59] Al-Masri M. S., Čerenkov Counting Technique. *Journal of Radioanalytical and Nuclear Chemistry (1996) 207:205-213*

[60] Vaca F., Manjon G., Garcia-Leion M., Efficiency Calibration of a Liquid Scintillation Counter for ^{90}Y Čerenkov Counting. *Nuclear Instruments & Methods In Physics Research A (1998) 406:267-275*

[61] Wiebe L. I., McQuarrie S. A., Ediss C., Maier-Borst W., Helus F., Liquid Scintillation Counting of Radionuclides Emitting High-energy Beta Radiation. *Journal of Radioanalytical and Nuclear Chemistry (1980) 60:385-394*

[62] Scarpitta S. C., Fisenne I. M., Čerenkov Counting as a Complement to Liquid Scintillation Counting. *Applied Radiation and Isotopes (1996) 47:795-800*

[63] Stamoulis K. C., Ioannides K. G., Karamanis D. T., Patiris D. C., Rapid Screening of ^{90}Sr Activity in Water and Milk Samples Using Čerenkov Radiation. *Journal of Environmental Radioactivity (2007) 93:144-156*

[64] Takiue M., Natake T., Fujii H., Aburai T., Accuracy of Čerenkov Measurement Using a Liquid Scintillation Spectrometer. *Applied Radiation and Isotopes (1996) 47:123-126*

[65] Rao D. D., Sudheendran V., Baburajan A., Chandramouli S., Hegde A. G., Mishra U. C., Measurement of High Energy Gross Beta and ^{40}K by Čerenkov Counting in Liquid Scintillation Analyser. *Journal of Radioanalytical and Nuclear Chemistry (2000)* 243:651-655

[66] Jabbar T., Khan K., Subhani M. S., Akhter P., Determination of ^{90}Sr in Environment of District Swat, Pakistan. *Journal of Radioanalytical and Nuclear Chemistry (2009)* 279:377-384

[67] Chang T. M., Chen S. C., King J. Y., Wang S. J., Rapid and Accurate Determination of $^{89, 90}Sr$ in Radioactive Samples by Čerenkov Counting. *Journal of Radioanalytical and Nuclear Chemistry (1996) 204:*339-347

[68] Guzzi G., Pietra R., Sabbioni E., Girardi F., Čerenkov Counting Rates of Radionuclides for Activation Analysis Purposes. *Journal of Radioanalytical and Nuclear Chemistry (1974) 20:751-767*

[69] Kossert K., Activity Standardization by Means of a New TDCR-Čerenkov Counting Technique. *Applied Radiation and Isotopes (2010) 68:1116 -1120*

[70] Feuerstein J., Boulyga S. F., Galler P., Stingeder G., Prohask T., Determination of ^{90}Sr in Soil Samples Using Inductively Coupled Plasma Mass Spectrometry Equipped with Dynamic Reaction Cell (ICP-DRC-MS). *Journal of Environmental Radioactivity (2008) 99:1764-1769*

[71] Kutschera W., Progress in Isotope analysis at Ultra-trace Level by AMS. *International Journal of Mass Spectrometry (2005) 242:145-160*

[72] Zhao X-L., Kieser W. E., Dai X., Priest N. D., Tremblay-Kramer S., Eliades J., Litherland A. E., Preliminary Studies of Pu Measurement by AMS Using PuF_4^-. *Nuclear Instruments & Methods in Physics Research B (2013) 294:356-360*

[73] Dai X., Cui Y., Christl M., Kramer-Tremblay S., Synal H., Ultra-trace Determination of Plutonium in Urine Samples Using a Compact Accelerator Mass Spectrometry System Operating at 300 kV. *Analytical Atomic Spectrometry (2012) 27:126-130*

[74] Arslan F., Behrendt M., Ernets W., *et al*., Trace Analysis of the Radionuclides ^{90}Sr and ^{89}Sr in Environmental Samples II: Accelerator Mass Spectrometry (AMS). *Chemie Angewandte International English (1995) 34:183-186*

[75] Eliades J., Zhao X-L., Litherland A. E., Kieser W. E., Online Ion Chemistry for the AMS Analysis of ^{90}Sr and $^{135, 137}$Cs. *Nuclear Instruments & Methods in Physics Research B, (2013) 294:361-363*

[76] Tumey S. J., Brown T. A., Hamilton T. F., Hillegonds D. J., Accelerator Mass Spectrometry of ^{90}Sr for Homeland and Security Environmental Monitoring, and Human Health. Lawrence Livermore National Laboratory, LLNL-JRNL-402381, 19 March 2008

[77] Litherland A. E., Ultrasensitive Mass Spectrometry with Accelerators. *Annual Review of Nuclear and Particle Science (1980) 30:437-473*

[78] Kieser W. E., Eliades J., Litherland A. E., Zhao X-L., Ye S. J., Cousins L., The Low Energy Isobar Separation for Anions. Progress Report, *Radiocarbon 52 (2010):236-242*

[79] Canadian Council of Ministers of the Environment, Protocols Manual for Water Quality Sampling in Canada. Available from: http://samplingh2o.ccme.ca/: [Accessed: 20 March 2013]

[80] Ontario Ministry of the Environment and Energy, Protocol for the Sampling and Analysis of Industrial/Municipal Waste Water, PIBS 2724E0, 1999

[81] Rowan D., Silke R., Carr J., Biota-sediment Accumulation Factors for Radionuclides and Sediment Associated Biota of the Ottawa River, *AECL Nuclear Review (2013) 2:3-16.* Available from: www.cnl.ca

[82] Lee D. R., Chaput T., Miller A., Wills C. A., Edibility of Sports Fishes in the Ottawa River Near Chalk River Laboratories. *AECL Nuclear Review (2013) 2:73-84.* Available from: www.cnl.ca

[83] Parsons P. J., Migration from a Disposal of Radioactive Liquid in *Sands. Health Physics (1963) 9:333-342*

[84] Killey R. W. D., Munch J. H., Radiostrontium Migration from a 1953-54 Liquid Release to a Sand Aquifer. *Water Pollution Research Journal of Canada (1987)* 22:107-128

[85] Lee D. R., Hartwig D. S., Zeolite Prevents Discharge of Strontium -90-contaminated Groundwater. Canadian Nuclear Society Waste Management, Decommissioning and Environmental Restoration for Canada's Nuclear Activities: Current Practices and Future Needs Ottawa, Ontario Canada May 8-11, 2005

[86] United States Environmental Protection Agency, Multi-Agency Radiological Laboratory Analytical Protocols Manual, NUREG-1576. EPA 402-B-04-001A. NTIS PB2004-105421, July 2004

[87] Hoffmann E., Charette J., Stroobant V., Mass Spectrometry Principles and Applications. New York: John Wiley & Sons Ltd. (1996) 31- 32

[88] Stow P., Comparison between SF-ICP-MS and Q-ICP-MS. Technical Presentation of High Resolution Inductively Coupled Mass Spectroscopy, Toronto Ontario, 19 September 2013, available from Isomass Analytic Inc., www.isomass.com

[89] International Standard ISO/IEC 17025. General Requirements for the Competence of Testing and Calibration Laboratories, ISO/IEC17025:2005(E). Available from Canadian Association for Laboratory Accreditation: www.cala.ca

[90] Environmental Protection Agency of U. S. Standard Method: Determination of Inorganic Anions in Drinking Water by Ion Chromatography. EPA-OGWDW/TSC (1997):300.1, Rev 1

[91] American Public Health Association. Standard Method for Dissolved Carbon Measurement: Automated Ultraviolet- pursulfate Digestion, APHA 5310C

[92] Makinen P. O., Handbook of Liquid Scintillation Counting. Turku Institute of Technology, Department of Telecommunications, Turku, Finland, 1995

[93] Health Physics Society. Performance Criteria for Radiobioassay. American National Standard. ANSI N13.30. American National Standard, New York, 2011

[94] Storm D. J., Lynch T. P., Weier D. R., Radiation Doses to Hanford Workers from Natural Ptassium-40. U. S. Department of Energy, DE-AC05-76RL01830, 2009. Available from www.pnl.gov. [Accessed: 13 November 2014]

[95] Ro C-U., Sirois A., Vet R. J., Time Trends in Canadian Air and Precipitation Chemistry Data. Proceedings of the Air and Waste Management Association's, 90th Annual Meeting and Exhibition, Toronto, Ontario, June 8-13, 1997

[96] Tayeb M., Dai X., Corcoran E. C., Kelly D. G., Evaluation of Interferences on Measurements of ^{90}Sr-^{90}Y by TDCR Čerenkov Counting Technique. *Journal of Radioanalytical and Nuclear Chemistry (2014) 300:409-414*

[97] Kellogg T. F., The Effect of Sample Composition and Vial Type on Čerenkov Counting in a Liquid Scintillation Counter. *Analytical Biochemistry (1983) 134:137-143*

[98] L'Annunziata M. F., Passo C. J., Čerenkov Counting of Yttrium-90 in the Dry State; Correlations with Phosphorus-32 Čerenkov Counting Data. *Applied Radiation and Isotopes (2002) 56:907-916*

[99] Currie L. A., Limits for Quantitative Detection and Quantitative Determination Applicable to Radiochemistry. *Analytical Chemistry (1968) 40:586-592*

[100] Atomic Energy of Canada Limited. Radioactive Emission Management. EnvP-509200-PRO-001. 2010 (Available through CNL Information Centre)

[101] Radiological Aspects- World Health Organization. Guidelines for Drinking Water Quality. Available from: http://www.who.int/water_sanitation_health/publications/2011/9789241548151_ch09.pdf [Accessed: Aug 2014]

[102] Mann P. S., Introductory Statistics, 6th Edition. 2007. John Wiley & Sons Inc., SBN 978-0-471-75530-2

[103] Butkalyuk P. S., Sapozhnikov Y. A., Rapid Determination of Strontium-90 in Seawater. *Moscow University Chemistry Bulletin (2009) 64, 165-167*

[104] Gagne A., Surett J., Kramer-Tremblay S., Dai X., Didychuk C., Lariviere D., A Bioassay Method for Americium and Curium in Feces. *Journal of Radioanalytical and Nuclear Chemistry* (2013) 295:477-482

[105] Tayeb M., Dai X., Kelly D. G., Corcoran E. C., Rapid Determination of Strontium-90 from Yttrium-90 in Seawater. *Journal of Radioanalytical and Nuclear Chemistry (In press)*

APPENDICES

Appendix A. Photos of Instruments and Apparatus

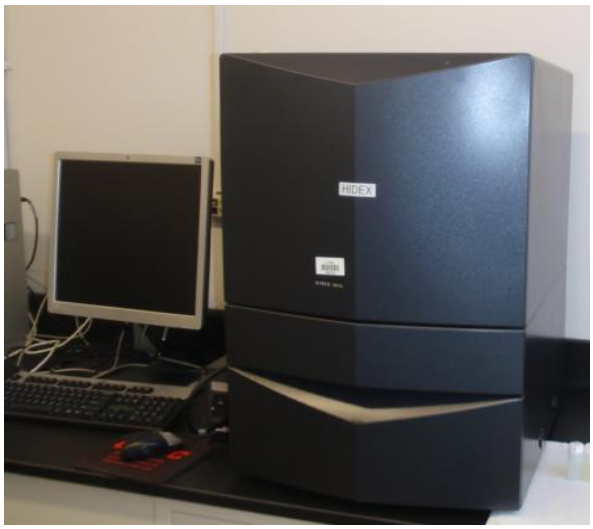

Figure A- 1. Hidex 300SL liquid scintillation counter

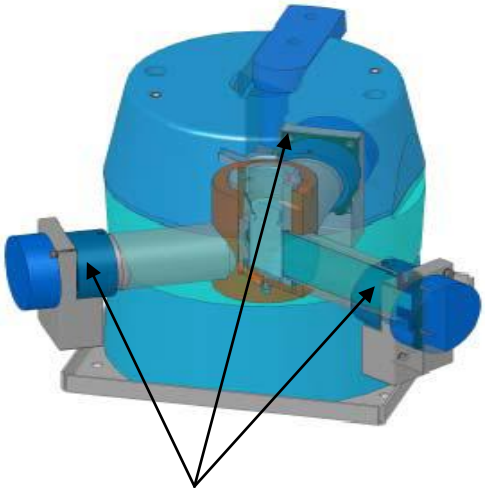

Figure A- 2. Detector assembly of Hidex 300SL liquid scintillation counter

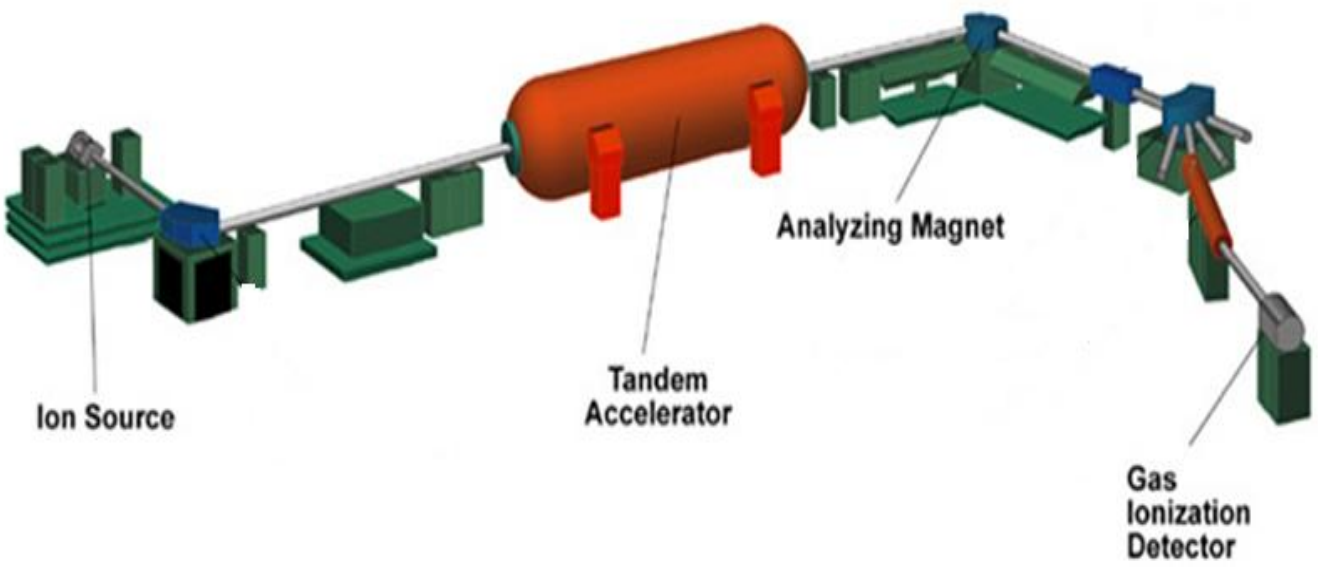

Figure A- 3. A schematic showing main parts of a tandem acceleratory mass spectrometer[(24)]

[(24)] Beta Analytic Inc. Introduction to Radiocarbon Determination by the Accelerator Mass Spectrometry. Available from: http://www.radiocarbon.com/accelerator-mass-spectrometry.htm [Accessed: 20 June 2013]

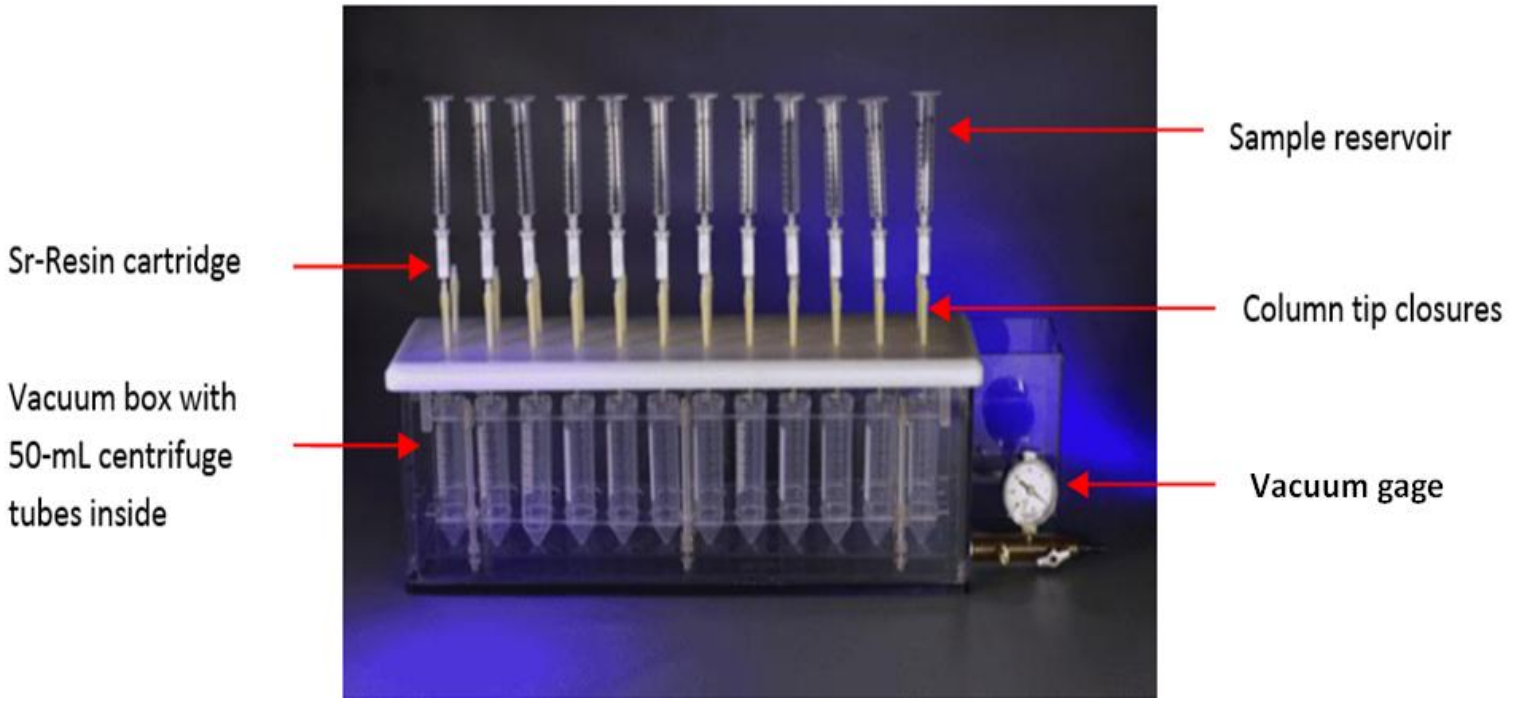

Figure A- 4. Photo of chromatography column assembly[(25)]

[(25)] Eichrom Technologies Inc., www.eichrome.com

Appendix B. Progress Review of Strontium-90 Determination by Accelerator Mass Spectrometry

As part of this research dissertation, development of a new ^{90}Sr target preparation technique using fluorides (*i.e.*, SrF_2) was designed with subsequent accelerator mass spectrometry (AMS) measurements conducted at the IsoTrace AMS facility (University of Toronto, Toronto, Ontario, Canada). Previous measurements of radionuclides by AMS using fluoride also had proven successful[(26, 27, 28)]. The SrF_2 is believed to be a good target source because it can produce SrF_3^- anion at the sputtering source of AMS. In general, the fluoride anions are called super halogen anions because of their unique properties, which are useful to AMS. For example, they show high electron binding energies (> 3.61 eV) which leads to relatively large current production at the sputtering ion source[(29)].

Based on preliminary experiments conducted at IsoTrace AMS facility, it was believed that Zr could be significantly attenuated in the NO_2 in an ISA (Isobar Separator for Anions); the latter being unique to the IsoTrace AMS facility[(29)]. In theory, with the use of ISA and the SrF_2 target, reduction factors for ion source production of ~ $3x10^5$ for ZrF_3–SrF_3 were anticipated with a theoretical detection sensitivity for $^{90}Sr/^{88}Sr$ of ~ $6x10^{-16}$ [(30)]. In practice, however, this detection sensitivity was not achievable. A number of technical difficulties arose at the IsoTrace AMS facility while conducting ^{90}Sr analysis, which limited the resources for measurement of samples. Consequently, the development of ^{90}Sr AMS method was not accomplished. The laboratory sample preparation of ^{90}Sr target, however, was successfully completed.

The AMS target development involved preparation of 30 samples of SrF_2 sources at various levels of ^{90}Sr, ~ 5 fg (equivalent to ~ 0.02 Bq) to ~ 1500 fg (equivalent to ~ 7 Bq) using micro-precipitation techniques. The SrF_2 precipitates were well mixed with PbF_2 (lead fluoride) powder and pressed into a 1.3 mm diameter hole in

---

[(26)] Zhao X. L., Kieser W. E., Dai X., Priest N. D., Tremblay-Kramer S., Eliades J., Litherland A. E., Preliminary Studies of Pu Measurement by AMS Using PuF_4^-. *Nuclear Instruments and Methods in Physics Research B (2013) 294:356-360*

[(27)] Arslan F., Behrendt M., Ernets W., *et al*., Trace Analysis of the Radionuclides ^{90}Sr and ^{89}Sr in Environmental Samples II: Accelerator Mass Spectrometry (AMS), *Chemie Angewandte International English (1995) 34:183-186*

[(28)] Tumey S. J., Brown T. A., Hamilton T. F., Hillegonds D. J., Accelerator Mass Spectrometry of ^{90}Sr for Homeland and Security Environmental Monitoring, and Human Health. Lawrence Livermore National Laboratory, LLNL-JRNL-402381, 19 March 2008

[(29)] Kieser W. E., Eliades J., Litherland A.E., Zhao X-L., Ye S. J., Cousins L., The Low Energy Isobar Separation for Anions. Progress Report, *Radiocarbon 52 (2010): 236-242*

[(30)] Eliades J., Zhao X-L., Litherland A. E., Kieser W. E., Online Ion Chemistry for the AMS Analysis of ^{90}Sr and $^{135,137}Cs$. *Nuclear Instruments and Methods in Physics Research B, (2013) 294: 361-363*

a stainless steel AMS target holder. The use of PbF_2 not only introduces fluoridation (donation of F), but it also enhances ionic conductivity. In conventional AMS target preparations, a metal powder such as Ag or Nb is usually added to enhance conductivity[27,29]. However, for the SrF_2+PbF_2 target, due to high ionic conductivity of PbF_2 (65-130 $J \cdot (K \cdot mol)^{-1}$)), there was no need for addition of metal powders. At the IsoTrace AMS facility, the targets were used to optimize the system conditions before actual measurements could be obtained. At the Cs^+ sputter ion source of AMS, the SrF_3^- anions were produced from the target SrF_2+PbF_2. Once the ions were produced, they entered the ISA where interferences, mainly from ^{90}Zr, were to be reactively suppressed in NO_2 gas. However, ISA optimization was required. Optimization of conditions for the best analyte transmission while suppressing most interferences was found to be quite challenging. The use of NO_2 gas, which is commonly used in the ISA, was anticipated to suppress Zr by a factor of more than a million without causing any trouble to Sr transmission. Unfortunately, during the actual analyses of ^{90}Sr, the high suppression factors for Zr and high transmission of Sr were not achievable. The main reason was because NO_2 was found to react with SrF_3^- (as well as with ZrF_3^- to attenuate it) to form an adduct at low energies. As such, the ISA had to be tuned to maintain as high an average energy as possible. But high ion energy made the ions hard to be confined in the subsequent steps. Consequently, this resulted in only 10 % transmission and over 90 % suppression of SrF_3^-. When O_2 instead of NO_2 was used in the ISA, because O_2 does not react with SrF_3^-, the transmission was improved to 33 %. However, further issues down the line reduced the transmission efficiency even further. The nominal terminal voltage of the accelerator at IsoTrace was 3 MeV. However, due to the age of the tandem accelerator, it had to operate at ~ 1.7 MeV terminal voltage instead. Operation at lower voltage was not suitable for effective transmission of $^{90}SrF_3^-$.

Besides the problems with ISA and tandem acceleration energies, additional challenges were encountered from impurities in the system. In general, in AMS several ion charge values are possible from the electron stripping of the anions. The preferred choice of charge state for the final ion detection is simply that with the highest available stripping yield[31]. Figure B-1 shows the acceleration energies needed for ions to a velocity such that on the average a total of three electrons are removed from the atom[31].

---

[31] Litherland A. E., Ultrasensitive Mass Spectrometry with Accelerators. *Annual Review of Nuclear Particle Science (1980) 30:437-473*

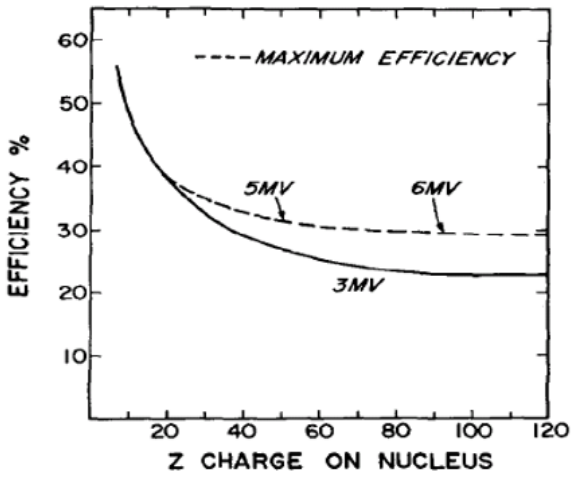

Figure B- 1. The efficiency for generating the + 3 charge state of an ion, by charge exchange in argon gas at 3 MeV energy and expected maximum efficiency at 5 MeV and 6 MeV acceleration energies[(6)]

From Figure B-1, for ^{90}Sr with mass 90, the efficiency of +3 charge state using a 3 MeV accelerator can be around 25 %. At the IsoTrace AMS facility, for both good efficiency and absence of surviving +3 interfering molecules, the detection of $^{90}Sr^{3+}$ was preferred. This was tried first and abandoned immediately. For $^{90}Sr^{3+}$, the mass-to-charge ratio is 30 (*i.e.*, $m{\cdot}z^{-1}$ = 90/3=30). This means that any impurities with mass 30 can interfere with $^{90}Sr^{3+}$ effective measurements. One of the major interferences arose from $^{60}Ni^{2+}$ ($m{\cdot}z^{-1}$ = 60/2=30). The flux of $^{60}Ni^{2+}$ in the spectrum was on the order of thousands counts per second, making $^{90}Sr^{3+}$ detection impossible. The fact that stainless steel target sample holders and press pins were used might have introduced significant amount of $^{60}Ni^{2+}$ in the system. Thus, $^{90}Sr^{3+}$ was unfavourable and, therefore, charge state +4 (*i.e.*, $^{90}Sr^{+4}$) was attempted. Although the final energy spectrum of $^{90}Sr^{4+}$ was clean due to the lack of interferences, the stripping efficiency of mass of $^{90}Sr^{4+}$ from $^{90}SrF_3^-$ was only about 3 % at ~ 1.7 MeV terminal voltage, which was several times lower than that of $^{90}Sr^{3+}$. Due to the low efficiency, only 10 $^{90}Sr^{4+}$ counts were collected in 3000 seconds from a target with 1500 fg ^{90}Sr. The counts were too low for such high ^{90}Sr content. Therefore, further optimization using charge state +2 (*i.e.*, $^{90}Sr^{2+}$) was considered. The $^{90}Sr^{2+}$ also suffered from excessive and variable doubly charged mass 90 molecules, which were too uncertain to be identified and to be controlled. Evaluation of all three different charges states that was tried with the focus shifting back to using +4 charge state. Using +4 charge state of a blank SrF_2+PbF_2 the followings results were reported: (i) transmission before ISA to the entry of the accelerator was 10 % ; (ii) transmission efficiency was 35 % for the SrF_3^- analyte through the ISA while suppressing ZrF_3^- by a factor of million; (iii) transmission efficiency from before ISA to the final Faraday cup was 0.16 %; (iv) the

background was low and excellent (collecting 0 counts) from all blank samples prepared from Sr+Pb+F micro-precipitation; (v) the detection sensitivity of ^{90}Sr was such that for every 5 fg of ^{90}Sr packed in a target, there was 1 $^{90}Sr^{4+}$ detected; (v) the beam transport efficiency form ion source exit to ISA was difficult to maintain stable and, therefore, longer lasting targets are needed. The longer lasting a target is, the closer the measured $^{90}Sr/^{88}Sr$ ratio agreed with the prepared ratio and; (vi) measured ratios of $^{90}Sr/^{88}Sr$ were in the range of ~ 10^{-10} to 10^{-12}.

The review of efforts made to optimize conditions for ^{90}Sr determination clearly indicated that there are a number of inefficiencies in the system set-up and that the system is also very complex. In addition, the inefficiencies with the current AMS facility at IsoTrace suggested that improvements are also needed in preparation of sample targets in order to lower $^{90}ZrF^{3-}$ and increase $^{90}ZrF^{-3}$ ionization yield. The amount of natural Zr in the sample target was found to be 10 times higher than estimated background. Therefore, further purification of Sr target samples was suggested for future samples. In the laboratory, glassware used in micro-precipitation of SrF_2 could have contributed to higher than expected Zr contents. Thus, for target preparation all sources of glassware should be avoided. Beakers and micro-centrifuge tubes that are made of Teflon PFA (perfluoroalkoxy) should be used for micro-precipitation of SrF_2. PFA is resistant to high temperatures, thus, sample could be adequately dried. Moist samples do not transmit effectively.

The $^{90}Sr/^{88}Sr$ of ~ 10^{-10}-10^{-12} achieved at ~ 1.7 MeV terminal voltage of the IsoTrace AMS is 4 orders of magnitude higher than the predicted theoretical limit of ~ 6 x 10^{-16} *(30)*. Even though the detection sensitivity of IsoTrace AMS was much higher than expected, the $^{90}Sr/^{88}Sr$ of ~ 10^{-10} to 10^{-12} is 10 fold better than the detection sensitivity obtained from a 5 MeV accelerator *(27)* and similarly comparable to those accelerators with 8-9 MeV terminal voltage *(28)*. Thus, the ISA of IsoTrace proved to be effective in removing ^{90}Zr interferences in our samples. In order to obtain the desired detection limits predicted, improvements needed to boost the overall system efficiency (*i.e.,* ionization, transmission and stripping). The inefficiency with the current IsoTrace experimental ISA set-up is illustrated in Table B-1. Table B-1 also tabulates the expected improvement in the new AMS system to be commissioned at the University of Ottawa (Ottawa, Ontario, Canada), which will operate at 2.8 MeV high voltage energy. Once commissioned, the measurements of ^{90}Sr will be tried at the new AMS facility and based on Table B-1, where better detection sensitivities than those achieved at IsoTrace AMS facility can be anticipated. However, this work will not form part of the present dissertation.

Table B-1. A comparison of efficiency of IsoTrace AMS with the new AMS system to be commissioned at the University of Ottawa[32]

	Fraction of Sr atoms leaving each segment of the AMS system	
Segment of AMS in the AMS system	**IsoTrace AMS (U of Toronto)**	**New AMS (U of Ottawa)**
Ionization: from Sr atoms in target to SrF_3^- in vacuum	~ 0.01 (unknown)	~ 0.01 (unknown)
Total fraction of Sr atom transmitted: SrF_3^- produced off target to reach ion source exit	~ 0.0002 ~ 0.3 (have to operate at 20keV extraction instead of the designed 35keV due to the limited bending power of the following magnet)	~ 0.1 ~ 0.5 (the magnet will be better, but will still have limited bending power)
SrF_3^- from ion source to ISA entrance	~ 0.3 (have to limit the beam phase space to 2mm-diameter and ±12mRad using a pair of apertures because that is what the current Isobar Separator can fully accept at vacuum)	1 (the new Isobar Separator reception is designed to take full phase space beam at vacuum from a Cs^+ sputter ion source)
SrF_3^- from ISA entrance to exit	~ 0.3 (the current Isobar Separator has not been designed for high transmission, and NO_2 causes damage to all fluoride anions)	~ (0.3 to 0.9) (improvement can be expected with proper full-column ISA design, and with the use of O_2 gas instead of NO_2)
SrF_3^- from ISA exit to tandem acceleratory entrance	~ 0.3 (have to go through an idle magnet box with un-designed matching optics)	1 (have to go through an analyzing magnet, with designed matching optics)
$SrF_3^- \rightarrow Sr^{+4}$ from tandem accelerator entrance to exit	~ 0.03 (have to use +4 charge state at a low (<1.7MeV) terminal voltage due to the age of the tandem accelerator not allowing operation at higher voltage	~ 0.3 (terminal voltage can be close to 3MeV, or, it is more probable to use +1 or +2 with higher stripper pressure for molecular collisional dissociation)
Sr^{+4} from tandem exit to final detector	~ 0.7 (uses a 5mm x 5mm 30nm SiN detector window, which is a bit too small for the beam spot at the detector entrance)	1
Total Sr atom fraction to be measured	**~ 2×10^{-6} (*i.e.*, ~ 2×10^{-4} %)**	**~ 1×10^{-3} (*i.e.*, ~ 0.1 %)**

[32] Zhao X-L., Update on the September 2013 Test of ^{90}Sr ISAMS [personnel communication, 15 September 2013]

Appendix C. Field Sample Collection Procedures and Analyses

C1. Field Safety Considerations Prior to Field Sample Collection

1. Obtain authorization for field work for a minimum of two people.
2. Prepare an emergency response plan, which should contain all of the necessary information: contact numbers for all persons involved with the project, Chalk River Laboratories' emergency contact numbers, and any other information necessary for an emergency situation.
3. At each site do a quick safety assessment prior to carrying out any work (*i.e.*, assess site location and access hazards, potential upstream, in-stream, and downstream hazards, safety gear required, *etc.*).
4. For collection of samples using a boat:
    i. Keep two paddles, a bailer, and an anchor on board.
    ii. Prior to collecting a sample, ensure that the anchor is secured.
    iii. Do not stand in the boat to obtain the water sample and position yourself securely.

C2. Water Quality Measurement *in-situ*

1. Calibrate the probes of pH/temperature meter (Beckman PHI 265) using buffer pH 4, 7, and 10 as per manufacturer instruction manual.
2. Calibrate the electric conductivity meter (YSI Model 30) using 2 standard solutions of potassium chloride, 0.01 M KCl and 0.1 M KCl at 25˚C as per manufacturer instruction manual.
3. Record data in calibration log book.

***Note**: Calibrate the meter probes daily and periodically throughout the day if required. Maintain a calibration log book and record the calibration data in order to track the performance of the meter. Keep calibration solutions in a cooler at temperatures close to the field water temperatures.*

4. Measure electric conductance, pH, and temperature *in-situ* from the boat:
    i. Lower the probe to approximately 10 cm depth beneath the surface.
    ii. Let the instrument stabilize, usually 1-2 min.
    iii. Record the readings in the field notebook.
5. Rinse the probe meters with de-ionized water in between sample locations.
6. Keep pH electrode sensors wet with sample water or tap water at all times during sampling (short-term storage).
7. Enter measurements in a spreadsheet and make temperature corrections for specific conductance based on KCl solution:
    i. If the temperature of the water sample is below 25˚C, add 2 % of the reading per degree to the specific conductance measurement reading of the sample obtained.

ii. If the temperature of the water sample is above 25˚C, subtract 2 % of the reading per degree from the specific conductance measurement reading of the sample obtained.
iii. If the temperature of the water sample is at 25˚C, report the exact measurement.

C3. Collecting Surface Water Samples Using a Boat

1. Anchor the boat securely.
2. Use a GPS (global positioning system) to accurately position the sampling location.
3. Record physical and meteorological conditions (*e.g.*, ambient temperature).
4. Take water samples from the upstream side to prevent contamination of the sample from gas or oil of the boat engine.
5. Use a ~ 4-L new polyethylene container with a handle for grabbing the water sample by lowering the container from the boat.
6. Note the date and time of sample collection using a waterproof marker, on an adhesive labelling tape that is affixed to the container.
7. Rinse the container with sample water three times before filling in order to remove any plasticizer used in production of the container.
8. Fill the container with sample water.
9. Cap the container immediately after filling.
10. Record the sample identification code on the adhesive labelling tape using a waterproof marker. Identify each of the samples by a unique code containing sampling location name and number (*e.g.*, PL1-3 for the first water sample collected from the third collection location of Perch Lake).
11. Put the container in a clean plastic bag and then in a chilled cooler and ship to the laboratory.

C4. Water Quality Measurement in the Laboratory

For those samples where *in-situ* measurement of water was not taken (*e.g.*, seawater samples), perform pH and conductivity measurements in the laboratory once the samples arrive:

1. Calibrate the probes of pH/temperature meter (Beckman PHI 265) using buffer pH 4, 7, and 10 as per manufacturer's instruction manual.
2. Calibrate the electric conductivity meter (YSI Model 30) using 2 standard solutions of potassium chloride, 0.01 M KCl and 0.1 M KCl at 25˚C as per manufacturer's instruction manual.
3. Record data in calibration log book.
4. Transfer a sub-sample of ~ 100 mL from the sample container into a 125-mL polyethylene bottle.
5. Rinse the electrode of conductivity meter with sample water in a separate container and discard water.

6. Place the electrode in the 150-mL polyethylene bottle.
7. Swirl the sample and allow 1-2 min for the meter to stabilize.
8. Record the reading in the lab notebook.
9. Rinse the electrode of pH meter with sample water in separate container and discard water.
10. Place the pH electrode in the 150-mL polyethylene bottle.
11. Swirl the sample and allow 1-2 min for the meter to stabilize.
12. Record the pH reading in the laboratory notebook.
13. Enter measurements in a spreadsheet and make temperature corrections for specific conductance as described in Appendix C2 step 7.

C5. Sample Filtration and Preservation

All water samples, including seawater and groundwater, are filtered and preserved as follows:

1. Filter the water samples through a 0.45 µm cellulose acetate membrane using a peristaltic pump.

   Note: *0.45 µm filter porosity is commonly used to separate particulate and dissolved matter.*

2. Separate a sub-sample of filtrate in a pre-labelled bottle for each of the chemical analyses such as anions, dissolved carbons, alkalinity, and dissolved metals.
3. Collect the remainder of the filtrate in two pre-labelled 2-L high density polyethylene bottles for ^{90}Sr method development.
4. Acidify the filtrate water with HNO_3 to 1 % by volume, which adjusts the pH of the water to < 2.
5. Rinse filtration equipment in between samples by pumping 1-2 L deionized water.
6. Acid wash filtration equipment with 5 % HNO_3 solution in between different sampling locations (*i.e.,* Ottawa River, Perch Lake, and Lower Bass Lake) and or types (*i.e.,* surface water, groundwater, and seawater):
   i. Pump ~ 500 mL of 5 % HNO_3 solution through the tubing of the filtration system.
   ii. Pump ~ 2 L deionized water.
   iii. Allow the equipment to air dry overnight.

Note*: Use a new filter membrane for each water sample. If the water contains lots of suspended particles, change the filter membrane frequently as needed.*

7. Store the bottles in a fridge with temperature ~ 5˚C until further analysis.

Appendix D. Efficiency Calibration of Strontium-85 and Yttrium-88

The γ spectrometer used in this dissertation for radiotracer γ ray measurement was a coaxial high purity germanium (HPGe) detector system with 25 % relative efficiency at γ energy 1.332 MeV of ^{60}Co. The detector was first calibrated for ^{85}Sr and ^{88}Y energies at specific geometries before measurements of unknown samples at the same geometries were taken. Known amounts (*i.e.*, ~ 70-80 Bq) of traceable ^{88}Y and ^{85}Sr reference standard solutions were spiked into diluted acidic solutions in 20-mL polyethylene plastic scintillation vials. Calibration samples volumes consisted of 10 mL, 15 mL, and 20 mL of 0.1 M HCl solution, which corresponded to the volumes of the unknown samples that were prepared for measurement at different stages of the method development experiments. The calibration sources were prepared in acid solutions to match the matrix of unknown samples and also to prevent the source uptake by the counting vials. After spiking, the samples were mixed well by agitating the vials. The vials were counted on the HPGe spectrometer at contact with and also 2.5 cm distance from the detector for approximately 2.5 h each. The net peak area was obtained and used to calculate the counting efficiency of each of the three γ rays of ^{88}Y (*i.e.*, 0.898 MeV, 1.836 MeV, and 2.734 MeV) and the 0.514 MeV γ ray of ^{85}Sr. The counting efficiencies for various geometries are shown in Figure D-1.

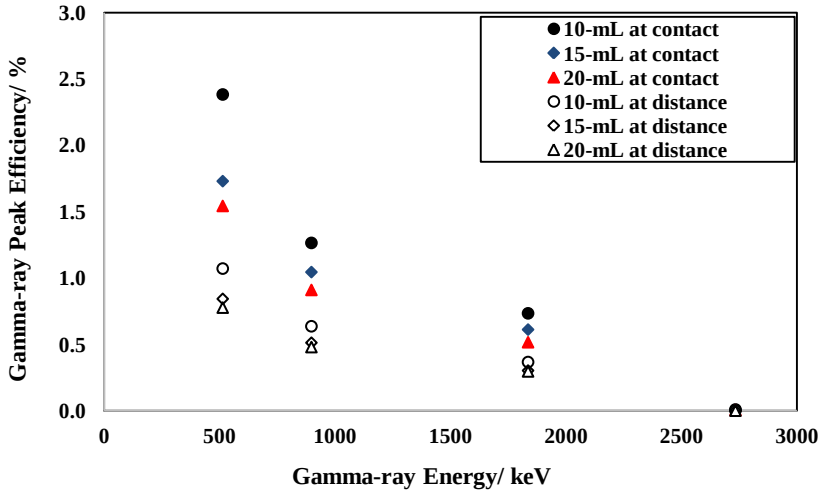

Figure D- 1. Calibration of ^{88}Y and ^{85}Sr γ-ray energies as a function of peak efficiency

As Figure D-1 illustrates, the peak efficiencies were higher when the samples were counted at contact position with the detector and, therefore, unknown samples were also counted at contact with the detector. Peak efficiencies at contact for all three volumes are tabulated in Table D-1 and Figure D-2. The corresponding peak

efficiencies (shaded in Table D-1) were used to determine activities of ^{88}Y and ^{85}Sr in unknown samples in Appendix L.

Table D-1. Peak efficiency calibration of ^{88}Y and ^{85}Sr at various geometries

Isotope	Matrix	Activity added /Bq	γ-ray energy /MeV	*I*	Net count rate /cps	FWHM[(33)]	ε_γ /%
^{88}Y	10 mL acidic solution	93.65	1.836	0.992	0.687±0.009	1.93	0.734±0.024
			0.898	0.937	1.184±0.012	1.54	1.264±0.040
			2.734	0.007	0.009±0.002	1.20	0.010±0.002
^{85}Sr		90.70	0.514	0.96	2.161±0.016	1.24	2.383±0.074
^{88}Y	15 mL acidic solution	57.12	1.836	0.992	0.349±0.004	2.0	0.612±0.020
			0.898	0.937	0.597±0.006	1.4	1.045±0.033
			2.734	0.007	0.003±0.001	0.5	0.005±0.001
^{85}Sr		50.90	0.514	0.96	0.880±0.007	1.18	1.730±0.054
^{88}Y	20 mL acidic solution	93.65	1.836	0.992	0.462±0.008	1.92	0.516±0.018
			0.898	0.937	0.814±0.010	1.51	0.910±0.029
			2.734	0.007	0.005±0.001	0.35	0.005±0.000
^{85}Sr		90.70	0.514	0.96	1.298±0.013	1.15	1.543±0.049

An example of γ peaks of one of the calibrated samples for ^{85}Sr and ^{88}Y is shown in Figure D-2. As illustrated in Figure D-2, all peaks were distinct and well resolved.

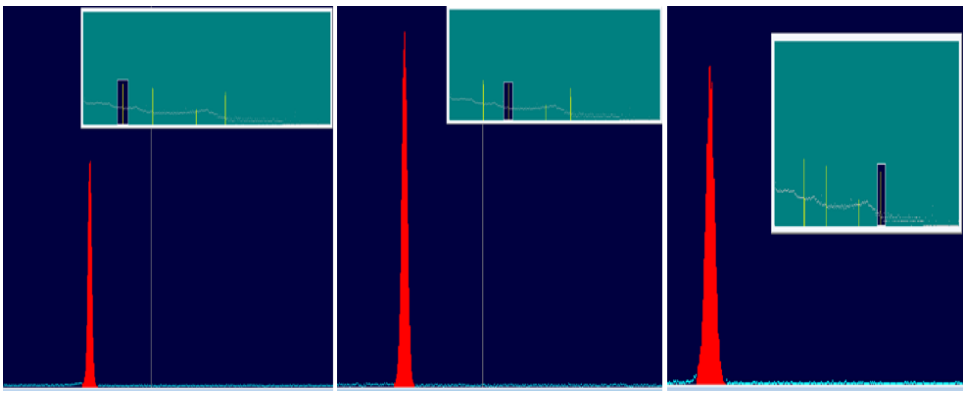

Figure D-2. Mixed standard sources of ^{88}Y and ^{85}Sr counted on the HPGe γ spectrometer (in 10 mL 0.1 M HCl, at contact). Peaks shown here are the spectrum of ^{85}Sr at 0.514 MeV (left) and two spectra of ^{88}Y at 0.898 MeV (centre) and 1.836 MeV (right).

[(33)] FWHM= full width half max; it is a measure of peak resolution in γ spectrometry.

Appendix E. Reagents and Materials Used in Experimentation Phase

Table E- 1. Chemical and radiological standards/solutions and material used in laboratory analysis of water samples

	Product Name	Manufacturer	Purpose
Radioactive Standard Solution	^{90}Sr-^{90}Y reference standard ($SrCl_2$ in 0.1 M HCl)	Eckert and Ziegler Isotope Products (Valencia, CA, USA)	Spike standard solution
	^{89}Sr reference standard ($SrCl_2$ in 0.1 M HCl)	Eckert and Ziegler Isotope Products (Valencia, CA, USA)	Spike standard solution
	^{85}Sr reference standard ($SrCl_2$ in 0.5 M HCl)	Eckert and Ziegler Isotope Products (Valencia, CA, USA)	Spike standard solution
	^{88}Y reference standard (Y_2Cl_3 in 0.1 M HCl)	Eckert and Ziegler Isotope Products (Valencia, CA, USA)	Spike standard solution
	^{137}Cs reference standard (CsCl in 0.1 M HCl)	Eckert and Ziegler Isotope Products (Valencia, CA, USA)	Spike standard solution
	^{210}Pb-^{120}Bi reference standard ($Pb(NO_3)_2$ in1.2 M HNO_3)	Eckert and Ziegler Isotope Products (Valencia, CA, USA)	Spike standard solution
	^{60}Co reference standard ($CoCl_2$ in 0.1 M HCl)	Eckert and Ziegler Isotope Products (Valencia, CA, USA)	Spike standard solution
Chemical Reagents	HNO_3 solution	Fisher Scientific Inc. (Ottawa, ON, Canada)	Preservative, dissolving agent
	HCl solution	Fisher Scientific Inc. (Ottawa, ON, Canada)	Preservative, column matrix etc.
	H_3PO_4 solution	Fisher Scientific Inc. (Ottawa, ON, Canada)	PO_4 source for co-precipitation
	NH_4OH solution	Fisher Scientific Inc. (Ottawa, ON, Canada)	Sample pH adjustment
	Na_2CO_3 salt	Fisher Scientific Inc. (Ottawa, ON, Canada)	CO_3 precipitation
	KCl salt	Fisher Scientific Inc. (Ottawa, ON, Canada)	Preparing ^{40}K source
	$Ca(NO_3)_2$ salt	Fisher Scientific Inc. (Ottawa, ON, Canada)	Ca source for co-precipitation
	$TiCl_3$ solution	Fisher Scientific Inc. (Ottawa, ON, Canada)	Co-precipitation of Y
	Y carrier solution (Y_2O_3 in 2 % HNO3)	Sigma-Aldrich (Oakville, ON, Canada)	Stable tracer for chemical yield
	Sr carrier solution ($Sr(NO_3)_2$ in 2 % HNO3)	Sigma-Aldrich (Oakville, ON, Canada)	Stable tracer for chemical yield
	pH buffer solutions	Fisher Scientific Inc. (Ottawa, ON, Canada)	pH meter calibration
	Ultima Gold AB cocktail	Perkin Elmer (Woodbridge, ON, Canada	Liquid scintillation cocktail

Table E-1. Continues

	Product Name	Manufacturer	Purpose
Materials	Sr-Resin® cartridges (2 mL, 50-100 um)	Eichrom Technologies Inc. (IL, USA)	Chromatographic separation of Sr
	DGA-N® resin cartridges (2 mL, 50-100 um)	Eichrom Technologies Inc. (IL, USA)	Chromatographic separation of Y
	7-mL liquid scintillation counting vials	Gamble Technologies (Mississauga, ON, Canada	Liquid scintillation counting of sample
	20-mL liquid scintillation counting vials	Perkin Elmer (Woodbridge, ON, Canada	Liquid scintillation counting of sample
	pH paper	Fisher Scientific Inc. (Ottawa, ON, Canada)	pH check
	Centrifuge tubes	Fisher Scientific Inc. (Ottawa, ON, Canada)	Centrifuging sample
	Food dye	Walmart (Pembroke, ON, Canada)	Colour quenching agent

Appendix F. Preparation of Reagents

All reagents are prepared in a fume hood.

F1. Preparation of 0.1 M HCl

1. In a 1-L volumetric flask, add 900 mL pure water.
2. Pipette 8.33 mL concentrated HCl (12 M).
3. Dilute to 1L with deionized water.

F2. Preparation of 0.1 M HNO_3

1. In a 1-L volumetric flask, add 900 mL pure water.
2. Pipette 6.25 mL concentrated HNO_3 (15.8M).
3. Dilute to 1L with deionized water.

F3. Preparation of 8 M HNO_3

1. In a 1-L volumetric flask, add 400 mL pure water.
2. Add 506 mL concentrated HNO_3 (15.8M) using a graduated cylinder.
3. Dilute to 1L with deionized water.

F4. Preparation of 0.05 M HCl

4. In a 1-L volumetric flask, add 900 mL pure water.
5. Pipette 4.17 mL concentrated HCl (12 M). Dilute to 1L with deionized water.

F5. Preparation of 2.6 M Na_2CO_3

1. In a 1-L Nalgene polyethylene plastic bottle, add 280 g of anhydrous Na_2CO_3.
2. Add 500 mL deionized water and dissolve the solid. Dilute to 1L.
3. Calculate the exact concentration as expressed by Eq. (F-1).

$$\left(\frac{1\ mol\ Na_2CO_3}{106\ g\ Na_2CO_3}\right)\left(\frac{280\ g\ Na_2CO_3}{1\ L}\right) = 2.6\ \frac{mol}{L}Na_2CO_3 \qquad \text{(F-1)}$$

F6. Preparation of 40 mg·mL^{-1} Ca Solution

1. In a 1-L Nalgene polyethylene plastic bottle, add 163.7 g of anhydrous $Ca(NO_3)_2$ salt.
2. Add 500 mL deionized water and dissolve the solid. Dilute to 1 L.
3. Calculate the exact concentration as per Eq. (F-2).

$$\left(\frac{1\ mol}{164.088\ g}Ca(NO_3)_2\right)\left(\frac{1\ mol\ Ca(NO_3)_2}{1\ mol\ Ca}\right)\left(\frac{40.078\ g}{1\ mol}Ca\right)\left(\frac{163.7\ g\ Ca(NO_3)_2}{1000\ mL}\right) = 40\ \frac{mg\ Ca}{mL} \qquad \text{(F-2)}$$

Appendix G. TDCR Čerenkov Counting Method Experimental

G1. Geometry Test Sample Preparation

TDCR Čerenkov counting test of sample geometry was performed using different sample volumes counted in plastic and glass scintillation counting vials of 7-mL and 20-mL capacity.

G.1.1. Sample Preparation in Plastic Vials

1. Label the caps of a number of 7-mL and 20-mL polyethylene plastic scintillation vials that are new and clean with a sample identification code, for example, SrCT3-1, representing Sr Čerenkov, Test 3, sample number 1.
2. Weigh the vials and record their weights in laboratory notebook.
3. Use four of the 7-mL plastic vials to transfer the following volumes of deionized water that is acidified as 0.1 M HCL solution using a calibrated 10-mL pipette: 1 mL, 3 mL, 5 mL, and 7 mL.
4. Use another set of four 7-mL plastic vials to transfer the same volumes as above for duplicate sample preparation.
5. In the eight of the 20-mL plastic vials, transfer the following volumes of using a calibrated 10-mL pipette: 3 mL, 5 mL, 7 mL, 10 mL, 13 mL, 15 mL, 18 mL, and 20 mL.
6. Repeat step 5 using another set of eight vials to prepare duplicate samples.
7. Weigh vials with samples in them and record the weight information in laboratory notebook.
8. Add a known amount (8-10 Bq) of traceable ^{90}Sr-^{90}Y radioactive standard in each of the 7-mL and 20-mL vials.
9. Seal the vials tight and shake well.
10. Weigh the vials and note the exact amount of the standard added.
11. Prepare four blank samples for the 7-mL vials by adding the following sample volumes of deionized water that is prepared as 0.1 M HCl into the 7-mL vials: 1 mL, 3 mL, 5 mL, and 7 mL.
12. Prepare eight blank samples for the 20-mL vials by adding the following sample volumes of 0.1 M HCl into the 20-mL vials: 3 mL, 5 mL, 7 mL, 10 mL, 13 mL, 15 mL, 18 mL, and 20 mL.
13. Prepare another set of 7-mL polyethylene vials from 0.1 M HNO_3 solution at volumes: 1 mL, 3 mL, 5 mL, and 7 mL.
14. Weigh vials with samples in them and record the weight information in laboratory notebook.
15. Add a known amount (8-10 Bq) of traceable ^{90}Sr-^{90}Y radioactive standard in each of the 7-mL and 20-mL vials.
16. Seal the vials tight and shake well.
17. Weigh the vials and note the exact amount of the standard added.

18. Prepare four blank samples for the 7-mL vials by adding the following sample volumes of deionized water that is prepared as 0.1 M HNO_3 solution into the 7-mL vials: 1 mL, 3 mL, 5 mL, and 7 mL.
19. Count samples on a low background Hidex LSC for 0.5 h.

G.1.2. Sample Preparation in Glass Vials

1. Label the caps of a number 7-mL and 20-mL low-potassium borosilicate glass scintillating vials that are new and clean with a sample identification code (*e.g.*, SrCT8-1).
2. Weigh the vials and record their weights in laboratory notebook.
3. Use three of the 7-mL glass vials to transfer the following volumes of deionized water acidified to 0.1 M HCl solution using a calibrated 10-mL pipette: 3 mL, 5 mL, and 7 mL.
4. Use another set of four 7-mL glass vials to transfer the same volumes as above for duplicate sample preparation.
5. In the four of the 20-mL glass vials, transfer the following volumes of the same solution using a calibrated 10-mL pipette: 10 mL, 15 mL, 18 mL, and 20 mL.
6. Repeat step 5 using another set of 4 vials to prepare duplicate samples.
7. Add a known amount (~ 8-10 Bq) of traceable ^{90}Sr-^{90}Y radioactive solution standard in each of the 7-mL and 20-mL vials.
8. Seal the vials tight and shake well.
9. Weigh the vials and note the exact amount of the standard added.
10. Count samples on low background Hidex LSC for 0.5 h.

G2. Colour Quenching Test Sample Preparation

Use yellow and brown food-grade dyes. Prepare brown dye by mixing red, green and yellow food-grade dyes in the proportions of 1:1:3, respectively. Prepare colour quenched samples in plastic and glass vials of 20-mL as follows:

1. Label the caps of a number of 20-mL plastic and glass scintillation vials that are new and clean with a sample identification code, for example, SrCT11-1.
2. Transfer 15 mL deionized water using a calibrated pipette into the vials.
3. In a set of eight plastic vials with 15 mL deionized water, add yellow dye in increasing drops (1 drop ~ 0.1 mL) with no colour added to the first sample.
4. In another set of eight plastic vials with 15 mL deionized water, add brown dye in increasing drops (1 drop ~ 0.1 mL).
5. In a set of six glass vials with 15 mL deionized water, add yellow dye in increasing drops (1 drop ~ 0.1 mL) (there is no need to repeat brown dye test in glass vials).
6. Prepare blank samples by adding 15 mL deionized water in each of 20-mL plastic and glass vials.
7. Seals vials tight and shake well.

8. Use a small portion, from each vial to measure absorbance on the Spectronic 200 UV-Visible spectrophotometer (Thermo Scientific Spectronic 200^{TM}):
    i. Following the instruction manual of the spectrophotometer take a background measurement for auto-subtraction of background.
    ii. Calibrate the instrument for zero absorption and 100 % transmission using deionized water sample in a quartz cuvette.
    iii. Transfer, using a disposal pipette, ~ 1 mL from each of the vials prepared in steps 2-6 within this section (Appendix G2) into the quartz cuvette.
    iv. Place the cuvette in the measurement chamber, close the lid, and obtain a measurement by pressing the designated button on the instrument.
    v. Record the maximum absorption and wavelength information reported by the instrument software, PiQue^{TM}, in laboratory notebook.
9. Seal the vials and count them on Hidex LSC to obtain background measurement of the quenched samples.
10. Weight the vials with samples and record weights.
11. Add a known amount (8-10 Bq) of traceable ^{90}Sr-^{90}Y radioactive standard solution into the coloured samples.
12. Seal the vials tight and shake well.
13. Weigh the vials again and note the exact amount of the standard added.
14. Recount the vials on the Hidex LSC.

G3. Preparation of Samples for Interfering Radionuclides Test

Prepare single radionuclide-containing samples using 15 mL of the deionized water prepared at 0.1M HCl in 20-mL plastic and glass scintillation vials as follows:

1. Label a number of 20-mL plastic and glass scintillation vials with the radionuclide symbol to be tested.
2. Add 15 mL solution into each vial.
3. Weigh vials and record weights in laboratory notebook.
4. For each of the radionuclides to be tested (*i.e.*, ^{90}Sr-^{90}Y, ^{32}P, ^{89}Sr, ^{210}Pb/ ^{210}Bi, ^{60}Co, and ^{137}Cs), add an exact amount of radioactivity.
5. Weigh vials and note the weights in laboratory notebook.
6. For ^{40}K, add a known amount (*i.e*., 0.5-1 g) of KCl, salt into the 15 mL deionized water, seal vial, and shake well to dissolve the salt.
7. Repeat steps 2-6 to prepare duplicate samples for each radionuclide test.
8. Prepare blank samples in each of plastic and glass vials from 15 mL deionized water.
9. Count vials on the Hidex LSC for 0.5 h.

Appendix H. Pre-concentration of Strontium-90 and Yttrium-90

H1. Procedure for Freshwater Strontium-90 and Yttrium-90 Co-precipitation

Use the procedure described below for the co-precipitation of unknown freshwater water samples, deionized water blank samples, and deionized water spiked samples:

1. Label 1-L clean glass beakers with sample identification code (*e.g.*, PL1-3 for Perch Lake sample 1 from sampling location 3).
2. Weigh beaker on a top loading balance and record mass in laboratory notebook.
3. Add 1L of pre-acidified unknown water sample to the beaker, weigh beaker with water in it, and record mass in the laboratory notebook.
4. For the spiked test samples and procedural blank samples, added 1L deionized water to the beaker, weigh the beaker with water in it, and record mass in the laboratory notebook.
5. Place a stir bar in the beaker.
6. Place the beaker on a stirring plate and start stirring.
7. Add approximately 1 mL of stable Sr carrier solution with concentration of 1000 $mg \cdot L^{-1}$ to all samples including blank and spiked sample for Sr chemical recovery monitoring, weigh the beaker, and record mass in the laboratory notebook.
8. Add ~ 1 mL of stable Y solution with concentration of 1000 $mg \cdot L^{-1}$ to all samples including blank and spiked sample for Y chemical recovery monitoring, weigh the beaker, and record mass in the laboratory notebook.
9. Mix the sample well.
10. For the spiked samples to be prepared at various concentrations of ^{90}Sr-^{90}Y (*i.e.*, 0-1 $Bq \cdot L^{-1}$, 5 $Bq \cdot L^{-1}$, 30 $Bq \cdot L^{-1}$, and 100 $Bq \cdot L^{-1}$), add known amounts of traceable ^{90}Sr-^{90}Y standard solution and record the exact mass of the standard solution added.
11. Remove a sub-sample equivalent to approximately 1 mL of water from the sample beaker and transfer it into a pre-weighed and pre-labelled 50-mL centrifuge tube for analysis of initial concentrations of Sr and Y by ICP-MS.
    i. Label a 50-mL centrifuge tube with sample code and letter A. For example, PL1-3A.
    ii. Weigh the 50-mL centrifuge tube and record the mass in the laboratory notebook.
    iii. Transfer approximately 1 mL of sample into the labelled and pre-weighed 50-mL centrifuge tube.
    iv. Record exact mass of the sample removed for ICP-MS analysis in the laboratory notebook.
    v. Add 0.1 M HNO_3 until the total volume reaches 20 mL.

vi. Record the final mass in the laboratory notebook.
vii. Seal the cap of the centrifuge tube with parafilm and send for ICP-MS analysis.

12. To the sample in the beaker, add 2 mL of 1 M $Ca(NO_3)_2$, solution (*i.e.*, ~ 80 mg Ca^{2+}) while stirring.
13. Add 1 mL of concentrated H_3PO_4 to each sample.
14. Continue stirring to mix reagents.
15. Using a transfer pipette, add concentrated NH_4OH solution, in a drop-wise manner, to each sample until the pH reaches 9-10 (check with pH paper).
16. Transfer half of the sample solution to a pre-weighed and pre-labelled 500-mL centrifuge tube.
17. Centrifuge at 4000 rpm for 5 min.
18. Gently decant the supernatant into a waste bottle for proper disposal.
19. Transfer the remainder of the sample solution to the same centrifuge tube.
20. Centrifuge at 4000 rpm for 5 min.
21. Gently decant the supernatant into a waste bottle for proper disposal.
22. To the precipitate in the 500-mL tube, add 100 mL deionized water, agitate the tube to loosen the precipitate, and centrifuge at 4000 rpm for 5 min.
23. Gently decant the supernatant into a waste bottle for proper disposal.
24. Weigh tube with precipitate in it and record mass in laboratory notebook.
25. Based on the mass of the precipitate, add a similar volume of concentrated HNO_3 solution to dissolve the precipitate (usually 10 mL). Sample is now ready for column extraction chromatography (Refer to Appendix I).

***Note**: It is important that the final sample is prepared in 8 M HNO_3 for column chromatography step (Appendix I). In case the dissolution is not complete by adding an amount equivalent to the precipitate size, add 5-6 mL of 8 M HNO_3 solution instead of concentrated HNO_3 to achieve complete dissolution.*

H2. Procedure for Seawater Yttrium-90 Co-precipitation

Use the procedure described below for the co-precipitation of seawater spiked and procedural blank samples:

1. Label 1-L clean glass beakers with sample identification code (*e.g.*, SWY-1 for seawater spiked sample 1)
2. Weigh beaker on a top loading balance and record mass in the laboratory notebook.
3. Add 1 L pre-acidified seawater to the beaker.
4. Weigh beaker with water in it and record mass of the water in the laboratory notebook.
5. Place a stir bar in the beaker.
6. Place beaker on stirring plate and start stirring.

7. Add ~ 1 mL of stable Y solution with concentration of 1000 $mg \cdot L^{-1}$ to all samples including procedural blank sample for Y chemical recovery monitoring, weigh beaker, and record in the laboratory notebook.
8. Mix the sample well.

Note: *There is no need to add stable Sr tracer as seawater naturally contains an ample amount of Sr (i.e., 6-8 $mg \cdot L^{-1}$), which can be traced.*

9. For spiked samples to be prepared at various concentrations of ^{90}Sr-^{90}Y (*i.e.*, 0-1 $Bq \cdot L^{-1}$, 5 $Bq \cdot L^{-1}$, 30 $Bq \cdot L^{-1}$, and 100 $Bq \cdot L^{-1}$), add known amounts of traceable ^{90}Sr-^{90}Y standard solution and record the exact mass of the standard solution added into the laboratory notebook.
10. To the spiked seawater samples with ^{90}Sr-^{90}Y of 5 $Bq \cdot L^{-1}$, 30 $Bq \cdot L^{-1}$, and 100 $Bq \cdot L^{-1}$, add a known amount (10-12 Bq) of traceable ^{88}Y standard for recovery monitoring by radiotracing option.
11. Record the exact mass of the ^{88}Y standard solution added into the laboratory notebook.
12. To all spiked samples, add a known amount (10-12 Bq) of traceable ^{85}Sr standard solution for chemical recovery monitoring by radiotracing option.
13. Record the exact mass of the ^{85}Sr standard solution added.

Note*: Avoid adding ^{88}Y in the low-level spiked (spiked with ^{90}Sr-^{90}Y at 0-1 $Bq \cdot L^{-1}$) samples because ^{88}Y and ^{90}Y are not separable and ^{88}Y strongly interferes with ^{90}Y spectrum. Also, there is no need for radiotracing option in the seawater procedural blank samples.*

14. Remove a sub-sample equivalent to approximately 1 mL of sample from the sample beaker and transfer it into a pre-weighed and pre-labelled 50-mL centrifuge tube for analysis of initial concentrations of Sr and Y by ICP-MS.
    i. Label a 50-mL centrifuge tube with sample code and letter A. For example, SWY-1A.
    ii. Weigh the 50-mL centrifuge tube and record the mass in the laboratory notebook
    iii. Transfer approximately 1 mL of sample into the labelled and pre-weighed 50-mL centrifuge tube
    iv. Record exact mass of the sample removed for ICP-MS analysis in laboratory notebook.
    v. Add 0.1 M HNO_3 until the total volume reaches 20 mL.
    vi. Record the final mass in the laboratory notebook.
    vii. Seal the cap of the centrifuge tube with parafilm and send for ICP-MS analysis.
15. To the sample in the beaker, using a transfer pipette add concentrated NH_4OH solution, drop-wise, while stirring to adjust pH to 5-6 (check with pH paper).

16. Continue stirring well.
17. While stirring, add 25 mL of saturated Na_2CO_3 solution in 5 mL portions using a calibrated 5-mL or 10-mL pipette.
18. Check pH of solution using precision pH paper. The pH should be ≤ 9.
19. Add concentrated NH_4OH solution, drop-wise, while stirring to adjust pH to 9.5-10 (check with precision pH paper). Calcium carbonate ($CaCO_3$) precipitate starts forming when solution turns basic, around pH 8.
20. Confirm the final pH is between pH 9.5-10 using a pH meter. Insert the probe of the pH meter into the solution.

***Note**: Ensure the pH meter probe is rinsed thoroughly in between samples to prevent the possibility of cross contamination.*

21. Transfer half of the sample solution to a pre-weighed and pre-labelled 500-mL centrifuge tube.
22. Centrifuge at 4000 rpm for 5 min.
23. Gently decant the supernatant into a pre-labelled 1-L polyethylene bottle and save until recovery results are obtained. Label the supernatant bottle with the sample code and letter B, for example, SWY-1B. If the recovery results are within the expected range (*e.g.,* 70-100 %), then properly dispose of the supernatant solution.
24. Transfer the remainder of the sample solution to the same centrifuge tube.
25. Centrifuge at 4000 rpm for 8 min.
26. Gently decant the supernatant and combine with its first half in the 1-L polyethylene bottle.
27. Keep the pellet in the 500-mL centrifuge tube.
28. Weigh the 500-mL centrifuge tube with pellet in it and record mass.
29. Add 10 mL of concentrated HNO_3 solution into the 500-mL centrifuge tube to dissolve the precipitate and mix well.

***Note**: $CaCO_3$ precipice is white and granular and should completely dissolve in 10 mL concentrated HNO_3 solution. Additional concentrated HNO_3 can be added to achieve complete dissolution, when needed.*

30. Transfer the sample solution in a 20-mL plastic scintillation counting vial.
31. Count the sample on the HPGe γ spectrometer for 0.5 h for the detection measurement of ^{88}Y and ^{85}Sr in the $CaCO_3$ precipitate.
32. After γ spectroscopy measurement is performed, remove 0.5 mL of the sample and transfer it into a pre-weighed and pre-labelled 50-mL centrifuge tube for analysis of Sr and Y by ICP-MS.
    i. Label a 50-mL centrifuge tube with sample code and letter C. For example, SWY-1C.

ii. Weigh the 50-mL centrifuge tube and record the mass in the laboratory notebook.
iii. Transfer approximately 0.5 mL of the dissolved precipitate into the labelled and pre-weighed 50-mL centrifuge tube.
iv. Record exact mass of the sample removed for ICP-MS analysis in laboratory notebook.
v. Add 0.1 M HNO_3 until the total volume reaches ~ 20 mL.
vi. Record the final mass in the laboratory notebook.
vii. Seal the cap of the centrifuge tube with parafilm and send for ICP-MS analysis.

33. Transfer the remainder of the dissolved precipitate solution to a 500 mL glass beaker for the subsequent precipitation step.
34. Rinse the 500-mL centrifuge tube with aliquots of deionized water and combine the rinse with the sample in the 500 mL beaker.
35. Dilute the sample with deionized water to 250 mL.

***Note**: Do not work with high salt conditions as further precipitation may not be effective.*

36. Place the beaker on a stirring plate, add a stirring bar and stir the sample.
37. Add ~ 3 mL of 20 % $TiCl_3$ solution (~ 230 mg Ti^{3+}) to the sample while stirring.
38. Check pH of the sample solution using pH paper. The pH should be < 2.
39. Adjust pH to 8-8.5 by adding concentrated NH_4OH solution drop-wise and with continuous stirring. Hydrous titanium oxide (HTiO) precipitate starts forming when pH of solution reached around 5.
40. Transfer half of the sample solution to a pre-weighed and pre-labelled 500-mL centrifuge tube.
41. Centrifuge at 4000 rpm for 5 min.
42. Gently decant the supernatant into a pre-labelled 500-mL polyethylene bottle and save until recovery results are obtained. Label the supernatant bottle with the sample code and letter D, for example, SWY-1D. If the recovery results are within the expected range, then properly dispose of the supernatant solution.
43. Keep the pellet in the 500-mL centrifuge tube.
44. Add 100 mL deionized water to the 500-mL centrifuge tube, agitate the tube to loosen the precipitate, and centrifuge at 4000 rpm for 5 min.
45. Gently decant the supernatant and discard.
46. Record the time for ^{90}Y decay correction as t_0.
47. Weight the 500-mL centrifuge tube with pellet in it and record mass in laboratory notebook.

***Note**: for the seawater method in this dissertation, the end of co-precipitation marks the start of decay of ^{90}Y even though on average ~ 20 % ^{90}Sr is expected in the sample. In the seawater method, time records are denoted by t and that of freshwater by T (see Appendix I).*

48. Add an amount equivalent to mass of the precipitate, of concentrated HNO_3 solution to the 500-mL centrifuge tube to dissolve the precipitate.

***Note:** HTiO precipitate is gel type and harder to dissolve compared to $CaCO_3$ precipitate. Also, it is important that the final sample is prepared in 8 M HNO_3 for column chromatography step (Appendix I). In case the dissolution is not complete by adding an amount equivalent to the precipitate size, add 5-6 mL 8 M HNO_3 solution instead of concentrated HNO_3 to achieve complete dissolution.*

49. Transfer the dissolved precipitate to a pre-labelled 20-mL polyethylene plastic scintillation counting vial.
50. Rinse the 500-mL centrifuge tube with aliquots of 8 M HNO_3 and combine the rinse with the sample in the 20-mL vial.
51. Measure the sample on a HPGe γ spectrometer for 0.5 h for ^{88}Y and ^{85}Sr radiotracing in the HTiO precipitate.
52. Once γ spectroscopy measurements are obtained, remove 0.5 mL of the dissolved precipitate and transfer it into a pre-weighed and pre-labelled 50-mL centrifuge tube for analysis of Sr and Y by ICP-MS.
    i. Label a 50-mL centrifuge tube with sample code and letter E. For example, SWY-1E.
    ii. Weigh the 50-mL centrifuge tube and record the mass in the laboratory notebook.
    iii. Transfer approximately 0.5 mL of the dissolved precipitate into the labelled and pre-weighed 50-mL centrifuge tube.
    iv. Note the exact mass of the sample removed for ICP-MS analysis.
    v. Add 0.1 M HNO_3 until the total volume reaches ~ 20 mL.
    vi. Record the final mass in the laboratory notebook.
    vii. Seal the cap of the centrifuge tube with parafilm and send for ICP-MS analysis.
53. Use the reminder of the sample for column extraction chromatography (Refer to Appendix I).

Appendix I. Procedure for Extraction Chromatography of Strontium-90 and Yttrium-90

I1. Extraction Chromatography Apparatus Set-up

1. Use a vacuum box with 12-holes as shown in the Figure A-4 in Appendix A.
2. For ^{90}Sr analysis, use Sr-Resin® (2 mL pre-packed column) and for ^{90}Y use DGA-N® resin (2 mL pre-packed column).
3. Label each column with a sample identification code.
4. Place a 50-mL labelled centrifuge tube in the inner rack of the vacuum box for each sample.
5. Place column tip closures:
   i. Fit a yellow outer tube for each column into the opening of the vacuum box lid.
   ii. Place a white inner tube into each yellow out tip. The white inner tubes cannot be used alone as they will not form an adequate seal with the holes on the lid.
6. Seal any unused openings (white inner tubes) on the vacuum box using vacuum manifold plugs to ensure a good seal is achieved during vacuum box operation.
7. Place a 2 mL Sr cartridge into the white inner tube. In the case of seawater, if not analyzing for ^{90}Sr, omit this step.
8. Place a 2 mL DGA-N® cartridge on top of the Sr cartridge. In the case of seawater, if not analyzing for ^{90}Sr, place the DGA-N® column directly into the white inner tube.
9. Attach a 20- mL syringe with luer lock to the top end of each column. The columns are now ready for pre-conditioning.

I2. Pre-conditioning of Extraction Chromatography Columns

1. Add 10 mL of deionized water to each column assembled in Appendix I1.
2. Attach the vacuum source pump, with a vacuum gauge in-line, to the vacuum box and turn on the vacuum pump.
3. Slowly raise the vacuum pressure to achieve approximately 3 $mL \cdot min^{-1}$ flow rate.
4. Once the reservoir is drained, stop the pump. Lift vacuum box lid and empty the deionized water down the drain.
5. Place the same centrifuge tubes back in the vacuum box.
6. Add 10 mL of 8 M HNO_3 to each column reservoir and turn on the pump.
7. Slowly raise the vacuum pressure to achieve approximately 3 $mL \cdot min^{-1}$ flow rate.
8. Once the reservoir is drained, stop the pump. Lift vacuum box lid and empty the HNO_3 solution into an acid waste bottle for disposal.

9. Place the same centrifuge tubes back in the vacuum box. The columns are now ready for loading with samples for extraction chromatography.

I3. Sample Loading and Extraction

1. Start with samples from Appendix H (samples were prepared in 8 M HNO_3).
2. Add the sample solutions into the 20-mL syringe reservoir of the column extraction system that are already assembled and preconditioned.
3. Turn on vacuum pump and adjust valve on the vacuum source to maintain a flow rate of ≤ 1 $mL \cdot min^{-1}$.
4. Once all samples have drained, turn off vacuum pump and release the vacuum pressure by turning the valve on the vacuum box.
5. Open the vacuum box and remove the 50-mL centrifuge tubes and save them in the laboratory until chemical recovery results are obtained and are as expected, after which these samples can be disposed of appropriately.
6. Place new and pre-labelled 50-mL centrifuge tubes in the inner rack of the vacuum box.
7. Rinse the columns with approximately 10 mL 8 M HNO_3. Keep flow rate at ≤ 3 $mL \cdot min^{-1}$.
8. Once all samples have drained, turn off vacuum pump and release pressure by turning the vacuum box valve.
9. Record the time of end of extraction for ^{90}Y decay correction. Samples are now extracted on the columns and ready to be eluted. For freshwater samples, this time is the start of ^{90}Y decay and is recorded as T_0.
10. Open the vacuum box and remove the 50-mL centrifuge tubes. Discard the 8 M HNO_3 rinse solution in to the acid waste bottle.

***Note**: Unlike the seawater method (Appendix H), for the freshwater method the end of column extraction, rather than the end of co-precipitation, marks the start of decay of ^{90}Y. This is because in the freshwater precipitation method both ^{90}Sr and ^{90}Y are precipitated together whereby ^{90}Sr, which is initially in equilibrium with ^{90}Y, continues to produce ^{90}Y. Thus, the decay correction of ^{90}Y does not start until ^{90}Sr and ^{90}Y separation step in the column chromatography procedure.*

I4. Yttrium Elution from DGA-N® Columns

1. Elute samples in 20-mL plastic scintillation counting vials that are pre-weighed and pre-labelled (caps only).
2. Place a 20-mL vials, with caps removed, for each column in the inner rack of the vacuum box.
3. Replace the inner and out tubes with new ones.
4. Split the Sr-Resin® and DGA-N® resins (if both were used)
5. Place the DGA-N® columns on the top of the new inner tubes.

6. Attach a clean 20-mL syringe reservoir on the top end of each DGA-N® column.
7. Add 10 mL of 0.05 M HCl solution in the syringe.

Note: For freshwater ^{90}Y elution, 10 mL 0.05 M HCl resulted in recoveries that were around 80 %. In order to improve recoveries, this volume was increased to 15 mL for seawater ^{90}Y elution from the column.

8. Turn on vacuum pump and adjust flow rate to ≤ 1 $mL \cdot min^{-1}$.
9. When all the solution has passed through the columns, stop the vacuum pump and remove the vacuum box lid.
10. Remove the 20-mL vials, put their caps and seal them.
11. Weigh the sample vials and record mass in the laboratory notebook.
12. Immediately count the sample for ^{90}Y Čerenkov emission on the Hidex LSC.
13. Count samples on the Hidex for 1 h. Record the start of the counting time for ^{90}Y decay correction as T_1 for freshwater samples and t_1 for seawater.
14. Once finished counted, remove a sub-sample for ICP-MS analysis of eluate[(34)]:
    i. Label a 50-mL centrifuge tube with sample code and letter F. For example, SWY-1F.
    ii. Weigh the 50-mL centrifuge tube and record the mass in the laboratory notebook.
    iii. Transfer approximately 0.5 mL of the eluate sample into the labelled and pre-weighed 50-mL centrifuge tube.
    iv. Record exact mass of the sample removed for ICP-MS analysis in laboratory notebook.
    v. Add 0.1 M HCl until the total volume reaches approximately 20 mL.
    vi. Record the final mass in the laboratory notebook.
    vii. Seal the cap of the centrifuge tube with parafilm and send for ICP-MS analysis.
15. Use 8 mL of the eluate sample for liquid scintillation analysis of ^{90}Y.
16. Add 12 mL Ultima Gold AB liquids scintillation cocktail to each vial with sample.
17. Seal vial and shake to mix.
18. Clean vial external surface with a damp kimwipe tissue.
19. Prepare a blank cocktail solution by mixing 10 mL 0.05 M HCl with 10 mL scintillation cocktail.
20. Count sample and blank vials on the Hidex LSC for 1 h.

[(34)] For the first four sweater samples (SWY-1 through SWY-4), an aliquot for the ICP-MS analysis of stable tracers was removed before Čerenkov counting measurement was obtained. For the rest of seawater and all of freshwater samples, this aliquot was removed after the Čerenkov counting of the sample. Thus, f <1 for Čerenkov counting of SWY-1 through SWY-4 in Table L-10.

21. Record the start of the counting time for ^{90}Y decay correction as t_1 for seawater and T_2 for freshwater samples.

I5. Strontium Elution form Sr-Resin® Columns

1. Elute samples in 20-mL plastic scintillation counting vials that are pre-weighed and pre-labelled.
2. Place a 20-mL vials, with caps removed, for each column in the inner rack of the vacuum box.
3. Replace the inner and outer tubes with new ones.
4. Place the Sr-Resin® columns on the top of the new inner tubes.
5. Attach a clean 20-mL syringe reservoir on the top end of Sr-Resin® column.
6. Add 8 mL deionized water in the syringe.
7. Turn on vacuum pump and adjust flow rate to ≤ 1 mL·min^{-1}.
8. When all the water has passed through the columns, stop the vacuum pump and remove the vacuum box lid.
9. Remove the 20-mL vials, put their caps and seal them.
10. Weigh the sample vials and record mass in the laboratory notebook.
11. Remove a sub-sample for ICP-MS analysis of eluate:
    i. Label a 50-mL centrifuge tube with sample code and letter G. For example, SWY-1G.
    ii. Weigh the 50-mL centrifuge tube and record the mass.
    iii. Transfer approximately 0.5 mL of the eluate sample into the labelled and pre-weighed 50-mL centrifuge tube.
    iv. Record exact mass of the sample removed for ICP-MS analysis in laboratory notebook.
    v. Add 0.1 M HNO_3 until the total volume reaches approximately 20 mL.
    vi. Record the final mass in the laboratory notebook.
    vii. Seal the cap of the centrifuge tube with parafilm and send for ICP-MS analysis.
12. Use the remainder of the eluate sample for liquid scintillation analysis of ^{90}Sr.
13. Add 12 mL liquids scintillation cocktail (UGAB) to each vial with sample.
14. Seal vial and shake to mix.
15. Clean vial external surface with a damp kimwipe tissue.
16. Prepare a blank cocktail solution by mixing 8 mL deionized water with 10 mL scintillation cocktail.
22. Count sample and blank vials on the Hidex LSC for 1 h. Record the start of the counting time for ^{90}Y decay correction as T_3 for freshwater samples (seawater were not processed using Sr-Resin®).
23. Recount the same sample vials on Hidex LSC for 1 h after ^{90}Y in-growth period (7-12 days after purification) and record the start of the re-counting time as T_4.

Appendix J. Non-Radiological Results

Table J- 1. pH and conductivity measurements of surface water samples

Sample Code	Collection, Analysis Date	pH	Temperature /˚C	Specific conductance /µS·cm^{-1}@ 25˚C
		Ottawa River		
ORU1-1, ORU2-1	July 17, 2013	7.45	26.8	59.3
ORD1-1, ORD2-1(Dup)	July 17, 2013	7.17	25.8	59.0
ORD1-2	July 17, 2013	-	-	-
ORD1-3	July 17, 2013	7.26	25.8	59.2
ORD1-4	July 17, 2013	-	-	-
ORD1-5	July 17, 2013	6.43	25.3	59.2
ORD1-6	July 17, 2013	7.23	26.2	59.0
ORD1-7	July 17, 2013	7.53	26.5	59.0
ORD1-8	July 17, 2013	7.82	26.9	59.0
Mean ±1σ		*7.27±0.43*	*26.2±0.59*	*59.1±0.13*
		Perch Lake		
PL1-1	July 18, 2013	6.40	27.7	118.5
PL1-2	July 18, 2013	6.44	27.6	117.4
PL1-3	July 18, 2013	6.45	28.1	117.9
PL2-3	July 18, 2013	6.38	27.9	118.0
PL1-4	July 18, 2013	6.37	27.8	118.1
PL1-5	July 18, 2013	6.50	28.7	118.1
PL1-6	July 18, 2013	6.56	28.8	113.7
PL1-7	July 18, 2013	6.40	28.8	113.7
PL1-8, PL2-8 (Dup)	July 18, 2013	6.54	29.2	111.7
Mean ±1σ		*6.45±0.07*	*28.3±0.59*	*116±2.5*
		Lower Bass Lake		
LBL1-1	July 23, 2013	6.82	25.1	92.1
LBL1-2	July 23, 2013	6.57	25.4	91.3
LBL1-3, LBL2-3(DUP)	July 23, 2013	6.57	25.8	90.5
LBL1-4	July 23, 2013	6.38	25.3	91.2
LBL1-5, LBL2-5(Dup)	July 23, 2013	6.51	25.5	91.1
LBL1-6	July 23, 2013	6.76	24.8	91.4
LBL1-7	July 23, 2013	6.57	25.3	91.4
LBL1-8	July 23, 2013	6.57	25.3	91.4
Mean ±1σ		*6.59±0.14*	*25.3±0.29*	*91.3±0.44*
Water Blank		5.57	17.6	3.0

Table J- 2. pH and conductivity measurements of groundwater samples

Sample code	Collection/ Analysis Date	pH	Temperature /˚C	Specific conductance /µS·cm^{-1}@ 25˚C
B-WS	Oct. 3, 2013	8.15	11.6	519
C-264	Oct. 24, 2013	6.20	9.8	409
610-35	Nov. 1, 2013	6.28	11.8	788
610-36	Nov. 1, 2013	6.92	11.8	1359
AA-98A	Oct. 22, 2013	5.71	13.1	666
C-112	Oct. 9, 2013	5.85	11.0	419
AA-69-B	Oct. 15, 2013	6.49	10.0	1412
AA-69-C	Oct. 15, 2013	6.11	10.2	485
AA-71-B	Oct. 15, 2013	6.25	9.8	724
AA-68	Oct. 16, 2013	6.60	10.0	173
LDA-21	Oct. 11, 2013	7.62	10.2	53.0
LDA-24	Oct. 9, 2013	7.13	9.1	286
Mean ±1σ		*7.0±0.7*	*11±2*	*608±422*
Water Blank	Oct. 9, 2013	5.57	17.6	3.00

Table J- 3. Dissolved metals concentrations in freshwater samples

Sample code	Na /mg·L^{-1}	K /mg·L^{-1}	Rb /mg·L^{-1}
ORU1-1	2.11E+00±0.13E+00	5.80E-01±1.70E-01	1.11E-03±0.06E-03
ORU2-1	2.15E+00±0.13E+00	6.50E-01±2.00E-01	1.28E-03±0.06E-03
ORD1-1	2.13E+00±0.13E+00	5.90E-01±1.80E-01	1.21E-03±0.06E-03
ORD2-1	2.12E+00±0.13E+00	5.80E-01±1.70E-01	1.21E-03±0.06E-03
ORD1-2	2.13E+00±0.13E+00	5.90E-01±1.80E-01	1.17E-03±0.06E-03
ORD1-3	2.16E+00±0.13E+00	5.60E-01±1.80E-01	1.18E-03±0.06E-03
ORD1-4	2.19E+00±0.13E+00	5.90E-01±1.70E-01	1.19E-03±0.06E-03
ORD1-5	2.16E+00±0.13E+00	6.00E-01±1.70E-01	1.11E-03±0.06E-03
ORD1-6	2.12E+00±0.13E+00	5.80E-01±1.70E-01	1.18E-03±0.06E-03
ORD1-7	2.15E+00±0.13E+00	6.10E-01±1.80E-01	1.14E-03±0.06E-03
ORD1-8	2.10E+00±0.13E+00	5.80E-01±1.80E-01	1.16E-03±0.06E-03
Mean±1σ	*2.14E+00*±0.03*E+00*	*5.92E-01*±0.23*E-01*	*1.18E-03*±0.05*E-03*
PL1-1	5.10E+00±0.30E+00	3.50E-01±1.70E-01	5.50E-04±0.01E-04
PL1-2	1.24E+01±0.07E+01	8.40E-01±1.80E-01	1.38E-03±0.07E-03
PL1-3	1.24E+01±0.07E+01	8.50E-01±1.80E-01	1.29E-03±0.06E-03
PL2-3	1.24E+01±0.07E+01	8.00E-01±2.00E-01	1.42E-03±0.07E-03
PL1-4	1.24E+01±0.07E+01	8.50E-01±1.80E-01	1.41E-03±0.07E-03
PL1-5	1.25E+01±0.07E+01	8.60E-01±1.80E-01	1.28E-03±0.06E-03
PL1-6	1.25E+01±0.08E+01	8.30E-01±1.70E-01	1.36E-03±0.07E-03
PL1-7	1.25E+01±0.08E+01	8.60E-01±1.80E-01	1.37E-03±0.07E-03
PL1-8	1.24E+01±0.07E+01	8.60E-01±1.80E-01	1.38E-03±0.07E-03
PL2-8	1.24E+01±0.07E+01	8.70E-01±2.00E-01	1.50E-03±0.08E-03
Mean±1σ	*1.17+01*±0.23*E+01*	*7.97E-01±1.60E-01*	*1.29E-03*±0.27*E-03*
LBL1-1	7.60E+00±0.50E+00	9.80E-01±1.80E-01	1.59E-03±0.08E-03
LBL1-2	7.50E+00±0.50E+00	9.50E-01±1.80E-01	1.58E-03±0.08E-03
LBL1-3	7.60E+00±0.50E+00	9.70E-01±1.80E-01	1.54E-03±0.08E-03
LBL2-3	7.60E+00±0.50E+00	9.90E-01±1.80E-01	1.63E-03±0.08E-03
LBL1-4	7.70E+00±0.50E+00	9.70E-01±1.80E-01	1.64E-03±0.08E-03
LBL1-5	7.60E+00±0.50E+00	9.50E-01±1.89E-01	1.58E-03±0.08E-03
LBL2-5	7.60E+00±0.50E+00	9.70E-01±1.80E-01	1.58E-03±0.08E-03
LBL1-6	7.60E+00±0.50E+00	9.60E-01±1.80E-01	1.62E-03±0.08E-03
LBL1-7	7.60E+00±0.50E+00	9.50E-01±1.80E-01	1.58E-03±0.08E-03
LBL1-8	7.60E+00±0.50E+00	9.80E-01±1.80E-01	1.58E-03±0.08E-03
Mean±1σ	*7.60E+00*±0.05*E+00*	*9.7E-01±0.14E-01*	*1.59E-03*±0.03*E-03*
Blank	*3.50E-02*±1.40E-02	<MDC	*<MDC*
MDC	2.00E-02	5.0E-02	2.00E-04

Table J-3. Continues

Sample Code	Cs /mg·L^{-1}	Mg /mg·L^{-1}	Ca /mg·L^{-1}
ORU1-1	1.10E-05±0.20E-05	1.75E+00±0.11E+00	6.60E+00±0.40E+00
ORU2-1	1.00E-05±0.20E-05	1.77E+00±0.11E+00	6.70E+00±0.40E+00
ORD1-1	9.00E-06±2.0E-06	1.78E+00±0.11E+00	6.80E+00±0.40E+00
ORD2-1	8.00E-06±2.0E-06	1.77E+00±0.11E+00	6.70E+00±0.40E+00
ORD1-2	9.00E-06±2.0E-06	1.78E+00±0.11E+00	6.80E+00±0.40E+00
ORD1-3	8.00E-06±2.0E-06	1.78E+00±0.11E+00	6.80E+00±0.40E+00
ORD1-4	9.00E-06±2.0E-06	1.82E+00±0.11E+00	6.90E+00±0.40E+00
ORD1-5	8.00E-06±2.0E-06	1.78E+00±0.11E+00	6.80E+00±0.40E+00
ORD1-6	1.00E-05±0.20E-05	1.77E+00±0.11E+00	6.70E+00±0.40E+00
ORD1-7	8.00E-06±2.0E-06	1.79E+00±0.11E+00	6.80E+00±0.40E+00
ORD1-8	8.00E-06±2.0E-06	1.76E+00±0.11E+00	6.700E+00±0.40E+00
Mean±1σ	*8.91E-06±1.0E-06*	*1.78E+00*±0.02E+00	*6.75E+00±0.08E+00*
PL1-1	<MDC	9.60E-01±0.01E+00	2.65E+00±0.16E+00
PL1-2	1.00E-05±0.20E-05	2.35E+00±0.14E+00	6.60E+00±0.40E+00
PL1-3	9.00E-06±2.0E-06	2.37E+00±0.14E+00	6.70E+00±0.40E+00
PL2-3	9.00E-06±2.0E-06	2.38E+00±0.14E+00	6.70E+00±0.40E+00
PL1-4	9.00E-06±2.0E-06	2.36E+00±0.14E+00	6.60E+00±0.40E+00
PL1-5	8.00E-06±2.0E-06	2.37E+00±0.14E+00	6.70E+00±0.40E+00
PL1-6	8.00E-06±2.0E-06	2.36E+00±0.14E+00	6.60E+00±0.40E+00
PL1-7	9.00E-06±2.0E-06	2.37E+00±0.14E+00	6.70E+00±0.40E+00
PL1-8	8.00E-06±2.0E-06	2.34E+00±0.14E+00	6.60E+00±0.40E+00
PL2-8	9.00E-06±2.0E-06	2.37E+00±0.14E+00	6.60E+00±0.40E+00
Mean±1σ	*8.78E-06*±0.67*E-06*	*2.22E+00*±0.44*E+00*	*6.25E+00±1.30E+00*
LBL1-1	<MDC	1.94E+00±0.12E+00	5.60E+00±0.30E+00
LBL1-2	<MDC	1.93E+00±0.12E+00	5.60E+00±0.30E+00
LBL1-3	<MDC	1.94E+00±0.12E+00	5.60E+00±0.30E+00
LBL2-3	<MDC	1.92E+00±0.12E+00	5.50E+00±0.30E+00
LBL1-4	<MDC	1.94E+00±0.12E+00	5.60E+00±0.30E+00
LBL1-5	<MDC	1.93E+00±0.12E+00	5.60E+00±0.30E+00
LBL2-5	<MDC	1.93E+00±0.12E+00	5.60E+00±0.30E+00
LBL1-6	<MDC	1.94E+00±0.12E+00	5.60E+00±0.30E+00
LBL1-7	<MDC	1.93E+00±0.12E+00	5.60E+00±0.30E+00
LBL1-8	<MDC	1.93E+00±0.12E+00	5.60E+00±0.30E+00
Mean±1σ	*<MDC*	*1.93E+00*±0.01E+00	*5.59E+00*±0.03E+00
Water Blank	<MDC	<MDC	<MDC
MDC	6.00E-06	4.00E-02	3.00E-02

Table J-3. Continues

Sample Code	Sr /mg·L^{-1}	Ba /mg·L^{-1}	Pb /mg·L^{-1}
ORU1-1	2.56E-02±0.16E-02	1.05E-02±0.08E-02	1.14E-04±0.06E-04
ORU2-1	2.59E-02±0.16E-02	1.10E-02±0.08E-02	1.10E-04±0.06E-04
ORD1-1	2.60E-02±0.16E-02	1.10E-02±0.08E-02	1.07E-04±0.06E-04
ORD2-1	2.59E-02±0.16E-02	1.11E-02±0.08E-02	1.12E-04±0.06E-04
ORD1-2	2.61E-02±0.16E-02	1.11E-02±0.08E-02	9.10E-05±0.05E-04
ORD1-3	2.60E-02±0.16E-02	1.12E-02±0.08E-02	1.03E-04±0.06E-04
ORD1-4	2.66E-02±0.16E-02	1.12E-02±0.08E-02	1.09E-04±0.06E-04
ORD1-5	2.61E-02±0.16E-02	1.11E-02±0.08E-02	1.32E-04±0.07E-04
ORD1-6	2.58E-02±0.16E-02	1.11E-02±0.08E-02	1.09E-04±0.06E-04
ORD1-7	2.60E-02±0.16E-02	1.09E-02±0.08E-02	1.01E-04±0.05E-04
ORD1-8	2.58E-02±0.16E-02	1.09E-02±0.08E-02	9.70E-05±0.05E-04
Mean±1σ	*2.60E-02±0.02E-02*	*1.10E-02*±0.02E-02	1.08E-04±0.02E-04
PL1-1	1.80E-02±0.30E-02	7.20E-03±0.06E-02	1.80E-04±0.09E-04
PL1-2	4.40E-02±0.30E-02	1.65E-02±0.11E-02	2.80E-04±0.10E-04
PL1-3	4.50E-02±0.30E-02	1.67E-02±0.11E-02	2.70E-04±0.10E-04
PL2-3	4.50E-02±0.30E-02	1.66E-02±0.11E-02	3.20E-04±0.10E-04
PL1-4	4.50E-02±0.30E-02	1.65E-02±0.11E-02	3.00E-04±0.10E-04
PL1-5	4.50E-02±0.30E-02	1.64E-02±0.11E-02	2.60E-04±0.10E-04
PL1-6	4.50E-02±0.30E-02	1.67E-02±0.11E-02	2.80E-04±0.10E-04
PL1-7	4.50E-02±0.30E-02	1.66E-02±0.11E-02	3.00E-04±0.10E-04
PL1-8	4.40E-02±0.30E-02	1.63E-02±0.11E-02	3.00E-04±0.10E-04
PL2-8	4.50E-02±0.30E-02	1.63E-02±0.11E-02	2.70E-04±0.10E-04
Mean±1σ	*4.21E-02±0.85E-02*	*1.56E-02±0.29E-02*	2.76E-04±0.05E-04
LBL1-1	4.80E-02±0.30E-02	1.39E-02±0.09E-02	<MDC
LBL1-2	4.80E-02±0.30E-02	1.38E-02±0.09E-02	5.80E-05±0.3E-05
LBL1-3	4.80E-02±0.30E-02	1.41E-02±0.09E-02	<MDC
LBL2-3	4.70E-02±0.30E-02	1.40E-02±0.11E-02	<MDC
LBL1-4	4.80E-02±0.30E-02	1.42E-02±0.10E-02	<MDC
LBL1-5	4.80E-02±0.30E-02	1.42E-02±0.10E-02	<MDC
LBL2-5	4.80E-02±0.30E-02	1.42E-02±0.09E-02	<MDC
LBL1-6	4.80E-02±0.30E-02	1.42E-02±0.10E-02	<MDC
LBL1-7	4.80E-02±0.30E-02	1.41E-02±0.10E-02	<MDC
LBL1-8	4.80E-02±0.30E-02	1.41E-02±0.09E-02	<MDC
Mean±1σ	*4.79E-02*±0.03E-02	*1.41E-02±0.01E-02*	5.80E-05±0.30E-05
Water Blank	<MDC	<MDC	<MDC
MDC	7.00E-03		5.00E-05

Table J-3. Continues

Sample Code	Fe /mg·L^{-1}	Th /mg·L^{-1}	U /mg·L^{-1}
ORU1-1	1.60E-01±0.11E-01	<MDC	5.60E-05±0.30E-05
ORU2-1	1.56E-01±0.12E-01	<MDC	6.20E-05±0.30E-05
ORD1-1	1.55E-01±0.12E-01	<MDC	6.60E-05±0.40E-05
ORD2-1	1.55E-01±0.10E-01	<MDC	7.20E-05±0.40E-05
ORD1-2	1.57E-01±0.12E-01	<MDC	6.50E-05±0.30E-05
ORD1-3	1.55E-01±0.13E-01	<MDC	6.00E-05±0.30E-05
ORD1-4	1.59E-01±0.13E-01	<MDC	6.20E-05±0.30E-05
ORD1-5	1.58E-01±0.12E-01	<MDC	6.40E-05±0.30E-05
ORD1-6	1.64E-01±0.14E-01	<MDC	6.30E-05±0.30E-05
ORD1-7	1.58E-01±0.10E-01	<MDC	6.30E-05±0.30E-05
ORD1-8	1.51E-01±0.10E-01	<MDC	6.20E-05±0.30E-05
Mean±1σ	*1.57E-01±0.03E-01*	<MDC	6.32E-05±0.10E-05
PL1-1	6.20E-01±*0.40*E-01	<MDC	<MDC
PL1-2	1.42E+00±0.09E+00	<MDC	<MDC
PL1-3	1.42E+00±0.10E+00	<MDC	<MDC
PL2-3	1.42E+00±0.09E+00	<MDC	<MDC
PL1-4	1.41E+00±0.09E+00	<MDC	<MDC
PL1-5	1.37E+00±0.09E+00	<MDC	<MDC
PL1-6	1.38E+00±0.09E+00	<MDC	<MDC
PL1-7	1.45E+00±0.09E+00	<MDC	<MDC
PL1-8	1.38E+00±0.09E+00	<MDC	<MDC
PL2-8	1.36E+00±0.09E+00	<MDC	<MDC
Mean±1σ	*1.32E+00*±0.25*E*+00	<MDC	<MDC
LBL1-1	7.00E-01±0.50E-01	<MDC	<MDC
LBL1-2	6.90E-01±0.40E-01	<MDC	<MDC
LBL1-3	7.00E-01±0.40E-01	<MDC	<MDC
LBL2-3	7.00E-01±0.50E-01	<MDC	<MDC
LBL1-4	7.00E-01±0.60E-01	<MDC	<MDC
LBL1-5	7.10E-01±0.40E-01	<MDC	<MDC
LBL2-5	7.10E-01±0.50E-01	<MDC	<MDC
LBL1-6	7.10E-01±0.50E-01	<MDC	<MDC
LBL1-7	7.10E-01±0.40E-01	<MDC	<MDC
LBL1-8	6.90E-01±0.50E-01	<MDC	<MDC
Mean±1σ	*7.02E-01±0.08E-01*	<MDC	<MDC
Water Blank	<MDC	<MDC	<MDC
MDC	9.00E-03	2.00E-04	5.00E-05

Table J- 4. Dissolved metals concentrations in groundwater samples

Sample code	Na /mg·L^{-1}	K /mg·L^{-1}	Rb /mg·L^{-1}
B-WS	1.00E+02±6.00E+00	7.90E-01±1.80E-01	8.70E-04±0.40E-04
C-264	4.40E+01±3.00E+00	1.70E+00±0.20E+00	4.20E-03±0.20E-03
610-35	8.10E+01±6.00E+00	3.40E+00±0.30 E+00	1.30E-03±0.10E-03
610-36	1.69E+02±1.20E+01	4.20E+00±0.30E+00	2.30E-03±0.10E-03
AA-98A	9.80E+01±7.00E+00	2.00E+00±0.20E+00	2.60E-03±0.10E-03
C-112	4.50E+01±3.00E+00	1.03E+01±0.07E+00	2.80E-03±0.10E-03
AA-69-B	2.04E+02±1.02E+01	3.60E+00±0.30E+00	2.00E-03±0.10E-03
AA-69-C	7.00E+01±4.00E+00	1.67E+00±0.20E+00	2.80E-03±0.10E-03
AA-71-B	9.90E+01±6.00E+00	2.80E+00±0.20E+00	8.00E-05±0.10E-03
AA-68	1.90E+01±1.10E+00	2.00E+00±0.20E+00	3.60E-03±0.20E-03
LDA-21	3.30E+00±2.00E-01	1.47E+00±0.19E+00	1.00E-03±0.10E-03
LDA-24	1.88E+00±1.10E-01	9.40E-01±1.80E-01	4.60E-04±0.20E-04
Mean±1σ	*7.78E+01*±6.20E+01	*2.91E+00*±2.60E+00	*2.00E-03*±1.30E-03
Water Blank	*3.50E-02*±1.40E-02	<MDC	<*MDC*
MDC	2.00E-02	5.00E-02	2.00E-04
Sample code	**Mg /mg·L^{-1}**	**Ca /mg·L^{-1}**	**Sr /mg·L^{-1}**
B-WS	5.00E-02±3.00E-02	2.61E-01±0.19E-01	9.40E-03±0.50E-03
C-264	2.72E+00±0.18E+00	9.30E+00±0.60E+00	8.20E-02±0.40E-02
610-35	1.11E+01±0.07E+00	4.00E+01±0.60E+01	1.87E-01±0.09E-01
610-36	1.17E+01±0.08E+00	6.70E+01±0.40E+01	3.10E-01±0.20E-01
AA-98A	2.70E+00±0.18E+00	8.60E+00±0.50E+00	8.20E-02±0.40E-02
C-112	4.30E+00±0.18E+00	1.31E+01±0.08E+01	1.06E-01±0.05E-01
AA-69-B	8.30E+00±0.50E+00	2.72E+01±0.16E+01	2.30E-01±0.10E-01
AA-69-C	3.30E+00±0.20E+00	9.10E+00±0.50E+00	8.01E-02±0.40E-02
AA-71-B	7.60E+00±0.50E+00	1.67E+01±0.10E+01	1.48E-01±0.07E-01
AA-68	1.33E+00±0.09E+00	8.60E+00±0.50E+00	5.90E-02±0.30E-02
LDA-21	1.36E+00±0.09E+00	4.30E+00±0.30E+00	3.00E-02±0.10E-02
LDA-24	8.60E-01±0.70E-01	4.00E+00±0.30E+00	4.30E-02±0.20E-02
Mean±1σ	*4.61E+00*±4.00E+00	*1.73E+01*±1.90E+01	*1.14E-01*±0.89E-01
Water Blank	<MDC	<MDC	<MDC
MDC	4.00E-02	3.00E-02	7.00E-03

Table J-4. Continues

Sample code	Cs /mg·L^{-1}	Ba /mg·L^{-1}	Fe /mg·L^{-1}
B-WS	1.10E-05±0.10E-05	2.10E-04±2.0E-05	7.00E-03±3.0E-03
C-264	8.00E-06±1.00E-06	1.08E-01±5.0E-03	1.54E+01±9.0E-01
610-35	< MDC	3.50E-02±2.0E-03	4.00E-03±3.0E-03
610-36	1.00E-05±0.10E-05	5.50E-02±3.0E-03	< MDC
AA-98A	4.00E-06±1.00E-06	1.01E-01±5.0E-03	4.10E+00±2.0E-01
C-112	< MDC	1.08E-01±5.0E-03	2.52E+00±1.5E-01
AA-69-B	< MDC	2.40E-01±1.0E-02	9.20E+00±6.0E-01
AA-69-C	< MDC	6.40E-02±3.0E-03	4.40E+00±3.0E-01
AA-71-B	< MDC	5.80E-02±3.0E-03	6.40E-02±5.0E-03
AA-68	< MDC	3.70E-02±2.0E-03	2.50E-02±3.0E-03
LDA-21	< MDC	3.30E-02±2.0E-03	< MDC
LDA-24	< MDC	1.12E-01±6.0E-03	< MDC
Mean±1σ	*8.25E-06*±3.10E-06	*7.93E-02*±6.20E-02	*3.97E+00*±5.3E+00
Water Blank	<MDC	<MDC	<MDC
MDC	6.00E-06	4.00E-03	9.00E-03

Sample code	Pb /mg·L^{-1}	Th /mg·L^{-1}	U /mg·L^{-1}
B-WS	2.20E-05±0.50E-05		2.60E-03±0.100E-03
C-264	2.50E-05±0.50E-05	3.30E-04±4.0E-05	< MDC
610-35	< MDC	< MDC	3.80E-04±0.30E-04
610-36	< MDC	< MDC	1.90E-03±0.10E-03
AA-98A	< MDC	4.50E-04±4.0E-05	< MDC
C-112	6.20E-05±0.50E-05	< MDC	< MDC
AA-69-B	5.00E-05±0.50E-05	3.10E-04±4.0E-05	2.40E-03±0.10E-03
AA-69-C	8.00E-05±0.60E-05	8.30E-04±5.0E-05	1.20E-02±0.10E-02
AA-71-B	6.00E-05±0.50E-05	< MDC	2.30E-03±0.10E-03
AA-68	5.60E-05±0.50E-05	< MDC	1.50E-04±0.200E-04
LDA-21	2.90E-03±0.10E-03	< MDC	2.40E-03±0.10E-03
LDA-24	6.40E-03±0.30E-03	< MDC	1.60E-02±0.10E-02
Mean±1σ	*1.07E-03*±2.20E-03	*4.80E-04*±2.41E-04	*4.46E-03*±5.60E-03
Water Blank	< MDC	< MDC	< MDC
MDC	5.00E-05	2.00E-04	5.0E-05

Table J- 5. Anion concentrations in freshwater samples

Sample code	F^- /mg·L^{-1}	Cl^- /mg·L^{-1}	NO_3^- /mg·L^{-1}	Br^- /mg·L^{-1}	PO_4^{3-} /mg·L^{-1}	SO_4^{2-} /mg·L^{-1}
			Ottawa River			
ORU1-1	< MDC	1.81	0.44	< MDC	0.05	4.23
ORU2-1(Dup)	< MDC	1.49	0.49	< MDC	0.05	4.99
ORD1-1	< MDC	1.45	0.50	< MDC	0.06	5.11
ORD2-1(Dup)	< MDC	1.43	0.46	< MDC	0.03	5.16
ORD1-2	< MDC	1.46	0.50	< MDC	< MDC	5.12
ORD1-3	< MDC	1.50	0.49	< MDC	< MDC	5.19
ORD1-4	< MDC	1.46	0.48	< MDC	0.04	5.16
ORD1-5	< MDC	1.50	0.50	< MDC	< MDC	5.20
ORD1-6	< MDC	1.47	0.51	< MDC	< MDC	5.20
ORD1-7	< MDC	1.52	0.52	< MDC	< MDC	5.20
ORD1-8	< MDC	1.38	0.47	< MDC	< MDC	5.09
Mean±1σ	*<MDC*	*1.50±0.11*	*0.49±0.02*	*< MDC*	*0.12±0.01*	*5.06±0.28*
			Perch Lake			
PL1-1	0.03	26.10	< MDC	< MDC	0.04	3.79
PL1-2	0.02	26.30	< MDC	< MDC	< MDC	3.87
PL1-3	0.01	26.60	< MDC	< MDC	< MDC	3.84
PL2-3(Dup)	0.02	26.40	< MDC	< MDC	< MDC	4.60
PL1-4	0.02	26.80	< MDC	< MDC	< MDC	3.89
PL1-5	0.05	26.70	< MDC	< MDC	< MDC	3.98
PL1-6	0.03	26.60	< MDC	< MDC	< MDC	3.91
PL1-7	0.06	26.50	< MDC	< MDC	< MDC	3.89
PL1-8	0.04	26.10	< MDC	< MDC	< MDC	3.81
PL2-8(Dup)	0.05	26.70	< MDC	< MDC	< MDC	3.93
Mean±1σ	*0.03±0.02*	*26.5±0.25*	*<MDC*	*< MDC*	*<MDC*	*3.95±0.23*
			Lower Bass Lake			
LBL1-1	< MDC	15.60	< MDC	< MDC	< MDC	2.74
LBL1-2	< MDC	15.60	< MDC	< MDC	< MDC	2.63
LBL1-3	< MDC	15.60	< MDC	< MDC	< MDC	2.55
LBL2-3(Dup)	< MDC	15.70	< MDC	< MDC	< MDC	2.68
LBL1-4	< MDC	15.50	< MDC	< MDC	< MDC	2.69
LBL1-5	< MDC	16.10	< MDC	< MDC	< MDC	2.67
LBL2-5(Dup)	< MDC	16.10	< MDC	< MDC	< MDC	2.72
LBL1-6	< MDC	15.80	< MDC	< MDC	< MDC	2.71
LBL1-7	< MDC	15.40	< MDC	< MDC	< MDC	2.66
LBL1-8	< MDC	14.70	< MDC	< MDC	< MDC	2.50
Mean±1σ	*< MDC*	*15.6±0.40*	*<MDC*	*< MDC*	*<MDC*	*2.65±0.08*
Blank	< MDC	<MDC	<MDC	<MDC	<MDC	<MDC
MDC	0.03	0.11	0.10	0.12	0.18	0.11

Table J- 6. Dissolved carbons in surface water samples

Location	Sample code	DOC /mg·L^{-1}	DIC /mg·L^{-1}
Ottawa River	ORU1-1	7.63	3.09
	ORU2-1	6.90	3.66
	ORD1-1	6.39	3.73
	ORD2-1	6.22	3.72
	ORD1-2	6.29	3.77
	ORD1-3	6.44	3.77
	ORD1-4	6.36	3.80
	ORD1-5	6.31	3.77
	ORD1-6	6.39	3.76
	ORD1-7	6.26	3.78
	ORD1-8	6.21	3.68
Mean±1σ		*6.49±0.42*	*3.68±0.20*
Perch Lake	PL1-1	13.0	0.304
	PL1-2	13.3	3.02
	PL1-3	13.5	2.91
	PL2-3	13.2	3.02
	PL1-4	13.2	2.91
	PL1-5	13.4	2.92
	PL1-6	13.5	2.93
	PL1-7	13.3	2.94
	PL1-8	13.2	2.87
	PL2-8	13.7	2.95
Mean±1σ		*13.3±3.9*	*2.68±1.1*
Lower Bass Lake	LBL1-1	4.75	3.93
	LBL1-2	4.64	3.85
	LBL1-3	4.65	3.92
	LBL2-3	4.67	3.90
	LBL1-4	4.62	3.84
	LBL1-5	4.60	3.88
	LBL2-5	4.58	3.91
	LBL1-6	4.62	3.92
	LBL1-7	4.67	3.85
	LBL1-8	4.58	3.90
Mean±1σ		4.64*±0.23*	3.89*±0.85*
Water Blank		0.24	0.07
MDC		0.05	0.05

Appendix K. TDCR Čerenkov Counting Results

Table K- 1. TDCR Čerenkov counting of ^{90}Sr-^{90}Y in aqueous solutions using various sample volumes in plastic vials (PV) and glass vials (GV). Samples were counted on low background Hidex LSC for 0.5 h counting time [35].

Sample code	Geometry	Vol /mL	Counts Dbl	Counts Trpl	Net TDCR	CR_N [36] /cps	$\varepsilon_{Čerenkov}$ /%	$\dot{\varepsilon}_{Čerenkov}$ [37] /%	A_i ^{90}Y /Bq
SrCT3-1	7 PV, HCl	1.01	12410±111	8793±94	0.74±0.02	6.42±0.06	71.9±1.6	71.9±1.5	8.94±0.22
SrCT3-2	7 PV, HCl	2.99	12400±111	8952±95	0.76±0.02	6.42±0.06	73.1±1.5	73.0±1.1	8.78±0.20
SrCT3-3	7 PV, HCl	5.01	12303±111	8752±94	0.75±0.02	6.36±0.06	72.2±1.6	72.1±1.3	8.80±0.21
SrCT3-4	7 PV, HCl	7.02	12221±111	8538±92	0.73±0.02	6.29±0.06	71.3±1.6	71.3±1.1	8.83±0.22
SrCT3-1Dup	7 PV, HCl	0.99	12344±111	8761±94	0.74±0.02	6.39±0.06	72.0±1.6	-	8.87±0.22
SrCT3-2Dup	7 PV, HCl	3.01	12353±111	8879±94	0.75±0.02	6.39±0.09	72.8±1.5	-	8.77±0.20
SrCT3-3Dup	7 PV, HCl	5.04	12256±111	8702±93	0.74±0.02	6.33±0.09	72.1±1.6	-	8.78±0.23
SrCT3-4Dup	7 PV, HCl	7.04	12362±111	8660±93	0.73±0.02	6.37±0.09	71.4±1.6	-	8.93±0.23
SrCT3-Blk1	7 PV, HCl	1.00	847±29	226±15	-	-	-	-	-
SrCT3-Blk2	7 PV, HCl	3.01	851±29	204±14	-	-	-	-	-
SrCT3-Blk3	7 PV, HCl	5.03	864±29	227±15	-	-	-	-	-
SrCT3-Blk4	7 PV, HCl	7.15	895±30	243±16	-	-	-	-	-
SrCT4-1	20 PV, HCl	3.00	12321±111	8342±91	0.70±0.03	6.39±0.09	69.0±1.8	68.6±1.3	9.26±0.28
SrCT4-2	20 PV, HCl	4.96	12256±111	8487±92	0.72±0.02	6.34±0.09	70.5±1.7	70.2±1.2	9.00±0.25
SrCT4-3	20 PV, HCl	7.02	12452±112	8590±93	0.72±0.02	6.45±0.09	70.1±1.8	70.7±1.2	9.20±0.26
SrCT4-4	20 PV, HCl	9.97	12465±112	8759±94	0.73±0.03	6.47±0.09	71.0±1.8	70.9±1.3	9.11±0.27
SrCT4-5	20 PV, HCl	13.07	12327±111	8548±92	0.72±0.02	6.35±0.09	70.6±1.7	70.7±1.2	9.00±0.25

[35] Calculation examples for different parameters using SrCT3-1 is presented in Appendix N.
[36] CR_N= Net count rate = sample count rate (CR_s) – blank count rate (CR_b)
[37] $\dot{\varepsilon}_{Čerenkov}$ = Average Čerenkov counting efficiency of sample and its duplicate. Results for sample and its duplicate are separated by vertical hatched line.

Table K-1. Continues

Sample code	Geometry	Vol /mL	Counts Dbl	Counts Trpl	Net TDCR	CR_N /cps	$\varepsilon_{Čerenkov}$ /%	$\dot{\varepsilon}_{Čerenkov}$ /%	$A_i^{90}Y$ /Bq
SrCT4-6	20 PV, HCl	15.1	12569±112	8746±94	0.72±0.02	6.50±0.09	70.6±1.8	70.7±1.2	9.21±0.26
SrCT4-7	20 PV, HCl	18.1	12348±111	8546±92	0.72±0.02	6.36±0.09	70.5±1.8	70.2±1.2	9.03±0.25
SrCT4-8	20 PV, HCl	20.1	12257±111	8475±92	0.72±0.02	6.31±0.09	70.4±1.8	69.8±1.2	8.97±0.26
SrCT4-1Dup	20 PV, HCl	3.00	12341±111	8243±91	0.69±0.03	6.40±0.06	68.3±1.9	-	9.37±0.27
SrCT4-2 Dup	20 PV, HCl	4.96	12361±111	8493±92	0.72±0.02	6.40±0.06	70.0±1.7	-	9.14±0.24
SrCT4-3 Dup	20 PV, HCl	7.02	12364±111	8697±93	0.73±0.02	6.41±0.06	71.2±1.8	-	9.00±0.24
SrCT4-4 Dup	20 PV, HCl	10.1	12558±112	8789±94	0.73±0.03	6.52±0.06	70.8±1.8	-	9.22±0.26
SrCT4-5 Dup	20 PV, HCl	13.1	12320±111	8560±93	0.73±0.02	6.35±0.06	70.7±1.7	-	8.98±0.23
SrCT4-6 Dup	20 PV, HCl	14.9	12372±111	8629±93	0.73±0.02	6.39±0.06	70.8±1.8	-	9.03±0.24
SrCT4-7 Dup	20 PV, HCl	18.1	12185±110	8358±91	0.72±0.02	6.27±0.06	70.0±1.7	-	8.96±0.24
SrCT4-8 Dup	20 PV, HCl	20.3	12145±110	8223±91	0.71±0.02	6.25±0.06	69.3±1.8	-	9.03±0.25
SrCT4-Blk1	20 PV, HCl	3.03	822±29	272±16	-	-	-	-	-
SrCT4-Blk2	20 PV, HCl	4.99	848±29	257±16	-	-	-	-	-
SrCT4-Blk3	20 PV, HCl	7.06	834±29	259±16	-	-	-	-	-
SrCT4-Blk4	20 PV, HCl	10.0	818±29	271±16	-	-	-	-	-
SrCT4-Blk5	20 PV, HCl	13.1	891±30	270±16	-	-	-	-	-
SrCT4-Blk6	20 PV, HCl	15.1	868±29	278±17	-	-	-	-	-
SrCT4-Blk7	20 PV, HCl	18.2	898±30	283±17	-	-	-	-	-
SrCT4-Blk8	20 PV, HCl	20.2	893±30	288±17	-	-	-	-	-
SrCT5-1	7 PV, HNO_3	1.00	12128±110	8332±91	0.72±0.02	6.28±0.06	70.1±1.7	70.4±1.2	8.95±0.23
SrCT5-2	7 PV, HNO_3	3.00	12241±111	8504±92	0.73±0.02	6.32±0.06	70.9±1.6	71.0±1.1	8.91±0.22
SrCT5-3	7 PV, HNO_3	5.03	12419±111	8677±93	0.73±0.02	6.40±0.06	71.3±1.5	71.5±1.1	8.97±0.21
SrCT5-4	7 PV, HNO_3	7.04	12026±110	8226±91	0.72±0.02	6.20±0.06	70.2±1.5	70.0±1.1	8.83±0.21

Table K-1. Continues

Sample code	Geometry	Vol /mL	Counts Dbl	Counts Trpl	Net TDCR	CR_N /cps	$\varepsilon_{Čerenkov}$ /%	$\dot{\varepsilon}_{Čerenkov}$ /%	$A_i^{90}Y$ /Bq
SrCT5-1Dup	7 PV, HNO_3	1.00	12318±111	8567±93	0.73±0.02	6.38±0.06	70.8±0.7	-	9.02±0.23
SrCT5-2 Dup	7 PV, HNO_3	2.96	12280±111	8547±92	0.73±0.02	6.34±0.06	71.0±1.6	-	8.93±0.22
SrCT5-3 Dup	7 PV, HNO_3	5.18	12472±112	8758±94	0.74±0.02	6.43±0.09	71.6±1.5	-	8.98±0.23
SrCT5-4 Dup	7 PV, HNO_3	7.04	12157±110	8257±91	0.71±0.02	6.27±0.09	69.8±1.5	-	8.98±0.23
SrCT5-Blk1	7 PV, HNO_3	0.99	827±29	227±15	-	-	-	-	-
SrCT5-Blk2	7 PV, HNO_3	3.00	860±29	219±15	-	-	-	-	-
SrCT5-Blk3	7 PV, HNO_3	5.14	900±30	225±15	-	-	-	-	-
SrCT5-Blk4	7 PV, HNO_3	7.06	864±29	206±14	-	-	-	-	-
SrCT7-1	7 GV, HCl	3.01	11851±109	7182±85	0.64±0.02	6.01±0.09	64.4±1.5	-	9.32±0.25
SrCT7-2	7 GV, HCl	5.03	11690±108	6816±83	0.61±0.02	5.97±0.09	62.2±1.6	-	9.60±0.28
SrCT7-3	7 GV, HCl	7.03	11206±106	6141±78	0.58±0.02	5.67±0.08	59.8±1.4	-	9.48±0.27
SrCT7-Blk1	7 GV, HCl	3.00	1042±32	263±16	-	-	-	-	-
SrCT7-Blk2	7 GV, HCl	5.02	942±31	247±16	-	-	-	-	-
SrCT7-Blk3	7 GV, HCl	7.00	1001±32	222±15	-	-	-	-	-
SrCT8-1	20 GV, HCl	9.92	12141±110	7310±85	0.64±0.06	6.07±0.06	64.5±3.0	-	9.42±0.72
SrCT8-2	20 GV, HCl	15.0	11990±109	6945±83	0.62±0.06	5.92±0.06	62.9±2.8	-	9.42±0.71
SrCT8-3	20 GV, HCl	18.0	11531±107	6474±80	0.60±0.07	5.70±0.06	61.5±2.9	-	9.28±0.76
SrCT8-4	20 GV, HCl	20.0	11360±107	6144±78	0.58±0.07	5.65±0.06	59.5±2.8	-	9.50±0.83
SrCT8-Blk1	20 GV, HCl	9.92	1215±35	307±18	-	-	-	-	-
SrCT8-Blk2	20 GV, HCl	15.0	1336±37	334±18	-	-	-	-	-
SrCT8-Blk3	20 GV, HCl	18.0	1266±36	298±17	-	-	-	-	-
SrCT8-Blk4	20 GV, HCl	20.0	1183±34	285±17	-	-	-	-	-

Note: Series SrCT7 and SrCT8 samples were not prepared in duplicates and, therefore, do not have $\dot{\varepsilon}_{Čerenkov}$ (average Čerenkov efficiency).

Table K- 2. TDCR Čerenkov counting of ^{90}Sr-^{90}Y in colour quenched (using yellow and brown food-grade dyes) aqueous solutions measured in plastic (PV) and glass (GV) vials on low background Hidex LSC.

Sample code	Description	Dye /mL	A_{ia} ^{90}Y /Bq	Backg. Dbl	Backg. Trpl	Sample Dbl	Sample Trpl	Net Dbl	Net Trpl
SrCT11-Blk	20 PV, Blank	0	8.80±0.11	297±17	87±9	3886±62	2670±52	3589±65	2583±53
SrCT11-1	20 PV, Yellow	0.1	8.85±0.11	254±16	74±9	3781±61	2400±49	3527±64	2326±50
SrCT11-2	20 PV, Yellow	0.2	8.81±0.11	264±16	77±9	3577±60	2112±46	3313±62	2035±47
SrCT11-3	20 PV, Yellow	0.3	8.83±0.11	247±16	72±8	3491±59	1978±44	3244±61	1906±45
SrCT11-4	20 PV, Yellow	0.4	8.88±0.11	223±15	65±8	3321±58	1760±42	3098±60	1695±43
SrCT11-5	20 PV, Yellow	0.5	8.86±0.11	216±15	63±8	3239±57	1651±41	3023±59	1588±41
SrCT11-6	20 PV, Yellow	0.6	8.87±0.11	199±14	58±8	3093±56	1461±38	2894±57	1403±39
SrCT11-7	20 PV, Yellow	0.7	8.86±0.11	220±15	64±8	2829±53	1277±36	2609±55	1213±37
SrCT11-8	20 PV, Yellow	0.8	8.85±0.11	202±14	59±8	2962±54	1311±36	2760±56	1252±37
SrCT12-1	20 PV, Brown	0.1	8.85±0.11	267±16	78±9	3658±60	2225±47	3391±63	2147±48
SrCT12-2	20 PV, Brown	0.2	8.85±0.11	234±15	68±8	3050±55	1519±39	2816±57	1451±40
SrCT12-3	20 PV, Brown	0.3	8.84±0.11	218±15	64±8	2849±53	1273±36	2631±55	1209±37
SrCT12-4	20 PV, Brown	0.4	8.86±0.11	205±14	60±8	2759±53	1073±33	2554±54	1013±34
SrCT12-5	20 PV, Brown	0.5	8.84±0.11	196±14	57±8	2418±49	868±29	2222±51	811±30
SrCT12-6	20 PV, Brown	0.6	8.85±0.11	181±13	53±7	2099±46	627±25	1918±48	574±26
SrCT12-7	20 PV, Brown	0.7	8.87±0.11	176±13	51±7	1896±44	539±23	1720±46	488±24
SrCT12-8	20 PV, Brown	0.8	8.88±0.11	171±13	50±7	1822±43	441±21	1651±45	391±22
SrCT13-1	20 GV, Blank	0	8.77±0.11	1262±36	299±17	11237±106	6360±80	9975±112	6061±82
SrCT13-2	20 GV, Brown	0.1	8.75±0.11	1174±34	279±17	10622±103	5531±74	9448±109	5252±76
SrCT13-3	20 GV, Brown	0.2	8.79±0.11	1118±33	265±16	10007±100	4766±69	8889±105	4501±71
SrCT13-4	20 GV, Brown	0.3	8.73±0.11	1066±33	253±16	9669±98	4420±66	8603±104	4167±65
SrCT13-5	20 GV, Brown	0.4	8.81±0.11	1024±32	243±16	9299±96	4099±64	8275±91	3856±62
SrCT13-6	20 GV, Brown	0.5	8.80±0.11	979±31	232±15	8706±93	3433±59	7727±88	3201±57

Table K-2. Continues

Sample code	TDCR	CR_N /cps	$\varepsilon_{Čerenkov}$ /%	A_i ^{90}Y /Bq	A_i/A_{ia}
SrCT11-Blk	0.72±0.02	5.98±0.10	70.3±1.4	8.51±0.22	0.967±0.03
SrCT11-1	0.66±0.02	5.88±0.10	65.9±1.4	8.93±0.24	1.01±0.03
SrCT11-2	0.61±0.02	5.52±0.10	62.4±1.4	8.84±0.25	1.00±0.03
SrCT11-3	0.59±0.02	5.41±0.10	60.4±1.4	8.95±0.26	1.01±0.03
SrCT11-4	0.55±0.02	5.16±0.09	57.3±1.4	9.02±0.27	1.02±0.03
SrCT11-5	0.53±0.02	5.04±0.09	55.5±1.4	9.07±0.28	1.02±0.03
SrCT11-6	0.49±0.02	4.82±0.09	52.3±1.3	9.22±0.29	1.04±0.03
SrCT11-7	0.47±0.02	4.35±0.09	50.7±1.4	8.58±0.29	0.97±0.03
SrCT11-8	0.45±0.02	4.60±0.09	49.8±1.3	9.25±0.31	1.05±0.03
SrCT12-1	0.63±0.02	5.65±0.10	63.9±1.4	8.85±0.24	1.00±0.03
SrCT12-2	0.52±0.02	4.69±0.09	54.7±1.4	8.58±0.27	0.97±0.03
SrCT12-3	0.46±0.02	4.38±0.09	50.2±1.4	8.73±0.30	0.99±0.03
SrCT12-4	0.40±0.02	4.26±0.08	45.0±1.3	9.46±0.34	1.07±0.04
SrCT12-5	0.37±0.02	3.70±0.08	42.3±1.4	8.76±0.34	0.99±0.04
SrCT12-6	0.30±0.02	3.20±0.07	36.4±1.4	8.78±0.40	0.99±0.05
SrCT12-7	0.28±0.02	2.87±0.07	35.0±1.5	8.20±0.40	0.93±0.05
SrCT12-8	0.24±0.02	2.75±0.07	30.6±1.4	9.00±0.48	1.01±0.05
SrCT13-1	0.61±0.01	5.54±0.06	61.9±0.8	8.95±0.15	1.02±0.02
SrCT13-2	0.56±0.01	5.25±0.05	57.9±0.8	9.06±0.16	1.04±0.02
SrCT13-3	0.51±0.01	4.94±0.05	54.0±0.8	9.14±0.17	1.04±0.02
SrCT13-4	0.48±0.01	4.78±0.05	52.3±0.8	9.15±0.17	1.05±0.02
SrCT13-5	0.47±0.01	4.60±0.05	50.8±0.8	9.06±0.17	1.03±0.02
SrCT13-6	0.41±0.01	4.29±0.05	46.5±0.8	9.24±0.19	1.05±0.02

Table K- 3. TDCR Čerenkov counting of ^{90}Sr-^{90}Y and other beta-emitting radionuclides measured in aqueous solutions in 20-mL plastic vials on low background Hidex LSC for 0.5 h counting time

Radionuclide tested	A_{ia} /Bq	Dbl	Trpl	CR_N /cps	$Eff_{Čerenkov}$ [38] /%	Avg Eff $_{Čerenkov}$ [39] /%
^{90}Sr-^{90}Y	9.25±0.16	12665±113	8860±94	6.58±0.07	71.1±1.4	70.5±1.1
^{90}Sr-^{90}Y Dup	8.89±0.15	12026±113	8365±91	6.22±0.10	70.0±1.7	
^{89}Sr	9.85±0.10	9606±98	5494±74	4.85±0.06	49.3±1.0	48.9±0.7
^{89}Sr Dup	9.89±0.10	9511±98	5265±73	4.80±0.06	48.6±1.0	
^{32}P	13.18±0.30	13895±118	8451±92	7.24±0.07	54.9±0.8	55.1±0.5
^{32}P Dup	13.18±0.30	13954±118	8464±92	7.27±0.07	55.2±0.8	
^{210}Pb-^{210}Bi	9.75±0.21	4045±64	1378±37	1.79±0.04	18.4±0.6	18.6±0.4
^{210}Pb-^{210}Bi Dup	9.86±0.22	4160±64	1398±37	1.85±0.04	18.8±0.6	
^{137}Cs	9.87±0.10	2414±49	731±27	0.85±0.03	8.6±0.3	8.5±0.3
^{137}Cs Dup	9.85±0.10	2378±49	730±27	0.83±0.03	8.4±0.3	
^{60}Co	11.62±0.12	2523±50	1155±34	0.94±0.03	8.1±0.3	8.0±0.2
^{60}Co Dup	12.14±0.12	2577±51	1230±35	0.97±0.03	8.0±0.3	
^{40}K	8.17±0.25	7376±86	3927±63	3.59±0.05	43.9±2.2	44.0±1.8
^{40}K Dup	16.12±0.48	14151±119	7610±87	7.35±0.07	45.6±3.1	
Blank DI Water[40]	None	823±29	270±16	-	-	-

[38] $Eff_{Čerenkov}$ = Counting efficiency of radionuclide obtained from Eq. (10) for all radionuclide and from Eq. (11) for ^{90}Y
[39] Avg Eff $_{Čerenkov}$ = Average of sample and duplicate counting efficiencies
[40] DI Water = Deionized water obtained Millipore Direct-Q5^{TM} water purification system

Table K- 4. TDCR Čerenkov counting of $^{-90}$Y and other beta-emitting radionuclides measured in aqueous solutions in 20-mL glass vials on low background Hidex LSC for 0.5 h counting time

Radionuclide tested	A_{ia} /Bq	Dbl	Trpl	CR_N /cps	$Eff_{Čerenkov}$ /%	Avg $Eff_{Čerenkov}$ /%
^{90}Sr-^{90}Y	13.19±0.16	16358±128	9778±99	8.42±0.07	63.8±0.9	63.8±0.67
^{90}Sr-^{90}Y Dup	13.21±0.16	16390±128	9626±98	8.44±0.07	63.9±0.9	
^{89}Sr	10.16±0.11	8821±94	3747±61	4.23±0.06	41.6±0.8	41.6±0.60
^{89}Sr Dup	10.16±0.11	8906±94	3801±62	4.28±0.06	42.1±0.8	
^{32}P	14.96±0.34	14347±120	6759±82	7.24±0.07	48.4±0.7	41.6±0.60
^{32}P Dup	13.22±0.30	12785±113	5942±77	6.37±0.07	48.2±0.8	
^{210}Pb-^{210}Bi	9.67±0.21	3835±62	1017±32	1.40±0.04	14.5±0.5	14.1±0.33
^{210}Pb-^{210}Bi Dup	9.75±0.21	3747±61	942±31	1.35±0.04	13.8±0.5	
^{137}Cs	9.86±0.10	2368±49	540±23	0.65±0.03	6.5±0.4	6.30±0.25
^{137}Cs Dup	9.88±0.10	2280±48	526±23	0.60±0.03	6.0±0.3	
^{60}Co	11.08±0.11	2795±53	915±30	0.84±0.04	7.6±4.4	6.30±0.25
^{60}Co Dup	10.68±0.11	2613±51	807±28	0.74±0.04	6.9±4.8	
^{40}K	8.26±0.25	6792±82	2572±51	3.04±0.05	36.8±5.0	38.0±1.4
^{40}K Dup	16.73±0.50	12913±114	5201±72	6.44±0.07	38.5±6.6	
Blank DI Water	None	1207±35	278±17	-	-	-

Table K- 5. TDCR Čerenkov counting of natural freshwater samples for their ^{90}Sr-^{90}Y content. Approximately 18-20 mL water samples were measured for 1 h on low background Hidex LSC.

Sample code	Raw Counts		TDCR	CR_N /cps	$\varepsilon_{Čerenkov}$ /%	$[A_i]$ ^{90}Y /Bq·L^{-1}	MDC /Bq·L^{-1}
	Dbl	Trpl					
ORFBlk	1801±42	608±25	0.34±0.02	0.50±0.01	39.9±2.1	< MDC	7.92
ORU1-1	1689±41	631±25	0.37±0.02	0.47±0.01	43.0±2.1	< MDC	7.55
ORU2-1(Dup)	1761±42	599±24	0.34±0.02	0.49±0.01	40.1±2.1	< MDC	8.36
ORD1-1	1658±41	580±24	0.35±0.02	0.46±0.01	40.9±2.1	< MDC	7.91
ORD1-2	1726±42	607±25	0.35±0.02	0.48±0.01	41.1±2.1	< MDC	7.93
ORD2-1(Dup)	1709±41	622±25	0.36±0.02	0.48±0.01	42.2±2.1	< MDC	7.92
ORD1-3	1723±42	633±25	0.37±0.02	0.48±0.01	42.5±2.1	< MDC	7.62
ORD1-4	1733±42	616±25	0.36±0.02	0.48±0.01	41.4±2.1	< MDC	7.91
ORD1-5	1688±41	619±25	0.37±0.02	0.47±0.01	42.4±2.1	< MDC	7.60
ORD1-6	1655±41	622±25	0.38±0.03	0.46±0.01	43.2±2.1	< MDC	7.27
ORD1-7	1746±42	625±25	0.36±0.02	0.49±0.01	41.7±2.1	< MDC	7.53
ORD1-8	1791±42	609±25	0.34±0.02	0.50±0.01	40.1±2.1	< MDC	8.06
PLFBlk	1909±44	747±27	0.39±0.02	0.53±0.01	44.5±2.1	< MDC	7.20
PL1-1	1955±44	795±28	0.41±0.02	0.54±0.01	45.8±2.1	< MDC	7.04
PL1-2	1963±44	772±28	0.39±0.02	0.55±0.01	44.7±2.0	< MDC	6.99
PL1-3	1912±44	781±28	0.41±0.02	0.53±0.01	46.0±2.1	< MDC	6.90
PL2-3(Dup)	1953±44	762±28	0.39±0.02	0.54±0.01	44.4±2.0	< MDC	7.22
PL1-4	1886±43	715±27	0.38±0.02	0.52±0.01	43.5±2.1	< MDC	7.32
PL1-5	1862±43	756±27	0.41±0.03	0.52±0.01	45.8±2.1	< MDC	6.98
PL1-6	1915±44	785±28	0.41±0.03	0.53±0.01	46.1±2.1	< MDC	6.85
PL1-7	1818±43	721±27	0.40±0.03	0.51±0.01	45.0±2.1	< MDC	7.07
PL1-8	1862±43	768±28	0.41±0.03	0.52±0.01	46.3±2.1	< MDC	6.83
PL2-8(Dup)	1967±44	816±29	0.42±0.02	0.55±0.01	46.5±2.1	< MDC	6.97
LBLFBlk	1861±43	672±26	0.36±0.02	0.52±0.01	41.9±2.1	< MDC	7.89
LBL1-1	1797±42	660±26	0.37±0.024	0.50±0.01	42.5±2.1	< MDC	7.61
LBL1-2	2003±45	747±27	0.37±0.02	0.56±0.01	43.0±2.0	< MDC	7.47
LBL1-3	1967±44	761±28	0.39±0.02	0.55±0.01	44.1±2.0	< MDC	7.32
LBL2-3(Dup)	1848±43	677±26	0.37±0.02	0.51±0.01	42.4±2.1	< MDC	7.60
LBL1-4	1867±4343	674±26	0.36±0.02	0.52±0.01	41.9±2.1	< MDC	7.64
LBL1-5	1916±44	744±27	0.39±0.02	0.53±0.01	44.3±2.1	< MDC	7.31
LBL2-5(Dup)	1924±44	710±27	0.37±0.02	0.53±0.01	42.6±2.0	< MDC	7.55
LBL1-6	1958±44	721±27	0.37±0.02	0.54±0.01	42.5±2.0	< MDC	7.53
LBL1-7	1757±42	612±25	0.35±0.02	0.49±0.01	40.8±2.1	< MDC	7.88
LBL1-8	1802±42	662±26	0.37±0.02	0.50±0.01	42.5±2.1	< MDC	7.60

Table K- 5. Continues

Sample code	Raw Counts		TDCR	CR_N /cps	$\varepsilon_{Čerenkov}$ /%	$[A_i]$ ^{90}Sr-^{90}Y /Bq·L^{-1}	MDC /Bq·L^{-1}
	Dbl	Trpl					
BWS	1808±43	657±26	0.36±0.02	0.50±0.01	42.1±2.1	< MDC	7.50
BWS-Dup	1739±42	611±25	0.35±0.02	0.48±0.01	41.1±2.1	< MDC	7.53
C264	1671±41	607±25	0.36±0.02	0.46±0.01	42.1±2.1	< MDC	7.75
C264-Dup	1624±40	549±23	0.34±0.02	0.45±0.01	39.9±2.1	< MDC	7.36
610-35	1786±42	655±26	0.37±0.02	0.50±0.01	42.4±2.1	< MDC	6.92
610-36	1807±43	648±25	0.36±0.02	0.50±0.01	41.7±2.1	< MDC	7.04
AA98A	1667±41	581±24	0.35±0.02	0.46±0.01	40.8±2.1	< MDC	7.99
AA98A-Dup	1702±41	625±25	0.37±0.02	0.47±0.01	42.5±2.1	< MDC	6.92
C-112	2157±46	928±30	0.43±0.02	0.60±0.01	47.8±2.0	< MDC	6.82
C-112-Dup	2109±46	899±30	0.43±0.02	0.59±0.01	47.5±2.0	< MDC	6.18
AA69B	23956±155	15793±126	0.66±0.02	6.65±0.04	65.8±1.4	469±13	4.69
AA69C	5565±75	3258±57	0.59±0.02	1.55±0.02	60.2±1.7	86.3±7.0	6.09
AA69C-Dup	5805±76	3405±58	0.59±0.02	1.61±0.02	60.3±1.6	78.0±6.5	5.12
AA71B	18487±136	12533±112	0.68±0.02	5.14±0.03	67.2±1.4	358±11	4.85
AA68A	101922±319	72374±269	0.71±0.02	28.3±0.08	69.6±1.3	2203±42	4.69
AA68A-Dup	116880±342	82121±287	0.70±0.02	32.5±0.08	69.1±1.3	2291±44	4.25
LDA21	658612±812	468585±685	0.71±0.01	183±0.2	69.7±1.3	13117±239	4.21
LDA24	64122±253	45262±213	0.71±0.02	17.8±0.06	69.3±1.3	1231±25	4.24
Spike	15985±126	11356±107	0.71±0.04	8.9±0.06	69.6±2.6	12.2±0.5	4.70
Blank 1	1066±33	505±22	-	-	-	-	-
Blank 2	1717±41	458±21	-	-	-	-	-

Table K- 6. TDCR Čerenkov counting of spiked ^{90}Sr-^{90}Y in colour quenched (brown food-grade dye) seawater samples measured in plastic vials on low background Hidex LSC for 0.5 h counting time.

Sample code	Dye /mL	A_{ia} ^{90}Y /Bq	Backgnd Dbl	Backgnd Trpl	Spiked Dbl	Spiked Trpl
SWY-Qnch 0	0	11.09±0.33	1047 ±32	375±19	14440±120	10030±100
SWY-Qnch 1	0.1	10.98±0.33	908 ±30	305±17	14086±119	9597±98
SWY-Qnch 2	0.2	10.98±0.33	891 ±30	320±18	13530±116	8686±93
SWY-Qnch 3	0.5	10.93±0.33	732 ±27	206±14	12230±111	6472±80
SWY-Qnch 4	0.7	11.00±0.33	763 ±28	220±15	11523±107	5751±76
SWY-Qnch 5	1.0	10.97±0.33	696 ±26	195±14	10919±104	5123±72
Blank Seawater	None	-	1146 ±34	417±20	-	-
Blank DI Water	None	-	895 ±30	323±18	-	-

Sample code	Net Counts Dbl	Net Counts Trpl	Count rate /cps	TDCR	ε_{Cerenk}	A_i ^{90}Y /Bq	A_i / A_{ia}
SWY-Qnch 0	13393±116	9655±98	7.44±0.07	0.72±0.01	70.4±0.7	10.57±0.13	0.95±0.03
SWY-Qnch 1	13178±115	9292±96	7.32±0.07	0.71±0.01	69.3±0.7	10.57±0.13	0.96±0.03
SWY-Qnch 2	12639±112	8366±91	7.02±0.07	0.66±0.01	66.0±0.7	10.63±0.14	0.97±0.03
SWY-Qnch 3	11498±107	6266±79	6.39±0.06	0.55±0.01	57.1±0.7	11.19±0.15	1.02±0.03
SWY-Qnch 4	10760±104	5531±74	5.98±0.06	0.51±0.01	54.6±0.7	10.94±0.16	0.99±0.03
SWY-Qnch 5	10223±101	4928±70	5.69±0.06	0.48±0.01	52.1±0.7	10.91±0.16	0.99±0.03

Appendix L. Liquid Scintillation Counting Results of Freshwater and Seawater Samples

Table L- 1. Čerenkov counting of spiked ^{90}Sr-^{90}Y in freshwater samples measured following radiochemical separation using DGA-N® resin. Counting time was either 0.5 or 1 h on a low background Hidex LSC[41].

Sample code	Vol/ L	Cnt time /h	Counts Dbl	Counts Trpl	Count rate /cps	TDCR	ε_{Cerenk}/ /%	T_1-T_0 /h	DY_{Cerenk}	$[A_i]$ ^{90}Y /Bq·L^{-1}	MDC /Bq·L^{-1}
PL1-1	1.01	0.5	7136±84	5047±71	3.96±0.05	0.71±0.01	69.4±1.0	3.9	0.958	6.51±0.15	0.10
PL1-3	1.00	0.5	6484±81	4389±66	3.60±0.04	0.68±0.01	67.2±1.0	4.0	0.958	6.45±0.11	0.08
PL1-3Dup	1.01	1.0	13777±117	9777±99	3.83±0.03	0.71±0.01	69.6±0.7	5.3	0.945	6.10±0.08	0.07
PL1-5	1.02	1.0	13871±118	9793±99	3.85±0.03	0.71±0.01	69.3±0.7	6.3	0.934	6.31±0.08	0.08
PL1-6	1.00	0.5	6549±81	4215±65	3.64±0.04	0.64±0.01	64.7±1.0	3.5	0.963	6.71±0.16	0.09
PL1-7	1.01	1.0	13787±117	9861±99	3.83±0.03	0.72±0.01	70.0±0.7	7.4	0.923	6.12±0.08	0.07
PL1-8	1.00	1.0	13058±114	9172±96	3.63±0.03	0.70±0.01	69.1±0.7	8.5	0.912	6.26±0.08	0.08
PL2-8	1.00	1.0	13272±115	9567±98	3.69±0.03	0.72±0.01	70.4±0.7	9.6	0.901	6.12±0.07	0.07
LBL1-1	1.00	1.0	2425±49	1089±33	0.67±0.01	0.45±0.02	49.4±0.4	4.6	0.951	0.21±0.10	0.13
LBL1-1Dup	1.00	1.0	1828±43	1045±32	0.51±0.01	0.57±0.02	59.2±1.7	0.9	0.990	0.37±0.05	0.09
LBL1-3	1.00	1.0	1920±44	1179±34	0.53±0.01	0.61±0.02	62.4±1.7	2.0	0.979	0.34±0.05	0.09
LBL2-3(Dup)	1.02	1.0	2134±46	1284±36	0.59±0.01	0.60±0.02	61.5±1.6	3.1	0.967	0.48±0.05	0.09
LBL1-4	1.02	0.5	909±30	526±23	0.50±0.02	0.58±0.03	59.7±2.5	4.5	0.953	0.32±0.07	0.12
LBL1-5	1.00	1.0	2473±50	1096±33	0.69±0.01	0.44±0.02	48.9±1.3	10.2	0.896	0.28±0.10	0.14
LBL1-7	1.00	0.5	763±28	398±20	0.42±0.01	0.52±0.03	55.2±2.6	4.5	0.952	0.56±0.06	0.10
LBL1-7Dup	1.00	1.0	2070±45	1235±35	0.57±0.01	0.60±0.02	61.1±1.6	4.2	0.956	0.45±0.05	0.09
LBL1-8	1.00	0.5	680±26	367±19	0.38±0.01	0.54±0.04	56.7±2.8	5.1	0.946	0.44±0.05	0.10

[41] Calculation examples using PL1-1 is presented in Appendix N.

Table L-1. Continues

Sample code	Vol /mL	Cnt time /h	Counts Dbl	Counts Trpl	Count rate /cps	TDCR	ε_{Cerenk}	T_1-T_0 /h	DY_{Cerenk}	$[A_i]^{90}Y$ /Bq·L^{-1}	MDC /Bq·L^{-1}
ORD1-1	1.00	0.5	396±20	115±11	0.22±0.01	0.29±0.03	35.6±2.8	1.7	0.981	<MDC	0.16
ORD1-2	1.00	0.5	349±19	130±11	0.19±0.01	0.37±0.04	42.9±3.3	2.3	0.976	0.15±0.05	0.13
ORD1-3	1.00	0.5	374±19	131±11	0.21±0.01	0.35±0.04	41.0±3.1	2.3	0.975	<MDC	0.14
B-WS	1.00	0.5	314±18	114±11	0.17±0.01	0.36±0.04	42.1±3.5	5.7	0.940	<MDC	0.14
AA69B	1.00	1.0	24185±156	17418±132	6.72±0.04	0.72±0.01	70.4±0.5	3.3	0.965	488±20	0.07
AA69C	1.00	1.0	5368±73	3630±60	1.49±0.02	0.68±0.02	67.1±1.1	4.4	0.954	92.0±5.1	0.07
AA69C-Dup	1.00	1.0	5048±71	3371±58	1.40±0.02	0.67±0.02	66.5±1.1	5.4	0.943	84.1±4.8	0.08
AA71B	1.00	1.0	15232±123	10870±104	4.23±0.03	0.71±0.01	69.9±0.7	6.5	0.932	343±14	0.07
Spike 1	1.00	0.5	4882±70	3365±58	2.71±0.04	0.69±0.02	68.1±1.1	0.6	0.994	4.51±0.12	0.08
Spike 2	1.00	0.5	4973±71	3156±56	2.76±0.04	0.64±0.01	64.0±1.1	0.6	0.994	4.84±0.13	0.09
Spike 3	1.00	1.0	12914±114	9118±95	3.59±0.03	0.71±0.01	69.3±0.7	1.1	0.988	5.51±0.13	0.07
Spike 4	1.00	0.5	6320±79	4514±67	3.51±0.04	0.71±0.01	69.9±1.0	1.2	0.987	5.46±0.14	0.10
Spike 5	1.00	0.5	6354±80	4491±67	3.53±0.04	0.71±0.01	69.4±1.0	1.7	0.981	5.67±0.14	0.10
Spike 6	1.00	1.0	11580±108	8263±91	3.22±0.03	0.71±0.01	69.9±0.8	10.7	0.891	5.35±0.11	0.08
Spike 7	1.00	1.0	2409±49	1479±38	0.67±0.01	0.61±0.02	62.4±1.5	11.3	0.885	0.65±0.06	0.09
Spike 8	1.00	0.5	1681±41	1065±33	0.93±0.02	0.63±0.03	63.9±1.9	2.3	0.976	1.09±0.07	0.11
Spike 9	1.00	0.5	25414±159	18416±136	14.1±0.09	0.73±0.01	70.7±0.5	2.8	0.970	23.1±0.4	0.10
Spike 10	1.00	0.5	94707±308	68805±262	52.6±0.17	0.73±0.01	70.8±0.3	3.4	0.964	95.0±1.5	0.10
MethodBlank 1	1.00	0.5	369±19	142±12	0.20±0.01	0.39±0.03	44.0±3.3	-	0.988	0.17±0.05	0.13
MethodBlank 2	1.00	0.5	325±18	137±12	0.18±0.01	0.42±0.04	47.1±3.6	-	0.987	<MDC	0.12
MethodBlank 3	1.00	0.5	780±28	441±21	0.43±0.02	0.57±0.02	58.7±1.7	-	0.987	0.21±0.03	0.12
MethodBlank 4	1.01	0.5	604±25	287±17	0.34±0.01	0.48±0.03	51.5±2.8	-	0.993	<MDC	0.14
BlankDI Water1	0.01	0.5	530±23	234±15	0.29±0.01	0.44±0.04	48.7±2.8	-	-	-	-
BlankDI Water2	0.01	0.5	302±17	124±11	0.17±0.01	0.41±0.04	46.2±3.7	-	-	-	-
Blank DI Water3	0.01	1.0	1059±33	488±22	0.29±0.01	0.46±0.03	50.3±2.1	-	-	-	-

Table L- 2. Liquid scintillation assay (LSA) of spiked ^{90}Sr-^{90}Y in freshwater samples measured following radiochemical separation on DGA-N® resin. Counting time was 1 h on a low background Hidex LSC.

Sample code	Vol /L	Counts Dbl	Counts Trpl	Count rate /cps	TDCR= ε_{LSA}	T_2-T_0 /h	DY_{LSA}	*f*	$[A_i]$ ^{90}Y /Bq·L^{-1}	MDC /Bq·L^{-1}
PL1-1	1.01	17749±133	16960±130	4.93±0.04	0.96±0.01	13	0.871	0.953	6.44±0.12	0.08
PL1-3	1.00	13861±118	13476±116	3.85±0.03	0.97±0.01	36	0.675	0.980	6.48±0.10	0.06
PL1-3Dup	1.01	16228±127	15575±125	4.51±0.03	0.96±0.01	29	0.730	0.965	6.53±0.11	0.08
PL1-5	1.02	15937±126	15226±123	4.43±0.03	0.96±0.01	30	0.721	0.971	6.52±0.11	0.08
PL1-6	1.00	14593±121	14280±119	4.05±0.03	0.98±0.01	23	0.779	0.981	6.00±0.11	0.06
PL1-7	1.01	15678±125	15008±123	4.35±0.03	0.96±0.01	31	0.713	0.970	6.31±0.11	0.08
PL1-8	1.00	15100±123	14358±120	4.19±0.03	0.95±0.01	32	0.704	0.972	6.49±0.11	0.08
PL2-8	1.00	14815±122	14125±119	4.11±0.03	0.95±0.01	33	0.696	0.954	6.32±0.11	0.08
LBL1-1	1.00	3162±56	2845±53	0.59±0.01	0.90±0.02	30	0.720	0.983	0.28±0.04	0.06
LBL1-1Dup	1.00	2977±55	2500±50	0.83±0.01	0.84±0.02	25	0.765	0.970	0.37±0.06	0.09
LBL1-3	1.00	3169±56	2698±52	0.88±0.02	0.85±0.02	26	0.756	0.964	0.43±0.06	0.09
LBL2-3(Dup)	1.02	3188±56	2692±52	0.89±0.02	0.84±0.02	27	0.747	0.970	0.46±0.06	0.09
LBL1-4	1.02	3234±57	2755±52	0.90±0.02	0.85±0.02	14	0.861	0.951	0.41±0.06	0.09
LBL1-5	1.00	3180±56	2871±54	0.59±0.01	0.90±0.02	37	0.670	0.983	0.30±0.04	0.06
LBL1-7	1.00	2079±46	1837±43	0.58±0.01	0.88±0.03	37	0.666	0.981	0.34±0.04	0.07
LBL1-7Dup	1.00	3131±56	2635±51	0.87±0.02	0.84±0.02	28	0.738	0.965	0.43±0.06	0.09
LBL1-8	1.00	2078±46	1817±43	0.58±0.01	0.87±0.03	39	0.658	0.981	0.36±0.04	0.07
ORD1-1	1.00	729±27	591±24	0.40±0.01	0.81±0.05	18	0.819	0.979	<MDC	0.05
ORD1-2	1.00	1316±36	1082±33	0.37±0.01	0.82±0.03	33	0.700	0.981	<MDC	0.07
ORD1-3	1.00	680±26	567±24	0.38±0.01	0.83±0.05	19	0.814	0.984	<MDC	0.05

Table L-2. Continues

Sample code	Vol /L	Counts Dbl	Counts Trpl	Count rate /cps	TDCR= ε_{LSA}	T_2-T_0 /h	DY_{LSA}	*f*	$[A_i]^{90}Y$ /Bq·L^{-1}	MDC /Bq·L^{-1}
B-WS	1.00	1645±41	1399±37	0.46±0.01	0.85±0.03	40	0.650	0.980	0.13±0.03	0.07
AA69B	1.00	24507±157	23207±152	6.81±0.04	0.95±0.01	27	0.750	0.952	471±15	0.05
AA69C	1.00	6250±79	5606±75	1.74±0.02	0.90±0.02	28	0.741	0.952	86.6±4.6	0.06
AA69C-Dup	1.00	6080±78	5470±74	1.69±0.02	0.90±0.02	29	0.732	0.952	80.7±4.4	0.06
AA71B	1.00	16061±127	15160±123	4.46±0.03	0.94±0.01	30	0.724	0.953	333±11	0.05
Spike 1	1.00	9537±98	9110±95	2.65±0.03	0.96±0.01	30	0.726	0.975	4.00±0.08	0.06
Spike 2	1.00	6277±79	6099±78	3.49±0.04	0.97±0.02	17	0.829	0.982	4.72±0.11	0.04
Spike 3	1.00	13760±117	12904±114	3.82±0.03	0.94±0.01	24	0.767	0.952	5.32±0.10	0.05
Spike 4	1.00	16688±129	15961±126	4.64±0.04	0.96±0.01	7	0.924	0.952	5.64±0.12	0.08
Spike 5	1.00	16677±129	15954±126	4.63±0.04	0.96±0.01	8	0.913	0.952	5.79±0.12	0.08
Spike 6	1.00	14448±120	13682±117	4.01±0.03	0.95±0.01	24	0.774	0.965	5.49±0.11	0.08
Spike 7	1.00	2703±52	2228±47	0.75±0.01	0.82±0.02	20	0.802	0.949	0.58±0.02	0.07
Spike 8	1.00	4780±69	4239±65	1.33±0.02	0.89±0.02	9	0.902	0.952	1.03±0.06	0.09
Spike 9	1.00	64059±253	62657±250	17.8±0.1	0.98±0.01	11	0.892	0.950	23.8±0.4	0.08
Spike 10	1.00	239175±489	235832±486	66.4±0.0	0.99±0.01	12	0.882	0.951	98.7±1.4	0.08
Method Blank 1	1.00	1307±36	1094±33	0.36±0.04	0.84±0.03	-	0.717	0.978	<MDC	0.07
Method Blank 2	1.00	1290±36	1125±34	0.36±0.04	0.87±0.04	-	0.818	0.981	<MDC	0.07
Method Blank 3	1.00	692±26	563±24	0.38±0.04	0.81±0.05	-	0.824	0.984	<MDC	0.05
Method Blank 4	1.01	2225±47	1779±42	0.62±0.04	0.80±0.02	-	0.935	0.951	<MDC	0.10
UGAB1[(42)]	0.02	1402±37	1160±34	0.39±0.04	0.83±0.03	-	-	-	-	-
UGAB2	0.02	1320±36	1181±34	0.37±0.04	0.90±0.04	-	-	-	-	-
UGAB3	0.02	2242±47	1891±43	0.41±0.04	0.84±0.03	-	-	-	-	-

[(42)] UGAB= Ultima Gold AB liquid scintillation cocktail. It was counted under the same conditions as the samples for background subtraction.

Table L- 3. Liquid scintillation assay (LSA) of spiked ^{90}Sr-^{90}Y in freshwater samples measured following radiochemical separation using Sr-Resin®. Counting time was 1 h on a low background Hidex LSC.

Sample code	Vol /L	Counts Dbl	Counts Trpl	Count rate /cps	TDCR= ε_{LSA}	T_3-T_0 /h	DSr_{LSA}	I_Y	*f*	$[A_i]$ ^{90}Sr / Bq·L^{-1}	MDC /Bq·L^{-1}
PL1-1	1.01	21960±148	21093±145	6.10±0.04	0.96±0.01	20	1.00	0.197	0.952	5.92±0.28	0.08
PL1-3	1.00	17958±134	17469±132	4.99±0.04	0.97±0.01	25	1.00	0.238	0.981	4.72±0.23	0.06
PL1-3Dup	1.01	23340±153	22381±150	6.48±0.04	0.96±0.01	18	1.00	0.179	0.951	6.48±0.29	0.08
PL1-5	1.02	23855±154	22869±151	6.63±0.04	0.96±0.01	19	1.00	0.189	0.951	6.58±0.30	0.08
PL1-6	1.00	19696±140	19016±138	5.47±0.04	0.97±0.01	6.0	1.00	0.063	0.985	6.18±0.25	0.06
PL1-7	1.01	23859±154	22819±151	6.63±0.04	0.96±0.01	20	1.00	0.199	0.951	6.63±0.30	0.08
PL1-8	1.00	23042±152	22033±148	6.40±0.04	0.96±0.01	22	1.00	0.208	0.968	6.23±0.29	0.08
PL2-8(Dup)	1.00	22346±149	21442±146	6.21±0.04	0.96±0.01	23	1.00	0.217	0.951	6.05±0.28	0.08
LBL1-1	1.00	3825±62	3482±59	0.71±0.01	0.91±0.02	6.6	1.00	0.069	0.979	0.34±0.05	0.06
LBL1-1Dup	1.00	3424±59	2904±54	0.95±0.02	0.85±0.02	14	1.00	0.140	0.950	0.41±0.07	0.09
LBL1-3	1.00	3407±58	2910±54	0.95±0.02	0.85±0.02	15	1.00	0.150	0.950	0.39±0.07	0.09
LBL2-3(Dup)	1.02	3414±58	2937±54	0.95±0.02	0.86±0.02	16	1.00	0.160	0.952	0.37±0.07	0.09
LBL1-4	1.02	3388±58	2887±54	0.94±0.02	0.85±0.02	21	1.00	0.207	0.950	0.33±0.07	0.09
LBL1-5	1.00	3716±61	3405±58	0.69±0.01	0.92±0.02	13	1.00	0.135	0.977	0.29±0.30	0.06
LBL1-7	1.00	2395±49	2162±46	0.66±0.01	0.90±0.03	26	1.00	0.247	0.981	0.27±0.05	0.07
LBL1-7Dup	1.00	3629±60	3077±55	1.01±0.02	0.85±0.02	17	1.00	0.170	0.953	0.46±0.07	0.09
LBL1-8	1.00	2251±47	1974±44	0.62±0.01	0.88±0.03	27	1.00	0.256	0.981	0.24±0.05	0.07
ORD1-1	1.00	3903±62	3052±55	0.36±0.01	0.78±0.02	7.0	1.00	0.073	0.980	<MDC	0.02
ORD1-2	1.00	1391±37	1120±33	0.39±0.01	0.81±0.03	22	1.00	0.210	0.981	<MDC	0.08
ORD1-3	1.00	3895±62	2522±50	0.36±0.01	0.65±0.02	10	1.00	0.106	0.980	<MDC	0.03

Table L-3. Continues

Sample code	Vol /L	Counts Dbl	Counts Trpl	Count rate /cps	TDCR= ε_{LSA}	T_3-T_0 /h	DSr_{LSA}	I_Y	*f*	$[A_i]$ ^{90}Sr /Bq·L^{-1}	MDC /Bq·L^{-1}
B-WS	1.00	1391±37	1144±34	0.39±0.01	0.82±0.03	28	1.00	0.266	0.979	<MDC	0.08
AA69B	1.00	40896±202	39541±199	11.4±0.1	0.97±0.01	20	1.00	0.196	0.954	518±22	0.08
AA69C	1.00	8576±93	7926±89	2.38±0.03	0.92±0.01	22	1.00	0.214	0.955	82.0±5.3	0.09
AA69C-Dup	1.00	9569±98	8948±95	2.66±0.03	0.94±0.01	21	1.00	0.205	0.955	97.8±6.0	0.08
AA71B	1.00	27269±165	26248±162	7.57±0.05	0.96±0.01	23	1.00	0.224	0.952	364±17	0.08
Spike 1	1.00	12894±114	12360±111	3.58±0.03	0.96±0.01	6.7	1.00	0.070	0.972	3.86±0.17	0.06
Spike 2	1.00	42092±205	34393±185	3.90±0.02	0.82±0.01	14	1.00	0.138	0.980	4.73±0.20	0.02
Spike 3	1.00	21576±147	20682±144	5.99±0.04	0.96±0.01	18	1.00	0.177	0.954	5.91±0.27	0.08
Spike 4	1.00	19919±141	19026±138	5.53±0.04	0.96±0.01	15	1.00	0.149	0.952	5.63±0.25	0.08
Spike 5	1.00	19733±140	18882±137	5.48±0.04	0.96±0.01	16	1.00	0.159	0.952	5.52±0.25	0.08
Spike 6	1.00	18485±136	17613±133	5.13±0.04	0.95±0.01	13	1.00	0.130	0.952	5.21±0.24	0.08
Spike 7	1.00	4019±63	3506±59	1.12±0.02	0.87±0.02	12	1.00	0.125	0.950	0.70±0.07	0.09
Spike 8	1.00	5449±74	4902±70	1.51±0.02	0.90±0.02	17	1.00	0.169	0.950	0.99±0.09	0.09
Spike 9	1.00	80733±284	78645±280	22.4±0.1	0.97±0.01	18	1.00	0.178	0.967	24.4±0.98	0.08
Spike 10	1.00	305997±553	299052±547	85.0±0.2	0.98±0.00	19	1.00	0.188	0.958	94.0±3.7	0.08
MethodBlank 1	1.00	1468±38	1154±34	0.41±0.01	0.79±0.03	-	1.00	0.081	0.989	<MDC	0.08
MethodBlank 2	1.00	1327±36	1120±33	0.37±0.01	0.84±0.03	-	1.00	0.086	0.979	<MDC	0.07
MethodBlank 3	1.00	629±25	516±23	0.35±0.01	0.82±0.05	-	1.00	0.169	0.980	<MDC	0.11
MethodBlank 4	1.01	2281±48	1749±42	0.63±0.01	0.77±0.02	-	1.00	0.139	0.951	<MDC	0.10
UGAB1	0.02	2186±47	1718±41	0.61±0.01	0.79±0.03	-	-	-	-	-	-
UGAB2	0.02	2230±47	1737±42	0.62±0.01	0.78±0.03	-	-	-	-	-	-
UGAB3	0.02	1404±37	1189±34	0.39±0.01	0.85±0.03	-	-	-	-	-	-

Table L- 4. Liquid scintillation assay (LSA) of spiked ^{90}Sr-^{90}Y in freshwater samples measured after ^{90}Y in-growth period of 7-12 days from the radiochemical separation on Sr-Resin®. Counting time was 1 h on a low background Hidex LSC.

Sample code	Vol /L	Counts Dbl	Counts Trpl	Count rate /cps	TDCR= ε_{LSA}	T_4-T_0 /h	DSr_{LSA}	I_Y	*f*	$[A_i]$ ^{90}Sr /Bq·L^{-1}	MDC /Bq·L^{-1}
PL1-1	1.01	32623±181	31712±178	9.06±0.05	0.97±0.01	149	1.00	0.800	0.952	6.07±0.09	0.08
PL1-3	1.00	31139±176	30513±175	8.65±0.05	0.98±0.01	227	0.999	0.914	0.981	5.50±0.38	0.06
PL1-3Dup	1.01	35372±188	34346±185	9.83±0.05	0.97±0.01	201	0.999	0.886	0.951	6.34±0.10	0.08
PL1-5	1.02	35592±189	34590±186	9.89±0.05	0.97±0.01	202	0.999	0.887	0.951	6.37±0.10	0.08
PL1-6	1.00	32695±181	32150±179	9.08±0.05	0.98±0.01	120	1.00	0.727	0.985	6.37±0.40	0.06
PL1-7	1.01	34275±185	33360±183	9.52±0.05	0.97±0.01	203	0.999	0.888	0.951	6.17±0.10	0.08
PL1-8	1.00	34265±185	33220±182	9.52±0.05	0.97±0.01	204	0.999	0.890	0.968	6.10±0.10	0.08
PL2-8(Dup)	1.00	32125±179	31161±177	8.92±0.05	0.97±0.01	205	0.999	0.891	0.951	5.78±0.09	0.08
LBL1-1	1.00	4695±69	4285±65	0.87±0.01	0.91±0.02	134	1.00	0.766	0.979	0.33±0.05	0.05
LBL1-1Dup	1.00	4079±64	3598±60	1.13±0.02	0.88±0.02	196	1.00	0.880	0.950	0.38±0.05	0.09
LBL1-3	1.00	4109±64	3589±60	1.14±0.02	0.87±0.02	197	1.00	0.882	0.950	0.39±0.05	0.09
LBL2-3(Dup)	1.02	3964±63	3489±59	1.10±0.02	0.88±0.02	198	1.00	0.883	0.952	0.35±0.04	0.09
LBL1-4	1.02	3962±63	3468±59	1.10±0.02	0.88±0.02	150	1.00	0.803	0.950	0.36±0.04	0.09
LBL1-5	1.00	4809±69	4160±64	0.89±0.01	0.87±0.02	141	1.00	0.782	0.977	0.39±0.05	0.06
LBL1-7	1.00	3205±57	3014±55	0.89±0.02	0.94±0.02	228	0.999	0.915	0.981	0.34±0.05	0.06
LBL1-7Dup	1.00	4224±65	3680±61	1.17±0.02	0.87±0.02	199	1.00	0.884	0.953	0.41±0.05	0.09
LBL1-8	1.00	2965±54	2739±52	0.82±0.01	0.92±0.02	229	0.999	0.916	0.981	0.30±0.05	0.07
ORD1-1	1.00	3593±60	2758±53	1.00±0.02	0.77±0.02	314	0.999	0.966	0.980	<MDC	0.07
ORD1-2	1.00	1384±37	1156±34	0.38±0.01	0.84±0.03	223	0.999	0.911	0.981	<MDC	0.07
ORD1-3	1.00	3747±61	2869±54	1.04±0.02	0.77±0.02	315	0.999	0.966	0.980	<MDC	0.07

Table L-4. Continues

Sample code	Vol /L	Counts Dbl	Counts Trpl	Count rate /cps	TDCR= ε_{LSA}	T_4-T_0 /h	DSr_{LSA}	I_Y	*f*	$[A_i]$ ^{90}Sr /Bq·L^{-1}	MDC /Bq·L^{-1}
B-WS	1.00	1317±36	1149±34	0.37±0.01	0.87±0.04	230	0.999	0.917	0.979	<MDC	0.07
AA69B	1.00	60549±246	59178±243	16.8±0.07	0.98±0.01	171	1.00	0.842	0.954	507±32	0.08
AA69C	1.00	11863±109	11188±106	3.29±0.03	0.94±0.01	173	1.00	0.846	0.955	85.2±7.0	0.08
AA69C-Dup	1.00	13304±115	12673±113	3.70±0.03	0.95±0.01	172	1.00	0.844	0.955	99.9±7.9	0.08
AA71B	1.00	39287±198	38114±195	10.9±0.05	0.97±0.01	174	1.00	0.847	0.952	360±24	0.08
Spike 1	1.00	22355±150	21873±148	6.21±0.04	0.98±0.01	220	0.999	0.907	0.972	3.92±0.08	0.06
Spike 2	1.00	29230±171	27978±167	8.12±0.05	0.96±0.01	316	0.999	0.967	0.980	4.41±0.37	0.05
Spike 3	1.00	30926±176	30028±173	8.59±0.05	0.97±0.01	168	1.00	0.838	0.954	5.67±0.38	0.08
Spike 4	1.00	29954±173	29131±171	8.32±0.05	0.97±0.01	143	1.00	0.788	0.952	5.65±0.37	0.08
Spike 5	1.00	29344±171	28500±169	8.15±0.05	0.97±0.01	144	1.00	0.791	0.952	5.52±0.36	0.08
Spike 6	1.00	29691±172	28701±169	8.25±0.05	0.97±0.01	195	1.00	0.879	0.952	5.28±0.37	0.08
Spike 7	1.00	5783±76	5297±73	1.61±0.02	0.92±0.02	188	1.00	0.869	0.950	0.77±0.09	0.09
Spike 8	1.00	7040±84	6499±81	1.96±0.02	0.92±0.02	146	1.00	0.793	0.950	0.99±0.10	0.08
Spike 9	1.00	121988±349	119987±346	33.9±0.10	0.98±0.00	147	1.00	0.795	0.967	24.3±1.5	0.08
Spike 10	1.00	461430±679	454597±674	128±0.2	0.99±0.00	148	1.00	0.798	0.958	93.2±5.5	0.08
Method Blank 1	1.00	1375±37	1176±34	0.38±0.01	0.86±0.03	-	-	-	0.989	<MDC	0.07
Method Blank 2	1.00	1324±36	1134±34	0.37±0.01	0.86±0.04	-	-	-	0.979	<MDC	0.07
Method Blank 3	1.00	3557±60	2684±52	0.99±0.02	0.76±0.02	-	-	-	0.980	<MDC	0.13
Method Blank 4	1.01	2220±47	1731±42	0.62±0.01	0.78±0.03	-	-	-	0.951	<MDC	0.10
UGAB1	0.02	1933±44	1529±39	0.54±0.01	0.79±0.03	-	-	-	-	-	-
UGAB2	0.02	2088±46	1639±40	0.58±0.01	0.79±0.03	-	-	-	-	-	-
UGAB3	0.02	3788±62	2858±53	1.05±0.02	0.75±0.02	-	-	-	-	-	-

Table L- 5. Chemical recovery of stable Y measured by ICP-MS in various stages of the seawater method development.

Developmental stage	Initial step	$CaCO_3$ precipitate		HTiO precipitate		Purified sample	
Sample code	Y_i [43] /mg	Y_f [44] /mg	Y_R /%	Y_f /mg	Y_R /%	Y_f /mg	Y_R /%
SWY-1	1.10±0.06	1.04±0.05	94.4±7.0	1.02±0.05	92.8±6.7	0.970±0.05	88.0±6.3
SWY-2	1.14±0.06	1.11±0.06	97.5±7.4	1.00±0.05	88.2±6.5	0.942±0.04	82.9±6.0
SWY-3	1.13±0.06	0.986±0.05	87.6±6.4	1.01±0.05	89.7±6.8	0.922±0.05	81.8±6.4
SWY-4	0.960±0.04	0.897±0.04	93.5±6.1	0.859±0.05	89.6±6.2	1.00±0.05	104.3±7.0
SWY-5	0.963±0.04	0.910±0.05	94.5±6.2	0.882±0.04	91.6±6.0	0.843±0.04	87.5±5.6
SWY-6	0.988±0.06	0.922±0.05	93.3±7.4	0.873±0.04	88.4±6.7	0.850±0.04	86.1±6.5
SWY-7	1.04±0.06	0.976±0.05	93.7±7.2	0.919±0.05	88.2±7.0	0.976±0.05	93.7±7.5
SWY-8	1.03±0.06	0.961±0.05	93.5±7.0	0.856±0.04	83.3±6.4	0.890±0.05	86.6±6.9
SWY-9	0.965±0.06	0.924±0.05	95.7±7.8	0.905±0.05	93.8±7.2	0.857±0.05	88.8±7.0
SWY-10	1.06±0.06	0.999±0.05	94.5±7.1	0.979±0.05	92.6±6.9	0.933±0.04	88.3±6.5
SWY-11	1.00±0.06	0.953±0.05	95.0±7.4	0.916±0.05	91.3±7.4	0.964±0.05	96.1±7.6
SWBlank-1	1.10±0.07	0.936±0.05	84.7±6.8	1.21±0.06	109±9	0.879±0.05	79.6±6.7
SWBlank-2	0.970±0.06	0.905±0.05	93.4±7.3	1.05±0.05	108±8	0.832±0.04	85.9±6.6
SWBlank-3	0.967±0.05	0.919±0.04	95.0±6.9	1.18±0.05	100±9	0.854±0.04	88.3±6.5
SWBlank-4	0.960±0.06	0.901±0.05	93.9±7.3	1.30±0.07	100±11	0.850±0.05	88.6±7.0

[43] Y_i= initial amount of Y to begin with
[44] Y_f= final amount of Y in the sample

Table L- 6. Chemical recovery of stable Sr measured by ICP-MS in various stages of the seawater method development.

Developmental stage	Initial step	$CaCO_3$ ppt		HTiO ppt		Purified sample	
Sample code	Sr_i [45] /mg	Sr_f [46] /mg	Sr_R /%	Sr_f /mg	Sr_R /%	Sr_f /mg	Sr_R /%
SWY-1	6.38±0.30	3.73±0.14	58.4±3.5	1.44±0.07	22.6±1.1	0.002±0.000	0.02
SWY-2	6.29±0.41	3.92±0.23	62.3±5.5	1.41±0.07	22.4±1.9	<2.334E-05	0.00
SWY-3	6.35±0.42	3.62±0.22	57.0±5.1	1.36±0.08	21.3±1.8	0.0002±0.0000	0.00
SWY-4	6.80±0.41	3.24±0.17	47.7±3.8	1.24±0.07	18.3±1.5	<4.971E-05	0.00
SWY-5	7.27±0.40	2.96±0.15	40.7±3.1	1.23±0.06	16.9±1.3	<1.176E-05	0.00
SWY-6	7.27±0.38	3.26±0.17	44.9±3.3	1.32±0.07	18.1±1.3	<1.187E-05	0.00
SWY-7	6.54±0.42	2.93±0.14	44.8±3.5	1.31±0.07	20.0±1.6	<3.109E-05	0.00
SWY-8	7.42±0.39	3.38±0.16	45.5±3.2	1.28±0.07	17.3±1.3	<1.222E-05	0.00
SWY-9	6.87±0.38	3.25±0.21	47.3±4.0	1.25±0.07	18.1±1.4	<3.753E-05	0.00
SWY-10	6.85±0.40	3.17±0.16	46.3±3.6	1.21±0.06	17.7±1.4	<5.091E-05	0.00
SWY-11	6.82±0.41	3.65±0.18	53.5±4.2	1.33±0.07	19.4±1.5	<3.506E-05	0.00
SWBlank-1	8.28±0.36	3.34±0.15	40.4±2.6	2.09±0.11	25.2±1.7	<1.387E-05	0.00
SWBlank-2	7.27±0.28	2.83±0.16	39.0±2.7	1.82±0.10	25.1±1.6	<1.873E-05	0.00
SWBlank-3	7.12±0.27	3.18±0.18	44.6±3.0	2.12±0.11	29.7±1.9	0.003±0.00	0.02
SWBlank-4	7.13±0.29	3.23±0.16	45.3±2.9	2.21±0.11	30.9±2.0	<1.331E-05	0.00
Mean ±1σ	7.0±0.5	3.3±0.3	47.8±6.9	1.5±0.4	21.5±4.5	0.002±0.001	0.02±0.00

[45] Sr_i = initial amount of Sr to begin with
[46] Sr_f = final amount of Sr in the sample

Table L- 7. Seawater ^{88}Y radiotracer recovery measured by HPGe γ spectrometry. Counting time was 0.5 h for counting of the dissolved precipitates and 1 h for purified samples.

Sample code	Description	Tracer	γ-energy /keV	*I*	*f*	CR_N /cps	ε_γ /%	$[A_i]$ /Bq·L^{-1}	$[A_{ia}]$ /Bq·L^{-1}	Recovery /%
SWY-1	15 mL pure sample	^{88}Y	898	0.937	0.753	0.072±0.006	1.05±0.03	9.75±0.82	12.6±0.4	77.7±6.9
SWY-2	15 mL pure sample	^{88}Y	898	0.937	0.759	0.087±0.006	1.05±0.03	11.7±0.8	12.5±0.4	93.7±7.3
SWY-3	15 mL pure sample	^{88}Y	898	0.937	0.759	0.077±0.005	1.05±0.03	10.3±0.8	12.4±0.4	82.7±6.5
SWY-4	20 mL $CaCO_3$ ppt	^{88}Y	898	0.937	1.000	0.093±0.008	0.91±0.03	10.9±1.0	12.6±0.4	87.1±8.2
SWY-4	20 mL HTiO ppt	^{88}Y	898	0.937	1.000	0.074±0.007	0.91±0.03	8.65±0.83	12.6±0.4	68.9±7.0
SWY-4	10 mLpure sample	^{88}Y	898	0.937	0.673	0.090±0.005	1.26±0.04	11.2±0.7	12.5±0.4	90.1±6.4
SWY-5	20 mL $CaCO_3$ ppt	^{88}Y	898	0.937	1.00	0.083±0.01	0.91±0.03	9.62±1.3	10.9±0.3	88.5±12.0
SWY-5	20 mL HTiO ppt	^{88}Y	898	0.937	1.00	0.10±0.01	0.91±0.03	12.1±1.2	10.9±0.3	104±14
SWY-5	10mLpure sample	^{88}Y	898	0.937	0.644	0.073±0.005	1.26±0.04	9.53±0.75	10.1±0.3	87.6±7.4
SWY-6	20 mL $CaCO_3$ ppt	^{88}Y	898	0.937	1.00	0.092±0.01	0.91±0.03	10.7±1.3	11.0±0.3	96.7±12.5
SWY-6	20 mL HTiO ppt	^{88}Y	898	0.937	1.000	0.091±0.01	0.91±0.03	10.5±1.3	11.0±0.3	95.5±11.9
SWY-6	10 mLpure sample	^{88}Y	898	0.937	0.658	0.076±0.005	1.26±0.04	9.70±0.74	10.9±0.3	89.0±7.3
SWY-7	20 mL $CaCO_3$ ppt	^{88}Y	898	0.937	1.00	n/a	-	n/a	n/a	-
SWY-7	20 mL HTiO ppt	^{88}Y	898	0.937	1.00	n/a	-	n/a	n/a	-
SWY-7	10 mLpure sample	^{88}Y	898	0.937	0.670	n/a	-	n/a	n/a	-

Table L-7. Continues

Sample code	Description	Tracer	γ-energy /keV	*I*	*f*	CR_N /cps	ε_γ /%	$[A_i]$ /Bq·L^{-1}	$[A_{ia}]$ /Bq·L^{-1}	Recovery /%
SWY-8	20 mL $CaCO_3$ ppt	^{88}Y	898	0.937	1.00	n/a	-	n/a	n/a	-
SWY-8	20 mL HTiO ppt	^{88}Y	898	0.937	1.00	n/a	-	n/a	n/a	-
SWY-8	10 mLpure sample	^{88}Y	898	0.937	0.649	n/a	-	n/a	n/a	-
SWY-9	20 mL $CaCO_3$ ppt	^{88}Y	898	0.937	1.00	0.088±0.008	0.91±0.03	10.2±1.0	12.7±0.4	80.3±8.4
SWY-9	20 mL HTiO ppt	^{88}Y	898	0.937	1.00	0.079±0.009	0.91±0.03	9.20±1.1	12.7±0.4	72.2±8.8
SWY-9	10 mLpure sample	^{88}Y	898	0.937	0.649	0.090±0.006	1.26±0.04	11.2±0.8	12.7±0.4	88.7±6.8
SWY-10	20 mL $CaCO_3$ ppt	^{88}Y	898	0.937	1.00	0.089±0.008	0.91±0.03	10.4±1.0	12.7±0.4	81.6±8.5
SWY-10	20 mL HTiO ppt	^{88}Y	898	0.937	1.00	0.096±0.007	0.91±0.03	11.2±0.9	12.7±0.4	88.2±7.7
SWY-10	10 mLpure sample	^{88}Y	898	0.937	0.664	0.088±0.006	1.26±0.04	11.1±0.8	12.6±0.4	88.0±6.8
SWY-11	20 mL $CaCO_3$ ppt	^{88}Y	898	0.937	1.00	0.11±0.008	0.91±0.03	12.2±1.1	12.4±0.4	97.7±8.9
SWY-11	20 mL HTiO ppt	^{88}Y	898	0.937	1.00	0.092±0.008	0.91±0.03	10.7±1.0	12.4±0.4	85.8±8.2
SWY-11	10 mLpure sample	^{88}Y	898	0.937	0.665	0.088±0.005	1.26±0.04	11.0±0.8	12.4±0.4	88.7±6.7

Note: Γ spectrometry of ^{88}Y in precipitates of SWY-1, SWY-2, and SWY-3 was not conducted due to unavailability of the instrument- denoted by "n/a" meaning "not applicable". Also, SWY-7 and SWY-8 were not spiked with ^{88}Y tracer and, therefore, no ^{88}Y was detected in the samples.

Table L- 8. Seawater ^{85}Sr radiotracer recovery measured by HPGe γ spectrometry. Counting time was 0.5 h for counting of the dissolved precipitates and 1 h for purified samples.

Sample code	Description	Tracer	γ-energy /keV	*I*	*f*	CR_N /cps	ε_γ /%	$[A_i]$ /Bq·L^{-1}	$[A_{ia}]$ /Bq·L^{-1}	Recovery /%
SWY-1	15 mL pure sample	^{85}Sr	514	0.960	0.753	ND	1.73±0.05	ND	11.3±0.3	ND
SWY-2	15 mL pure sample	^{85}Sr	514	0.960	0.759	ND	1.73±0.05	ND	11.2±0.3	ND
SWY-3	15 mL pure sample	^{85}Sr	514	0.960	0.759	ND	1.73±0.05	ND	11.2±0.3	ND
SWY-4	20 mL $CaCO_3$ ppt	^{85}Sr	514	0.960	1.00	0.055±0.007	1.54±0.05	3.71±0.5	10.9±0.3	34.0±4.7
SWY-4	20 mL HTiO ppt	^{85}Sr	514	0.960	1.00	0.094±0.004	1.54±0.05	0.64±0.30	10.9±0.3	5.8±2.8
SWY-4	10 mLpure sample	^{85}Sr	514	0.960	0.673	ND	2.38±0.07	ND	10.8±0.3	ND
SWY-5	20 mL $CaCO_3$ ppt	^{85}Sr	514	0.960	1.00	0.091±0.01	1.54±0.05	6.09±0.70	10.4±0.3	58.5±6.9
SWY-5	20 mL HTiO ppt	^{85}Sr	514	0.960	1.00	0.021±0.005	1.54±0.05	1.41±0.34	10.4±0.3	13.6±3.3
SWY-5	10 mLpure sample	^{85}Sr	514	0.960	0.644	ND	2.38±0.07	ND	10.4±0.3	ND
SWY-6	20 mL $CaCO_3$ ppt	^{85}Sr	514	0.960	1.00	0.10±0.01	1.54±0.05	6.88±0.71	10.4±0.3	66.4±7.1
SWY-6	20 mL HTiO ppt	^{85}Sr	514	0.960	1.00	0.017±0.006	1.54±0.05	1.15±0.37	10.4±0.3	11.1±3.6
SWY-6	10 mLpure sample	^{85}Sr	514	0.960	0.658	ND	2.38±0.07	ND	10.2±0.3	ND
SWY-7	20 mL $CaCO_3$ ppt	^{85}Sr	514	0.960	1.00	0.046±0.005	1.54±0.05	3.13±0.35	10.4±0.3	30.2±3.5
SWY-7	20 mL HTiO ppt	^{85}Sr	514	0.960	1.00	0.025±0.003	1.54±0.05	1.67±0.23	10.4±0.3	16.1±2.3
SWY-7	10 mLpure sample	^{85}Sr	514	0.960	0.670	0.0006±0.001	2.38±0.07	ND	10.3±0.3	ND

Table L-8. Continues

Sample code	Description	Tracer	γ-energy /keV	*I*	*f*	CR_N /cps	ε_γ /%	$[A_i]$ /Bq·L^{-1}	$[A_{ia}]$ /Bq·L^{-1}	Recovery /%
SWY-8	20 mL $CaCO_3$ ppt	^{85}Sr	514	0.960	1.00	0.10±0.01	1.54±0.05	6.73±0.70	10.3±0.3	65.0±7.1
SWY-8	20 mL HTiO ppt	^{85}Sr	514	0.960	1.00	0.029±0.006	1.54±0.05	1.96±0.38	10.4±0.3	18.9±3.7
SWY-8	10 mLpure sample	^{85}Sr	514	0.960	0.649	ND	2.38±0.07	ND	10.2±0.3	ND
SWY-9	20 mL $CaCO_3$ ppt	^{85}Sr	514	0.960	1.00	0.071±0.007	1.54±0.05	4.74±0.51	12.3±0.4	38.6±4.3
SWY-9	20 mL HTiO ppt	^{85}Sr	514	0.960	1.00	0.021±0.005	1.54±0.05	1.38±0.34	12.3±0.4	11.2±2.8
SWY-9	10 mLpure sample	^{85}Sr	514	0.960	0.649	ND	2.38±0.07	ND	12.3±0.4	ND
SWY-10	20 mL $CaCO_3$ ppt	^{85}Sr	514	0.960	1.00	0.073±0.008	1.54±0.05	4.89±0.55	12.3±0.4	39.7±4.6
SWY-10	20 mL HTiO ppt	^{85}Sr	514	0.960	1.00	0.016±0.005	1.54±0.05	1.05±0.34	12.3±0.4	8.5±2.8
SWY-10	10 mLpure sample	^{85}Sr	514	0.960	0.664	ND	2.38±0.07	ND	12.2±0.4	ND
SWY-11	20 mL $CaCO_3$ ppt	^{85}Sr	514	0.960	1.00	0.082±0.008	1.54±0.05	5.44±0.58	10.7±0.3	50.7±5.7
SWY-11	20 mL HTiO ppt	^{85}Sr	514	0.960	1.00	0.014±0.004	1.54±0.05	0.93±0.30	10.7±0.3	8.6±2.8
SWY-11	10 mLpure sample	^{85}Sr	514	0.960	0.665	ND	2.38±0.07	ND	10.6±0.3	ND

Note: As it was expected, no ^{85}Sr was detected in pure samples following radiochemical separation on DGA-N® resin-denoted by "ND" meaning "not detected".

Table L- 9. ^{88}Y radiotracer recovery in purified seawater samples measured by liquid scintillation assay on a low background Hidex LSC for a counting time of 1 h.

Sample code	ROI 100-300		CR_N /cps	^{88}Y DY	A_i ^{88}Y /Bq	A_{ia} ^{88}Y /Bq	Recovery /%
	Dbl	Trpl					
SWY-1	5310±73	3735±61	0.94±0.02	0.960	9.89±0.23	12.7±0.38	78.2±6.9
SWY-2	5671±75	4117±64	1.05±0.02	0.953	10.5±0.22	12.8±0.38	82.3±7.2
SWY-3	5451±74	3902±62	0.99±0.02	0.946	10.4±0.23	12.8±0.38	81.3±7.2
SWY-4	7728±88	5508±74	1.42±0.02	0.898	12.1±0.22	12.6±0.38	96.3±8.4
SWY-5	6095±78	4295±66	1.19±0.02	0.896	9.34±0.18	11.0±0.38	85.2±7.5
SWY-6	5870±77	4099±64	1.14±0.02	0.890	9.36±0.19	11.1±0.38	84.2±7.4
SWY-9	5567±75	381±20	1.33±0.02	0.896	11.2±0.19	12.8±0.38	87.4±7.6
SWY-10	5693±75	390±20	1.36±0.02	0.890	11.4±0.19	12.8±0.38	89.0±7.7
SWY-11	5754±76	394±20	1.38±0.02	0.885	11.6±0.19	12.6±0.38	92.0±8.0
UGAB1	765±28	354±19	-	-	-	-	-
UGAB2	825±29	407±20	-	-	-	-	-
UGAB3	793±28	375±19	-	-	-	-	-
UGAB4	798±28	389±20	-	-	-	-	-

Table L- 10. Čerenkov counting of spiked ^{90}Sr-^{90}Y in seawater samples that were measured following radiochemical separation using DGA-N® resin. Samples were counted on a low background Hidex LSC for a counting time of 1 h.

Sample code	Vol /L	$[A_{ia}]$ ^{90}Y /Bq·L^{-1}	A_{ia} ^{88}Y /Bq[47]	^{88}Y-^{90}Y Mixed counts (C_{YY})		^{88}Y counts (C_{Y88})		^{88}Y Recovery (γ-spec) /%	^{88}Y counts (C_{Y88}) R_{Corr}[48]	
				Dbl	Trpl	Dbl	Trpl		Dbl	Trpl
SWY-1	1.00	5.02±0.18	12.7±0.38	12186±110	8252±91	1667±41	847±29	77.7±6.9	1295±36	658±26
SWY-2	1.00	4.95±0.18	12.8±0.38	12132±110	8240±91	1647±41	837±29	93.7±7.3	1543±39	784±28
SWY-3	1.00	5.00±0.18	12.8±0.37	12172±110	8181±90	1648±41	838±29	82.7±6.5	1363±37	693±26
SWY-4	1.00	5.98±0.21	12.6±0.38	14911±122	10323±102	1719±41	874±30	90.1±6.4	1549±39	787±28
SWY-5	1.01	4.72±0.17	11.0±0.33	14076±119	9645±98	1971±41	1002±32	87.6±7.4	1726±42	877±30
SWY-6	1.01	4.72±0.17	11.1±0.33	13724±117	9382±97	1943±41	988±31	89.0±7.3	1729±42	879±30
SWY-7	1.00	0.58±0.02	-	-	-	-	-	-	-	-
SWY-8	1.01	0.59±0.02	-	-	-	-	-	-	-	-
SWY-9	1.01	20.0±0.72	12.8±0.39	46081±215	33049±182	1686±41	857±29	88.7±6.8	1495±39	760±28
SWY-10	1.01	33.7±1.2	12.8±0.38	73512±271	53331±231	1692±41	860±29	88.0±6.8	1489±39	757±28
SWY-11	1.01	93.6±3.4	12.6±0.38	194975±442	142703±378	1715±41	872±30	88.7±6.7	1522±39	773±28
SWBlank-1	1.01	-	-	1124±34	518±23	-	-	-	-	-
SWBlank-2	1.00	-	-	1202±35	571±24	-	-	-	-	-
SWBlank-3	1.00	-	-	1190±34	595±24	-	-	-	-	-
SWBlank-4	1.02	-	-	1330±36	650±25	-	-	-	-	-
Blank DI Water1	0.01	-	-	1027±32	486±22	-	-	-	-	-
Blank DI Water2	0.01	-	-	1095±33	548±23	-	-	-	-	-

[47] Note that the activity and not the activity concentrations of spiked ^{88}Y was used for determination of coincidence counts.
[48] Contributions of ^{88}Y to coincidence counts are corrected based on chemical recovery of ^{88}Y shown in the present Table.

Table L-10. Continues

Sample code	^{90}Y counts Dbl	^{90}Y counts Trpl	CR_N /cps	TDCR	ε_{Cerenk} /%	t_1-t_0 /h	DY_{Cerenk}	*f*	$[A_i]$ ^{90}Y /Bq·L^{-1}	B_{ri} /%	MDC /Bq·L^{-1}
SWY-1	9864±99	7108±84	2.74±0.03	0.721±0.01	70.4±0.6	0.8	0.992	0.976	4.56±0.33	-9.2	0.07
SWY-2	9562±98	6970±83	2.66±0.03	0.73±0.01	71.1±0.6	1.8	0.981	0.976	4.70±0.35	-5.1	0.07
SWY-3	9782±99	7002±84	2.72±0.03	0.72±0.01	70.1±0.6	2.9	0.969	0.976	4.99±0.40	-0.2	0.08
SWY-4	12350±111	9044±95	3.43±0.03	0.73±0.01	71.2±0.6	5.1	0.946	0.968	5.25±0.37	-12.2	0.06
SWY-5	11210±106	8195±91	3.11±0.03	0.73±0.01	71.2±0.6	1.7	0.982	1.00	5.04±0.39	6.9	0.07
SWY-6	10855±104	7930±89	3.01±0.03	0.73±0.01	71.1±0.6	2.8	0.970	1.00	5.03±0.39	6.5	0.07
SWY-7	2240±47	1292±36	0.62±0.01	0.69±0.02	68.3±1.2	4.4	0.924	1.00	0.54±0.04	-7.8	0.07
SWY-8	2399±49	1396±37	0.35±0.01	0.65±0.02	65.4±1.2	0.5	0.995	1.00	0.61±0.05	4.1	0.07
SWY-9	43490±209	31741±178	12.1±0.1	0.73±0.01	71.1±0.3	0.7	0.992	1.00	19.2±1.52	-4.3	0.07
SWY-10	70929±266	52026±228	19.7±0.1	0.73±0.01	71.3±0.2	1.8	0.980	1.00	31.8±2.35	-5.8	0.07
SWY-11	192441±439	141438±376	53.5±0.1	0.74±0.01	71.4±06	6.2	0.773	1.00	102.7±8.14	-9.7	0.06
SWBlank-1	1124±34	518±23	0.00	0.00	47.2±7.6	3.9	0.959	1.00	<MDC	-	0.12
SWBlank-2	1202±35	571±24	0.02±0.01	0.032±0.001	47.2±7.6	5.0	0.948	1.00	<MDC	-	0.11
SWBlank-3	1190±34	595±24	0.01±0.01	0.440±0.018	48.6±1.5	6.1	0.936	1.00	<MDC	-	0.10
SWBlank-4	1330±36	650±25	0.05±0.01	0.405±0.016	45.7±1.4	7.1	0.926	1.00	0.14±0.03	-	0.11

Table L- 11. Liquid scintillation assay (LSA) of spiked ^{90}Sr-^{90}Y in seawater samples measured following radiochemical separation using DGA-N® resin. Samples were counted on low background Hidex LSC for a counting time of 1 h.

Sample code	Vol /L	^{88}Y-^{90}Y count ($C1_{YY}$)[49]		^{88}Y-^{90}Y count ($C2_{YY}$)[50]		^{88}Y count ($C1_{Y88}$)[51]		^{88}Y count ($C2_{Y88}$)[52]		^{88}Y Recovery (γ-spec)	^{88}Y count ($C2_{Y88}$)R_{Corr}[53]		^{90}Y count ($C2_{Y90}$)[54]	
		Dbl	Trpl	Dbl	Trpl	Dbl	Trpl	Dbl	Trpl		Dbl	Trpl	Dbl	Trpl
SWY-1	1.00	5310	3735	5315	5251	4229	290	967	965	0.777	751	750	3444±31	3417±31
SWY-2	1.00	5671	4117	5536	5478	4389	301	1003	1002	0.937	940	939	3476±59	3455±59
SWY-3	1.00	5451	3902	5234	5197	4223	289	965	964	0.827	798	797	3316±58	3316±58
SWY-4	1.00	7728	5508	8177	8114	5625	385	1286	1284	0.901	1159	1157	5726±75	5705±20
SWY-5	1.01	6095	4295	6891	6836	7029	481	1607	1604	0.876	1408	1405	4115±64	4108±64
SWY-6	1.01	5870	4099	6825	6773	6644	455	1519	1516	0.890	1352	1349	4104±64	4101±64
SWY-7	1.00	-	-	1943	1883	-	-	-	-	-	-	-	1943±44	1883±43
SWY-8	1.01	-	-	1887	1837	-	-	-	-	-	-	-	1887±32	1837±23
SWY-9	1.01	7516	5464	20483	20429	5567	381	1273	1271	0.887	1129	1127	18009±75	18012±20
SWY-10	1.01	7712	5651	32198	32142	5693	390	1301	1299	0.880	1145	1143	29708±75	29709±20
SWY-11	1.01	9830	7442	92254	92189	5754	394	1315	1313	0.887	1166	1165	89831±76	89808±20
SWBlank-1	1.01	-	-	1466	1419	-	-	-	-	-	-	-	1466±32	1419±24
SWBlank-2	1.00	-	-	1430	1385	-	-	-	-	-	-	-	1430±30	1385±22
SWBlank-3	1.00	-	-	1362	1312	-	-	-	-	-	-	-	1362±31	1312±22
SWBlank-4	1.02	-	-	1342	1287	-	-	-	-	-	-	-	1342±30	1287±22
UGAB1	0.02	765	354	1120	1084	-	-	-	-	-	-	-	-	-
UGAB2	0.02	793	375	1345	1290	-	-	-	-	-	-	-	-	-
UGAB3	0.02	798	389	1293	1253	-	-	-	-	-	-	-	-	-

[49] $C1_{YY}$ = Coincidences in counting channels 100-300 of Hidex LSC for mixed contributions of ^{88}Y and ^{90}Y
[50] $C2_{YY}$ = Coincidences in counting channels 300-800 of Hidex LSC for mixed contributions of ^{88}Y and ^{90}Y
[51] $C1_{Y88}$ = Coincidences in counting channels 100-300 of Hidex LSC for contribution of ^{88}Y alone
[52] $C2_{Y88}$ = Coincidences in counting channels 300-800 of Hidex LSC for contribution of ^{88}Y alone
[53] $(C2_{Y88})R_{corr}$ = Coincidences in counting channels 300-800 of Hidex LSC after chemical recovery correction of ^{88}Y for actual contribution of ^{88}Y
[54] $C2_{Y90}$ = Coincidences in counting channels 300-800 of Hidex LSC channels for contributions of ^{90}Y alone

Table L-11. Continues

Sample code	CR_N /cps	TDCR= ε_{LSA}	t_2-t_0 /h	DY_{LSA}	f [55]	$[A_i]$ ^{90}Y /Bq·L^{-1}	$[A_{ia}]$ ^{90}Y /Bq·L^{-1}	B_{ri} /%	MDC /Bq·L^{-1}
SWY-1	0.96±0.01	1.00±0.03	6.3	0.934	0.247	4.70±0.38	5.02±0.18	-6.5	0.20
SWY-2	0.97±0.01	1.00±0.03	7.4	0.923	0.260	4.84±0.39	4.95±0.18	-2.3	0.20
SWY-3	0.92±0.01	1.00±0.03	8.5	0.912	0.250	4.92±0.42	5.00±0.18	-1.7	0.21
SWY-4	1.59±0.02	1.00±0.03	16.6	0.836	0.327	5.81±0.42	5.98±0.21	-2.8	0.11
SWY-5	1.20±0.02	1.00±0.03	16.9	0.833	0.330	4.36±0.34	4.72±0.17	-7.6	0.14
SWY-6	1.17±0.02	1.00±0.03	18.0	0.823	0.336	4.67±0.37	4.72±0.17	-1.0	0.14
SWY-7	0.54±0.01	0.98±0.02	17.9	0.798	0.330	0.59±0.05	0.58±0.02	0.9	0.16
SWY-8	0.14±0.01	0.99±0.04	15.7	0.844	0.351	0.56±0.06	0.59±0.02	-5.5	0.13
SWY-9	5.00±0.02	1.00±0.04	16.8	0.833	0.330	20.4±1.4	20.0±0.7	1.6	0.13
SWY-10	8.25±0.02	1.00±0.03	17.9	0.824	0.336	33.6±2.3	33.7±1.2	-0.4	0.13
SWY-11	25.0±0.02	1.00±0.03	17.7	0.826	0.335	93.6±7.3	93.6±3.4	0.0	0.11
SWBlank-1	0.03±0.01	0.97±0.04	19.1	0.813	0.351	0.13±0.04	-	-	0.05
SWBlank-2	0.02±0.01	0.97±0.05	20.2	0.804	0.356	<MDC	-	-	0.05
SWBlank-3	-0.00±0.01	0.96±0.04	21.2	0.794	0.342	<MDC	-	-	0.05
SWBlank-4	-0.01±0.01	0.96±0.04	22.3	0.785	0.331	<MDC	-	-	0.04

[55] Note that the *f* values are lower for SWY-1 through SWY-3. That is because in the initial developmental procedure, larger volume (>15 mL) of the stripping solution (0.05 M HCl) was used under the assumption that larger volume may result in better chemical recoveries. However, no observable differences in chemical recoveries were noted by using larger stripping solution. Thus,12-15 mL of 0.05 M HCl was used for the remainder of the samples because where the chemical recoveries remains unchanged.

Appendix M. Correction of Radiotracer Contributions to Measured Activity of Yttrium-90 in Seawater Samples

In the seawater method development, ^{88}Y was used for chemical recovery tracing. On one hand the ^{88}Y as a tracer provides a quick and convenient way of radiochemical recovery determination by γ spectrometry of its high energy γ ray. On the other hand, ^{88}Y interferes with ^{90}Y Čerenkov counting and liquid scintillation assay (LSA) measurements. Because both ^{90}Y and ^{88}Y isotopes are chemically the same, they are not separable in the radiochemical purification procedures. In the present dissertation, ^{88}Y tracer in the purified samples, which were also spiked with ^{90}Y (in equilibrium with ^{90}Sr), contributed to ~ 10 % Čerenkov emission in the default region of interest (ROI) of ^{90}Y Čerenkov counting. In addition, when counted in liquid scintillation cocktail (UGAB), the electron capture (EC) emission of ^{88}Y also contributed by ~15 % to β^- emission in the ROI of ^{90}Y β^--ray counting. Figure M-1 demonstrates that the spectral emissions of ^{88}Y and ^{90}Y, which were counted in transparent solutions by Čerenkov counting using Hidex LSC, overlap in the same region (channels 50-350).

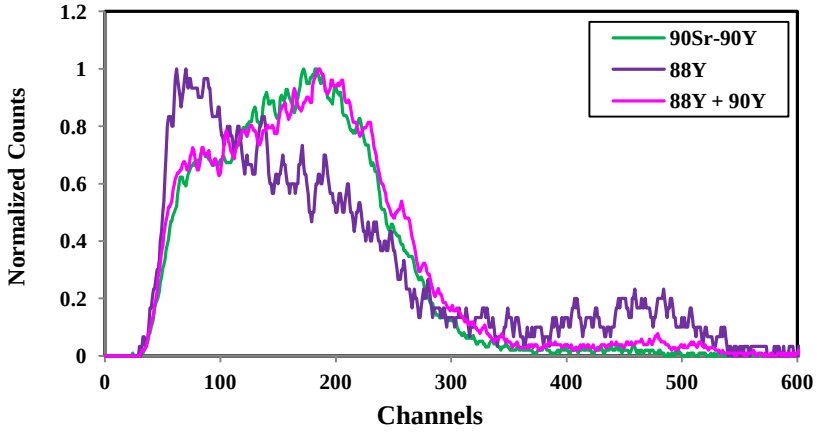

Figure M- 1. A comparison of normalized spectra obtained by counting spiked radionuclides in transparent solution by Čerenkov counting on a low background Hidex LSC. The radionuclides were: pure ^{88}Y standard (~ 20 Bq); ^{90}Y (~ 5 Bq) in equilibrium with ^{90}Sr; and mixed standards ^{88}Y (~ 10 Bq) and ^{90}Y (~ 5 Bq).

Unlike ^{88}Y, ^{85}Sr did not show any Čerenkov emissions and, therefore, was not an interference. Although the EC emission of ^{85}Sr measured by LSA could cause interference towards ^{90}Y LSA, the separation of ^{85}Sr from ^{90}Y was achieved on the DGA-N® columns prior to ^{90}Y liquid scintillation assay. Thus, no mathematical subtraction of ^{85}Sr from ^{90}Y was required in this dissertation.

In order to subtract the contribution of ^{88}Y tracer and obtain ^{90}Y measurements accurately, mathematical corrections were applied to determine net ^{90}Y

coincidences prior to activity determination is seawater spiked samples. In the approach to correct for ^{88}Y contribution ROI of ^{90}Y, a known amount (8.55 Bq) of pure ^{88}Y standard solution was spiked in 0.5 M HCl solution and counted on Hidex LSC for a counting time of 1 h. A blank 0.5 M HCl solution was also counted for background subtraction. The net double and triple counts of the pure ^{88}Y standard in the default counting ROI of ^{90}Y were obtained and used in Eq. (M-1) to determine the net activity of ^{90}Y in the samples that were spiked with both ^{90}Y and ^{88}Y tracer.

$$(C_{Y90})_{dbl} = Net\ (C_{YY})_{\mathrm{dbl}} - Net\ (C_{Y88})_{\mathrm{dbl}} \quad \text{(M-1)}$$

In Eq. (M-1), $(C_{Y90})_{dbl}$ represents net double coincidence counts of ^{90}Y; $(C_{YY})_{\mathrm{dbl}}$ shows net double coincidence counts obtained from counting of a sample containing mixed ^{90}Y and ^{88}Y standard sources; and $(C_{Y88})_{\mathrm{dbl}}$ is the net double coincidence counts due to ^{88}Y alone in the sample containing both ^{90}Y and ^{88}Y and determined by Eq. (M-2):

$$(C_{Y88})_{dbl} = \frac{(\bar{A}_{Y88})}{(A_{Y88})} \times (\bar{C}_{Y88})_{dbl} \quad \text{(M-2)}$$

where $\bar{A}_{Y88}$ is activity of pure ^{88}Y standard, which was 8.55 Bq; $(\bar{C}_{Y88})_{dbl}$ shows net double coincidences of pure ^{88}Y standard; and A_{Y88} is ^{88}Y tracer that was added in the sample containing ^{90}Y and was a known quantity. The corresponding triple coincidence counts were obtained in the same manner. Coincidence counts in Eq. (M-2) and Eq. (M-3) were obtained from counting window comprised of channels 50-350 on Hidex LSC.

The corresponding net double and triple coincidences for $\bar{A}_{Y88}$ were found to be $(\bar{C}_{Y88})_{dbl}$ 2528= and $(\bar{C}_{Y88})_{trpl}$=1285, respectively, which were used in Eq. (M-2) for all spiked seawater samples. Eq. (M-2) is valid under the assumption that the counting efficiency of pure ^{88}Y tracer does not significantly change when slightly different quantities of the tracer, for example, quantities in the range used in this dissertation (*i.e.*, 10.5-12.5 Bq) are spiked for radiotracing in the sample. A separate experiment, which is beyond the scope of discussion in this dissertation, had validated this hypothesis.

An example of ^{90}Y radioactivity calculation in the mixed ^{90}Y and ^{88}Y is described below using seawater sample SWY-1. The parameters for SWY-1 as shown in Table L-10 were:

- A_{Y88} = 12.652 Bq (^{88}Y tracer activity added to SWY-1)
- $(C_{YY})_{\mathrm{dbl}}$ = 12186, which is gross counts.
- Net $(C_{YY})_{\mathrm{dbl}}$ = 2186-1027 (corresponding blank, DI Water 1) = 11159
- $(C_{YY})_{\mathrm{trpl}}$ = 8252, which is gross counts.

- Net $(C_{YY})_{\text{trpl}}$ = 8252-486 (corresponding blank, DI Water 1) = 7766

Also, as discussed earlier: $(\bar{A}_{Y88})$= 8.551 Bq; $(\bar{C}_{Y88})_{dbl}$= 2528; and $(\bar{C}_{Y88})_{trpl}$= 1285

Thus, net coincidences for 12.652 Bq ^{88}Y spiked was determined as per Eq. (M-2). Also, because from the purified sample an aliquot was removed for stable Y chemical recovery determination before Čerenkov counting was obtained, therefore, the fraction measured for SWY-1 was f = 0.976 (Table L-10).

$$(C_{Y88})_{dbl} = \left(\frac{(\bar{A}_{Y88})}{\left(\frac{A_{Y88}}{f}\right)}\right) \cdot (\bar{C}_{Y88})_{dbl} = \left(\frac{8.551}{\frac{12.652}{0.976}}\right) \cdot 2528 = 1708.6 = 1667$$

$$(C_{Y88})_{trpl} = \left(\frac{(\bar{A}_{Y88})}{\left(\frac{A_{Y88}}{f}\right)}\right) . (\bar{C}_{Y88})_{trpl} = \left(\frac{8.551}{\frac{12.652}{0.976}}\right) \cdot 1285 = 868.5 = 847$$

Furthermore, the $(C_{Y88})_{dbl}$ and $(C_{Y88})_{trpl}$ needed to be corrected for the actual fraction of ^{88}Y that remained in the sample after the radiochemical separation. Therefore, the chemical recovery of ^{88}Y in SWY-1, which was 77.7 % (Table 7 and Table L-10) was used to achieve the accurate contributions of ^{88}Y:

$$(C_{Y88})_{dbl}R_{corr} = 1667 \cdot 0.777 = 1295$$

$$(C_{Y88})_{trpl}R_{corr} = 847 \cdot 0.777 = 658$$

Finally, net counts due to ^{90}Y alone were determined as follows:

$(C_{Y90})_{dbl}$= *Net* $(C_{YY})_{\text{dbl}} - (C_{Y88})_{\text{dbl}}$ = 11159 − 1295 = 9864

$(C_{Y90})_{dbl}$= *Net* $(C_{YY})_{\text{dbl}} - (C_{Y88})_{\text{dbl}}$ = 7766 – 658 = 7108

The net coincidences found above represent the contributions towards counts from ^{90}Y spiked activity alone, which were processed further for the determination of ^{90}Y measured activity in the sample. Because the count rates obtained after the mathematical correction represent net sample count rates, CR_N, where the blank is already subtracted, therefore, the activity calculation formula shown in Eq. (17) of Section 5.3.2.1 was modified for seawater ^{90}Y activity measurements as shown below:

$$[A_i] = A_{Y\ Cerenk}\ (Bq \cdot L^{-1}) = \frac{CR_N}{\varepsilon_{Cerenk} \cdot R \cdot f \cdot V \cdot DY_{Cerenk}} \qquad \text{(M-3)}$$

Using parameters in Table M-10 and chemical recovery of stable Y in Table M-5, the ^{90}Y Čerenkov emission in 1.002 L SWY-1 seawater sample was determined to be 4.56±0.33 Bq·L^{-1} (uncertainty calculations are discussed in Appendix N):

$$A_{Y\ Cerenk}\ (Bq \cdot L^{-1}) = \frac{2.74}{0.704 \cdot 0.880 \cdot 0.976 \cdot\ 1.002 \cdot 0.992} = 4.56\pm0.33\ \text{Bq}\cdot\text{L}^{-1}$$

In addition to Čerenkov emission, a preliminary liquid scintillation assay of ^{88}Y on Hidex LSC had demonstrated that ^{88}Y exhibits its EC emission peak in the channels 100-800, Figure M-2. The ^{90}Y counting window was set at channels 300-800 to exclude the prominent peak of ^{88}Y. Although, cutting ^{90}Y counting window at channels 300 eliminated a large fraction of ^{88}Y interference, a small peak of ^{88}Y in window 300-800 remained to affect the accurate determination of ^{90}Y. This contribution was mathematically subtracted.

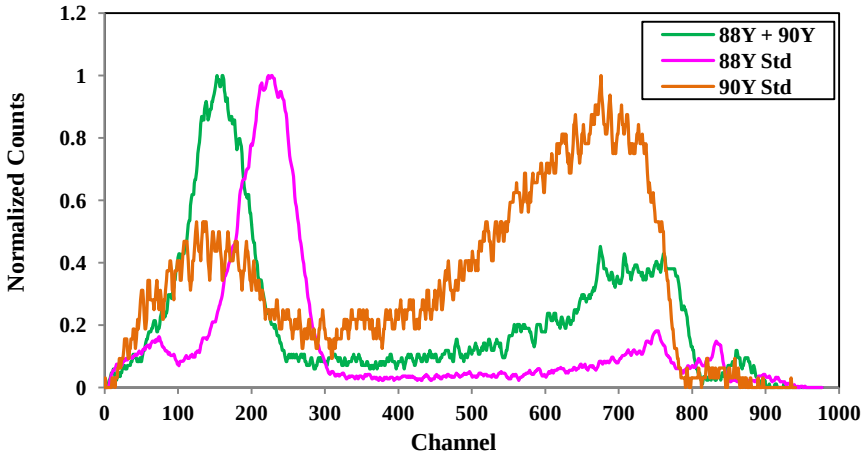

Figure M- 2. A comparison of normalized spectra of pure ^{88}Y (pink), pure ^{90}Y (brown), and mixed ^{90}Y and ^{88}Y (green). The sources were measured in scintillation cocktail on a low background Hidex LSC.

For the mathematical correction of ^{88}Y contribution in the counting region of ^{90}Y LSA, coincidence counts in channels 100-800 were used. The counting window of 100-800 was grouped into two windows: counting window 1 (C1) comprised of channels 100-300, and counting window 2 (C2) consisting channels 300-800. Also, a ^{88}Y standard spiked in scintillation cocktail was counted on Hidex LSC. For this ^{88}Y spiked standard, the counting windows are denoted as $\overline{C1}_{Y88}$ and $\overline{C}2_{Y88}$ comprised of channels 100-300 and 300-800, respectively, Figure M-3a. For the sample containing mixed sources of ^{90}Y and ^{88}Y tracer, the counting regions were divided into $C1_{YY}$ (channels 100-300) and $C2_{YY}$ (channels 300-800), Figure M-3b. Because the C2 constitutes the default region of interest for ^{90}Y, therefore, contributions of ^{88}Y in this region needed to be subtracted using Eq. (M-4):

$$(C2_{Y90}\ )_{dbl} = Net(C2_{YY}\ )_{dbl} - \ Net\ (C2_{Y88}\ )_{dbl} \quad \text{(M-4)}$$

where $(C2_{Y90}\ )_{dbl}$ represents double coincidence of ^{90}Y alone in the mixed ^{88}Y and ^{90}Y source in the counting window 300-800; $(C2_{YY}\ )_{dbl}$ is double coincidence counts due to both ^{88}Y and ^{90}Y in the sample containing mixed ^{88}Y and ^{90}Y in window 300-800 (obtained from the analysis report); and $(C2_{Y88}\ )_{dbl}$ represents double coincidence counts due to ^{88}Y alone in the sample containing mixed ^{88}Y and ^{90}Y in window 300-800 (is unknown). The expression in Eq. (M-4) shows the relationship between double coincidence counts, which is also true for their corresponding triple coincidence counts.

Coincidence counts due to ^{88}Y alone ($C1_{Y88}$ and $C2_{Y88}$) in the mixed sample were unknown and calculated from the mathematical relationships that exist between counts and activity emission in theory, in general. They are shown in Eq. (M-5) through Eq. (M-7) and in Figure M-3.

$$(\overline{C1}_{Y88})_{dbl}\ \cdot\ (\ C2_{Y88}\ )_{dbl} = (\overline{C2}_{Y88})_{dbl} \cdot (\ C1_{Y88}\ )_{dbl} \quad \text{(M-5)}$$

Also, as per Eq. (M-2) (per assumption that the counting efficiency of pure ^{88}Y tracer does not significantly change when slightly different quantities of the tracer changes), the $C1_{Y88}$ can be determined as expressed by M-6:

$$(C_{1Y88})_{dbl} = \left(\frac{\bar{A}_{Y88}}{A_{Y88}}\right) \cdot\ (\overline{C1}_{Y88})_{dbl} \quad \text{(M-6)}$$

Rearranging of Eq. (M-5) gives Eq. (M-7):

$$(C2_{Y88})_{dbl} = \left(\frac{\overline{C2}_{Y88}}{\overline{C1}_{Y88}}\right) \cdot (C1_{Y88})_{dbl} \quad \text{(M-7)}$$

In equations above, $(\ C1_{Y88}\ )_{dbl}$ is the coincidence counts of ^{88}Y alone in the mixed spiked standards ^{88}Y and ^{90}Y in ROI 100-300; A_{Y88} represents spiked activity of ^{88}Y tracer added in the sample containing ^{90}Y, which was a known quantity; and $\bar{A}_{Y88}$ is the activity of pure ^{88}Y standard counted in liquid scintillation cocktail on Hidex in window 100-300. The parameters for $\bar{A}_{Y88}$, which were used for mathematical corrections in equations above were:

- $(\bar{A}_{Y88})$= 12.927 Bq
- $(\overline{C1}_{Y88})_{dbl}$ =16733
- $(\overline{C1}_{Y88})_{trpl}$ =1146
- $(\overline{C2}_{Y88})_{dbl}$ =3825
- $(\overline{C2}_{Y88})_{trpl}$ =3819

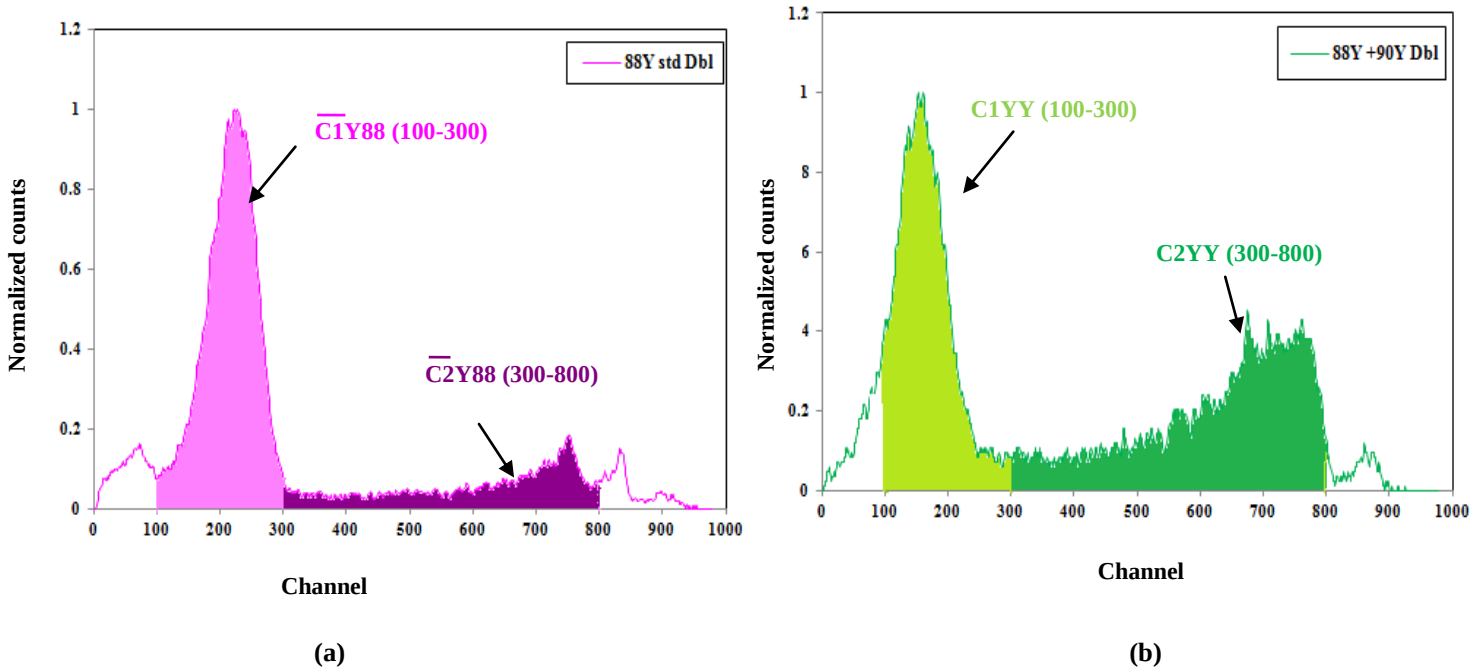

Figure M- 3. Normalized double coincidence spectra of pure ^{88}Y (a) and an example of mixed ^{88}Y and ^{90}Y (b) both measured in liquid scintillation cocktail on Hidex LSC for 1 h following radiochemical separation by DGA-N®.

An example of ^{90}Y activity determination by its liquid scintillation assay on Hidex in the presence of mixed ^{90}Y and ^{88}Y spiked sources is described using purified seawater sample SWY-1. Both double and triple coincidences were mathematically corrected. The ^{88}Y standard source parameters were also used. In addition, because a fraction of the purified SWY-1 was measured, therefore, that also was incorporated in the calculations below. For SWY-1 the LSA fraction measured was f = 0.247 (Table L-11). In SWY-1 example, the ^{88}Y tracer contribution in window 100-300 using Eq. (M-6) was:

$$Net\ (C_{1Y88}\ )_{dbl} = \left(\frac{\bar{A}_{Y88}}{\frac{A_{Y88}}{f}}\right) \cdot\ (\overline{C1}_{Y88})_{dbl} = \left(\frac{12.927}{\frac{12.652}{0.247}}\right) 16733 = 4229$$

$$Net\ (C_{1Y88}\ )_{trpl} = \left(\frac{\bar{A}_{Y88}}{\frac{A_{Y88}}{f}}\right) \cdot (\overline{C1}_{Y88})_{trpl} = \left(\frac{12.927}{\frac{12.652}{0.247}}\right) 1146 = 290$$

In SWY-1 example, the ^{88}Y tracer contribution in the window 300-800 as per Eq. (M-7) was determined to be:

$$Net\ (C2_{Y88})_{dbl} = \left(\frac{(\overline{C2}_{Y88})_{dbl}}{(\overline{C1}_{Y88})_{dbl}}\right) \cdot (\ C1_{Y88})_{dbl} = \left(\frac{3825}{16733}\right) 4229 = 967$$

$$Net\ (C2_{Y88})_{trpl} = \left(\frac{(\overline{C2}_{Y88})_{trpl}}{(\overline{C1}_{Y88})_{trpl}}\right) \cdot (\ C1_{Y88})_{trpl} = \left(\frac{3819}{1146}\right) 290 = 965$$

The chemical recovery of ^{88}Y in the sample was used to obtain the accurate contributions of ^{88}Y. Thus using ^{88}Y recovery of 77.7 % in SWY-1, the corrected coincidences were:

$$Net\ (C2_{Y88}\ )_{dbl}\ R_{corr} = 967\ \cdot 0.777 = 751$$

$$Net\ (C2_{Y88}\ )_{trpl}\ R_{corr} = 965\ \cdot 0.777 = 750$$

The ^{88}Y contributions were subtracted from overall net counts in the ROI of ^{90}Y LSA in SWY-1 (window 300-800) using Eq. (M-4). The gross counts of SWY-1 in ROI 300-800 as shown in Table L-11 were:

- $(C2_{YY})_{dbl}$ =5315
- $(C2_{YY})_{trpl}$ =5251

Note that the coincidence counts shown above are gross values. Therefore, net coincidences were obtained after blank subtraction. The parameters for the

corresponding blank counted in the same batch with SWY-1 (*i.e.*, UGAB1) for its window 300-800 as shown in Table L-11 were:

- $(C2_{YY})_{dbl}$ =1120
- $(C2_{YY})_{trpl}$ =1084

Therefore, using net counts in Eq. (M-4):

$(C2_{Y90})_{dbl} = Net\ (C2_{YY})_{dbl} - Net\ (C2_{Y88})_{dbl}$= (5315 − 1120)−751 = 3444

$(C2_{Y90})_{trpl} = Net\ (C2_{YY})_{trpl} - Net\ (C2_{Y88})_{trpl}$= (5251− 1084) −750 = 3417

The net coincidences found above represent the contributions towards counts from ^{90}Y spiked activity alone and were processed further to determine ^{90}Y in the seawater sample. Because the count rates obtained after the mathematical correction represent net sample count rates, CR_N, where the blank is already subtracted, therefore, the activity calculation formula shown in Eq. (18) of Section 5.3.2.1 was modified for seawater ^{90}Y LSA measurements:

$$[A_i] = A_{Y\ LSA}\ (Bq \cdot L^{-1}) = \frac{CR_N}{\varepsilon_{LSA} \cdot R \cdot f \cdot V \cdot DY_{LSA}} \quad \text{(M-8)}$$

Given the parameters in Table L-11 and chemical recovery of stable Y in Table L-5, the ^{90}Y activity based on LSA on Hidex LSC for 1.002 L seawater sample SWY-1 was 4.70±0.38 Bq·L^{-1} (uncertainty calculations are discussed in Appendix N):

$$A_{Y\ LSA}\ (Bq \cdot L^{-1}) = \frac{0.957}{1.00 \cdot 0.880 \cdot 0.247 \cdot 1.002 \cdot 0.934}$$ = 4.70±0.38 Bq·L^{-1}

Appendix N. Example Calculations

N1. Calculations for TDCR Čerenkov of ^{90}Sr-^{90}Y Activities

For SrCT3-1, its duplicate SrCT3-1Dup, and its corresponding blank sample SrCT3-Blk1 in Table K-1 (Appendix K):

1. TDCR

$$\text{TDCR} = \frac{(C_{trpl})_s - (C_{trpl})_b}{(C_{dbl})_s - (C_{dbl})_b} \quad \text{(N-1)}$$

Where $(C_{trpl})_s$ and $(C_{trpl})_b$ represent triple coincidence counts of sample and blank, respectively; and $(C_{dbl})_s$ and $(C_{dbl})_b$ represent double coincidence counts of sample and blank, respectively.

$$\text{TDCR} = \frac{(8793)_s - (226)_b}{(12410)_s - (847)_b} = 0.741 = 74.1\%$$

2. Uncertainty in TDCR

In general, the relative precision of 1 σ (standard deviation) at 68 % confidence level is commonly used in counting statistics to find the uncertainty in sample counts (σ_s):

$$\sigma_s = \sqrt{Total\ counts\ of\ sample} \quad \text{(N-2)}$$

For net counts, μ, where μ= sample gross counts- background counts, the uncertainty in net counts is the quadrature sum of uncertainties in the sample (σ_s) and background (σ_b):

$$\sigma_\mu = \sqrt{(\sigma_s)^2 + (\sigma_b)^2} \quad \text{(N-3)}$$

Thus, for the triple and double counts, Eq. (N-3) can be modified as Eq. (N-4) and uncertainty in coincidence counts can be propagated using general uncertainty propagation rule [(56)] as shown in Eq. (N-5).

$$\sigma(TDCR)_{\mu} = \sqrt{\left(\sigma_{(TDCR)s}\right)^2 + \left(\sigma_{(TDCR)_b}\right)^2} \quad \text{(N-4)}$$

$$(\sigma_{\mathrm{TDCR}}) = \left(\frac{\mathrm{C_{trpl}}}{\mathrm{C_{dbl}}}\right) \cdot \left(\sqrt{(\sigma\ \mathrm{C_{trpl}}/\ \mathrm{C_{trpl}})^2 + (\sigma\ \mathrm{C_{dbl}}/\ \mathrm{C_{dbl}})^2}\right) \quad \text{(N-5)}$$

Thus, uncertainty in TDCR of sample SrCT3-1 and its corresponding blank SrCT3-Blk1 can be used to find the net TDCR uncertainty as follows:

$$(\sigma_{\mathrm{TDCR}})_{\mathrm{s}} = \left(\frac{8793}{12410}\right) \cdot \left(\sqrt{(\sqrt{8793}/8793)^2 + (\sqrt{12410}/12410)^2}\right) = 0.00987$$

$$(\sigma_{\mathrm{TDCR}})_{\mathrm{b}} = \left(\frac{226}{847}\right) \cdot \left(\sqrt{(\sqrt{226}/226)^2 + (\sqrt{847}/847)^2}\right) = 0.0199$$

$$\sigma(TDCR)_{\mu} = \sqrt{(0.00987)^2 + (0.0199)^2} = 0.022 = 2.2\ \%$$

Thus, for SrCT3-1 the TDCR±σ is 0.741±0.022.

3. Counting efficiency of ^{90}Y

For SrCT3-1 with TDCR of 0.741±0.022, the counting efficiency of ^{90}Y was obtained using Eq. (12) in Section 5.3.1.1.

$\mathcal{E}_{\check{\mathrm{C}}\mathrm{erenkov}} = 0.9 \cdot (0.741)^{0.75} = 0.719$

The uncertainty in $\mathcal{E}_{\check{\mathrm{C}}\mathrm{erenkov}}$ of SrCT3-1 was propagated using power rule [(56)] as per Eq. (N-6).

$$\sigma(\mathcal{E}_{\check{\mathrm{C}}\mathrm{erenkov}}) = 0.9 \cdot \{0.75 * (\mathrm{TDCR})^{0.75-1}\} \cdot \sigma(TDCR)_{\mu} \quad \text{(N-6)}$$

[(56)] Mann P. S., Introductory Statistics, 6th Edition. 2007. John Wiley & Sons Inc., SBN 978-0-471-75530-2

$\sigma(\varepsilon_{Čerenkov}) = 0.9 \cdot\{0.75*(0.741)^{0.75-1}\} \cdot (0.022) = 0.016$

For those samples where there was a sample and a duplicate, the average of the Čerenkov counting efficiencies of the sample and the duplicate were taken and shown as $\dot{\varepsilon}_{Čerenkov}$ in Table K-1. The uncertainty on $\dot{\varepsilon}_{Čerenkov}$ was the quadrature sum of uncertainties in the sample $\varepsilon_{Čerenkov}$ and duplicate $\varepsilon_{Čerenkov}$.

4. Measured Čerenkov activity of ^{90}Y

The measured activities were determined as per Eq. (13) shown in Section 5.3.1.1.

For example for SrCT3-1, the net count rates ($CR_s - CR_b$) in Eq. (14) is 6.424±0.064 in Table L-1. Thus:

$$A_i = A_{Y\ TDCR}\ (Bq) = \frac{CR_s - CR_b}{\varepsilon_{Cerenk}} = \frac{6.424}{0.719} = 8.94 \text{ Bq}$$

The uncertainty in activity of ^{90}Y was propagated as below:

$$\sigma\left(A_{Y\ TDCR}\ (Bq)\right) = \frac{6.424}{0.719}\left(\sqrt{(0.064/6.424)^2 + (0.016/0.719)^2}\right) = 0.22$$

Thus, the A_i of SrCT3-1 was determined to be 8.94±0.22 Bq.

5. Bias in ^{90}Y measured activity

Relative bias (B_{ri}) for individual measurements was determined using Eq. (15) in Section 5.3.11. For example for SrCT3-1, the bias was determined as shown below:

$$B_{ri} = \frac{A_i - A_{ai}}{A_{ai}} = \frac{8.94 - 9.28}{9.28} = 0.0366 = -3.7\ \%$$

The relative precision (S_B) for replicates was the dispersion in bias measurements as shown in Eq. (16) in Section 5.3.1.1. For example, for replicates of geometry test in 7-mL vials for samples and duplicates of SrCT3-1 through SrCT3-4 in Table 16 in Section 5.3.1.1 the S_B was determined using Excel and found to be -5.1 %.

N2. Example Calculations for Determination of Activity Concentrations of Freshwater Strontium-90 and Yttrium-90

Measured activity concentrations, [A_i], of spiked freshwater were determined using four different methods. All four methods used the generic activity concentration calculation formulas. An example of activity concentration calculations for Čerenkov counting of ^{90}Y in PL1-1 is described here.

The Čerenkov emission of ^{90}Y in 1.01 L sample of PL1-1 following radiochemical separation was calculated using Eq. (18) in Section 5.3.2.1 and variables for PL1-1 tabulated in Table L-1 (Appendix L). The variables were: the time elapsed between ^{90}Y extraction on the DGA-N® resin and its start of counting on the Hidex LSC (T_1-T_0) was 3.9 h; the decay constant ^{90}Y is λ_Y = 0.011 h^{-1}; the chemical recovery of stable Y was found to be 80.7 % (Table 25); fraction of sample measured was *f* =1 because the entire purified sample was Čerenkov counted. The corresponding blank sample was DI Water 1 in Table L-1 which was used to subtract background effects.

Therefore: $DY_{Cerenk}=e^{-(T_1-T_0)\cdot\lambda_Y}= e^{-(3.9)\cdot 0.011}= 0.958$

$$[A_i] = A_{YCerenk}\ (Bq\cdot L^{-1}) = \frac{\frac{CR_S}{(\varepsilon_{Cerenk})_S} - \frac{CR_b}{(\varepsilon_{Cerenk})_b}}{R\cdot f\cdot V\cdot DY_{Cerenk}} = \frac{\frac{3.96}{0.694} - \frac{0.29}{0.487}}{0.807\cdot 1\cdot 1.01\cdot 0.958}$$

$A_{YCerenk}\ (Bq\cdot L^{-1})$ = 6.51±0.15 Bq·L^{-1}

The uncertainty in activity concentrations were propagated the same way as the ^{90}Y Čerenkov counting by TDCR as described in earlier section of this Appendix (Appendix N1).

Similarly, using the variables in Table L-2 through Table L-4, the activity concentrations of the other three methods of activity measurement (*i.e.*, ^{90}Y by LSA, ^{90}Sr by LSA initially, and ^{90}Sr by LSA after ^{90}Y in-growth period) were determined. The in-growth (I_Y) of ^{90}Y in ^{90}Sr activity, which was used for correction of ^{90}Sr activity was obtained using Eq. (21), Section 5.3.2.1. The decay constant ^{90}Y is λ_Y=0.011 h^{-1}and that of ^{90}Sr is λ_{Sr}=2.746x10^{-6} h^{-1}. An example of I_Y determination using PL1-1 parameters in Table L-3 is shown below:

$$I_Y = \left(\frac{\lambda_Y}{\lambda_Y - \lambda_{Sr}}\right)\cdot\left(e^{-\lambda_{Sr}\cdot(T_3-T_0)} - e^{-\lambda_Y\cdot(T_3-T_0)}\right) = \left(\frac{0.011}{0.011 - 2.746\text{x}10^{-6}}\right)\cdot$$

$$\left(e^{-2.746\text{x}10^{-6}\cdot(20)} - e^{-0.011\cdot(20)}\right) = 0.197$$

N3. Example Calculations for Determination of Seawater Radiotracers Activities

The seawater radiotracing was performed using ^{88}Y and ^{85}Sr. The ^{88}Y was measured by both γ spectrometry and liquid scintillation assay. The ratio of measured to expected activity of ^{88}Y in samples was used as the chemical recovery of ^{88}Y in the sample. An example calculation of ^{88}Y activity in 1.002±0.009 L seawater sample of SWY-1 is presented here. In Table L-7 (Appendix L), for the ^{88}Y γ ray of 0.898 MeV, which has an emission probability of I = 0.937, the counting efficiency was found to be ε_γ=1.05±0.03 %. Using Eq. (23) in Section 5.3.2.2, the activity concentration of ^{88}Y was measured as shown below:

$$[A_i] = A_\gamma \pm \sigma\ (Bq \cdot L^{-1}) = \frac{CR_S}{\varepsilon_\gamma \cdot I \cdot f \cdot V} \pm \left\{\left(\frac{CR_S}{\varepsilon_\gamma \cdot I \cdot f \cdot V}\right) \cdot \left(\sqrt{(\sigma CR_s/CR_s)^2 + (\sigma\varepsilon_\gamma/\varepsilon_\gamma)^2 + (\sigma V/V)^2}\right)\right\}$$

$$= \left(\frac{0.072}{0.01045 \cdot 0.937 \cdot 0.753 \cdot 1.002}\right) \pm \left\{\left(\frac{0.072}{0.01045 \cdot 0.937 \cdot 0.753 \cdot 1.002}\right) \cdot \sqrt{(0.005/0.072)^2 + (0.00033/0.01045)^2 + (0.009/1.002)^2}\right\}$$

$A_\gamma \pm \sigma\ (Bq \cdot L^{-1})$ = 9.75 ± 0.82 Bq·L^{-1}

The measured activity of ^{88}Y was used to determine the recovery of ^{88}Y in purified SWY-1. The spiked activity, [A_{ia}], which was an exact and known amount, was 12.55 Bq·L^{-1}. Thus, the recovery was:

$$R \pm \sigma(\%) = \left[\frac{9.75 \pm 0.82}{12.55 \pm 0.38} \pm \left\{\left(\frac{12.55 \pm 0.38}{9.75 \pm 0.82}\right) \cdot \cdot \sqrt{(0.38/12.55)^2 + (0.82/9.75)^2}\right\}\right] \cdot 100$$

$R \pm \sigma$ = 77.7±6.9 %